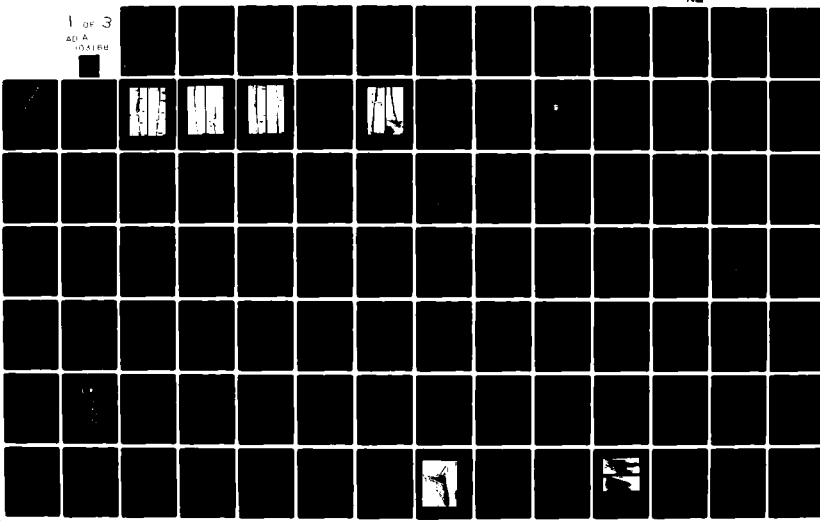


AD-A103 168 ENVIRONMENTAL SCIENCE AND ENGINEERING INC GAINESVILLE FL F/G 8/10
ANALYSIS OF COASTAL SEDIMENT TRANSPORT PROCESSES FROM WRIGHTSVI--ETC(U)
JUN 81 T C WINTON, I B CHOU, G M POWELL DACW72-79-C-0001
CERC-MR-81-6 NL

UNCLASSIFIED

1 of 3
AD-A
03464



AD A103168

LEVEL

MR 81-6

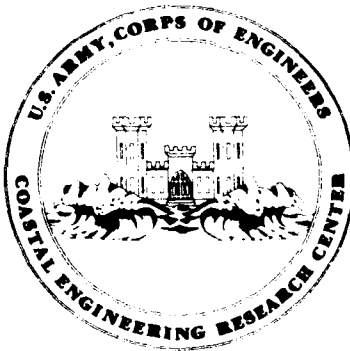
12

Analysis of Coastal Sediment Transport Processes From Wrightsville Beach to Fort Fisher, North Carolina

by

T. C. Winton, I. B. Chou,
G. M. Powell, and J. D. Crane

MISCELLANEOUS REPORT NO. 81-6
JUNE 1981



Approved for public release;
distribution unlimited.

Prepared for

U.S. ARMY, CORPS OF ENGINEERS
COASTAL ENGINEERING
RESEARCH CENTER

Kingman Building
Fort Belvoir, Va. 22060

81 8 21 059

DMC FILE COPY

Reprint or republication of any of this material shall give appropriate credit to the U.S. Army Coastal Engineering Research Center.

Limited free distribution within the United States of single copies of this publication has been made by this Center. Additional copies are available from:

*National Technical Information Service
ATTN: Operations Division
5285 Port Royal Road
Springfield, Virginia 22161*

The findings in this report are not to be construed as an official Department of the Army position unless so designated by other authorized documents.

UNCLASSIFIED

SECURITY CLASSIFICATION OF THIS PAGE (When Data Entered)

DD FORM 1 JAN 73 1473 EDITION OF 1 NOV 68 IS OBSOLETE

UNCLASSIFIED

SECURITY CLASSIFICATION OF THIS PAGE (When Data Entered)

UNCLASSIFIED

SECURITY CLASSIFICATION OF THIS PAGE(When Data Entered)

7 The historical position of the MLW, MSL, and MHW contours, relative to a fixed base line, is plotted for the period between 1964 and 1975. An equivalent volumetric erosion or accretion between successive surveys is determined by multiplying the average excursion distance of the contours by a constant of proportionality.

The plots of excursion distance versus time for the MLW, MSL, and MHW contours also show the time response of the beach fills. This response is described by a mathematical function.

The alongshore components of wave-induced energy flux are also determined within the study area through wave refraction analysis. This information, together with the information on volumetric change, is used in a sediment budget analysis to determine the coefficient of alongshore sediment transport and the inlet trapping characteristics.

PREFACE

This report is published to provide coastal engineers with a comprehensive engineering analysis of coastal sediment transport processes along a 42-kilometer segment of the North Carolina shoreline from Wrightsville Beach to Fort Fisher. Included is an interpretation of the littoral processes, long-shore transport, and the behavior and success of beach nourishment projects at Wrightsville and Carolina Beaches. The work was carried out under the evaluation and shore protection structures program of the Coastal Engineering Research Center (CERC).

The report was prepared by T.C. Winton, I.B. Chou, G.M. Powell, and J.D. Crane of Environmental Science and Engineering, Inc. (ESE), Gainesville, Florida, under CERC Contract No. DACW 72-79-C-0001.

The authors acknowledge the efforts and many helpful comments provided by Dr. R. Weggel, Chief, Evaluation Branch, CERC, Dr. T.Y. Chiu, University of Florida, Department of Coastal Engineering, and the staff of the U.S. Army Engineer District, Wilmington.

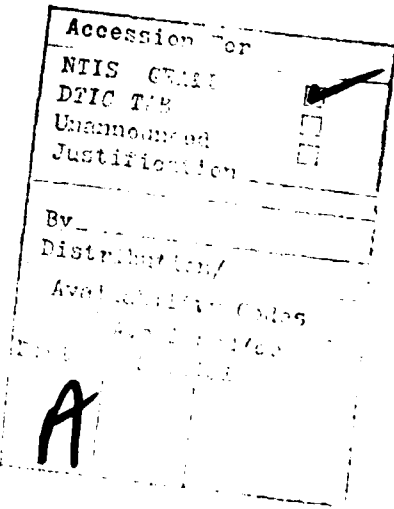
G. Hawley and Dr. R. Weggel were the CERC contract monitors for the report, under the general supervision of N.E. Parker, Chief, Engineering Development Division.

Comments on this publication are invited.

Approved for publication in accordance with Public Law 166, 79th Congress, approved 31 July 1945, as supplemented by Public Law 172, 88th Congress, approved 7 November 1963.



TED E. BISHOP
Colonel, Corps of Engineers
Commander and Director



CONTENTS

	Page
CONVERSION FACTORS, U.S. CUSTOMARY TO METRIC (SI).....	8
I INTRODUCTION.....	9
II STUDY AREA.....	10
III DATA COLLECTION.....	18
1. Beach Profiles.....	18
2. Wave Data.....	18
3. Beach Sand Data.....	23
IV ANALYSIS OF BEACH PROFILE DATA.....	25
1. Excursion Distance Technique.....	25
2. Historical Events Affecting Excursion Distance Analysis.....	25
3. Excursion Distance Analysis.....	27
4. Beach Behavior from 1965 to 1975.....	45
V LONGSHORE SEDIMENT TRANSPORT ANALYSIS.....	62
1. Introduction.....	62
2. Wave Refraction Analysis.....	62
3. Energy Flux Computation.....	70
4. Longshore Sediment Transport Model.....	73
5. Sediment Budget.....	78
VI BEACH-FILL PERFORMANCE.....	82
VII SUMMARY AND CONCLUSIONS.....	92
LITERATURE CITED.....	96
 APPENDIX	
A WRIGHTSVILLE BEACH EXCURSION DISTANCE PLOTS.....	99
B CAROLINA BEACH EXCURSION DISTANCE PLOTS.....	125
C MASONBORO BEACH EXCURSION DISTANCE PLOTS.....	145
D KURE BEACH EXCURSION DISTANCE PLOTS.....	158
E FISHER BEACH EXCURSION DISTANCE PLOTS.....	170
F COMPARATIVE SHORT BEACH PROFILES.....	182
G WAVE REFRACTION PLOTS.....	196
 TABLES	
1 Cross references for beach profile data.....	21
2 Repetitive short and long profiles measured along the study area.....	23
3 Beach sand grain-size data.....	24
4 Beach-fill evaluation.....	26

CONTENTS

TABLES--Continued

	Page
5 Historical events affecting beach volumes during study period, 1965-1975.....	29
6 Volumetric and excursion losses due to rise in MSL.....	41
7 Average long-term excursion rates along Wrightsville Beach.....	50
8 Seasonal variation in MLW, MSL, and MHW position along Wrightsville Beach.....	51
9 Wrightsville Beach, 1970 beach-fill data.....	53
10 Average long-term excursion rates along Carolina Beach.....	58
11 Seasonal variation in MLW, MSL, and MHW positions, Carolina Beach.....	59
12 1965 to 1971 beach-fill data, Carolina Beach.....	61
13 Statistical wave climate parameters for the study area.....	65
14 Selected seasonal wave parameters used in the wave refraction analysis.....	66
15 Predicted and measured distribution of wave energy at Wrightsville Beach.....	67
16 Value of β for Wrightsville and Carolina Beaches.....	76
17 Annual volumetric changes in beach cell volume and losses due to sea level rise and wave overtopping.....	78
18 Energy flux values at cell boundaries.....	81
19 Efficiency factors α for Wrightsville and Carolina Beach sediment budgets.....	81
20 Granulometric data for Wrightsville Beach 1970 beach fill.....	84
21 Average granulometric data for Carolina Beach 1965 beach fill.....	91

FIGURES

1 Wrightsville Beach to Fort Fisher, North Carolina study area.....	11
2 Aerial photo map of study area from Figure Eight Island to Masonboro Beach, North Carolina.....	13
3 Aerial photo map of study area from Masonboro Beach to Carolina Beach, North Carolina.....	14
4 Aerial photo map of study area from Carolina Beach to Fort Fisher, North Carolina.....	15
5 Aerial photo map of study area from Fort Fisher to Cape Fear, North Carolina.....	17
6 Profile station location map, WB1 to MB27.....	19
7 Profile station location map, MB28 to FB21.....	20

CONTENTS

FIGURES--Continued

	Page
8 Distribution of beach fills along study area.....	28
9 Comparative short profiles, Wrightsville Beach.....	30
10 Comparative long profiles, Wrightsville Beach.....	31
11 Distance from the base line to stated contours at WB15.....	32
12 Distance from the base line to stated contours at CB71.....	33
13 Distance from the base line to stated contours at MB17.....	34
14 Distance from the base line to stated contours at KB17.....	35
15 Distance from the base line to stated contours at FB10.....	36
16 Distance from the base line to stated contours at WB15.....	38
17 Distance from the base line to stated contours at CB71.....	39
18 Schematization of beach-fill response.....	40
19 Definition sketch for beach-fill response.....	43
20 Semilog plots of excursion distance versus time after fill placement for profile WB15.....	43
21 Distance from the base line to stated contours at WB3.....	46
22 Distance from the base line to stated contours at WB16.....	47
23 Distance from the base line to stated contours at WB47.....	49
24 Comparison of measured and computed volumetric change along Carolina Beach.....	50
25 Relative seasonal change in beach slope for Wrightsville Beach.....	51
26 Semilog plots of normalized excursion distance versus time after fill placement for MHW, MLW, and MSL contours (1970 beach fill).....	52
27 Distance from the base line to stated contours at CB2.....	55
28 Distance from the base line to stated contours at CB64.....	56
29 Distance from the base line to stated contours at CB119.....	57
30 Comparison of measured and computed volumetric change along Wrightsville Beach.....	58
31 Semilog plots of normalized excursion distance versus time after fill placement for 1965 beach fill.....	59
32 Semilog plots of normalized excursion distance versus time after fill placement for 1971 beach fill.....	60
33 Wave directions used in refraction analysis.....	64

CONTENTS

FIGURES--Continued

	Page
34 A three-dimensional line drawing representation of the offshore bathymetry (view looking onshore from southeast).....	68
35 Wave refraction diagram for a medium period wave ($T = 10.5$ seconds; $H = 1.40$ meters from the east).....	71
36 Wave refraction diagram for a medium period wave ($T = 10.5$ seconds; $H = 1.40$ meters from the east) with crossed wave waves eliminated.....	71
37 Northerly and southerly components of longshore energy flux along study area.....	74
38 Net annual longshore energy flux along study area.....	74
39 Comparison of measured and computed volumetric change along Wrightsville Beach.....	77
40 Comparison of measured and computed volumetric change along Carolina Beach.....	77
41 Beach-cell schematization.....	80
42 Sediment budget schematics for Wrightsville Beach and Carolina Beach...	80
43 Wrightsville Beach 1970 beach fill.....	83
44 Response of foreshore slope after Wrightsville Beach 1970 beach fill...	86
45 View of Wrightsville Beach looking north-northeast.....	88
46 Views of Carolina Beach shoreline before and after construction of 1965 beach-fill project.....	91

CONVERSION FACTORS, U.S. CUSTOMARY TO METRIC (SI) UNITS OF MEASUREMENT

U.S. customary units of measurement used in this report can be converted to metric (SI) units as follows:

Multiply	by	To obtain
inches	25.4	millimeters
	2.54	centimeters
square inches	6.452	square centimeters
cubic inches	16.39	cubic centimeters
feet	30.48	centimeters
	0.3048	meters
square feet	0.0929	square meters
cubic feet	0.0283	cubic meters
yards	0.9144	meters
square yards	0.836	square meters
cubic yards	0.7646	cubic meters
miles	1.6093	kilometers
square miles	259.0	hectares
knots	1.852	kilometers per hour
acres	0.4047	hectares
foot-pounds	1.3558	newton meters
millibars	1.0197×10^{-3}	kilograms per square centimeter
ounces	28.35	grams
pounds	453.6	grams
	0.4536	kilograms
ton, long	1.0160	metric tons
ton, short	0.9072	metric tons
degrees (angle)	0.01745	radians
Fahrenheit degrees	5/9	Celsius degrees or Kelvins ¹

¹ To obtain Celsius (C) temperature readings from Fahrenheit (F) readings, use formula: $C = (5/9)(F - 32)$.

To obtain Kelvin (K) readings, use formula: $K = (5/9)(F - 32) + 273.15$.

ANALYSIS OF COASTAL SEDIMENT TRANSPORT PROCESSES FROM
WRIGHTSVILLE BEACH TO FORT FISHER, NORTH CAROLINA

by

T.C. Winton, I.B. Chou, G.M. Powell, and J.D. Crane

I. INTRODUCTION

This report presents a comprehensive engineering analysis of the coastal sediment transport processes along a 42-kilometer segment of the North Carolina shoreline from Wrightsville Beach to Fort Fisher. Included in the analysis is an interpretation of all available data describing the littoral processes, longshore transport, and the behavior and success of beach nourishment projects at Wrightsville Beach and at Carolina Beach, North Carolina.

Several coastal engineering studies have been conducted within the study area to assess the nearshore coastal processes and shoreline erosion trends. Vallianos (1970) investigated the influence of the manmade Carolina Beach Inlet on the volumetric erosion trends of the Masonboro and Carolina beach shorelines. He presented a preliminary assessment of the impact of Masonboro Inlet north jetty on the longshore transport trends for Wrightsville and Masonboro beach shorelines, and an evaluation on the performance of the 1965 Carolina Beach beach fill.

Jarrett (1977) conducted a study for the 30-kilometer segment of shoreline from Wrightsville Beach to Kure Beach in relation to an environmental assessment of coastal erosion as affected by Carolina Beach Inlet. He estimated the annual rate of littoral transport between nine littoral cells by using a calibrated energy flux-wave refraction sediment budget approach. Jarrett refined Vallianos' (1970) bypassing rates for both Masonboro and Carolina Beach Inlet and reassessed the magnitude of the impact on shore process of manmade changes occurring during the study period. The results of this study are also available in reports by the U.S. Army Engineer District, Wilmington (1976; 1977).

The U.S. Army Engineer District, Wilmington (1974), presented historic shoreline changes in the vicinity of Fort Fisher between 1865 and 1973. Several plans were recommended to protect the historic Fort Fisher battlements from critical dune erosion.

Large quantities of data, some of which are not available to previous investigators, were evaluated during this study. Much of the field data were collected from 1964 to 1975 for shoreline erosion studies conducted by the U.S. Army Engineer District, Wilmington, and in part for the Coastal Engineering Research Center's (CERC) Beach Evaluation Program (BEP). Profile surveying and the collection of other data used in this report were coordinated by CERC. Data evaluated include repetitive beach profiles, sand data, bathymetry surveys, wave gage records, dredging records, meteorological records, coastal structure design, coastal geomorphological studies, shoreline erosion studies, aerial photography, and beach photography.

Appendices A to G present a graphic description of the shoreline changes along the study area between 1964 and 1975. These plots allow a quantitative assessment and interpretation of beach response to seasonal climatic changes, storm events, beach-fill projects, and coastal engineering structures. Long-term trends are identified and used to establish a sediment budget model of Wrightsville and Carolina Beaches. The analysis of the excursion distance response of the mean low water (MLW), mean sea level (MSL), and mean high water (MHW) contours of profiles along Wrightsville and Carolina Beaches permitted the formulation of a mathematical description of post beach-fill performances.

All analyses and interpretations of results are included in this report. Supplementary data are provided in eight unpublished volumes (I to VIII) which are available from the CERC technical library. Volume I contains five sections: Section A provides a beach profile documentation for the entire study shoreline; Section B presents storm histories (accounts of the major storms occurring in the study area); Section C provides a wave refraction analysis of the area including wave gage data for selected wave spectra plots, selected data from CERC's Littoral Environment Observation (LEO) program, and wave refraction plots; Section D presents plots and tabulated values of the gross northerly and southerly, and the net longshore energy flux distribution; and Section E provides data on volumetric changes which occurred within all inlets along the study area. Comparative short and long beach profiles, beach profile data, MSL excursion rate tables, MSL volumetric change plots and tables, and selected sand data are presented for Wrightsville Beach (Vols. II, III, and IV), Masonboro Beach (Vol. V), Carolina Beach (Vols. VI and VII), Kure Beach (Vol. VIII, Sec. I), and Fort Fisher (Vol. VIII, Sec. J).

II. STUDY AREA

The study area is part of the tidewater region of the Atlantic Coastal Plain, consisting of a series of low, narrow, sandy barrier islands and peninsular beaches located in New Hanover County, North Carolina. The islands front the Atlantic Ocean just north of Cape Fear and are separated from the mainland by either the Cape Fear River estuary or by Myrtle Grove, Masonboro, Greenville, and Middle Sounds. The five coastal sites in the 42-kilometer study are (from north to south) Wrightsville Beach, Masonboro Beach, Carolina Beach, Kure Beach, and Fort Fisher. Figure 1 shows the study area and the location of the five study segments.

The beach sands are generally fine and composed of quartz sand with a shell content ranging from 0 to 42 percent. The direct sources of littoral materials for the study area are the adjacent beaches, dunes, and bluffs (direction of transport depending on direction of wave attack) as a result of erosion, and the nearshore ocean bottom areas, from which material is brought onto shore. A complete description of the geomorphology and geologic history of the study area has been summarized by Pierce (1970).

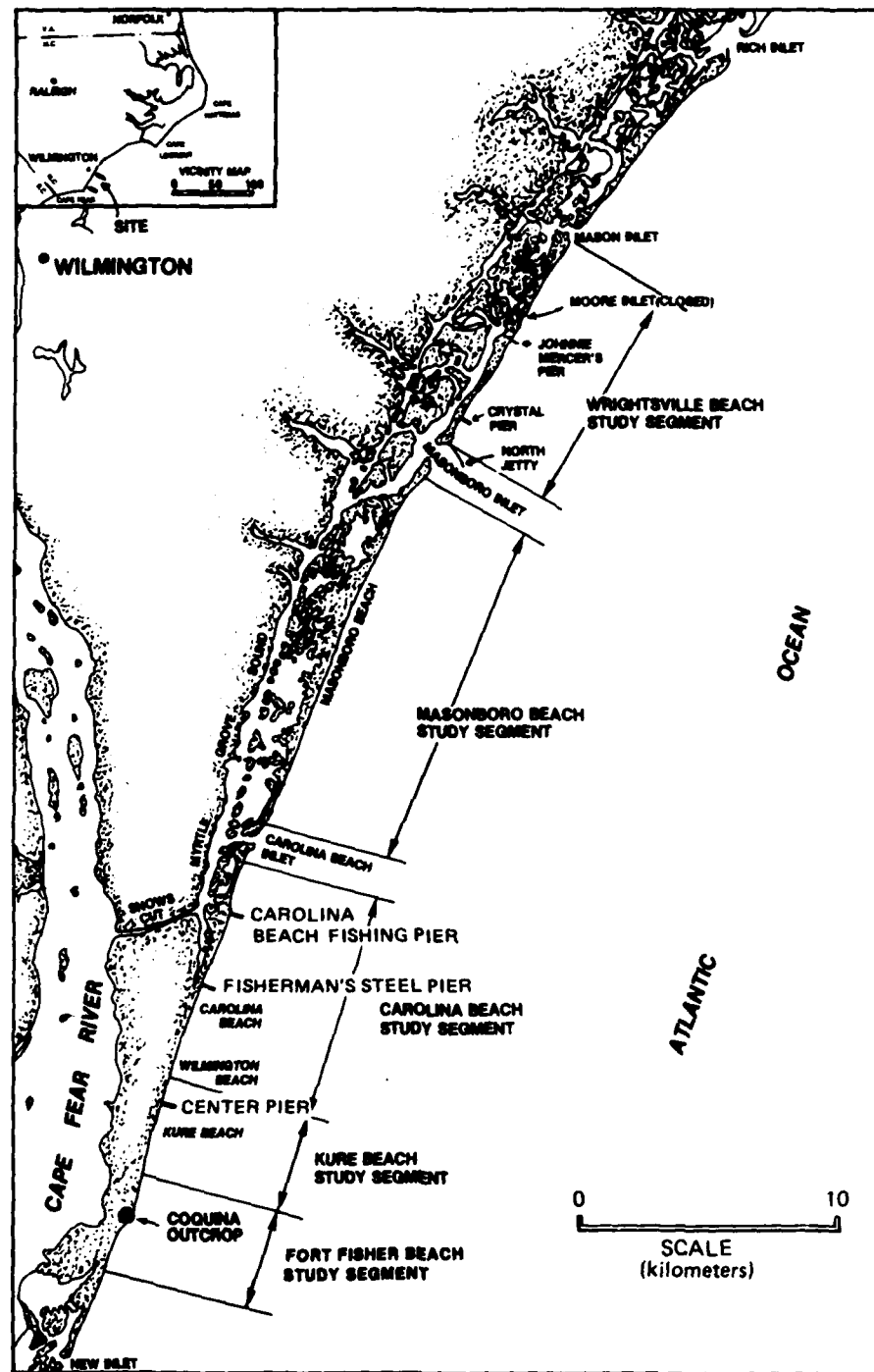


Figure 1. Wrightsville Beach to Fort Fisher, North Carolina, study area.

Based on data recorded by CERC's wave gage located at Wrightsville Beach, the annual significant wave height is 0.76 meter (2.5 feet). Wave observations along Wrightsville Beach indicate that 98 percent of the observed wave energy approaches from the eastern and southeastern quadrants. The dominant direction of littoral transport is from north to south; however, reversals in transport direction along the beaches do occur. The mean and spring tidal ranges are 1.2 and 1.4 meters, respectively; the difference between MSL and MLW is 0.57 meter.

Wrightsville Beach is about 6.75 kilometers in length, with an average dune height of 4 meters above MSL. The beach faces approximately east-southeast, has an average beach slope from MHW to the -6.0 meter (MSL) depth contour of 1 on 37.2, and contains beach sediments with a mean grain size of 0.27 millimeter. The ocean shoreline of Wrightsville Beach was modified in 1965 by the construction of a hurricane and storm protection project. Initially, 2,288,000 cubic meters of fill material was placed along 5,100 meters of beach north of Masonboro Inlet with artificial dune heights constructed to an approximate elevation of +2.5 meters (MSL) for storm protection purposes. The northern transition section included the closure of Moore Inlet, which had previously separated Wrightsville Beach from Shell Island. In spring 1966, an additional 244,000 cubic meters of fill material from the Masonboro Inlet was placed between Johnnie Mercer's Pier and Crystal Pier. In October 1966, a final deposition of 32,100 cubic meters of material from the estuarial area behind Shell Island was placed along the northernmost 610 meters within the town limits of the Wrightsville Beach project shoreline.

In 1970, a renourishment of the central shoreline of Wrightsville Beach was required. A total of 1,053,600 cubic meters of fill material obtained from a shoal in the Banks Channel and the sound area behind Shell Island was placed on the beach, beginning at a point approximately 1.83 kilometers north of Masonboro Inlet and extending to the northern city limits of Wrightsville Beach. Figure 2 is an aerial photo strip map showing the Wrightsville Beach shoreline.

Masonboro Island is bordered by Masonboro Inlet to the north, and by Carolina Beach Inlet (opened in 1952 by local interest groups) to the south (Figs. 2 and 3). It is a very narrow, low-lying uninhabited island approximately 12.5 kilometers long with a shoreline orientation from north-northeast to south-southwest. The natural dune heights along the island range from 3 to 10 meters (MSL), and the median grain size is 0.34 millimeter. The average beach slope is approximately 1 on 59.

Carolina Beach is located just south of the Carolina Beach Inlet and extends about 4.3 kilometers southward to Kure Beach (Figs. 3 and 4). The northern end of Carolina Beach has experienced high erosion rates since the opening of Carolina Beach Inlet (Vallianos, 1970), which have affected the efficiency of a hurricane and shore protection project constructed in 1965. The 4.27 kilometers of shoreline fronting the town of Carolina Beach was nourished with about 2,014,000 cubic meters of fill material obtained from the Carolina Beach harbor. However, by 1967, erosion of the northern 1.2 kilometers of the project beach was so severe that emergency action was required. Approximately 314,000 cubic

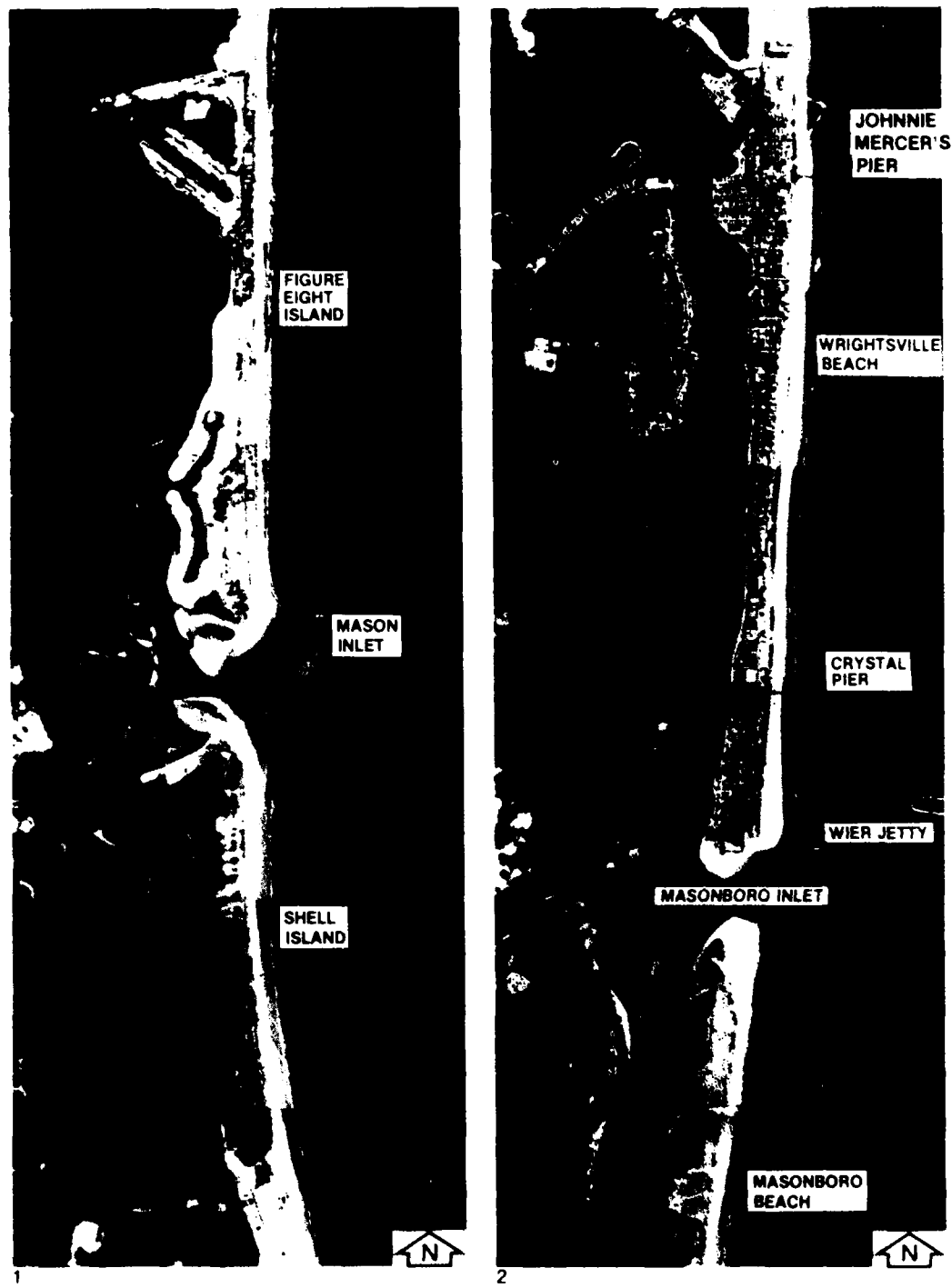


Figure 2. Aerial photo map of study area from Figure Eight Island to Masonboro Beach, North Carolina.

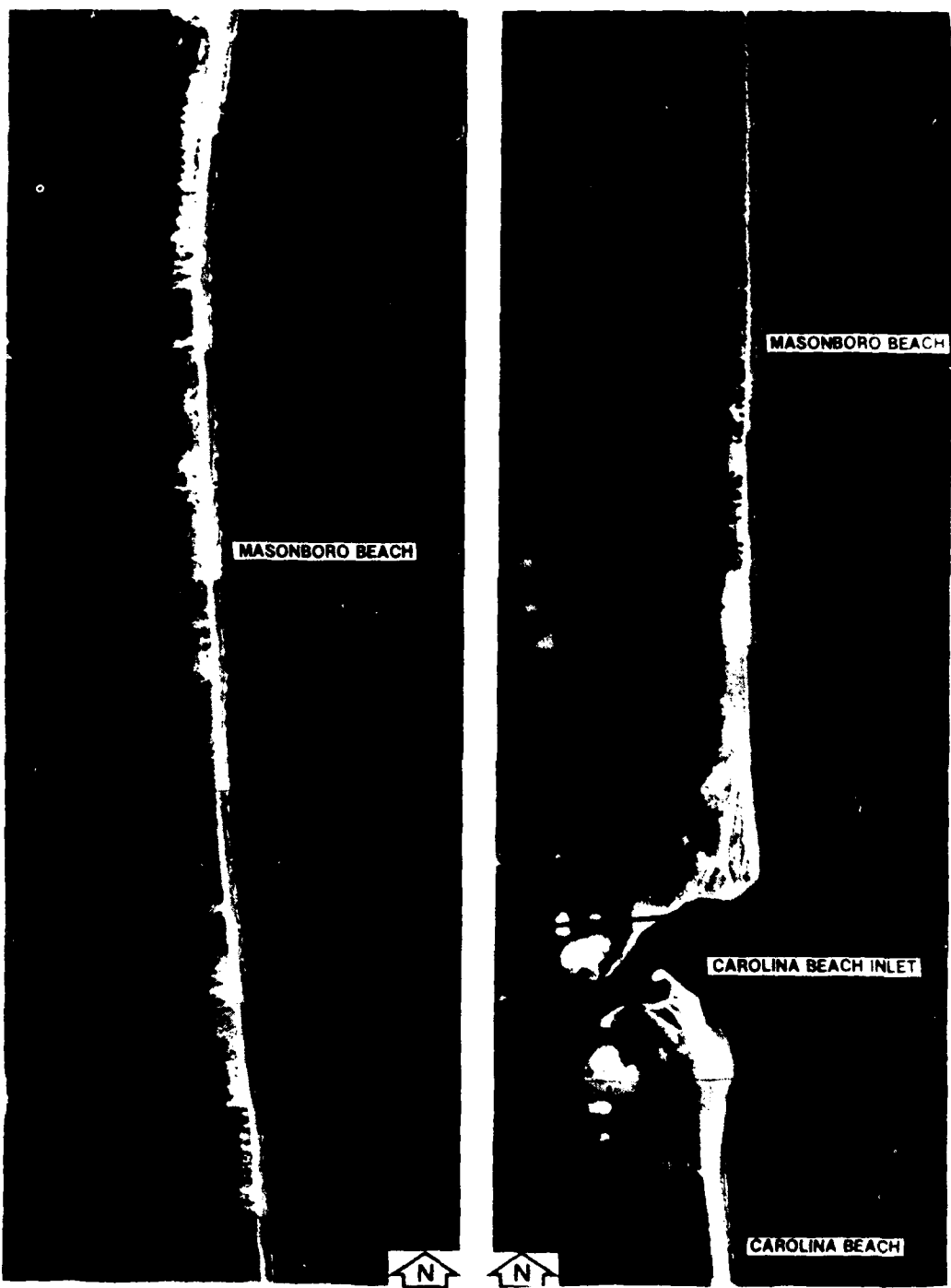


Figure 3. Aerial photo map of study area from Masonboro Beach to Carolina Beach, North Carolina.

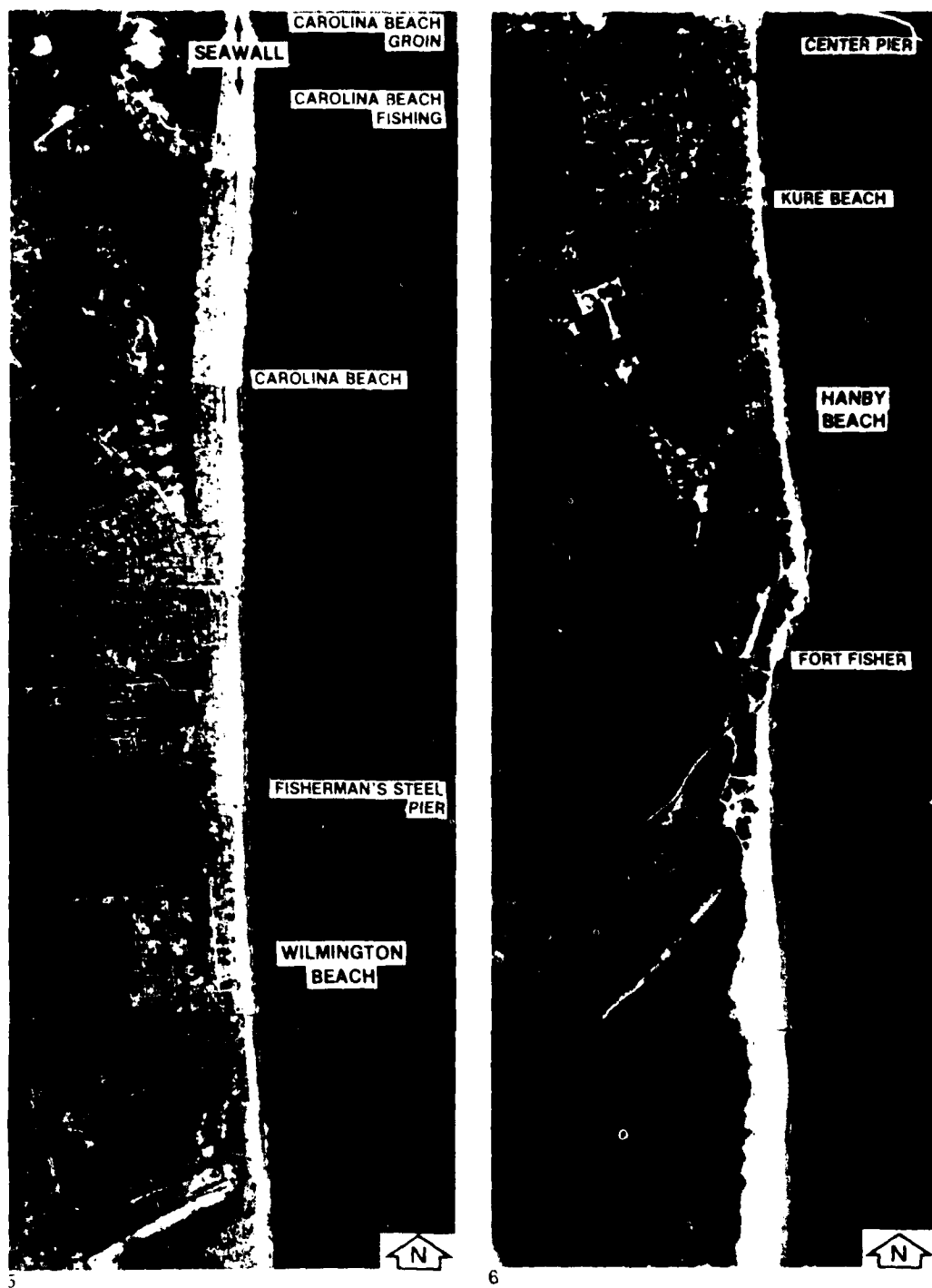


Figure 4. Aerial photo map of study area from Carolina Beach to Fort Fisher, North Carolina.

meters of fill material was distributed there and 83,400 cubic meters of sand was placed to form a new 520-meter transition section from the original northern limits of the project beach. A temporary wooden groin was constructed at the transition junction between the two fill sites.

Despite the 1967 emergency action, serious erosion continued, requiring the supplemental emergency construction in 1970 of a 335-meter rubble-mound seawall extending southward from the northern boundary of the project. In conjunction with the seawall construction, 264,500 cubic meters of fill material from the sediment trap located inside Carolina Beach Inlet was placed along the northern 1.2 kilometers of shoreline. By late spring 1971, the southern 3.47 kilometers of the project beach had been partially restored with approximately 581,000 cubic meters of material from a borrow area located in the Cape Fear River. The rubble-mound seawall was extended an additional 290 meters southward in 1973. The severe erosion trend of the northern project limits continued despite the numerous remedial measures taken.

Kure Beach has a shoreline about 4.25 kilometers in length, and is situated between Carolina Beach to the north and Fort Fisher to the south (Fig. 4). The city of Kure Beach and the unincorporated towns of Wilmington Beach and Hanby Beach are located in this segment. Dune heights average 2.5 meters above MSL along this segment; beaches have a median sand grain size of 0.30 millimeter and an average beach profile slope of 1 on 30. The beaches along this shoreline remained relatively stable during the study period.

Fort Fisher, the southermost segment of shoreline studied, is approximately 6.25 kilometers long and extends southward from Kure Beach to just north of New Inlet (Figs. 4 and 5). The mean grain size of the beach sand is 0.27 millimeter and the average slope is approximately 1 on 36. The northern 1.6 kilometers of shoreline is a sandy beach, mostly undeveloped, which varies in width from 27 to 55 meters. This section remained relatively stable during the study period. The central stretch of beach contains the historic remains of a Confederate Army fortification known as Fort Fisher, which was built adjacent to New Inlet. Since the closure of this inlet in 1883, rapid erosion exposed an outcrop of coquina rock located adjacent to the remains of the fort (Fig. 1). The sandy beach fronting Fort Fisher varied in width from 0 to 45 meters during mean tide levels, and the sand bluff along the backshore continued to erode at a critical rate, thus requiring construction of an emergency rubble revetment. In July 1965, additional rubble was placed along both the northern and southern flanks; 11,500 cubic meters of sand was also placed along 213 meters of shore north of the revetment. In May 1967, an extratropical cyclone caused severe erosion to the 1965 emergency fill which required placement of another 11,500 cubic meters of sand along the same beach section. In 1970, further emergency measures were implemented by placement of a limestone revetment along a part of the upland bluff which had previously been protected by the beach fills. The southernmost 4.58 kilometers of shore is an accreting sandspit characterized by low topography and a sandy beach with widths between 60 and 275 meters.

The study area and the beach-fill projects are further described in Vallianos (1970), U.S. Army Engineer District, Wilmington (1970, 1974, and 1977), and Jarrett (1977).

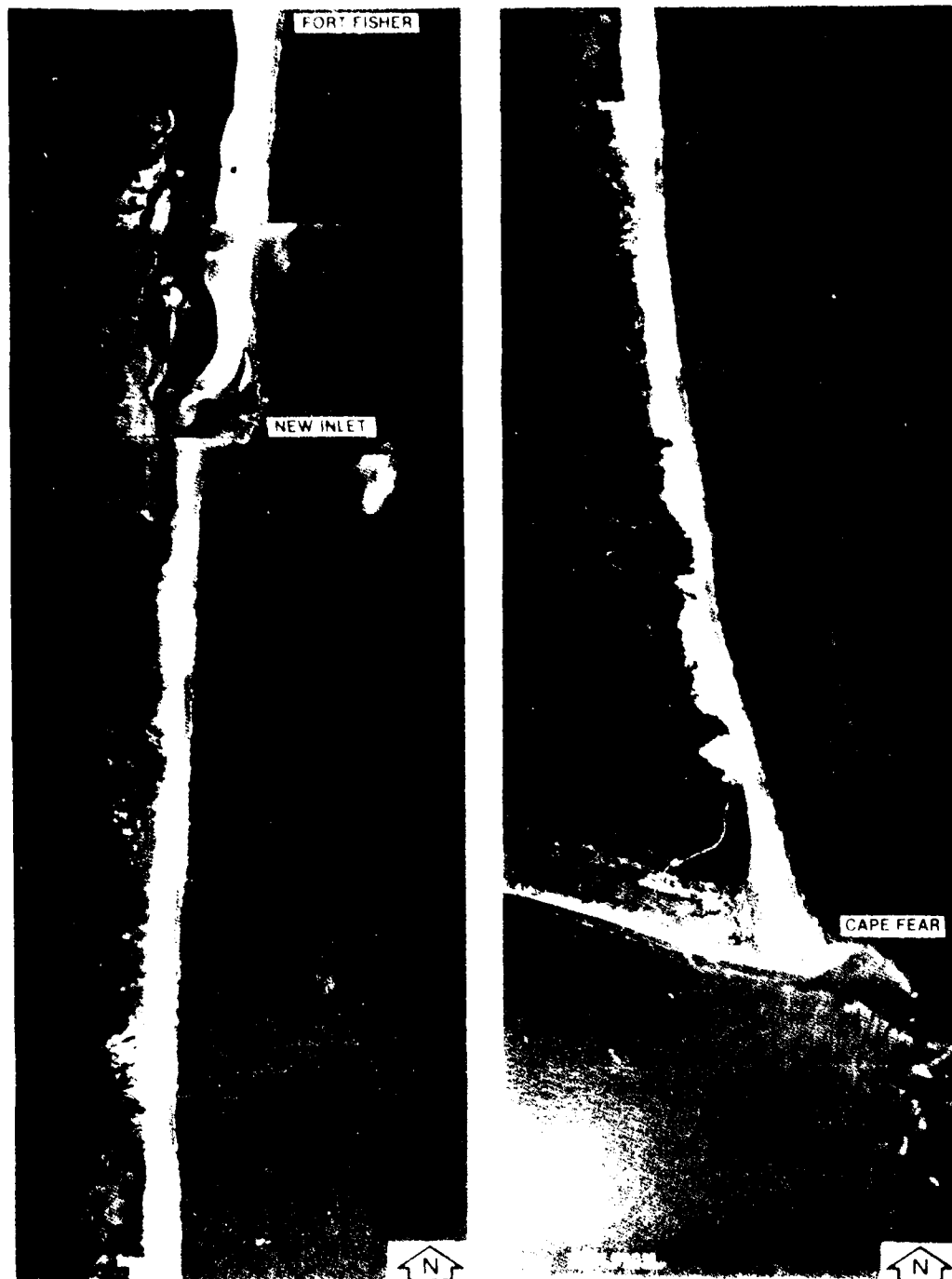


Figure 5. Aerial photo map of study area from Fort Fisher to Cape Fear, North Carolina.

III. DATA COLLECTION

1. Beach Profiles.

The sediment budget analysis performed in the study area was based on the beach profile data provided by CERC. Beach surveys were taken at 241 stations along the shoreline, and each profile was perpendicular to the local shoreline. The survey stations were numbered sequentially from north to south and were prefixed by the abbreviation of the corresponding beach name; e.g., WB for Wrightsville Beach (50 stations), MB for Masonboro Beach (31 stations), CB for Carolina Beach (119 stations), KB for Kure Beach (20 stations), and FB for Fort Fisher Beach (21 stations). Station CB2 would therefore represent the second station from the north in Carolina Beach. Figures 6 and 7 show the relative locations of all the stations.

The beach surveys were conducted by contractor for U.S. Army Engineer District, Wilmington, from 1963 to 1975. Most profiles were measured by level and tape and extended to only about 2.4 meters (8 feet) or less below MSL. These profiles were referred to as short profiles. Long profiles were measured to a depth of 12.2 meters (40 feet) using a depth sounder. Table 1 shows the survey stations, along with CERC's station reference codes, which indicates long profiles by the letter L.

About 2,952 repetitive beach profiles were taken during 399 surveys, including 2,815 short profiles and 137 long profiles. Table 2 shows the number of short and long profiles for each beach. Table 2 and Figures 6 and 7 show that Wrightsville and Carolina Beaches have much better temporal and spatial resolution than the rest of the study area. Of the entire beach data, 89 percent of the profiles were taken on Wrightsville and Carolina Beaches. The Fort Fisher Beach, Kure Beach, and Masonboro Beach profile data were of insufficient quantity to permit a valid analysis.

All data are available in supplementary data Volumes I to VIII from the CERC library.

2. Wave Data.

The wave climate data for the study area are from the following sources:

- (a) A CERC wave gage, located on Johnnie Mercer's Pier at Wrightsville Beach, which operated from March 1971 to February 1975. The gage was located in 5.2 meters (17 feet) of water, and the recorded wave data represent approximately all waves reaching Wrightsville Beach from all seaward directions. However, wave direction could not be differentiated by the gage. The wave gage data for this study with selected wave spectral plots are presented in supplementary data Volume I.

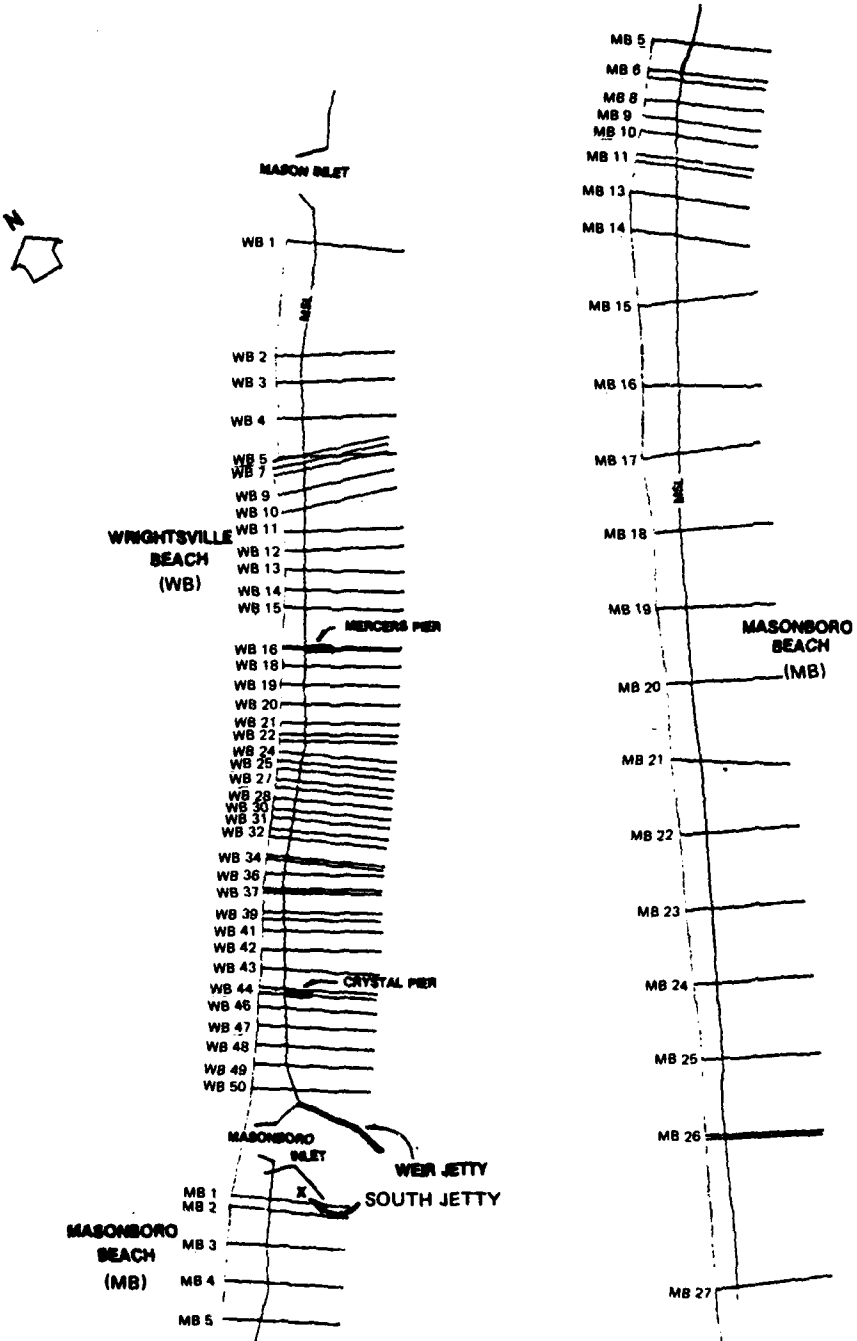


Figure 6. Profile station location map, WB1 to MB27.

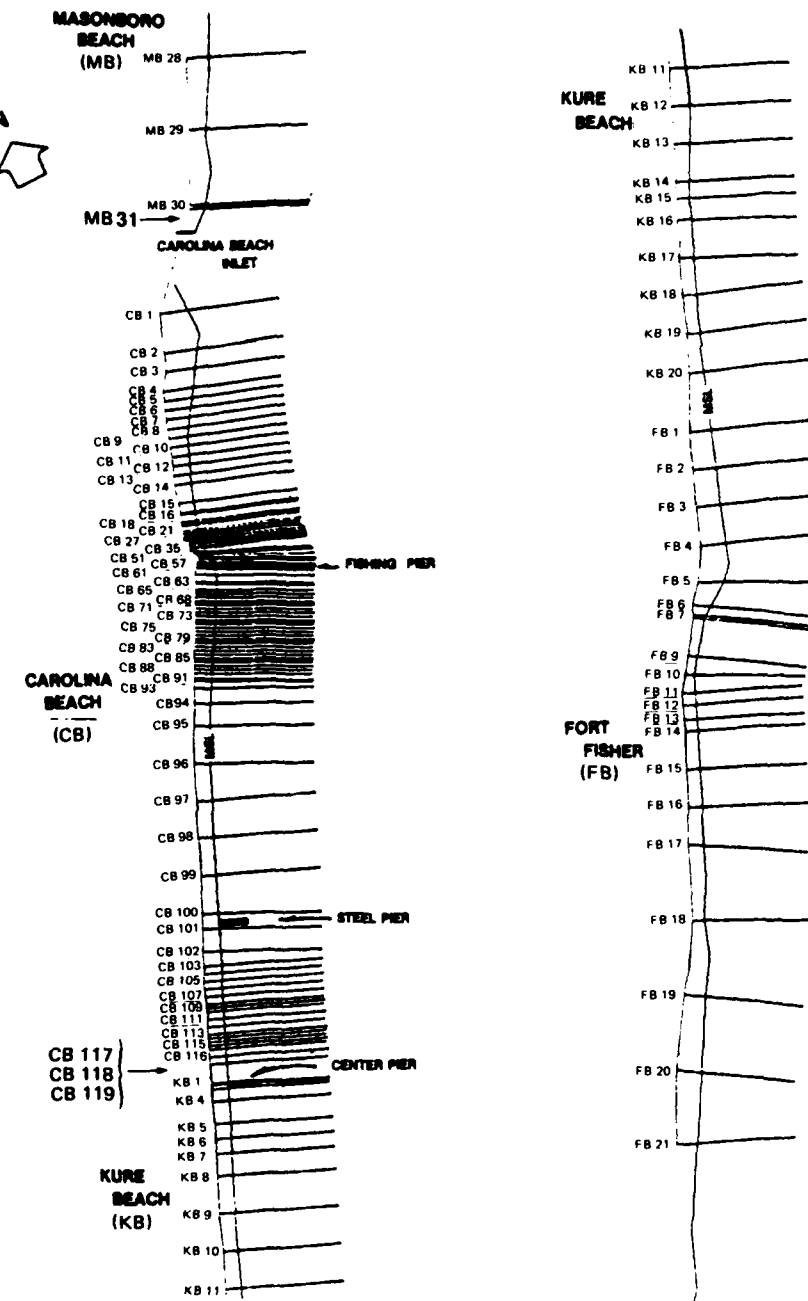


Figure 7. Profile station location map, MB28 to FB21.

Table 1. Cross references for beach profile data.

Profile	CBNC no.	Transsect distance (ft.)	Transsect bearing (degrees)	Profile bearing (degrees)	CBNC reference code	Profile	CBNC no.	Transsect distance (ft.)	Transsect bearing (degrees)	Profile bearing (degrees)	CBNC reference code
WB 1	227+02	0030	34.33	125.32	US044 WL017 15 1	WB 23	270+04	2020	18.03	110.70	WS026 WL009
WB 2	198+04	700	27.52	117.32	US043 WL016 15 2	WB 24	299+00	2000	20.17	111.73	WS027
WB 3	189+04	997	27.40	117.40	15 3	WB 25	310+02	1998	23.33	112.49	WS028 WL010
WB 4	179+02	999	27.38	117.50	US042 15 4	WB 26	330+00	100	23.42	112.42	
WB 5	169+00	104	34.22	117.48	US041	WB 27	331+00	3900	22.06	113.12	WS029
WB 6	168+04	250	47.77	104.00	15 5	WB 28	370+09	1899	19.43	109.45	WS030
WB 7	166+04	106	16.08	104.08	US040 WL015 15 6	WB 29	389+00	2902	19.67	109.67	WS031 WL011
WB 8	155+00	514	16.08	104.08	US037	WB 30	410+00	76	19.45	109.45	WL012
WB 9	157+00	406	16.37	104.37	US038 15 7	WB 31	410+00	2858	19.45	109.45	WS032
WB 10	155+00	540	20.32	104.37	US037	CB 1	199+00	999	35.73	104.05	CS052
WB 11	149+95	495	27.27	117.27	US034 15 8	CB 2	190+00	500	14.03	104.05	CS053 CL015
WB 12	145+00	400	27.27	117.27	US035	CB 3	185+00	500	14.03	104.05	CS054
WB 13	146+20	520	31.08	121.08	US034 15 9	CB 4	180+00	285	14.03	104.05	CS055
WB 14	133+00	479	31.08	121.08	US033	CB 5	177+50	250	45.33	104.03	177+50
WB 15	130+21	1025	31.16	121.16	US032 WL014 15 10	CB 6	175+00	250	14.03	104.05	175+00
WB 16	119+94	48	38.42	126.42	US031 15 11	CB 7	172+50	249	14.03	104.05	172+50
WB 17	119+28	428	38.42	126.42	US030 15 12	CB 8	170+01	251	14.03	104.05	CS047
WB 18	115+00	503	38.42	126.42	US029	CB 9	167+50	250	14.03	104.05	167+50
WB 19	109+97	497	38.42	126.42	US028 15 13	CB 10	165+00	250	14.03	104.05	CS048 142+50
WB 20	105+00	503	38.42	126.42	US027	CB 11	162+50	249	14.03	104.05	
WB 21	99+97	277	38.42	126.42	US026 WL013 15 14	CB 12	160+01	251	14.03	104.05	CS047 CL014
WB 22	97+00	260	38.42	126.42	US025	CB 13	157+50	249	14.03	104.05	157+50
WB 23	95+00	264	38.42	126.42	US024	CB 14	155+01	500	14.03	104.05	CS046
WB 24	92+36	239	35.28	125.28	US023	CB 15	150+01	251	14.03	104.05	CS045 CL013
WB 25	89+97	197	35.28	125.28	US022 15 15	CB 16	147+50	50	2.55	104.05	CS044
WB 26	88+00	300	35.28	125.28	US021	CB 17	147+00	199	14.03	104.05	147+00
WB 27	85+00	200	33.28	125.28	US020	CB 18	145+01	51	14.03	104.05	CS043 CL012
WB 28	80+00	284	35.28	125.28	US019	CB 19	144+50	50	14.03	104.05	144+50
WB 29	80+16	298	35.28	125.27	US018 WL012 15 16	CB 20	144+00	150	14.03	104.05	144+00
WB 30	77+10	210	35.37	125.27	US012	CB 21	142+50	50	14.03	104.05	CS042
WB 31	75+00	300	35.27	125.27	US016	CB 22	142+00	25	14.03	104.05	142+00
WB 32	72+00	202	35.27	125.27	US011	CB 23	141+75	50	14.03	104.05	
WB 33	69+98	470	35.77	125.77	US015 WL010 15 17	CB 24	141+25	23	14.03	104.05	CS043
WB 34	65+00	100	35.77	125.77	US014	CB 25	141+00	25	14.03	104.05	CS041
WB 35	64+00	400	35.77	125.77	US019	CB 26	140+75	50	14.03	104.05	CS044+00M
WB 36	60+00	400	38.83	126.83	US013 15 18	CB 27	140+25	25	14.03	104.05	CS043+00M
WB 37	54+00	100	38.83	126.83	US008	CB 28	140+00	75	14.03	104.05	CS040 CL011
WB 38	55+00	562	38.83	126.83	US012	CB 29	139+75	25	14.03	104.05	CS043+00M
WB 39	49+98	198	38.72	126.72	US011 15 19	CB 30	139+50	25	14.03	104.05	CS042+75M
WB 40	40+00	300	38.72	126.72	US007	CB 31	139+25	25	14.03	104.05	CS042+50M
WB 41	45+00	503	38.72	126.72	US010	CB 32	139+00	25	14.03	104.05	CS037
WB 42	39+97	474	30.59	129.59	US009 WL006 15 20	CB 33	138+75	25	14.03	104.05	CS037
WB 43	35+23	310	31.48	123.48	US008	CB 34	138+50	25	14.03	104.05	CS081+75M
WB 44	30+13	153	32.47	123.47	US007 WL005 15 21	CB 35	138+25	25	14.03	104.05	CS081+50M
WB 45	20+60	300	31.47	123.47	US006 15 23	CB 36	138+00	25	14.03	104.05	CS038
WB 46	25+00	470	32.47	123.47	US005	CB 37	137+75	25	14.03	104.05	CS081+25M
WB 47	20+02	562	32.47	123.47	US004 WL004 15 22	CB 38	137+50	25	14.03	104.05	CS081+75M
WB 48	15+00	500	32.47	122.43	US003 WL003	CB 39	137+25	25	14.03	104.05	CS080+50M
WB 49	10+00	650	32.43	122.43	US002 WL002 15 23	CB 40	127+00	15	14.73	108.03	CS037
WB 50	3+50	3160	40.23	121.70	US001 WL001 15 24	CB 41	136+85	10	14.73	108.03	+0.00FACE
WB 1	7+00	300	40.23	125.73	US004	CB 42	136+75	10	14.73	108.03	CS080+00
WB 2	10+00	1000	32.47	125.73	US005	CB 43	136+45	15	14.73	108.03	+0.00FACE
WB 3	20+00	1000	32.47	122.47	US006	CB 44	136+20	25	14.73	108.03	EDR04+75S
WB 4	30+00	1000	32.40	122.47	US007	CB 45	136+25	25	14.73	108.03	EDR04+50S
WB 5	40+00	800	32.40	122.47	US006	CB 46	136+00	25	14.73	108.03	EDR04+75S
WB 6	40+00	200	32.40	122.48	US009 WL001	CB 47	135+75	25	14.73	108.03	EDR01+90S
WB 7	50+00	570	32.40	122.40	US008	CB 48	135+50	25	14.73	108.03	EDR01+25S
WB 8	55+70	430	34.40	122.40	US001 WL002	CB 49	135+25	25	14.73	108.03	EDR01+50S
WB 9	40+00	600	34.40	124.40	US012	CB 50	135+00	25	22.00	110.02	CS034 CL010
WB 10	64+00	599	34.40	124.40	US013 WL003	CB 51	134+75	30	22.00	112.00	CS034
WB 11	49+99	291	34.42	124.40	US014	CB 52	134+50	25	22.00	112.00	CS035
WB 12	72+00	799	34.42	124.40	US015 WL004	CB 53	134+25	25	22.00	112.00	CS033
WB 13	79+97	1001	24.43	124.42	US016 WL005	CB 54	134+00	75	22.00	112.00	CS033
WB 14	90+00	2243	20.75	124.43	US017 WL006	CB 55	133+75	25	22.00	112.00	CS033
WB 15	110+00	1800	23.37	107.73	US018	CB 56	133+50	40	22.00	112.00	CS032
WB 16	130+99	1900	26.72	116.47	US017	CB 57	132+40	10	22.00	112.00	CS032
WB 17	149+99	2000	13.43	106.72	US020 WL007	CB 58	132+50	50	22.00	112.00	CS031
WB 18	170+00	2000	24.22	111.50	US021	CB 59	132+00	50	22.00	112.00	CS030
WB 19	190+02	2053	17.41	113.72	US022	CB 60	131+50	150	22.00	112.00	131+50
WB 20	210+00	2060	23.04	112.73	US023 WL006	CB 61	130+00	200	22.00	112.00	CS029 CL007
WB 21	230+00	2068	12.75	116.75	US024	CB 62	128+00	50	22.00	112.00	128+00
WB 22	230+00	1976	21.70	111.70	US023	CB 63	127+50	150	22.00	112.00	CS028

Note--Coastal structures at profiles WB17 (Johnnie Mercer's Pier), WB45 (Crystal Pier), CB42 (groin), and CB57 (fishing pier).

Table 1. Cross references for beach profile data--Continued.

Profile	CBNC No.	Transsect distance (ft.)	Transsect bearing (degrees)	Profile bearing (degrees)	CBNC reference code	Profile	CBNC No.	Transsect distance (ft.)	Transsect bearing (degrees)	Profile bearing (degrees)	CBNC reference code
CB 44	128+00	100	22.00	112.00	136+00	CB112	10+00	200	17.33	107.33	CB002 CL001
CB 45	125+00	100	22.00	112.00	C5027 CL008	CB113	0+00	100	17.20	107.20	C5007
CB 46	124+00	100	22.00	112.00	124+00	CB114	7+00	100	17.20	107.20	C5006
CB 47	123+00	50	22.00	112.00	123+00	CB115	6+00	100	17.20	107.20	C5005
CB 48	122+50	50	22.00	112.00	C5024	CB116	5+00	100	17.20	107.20	C5004
CB 49	122+00	100	22.00	112.00	122+00	CP317	4+00	200	17.20	107.20	C5003
CB 50	121+00	100	22.00	112.00	121+00	CP118	2+00	200	17.20	107.20	C5002
CB 51	120+00	100	22.00	112.00	C5023 CL007	CB119	0+00	503	16.65	107.20	C5001
CB 52	119+00	100	22.00	112.00	119+00	KB 1	5+00	47	16.65	108.65	KB001 -3+00 -3+00 CB-3+00
CB 53	118+00	50	22.00	112.00	118+00	KB 2	5+50	125	17.23	108.65	CPKBDL550
CB 54	117+50	50	22.00	112.00	C5024	KB 3	6+75	325	17.35	107.35	KB002
CB 55	117+00	100	22.00	112.00	C5024	KB 4	10+00	600	17.35	107.35	KB003 -10+00-10+00 CB-10+00
CB 56	116+00	100	22.00	112.00	116+00	KB 5	16+00	400	17.40	107.35	KB004 -15+00-15+11 CB-15+00
CB 57	115+00	100	22.00	112.00	C5023 CL006	KB 6	20+00	400	17.35	107.35	KB005 -20+00-20+16 CB-20+00
CB 58	114+00	100	22.00	112.00	114+00	KB 7	24+00	600	17.43	107.43	KB006 CL001
CB 59	113+00	50	22.00	112.00	C5013	KB 8	30+00	1000	17.40	107.40	KB007
CB 60	112+50	50	22.00	112.00	112+50	KB 9	40+00	995	17.40	107.40	KB008
CB 61	112+00	100	22.00	112.00	C5022	KB 10	49+99	1000	17.42	107.40	KB009 KL002
CB 62	111+00	100	22.00	112.00	C5011	KB 11	59+99	1000	17.40	107.40	KB010
CB 63	110+00	100	22.00	112.00	C5021 CL003	KB 12	69+99	1000	17.40	107.40	KB011
CB 64	109+00	100	22.00	112.00	C5019	KB 13	79+99	995	17.37	107.35	KB012 KL003
CB 65	108+00	50	22.00	112.00	108+00	KB 14	89+98	438	17.38	107.38	KB013
CB 66	107+50	50	22.00	112.00	107+50	KB 15	94+36	542	18.78	107.35	KB014
CB 67	107+00	100	22.00	112.00	C5017	KB 16	99+92	1000	18.78	108.78	KB015
CB 68	106+00	100	22.00	112.00	106+00	KB 17	109+98	1000	14.68	108.78	KB016 KL004
CB 69	105+00	100	22.00	112.00	C5020	KB 18	119+98	1000	13.67	103.65	KB017
CB 70	104+00	150	22.00	112.00	104+00	KB 19	129+98	1000	13.67	103.68	KB018
CB 71	102+50	50	22.00	112.00	102+50	KB 20	139+98	1545	20.25	103.67	KB019
CB 72	102+00	199	22.00	112.00	102+00	FB 1	52+00	1000	14.77	104.77	FB001
CB 73	100+01	401	20.87	110.87	C5019 CL004	FB 2	53+00	1000	14.75	104.77	FB002 FL001
CB 74	96+00	600	20.87	110.87	96+00	FB 3	54+00	1011	14.85	104.65	FB003
CB 75	90+00	1000	20.87	110.87	C5018	FB 4	55+01	1000	25.63	104.65	FB004
CB 76	86+00	1005	17.43	110.87	C5017	FB 5	56+017	422	36.65	110.65	FB005 FL002
CB 77	70+00	995	17.12	107.12	C5016 CL003	FB 6	56+6+39	292	18.67	116.45	FB006
CB 78	69+02	1003	17.17	106.95	C5013	FB 7	56+6+91	99	24.32	116.45	FB007
CB 79	59+99	995	19.33	106.95	C5014	FB 8	56+9+90	1000	26.32	116.45	FB008
CB100	40+03	403	20.40	110.40	C5013 CL002	FB 9	57+9+90	500	23.80	116.32	FB009
CB101	36+00	579	20.40	110.40	C5012	FB 10	58+4+90	505	23.89	111.21	FB010
CB102	30+01	485	19.57	110.40	C5011	FB 11	58+9+93	309	16.30	106.30	FB011 FL003
CB103	26+00	200	17.33	107.33	26+00	FB 12	59+3+02	400	16.78	106.30	FB012
CB104	24+00	200	17.33	107.33	24+00	FB 13	59+7+02	300	17.33	106.78	FB013
CB105	22+00	199	17.33	107.33	22+00	FB 14	60+0+02	999	17.53	106.78	FB014
CB106	20+01	201	17.33	107.33	C5010	FB 15	61+0+01	999	16.20	107.53	FB015
CB107	18+00	200	17.33	107.33	18+00	FB 16	62+0+00	1004	16.37	105.20	FB016
CB108	16+00	100	17.33	107.33	16+00	FB 17	63+0+04	1990	16.64	114.18	FB017
CB109	13+00	100	17.33	107.33	C5009	FB 18	65+6+03	1995	26.10	110.60	FB018 FL004
CB110	14+00	200	17.33	107.33	14+00	FB 19	66+9+97	2004	26.00	116.12	FB019
CB111	12+00	200	17.33	107.33	12+00	FB 20	69+0+03	1990	20.00	116.02	FB020
						FB 21	71+0+00		106.00	FB021 FL005	

Note--Coastal structures at profiles CB101 (Fisherman's Steel Pier) and KB2 (Center Pier).

Table 2. Repetitive short and long profiles measured along the study area.

Beach	First survey (yr)		Last survey (yr)		Ranges (No.)		Profiles (No.)		Surveys (No.)
	Short	Long	Short	Long	Short	Long	Short	Long	
Wrightsville	1963	1965	1974	1970	50	17	1,562	39	310
Masonboro	1964	1969	1973	1971	31	12	93	23	14
Carolina	1965	1967	1973	1971	119	15	956	62	81
Kure	1969	1969	1973	1970	20	4	101	8	17
Fort Fisher	1969	1970	1973	1970	21	5	103	5	8

- (b) Visual observations by U.S. Coast Guard personnel from the Frying Pan Shoals Light Tower. The wave data with the monthly wave statistics were provided by CERC.
- (c) Long-term deepwater wave statistics provided in the Summary of Synoptic Meteorological Observations (SSMO) (U.S. Naval Weather Service Command, 1975).
- (d) CERC's wave observation program at Wrightsville Beach provided visual observations of wave conditions, recorded daily at Johnnie Mercer's Pier between June 1970 and December 1973. CERC provided the monthly statistical analysis of these shore-based wave observations including breaking wave height, period, and direction. The wave data collected at Wrightsville Beach during the study period are available in supplementary data Volumes II, III, and IV.

3. Beach Sand Data.

Beach sand data for certain profiles within the study area from 1969 to 1971 were provided by CERC. Samples were collected along the profile azimuth from the dune crest, the berm, and at MHW, MSL, MLW, -1.8 meters (-6 feet) (MLW), -3.66 meters (-12 feet) (MLW), and -5.49 meters (-18 feet) (MLW). Frequency of sand sample collection was not consistent from beach to beach or from profile to profile. The sand was analyzed for basic engineering properties including grain-size distribution, median grain size, standard deviation, fall velocity, and composition. Grain-size analyses are summarized in Table 3. The complete sand data are presented in supplementary data volumes for each beach segment (except for Kure Beach).

Table 3. Beach sand grain-size data.

Station	MHW		MSL		MLW	
	1	2	1	2	1	2
WB15	2.28	0.29	2.18	0.32	2.02	0.50
WB16	1.67	0.72	1.59	0.90	1.77	0.88
WB19	2.09	0.34	2.09	0.35	2.20	0.38
WB25	1.69	0.52	1.31	0.70	1.13	1.07
WB29	1.56	0.82			2.19	0.59
WB42			2.10	0.70	2.61	0.50
WB47	1.09	0.72	1.07	0.85	1.38	0.97
WB50	2.18	0.36	2.19	0.57	2.05	0.68
MB4	2.24	0.28	2.06	0.45	1.91	0.63
MB14					2.00	0.49
MB20	0.83	0.61	1.53	0.72	1.56	0.95
MB23	1.16	0.49	1.33	0.46	1.22	0.76
MB26	0.89	0.77	1.33	0.56		
MB29	1.83	0.44			0.76	0.67
CB1					1.60	0.62
CB3					1.47	0.62
CB12	1.52	0.43	1.19	0.63	1.46	0.47
CB61	1.76	0.30	1.20	0.35	0.82	0.40
CB77			0.79	0.37	1.33	0.47
CB97	1.36	0.38	0.95	0.51	0.84	0.33
CB112	1.51	0.38	1.66	0.31	0.80	0.60
FB11	2.04	0.30	1.95	0.53	2.28	0.64
FB18	1.73	0.37	1.21	0.57	1.61	0.55

¹ = mean value of ϕ .

² = standard deviation of ϕ .

NOTE-- $\phi = -\log_2 D$, where D = sand diameter in millimeters.

IV. ANALYSIS OF BEACH PROFILE DATA

1. Excursion Distance Technique.

If successive aerial photos of a beach face are compared with each other and a change in location of the beach is noted, then this change is indicative of either a period of erosion or accretion. Horizontal displacement of the planform position of any one point on the beach, from one survey to another, is the excursion distance for that point for the survey period. On an accreting beach, the excursion distance of a point relative to its initial position is positive, and on an eroding beach, it is negative. The rate of change of the excursion distance with time is the excursion rate.

If successive beach profiles are reduced to a common base line, the excursion distance of each point on the profile indicates the magnitude of the onshore-offshore movement. The relative magnitude of the excursion distances between two or more points on the same profile identifies and quantifies the change in beach slope between those points. Beach excursions can be converted to volumetric changes for the entire active profile by applying to the excursion distances a volumetric equivalent factor. This factor was developed from measured changes at two piers located along Wrightsville Beach (U.S. Army Engineer District, Wilmington, 1977), which showed that for a closure depth of approximately 8.23 meters, each meter of excursion was equivalent to 8.23 cubic meters of change for the entire active profile per meter of beach front. Equivalently in English units, for a closure depth of 27 feet, each foot of excursion was equivalent to 1 cubic yard of change for the entire active profile per foot of beach front. Consequently, excursion distance analysis is a simple but powerful technique which is used to identify and quantify both long-term beach changes and the response of a beach to short-term impacts resulting from storm activity, beach fills, and other man-induced changes.

2. Historical Events Affecting Excursion Distance Analysis.

Meaningful interpretation of excursion distance plots can only be performed if known short-term or sudden impact events are identified and accounted for within the analysis. In order to do this, all major erosion-causing storms and all man-related activities which cause erosion-accretion during the study period must be abstracted from the historical records.

Table 4 lists all beach-fill changes reported along the study area beaches from 1965 to 1974. The initial fill excursion distances in the table were estimated by applying the volumetric equivalent factor of 8.23 cubic meters of change for each meter excursion per meter beach

Table 4. Beach-fill evaluation.¹

Beach	Date	Location ² (ft.)	Profile station	FILL length (ft.)	FILL volume (cu. ft.)	FILL excavation distance (ft.)	Vol. sorting logistics (cu. ft.)	Excav. loss (cu. ft.)	Net volume (cu. ft.)	Net excavation distance (ft.)	Comments
Wrightsville											
	Spring 1965	1.9-7.0	1819-1820	5,130	2,290,071	54.6					Completion of 18' jetty in spring 1965
	Spring 1966	3.35-6.1	1819-1825	2,750	244,000	10.8	331,600	-7.9	2,224,700	+46.7	
	Oct. 1966	3.35-4.0	1819-1821	650	32,136	6.5					
	Spring 1970	2.75-4.6	1815-1821	1,850	1,053,600	69.2	573,856	-37.7	480,000	+31.50	
Carolina											
	Apr. 1965	22.35-26.5	C816-C815	4,275	2,013,854	57.2	617,250	-25.0			+32.2
	Mar. 1967	21.75-22.25	C812-C816	500	83,400	20.3					
	Mar. 1967	22.25-23.5	C818-C825	1,220	231,075	23.0	157,240	-11.1	157,250	+10.5	
	May 1967	23.0-23.7	C871-C863	700	88,000	15.3	26,800	-4.7			+11.6
	Aug. 1968	23.0-23.7	C871-C863	700	74,200	12.9	0				No sorting losses
	Dec. 1970	22.25-23.5	C816-C825	1,220	265,000	26.4	52,000	-5.2	213,000	+21.2	
	Dec. 1970	22.25-22.6	C816-C824	335	—	—	0				Completion of rubble-and-seawall
	May 1971	23.0-26.5	C871-C815	3,500	316,000	11.0	0				Extension of rubble-and-seawall
	Sept. 1973	22.6-22.9	C854-C864	300							
Port Fisher											
	July 1965	32.7-33.0		220	11,300	6.4					Additional rubble added to revetment
	Oct. 1967	32.7-33.0		220	11,500	6.4					Beach fill placed along eroding bluff
	1970	32.7-33.0									Severe loss to 1965 beach fill due to May 1967 extratropical cyclone
											Limestone revetment added

¹Data from U.S. Army Engineer District, Wilmington (1970, 1974) and Jarrett (1977).²Distances from northern end of study area (MHI).

front. The excursion loss due to sorting was determined in the same manner from estimates on the volume of beach fill lost due to sorting or from volumetric loss calculations based on the critical ratios of the beach-fill material. Note that the initial fill distance, the excursion loss (due to sorting), and the net fill excursion are only comparison estimates and should not be considered as absolute values. Figure 8 shows the spatial distribution of the beach-fill excursions along the study area, with an obvious concentration of fill activity in front of the townships of Wrightsville Beach and Carolina Beach. Areas of reported net beach fill are shown to extend in some places to approximately 100 meters (300 feet). Because these values only reflect the fill excursion remaining after the initial loss period and do not consider the fill loss due to storm-induced or long-term (annual) erosion rates, they are slightly misleading. Most fills were placed after the previous fill had been severely eroded away.

Table 5 presents all historical events influencing beach volumes since 1965, with a brief description of each event. Storms were included in this table only if noted beach erosion occurred, if associated storm surge was noted, or if the windspeeds were in excess of 80 kilometers per hour (50 miles per hour). A complete list of all storms during the study period is available in supplemental data Volume I, Section B.

3. Excursion Distance Analysis.

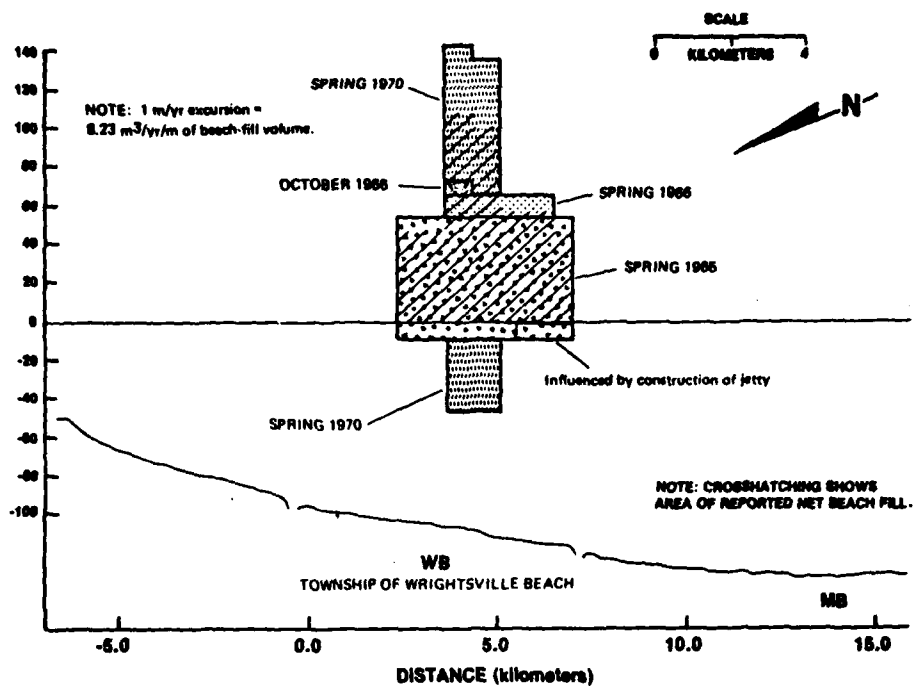
Selected beach profiles from all stations were plotted at a small scale and visually checked for accuracy and acceptability of data points. Larger scale profiles were then drawn to compare sequential outlines. Areas of erosion from one sequential profile to the next were highlighted by a dot-screen pattern. Typical short and long beach profile plots are shown in Figures 9 and 10. All of the larger scale plots of the short and long beach profiles are contained within supplemental data Volumes II to VIII.

A common base line was established for each sequential profile and the horizontal distance from that base line to the location of the MHW, MSL, MLW, -1.83 meters (-6 feet), -3.66 meters (-12 feet), and -5.49 meters (-18 feet) contours were calculated. These distances were plotted against time of measurement, and the relative distance between the first and subsequent distances represents the excursion distance through time for each contour.

A sample plot from each beach is shown in Figures 11 to 15. A linear regression ("least squares") line which mathematically "best fits" all data points is drawn on these plots. One straight line is not representative of the average excursion rates between the years 1965 and 1975, especially for Wrightsville and Carolina Beaches.

When few data points exist, the scatter due to seasonal fluctuations, prior storm erosion, etc., can totally mask the longer term or

APPROX. EXCURSION DISTANCE OF HISTORIC BEACH FILLS.



APPROX. EXCURSION DISTANCE OF HISTORIC BEACH FILLS.

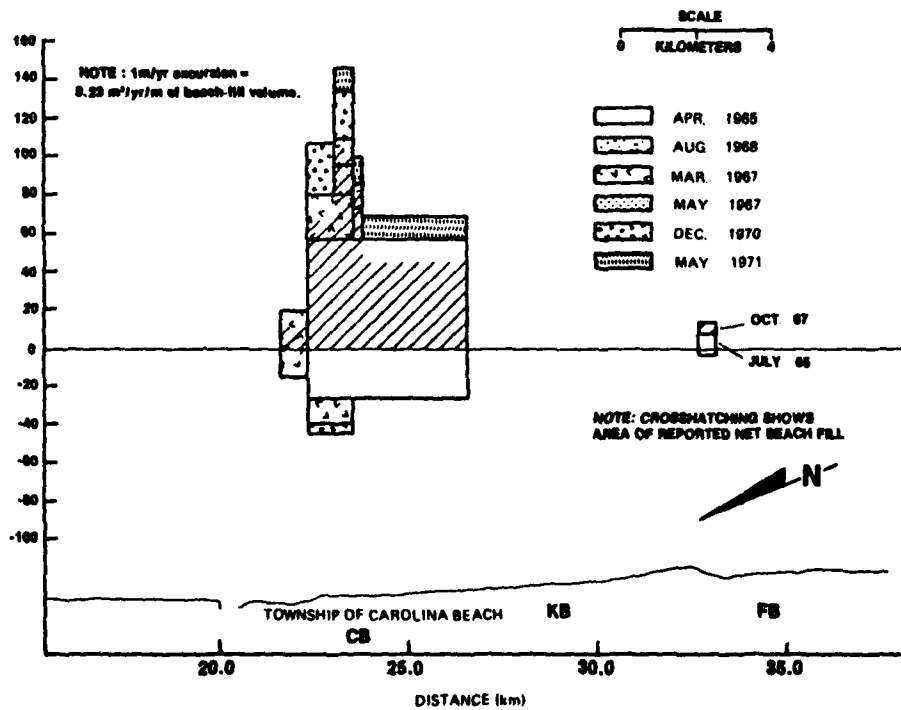


Figure 8. Distribution of beach fills along study area.

Table 5. Historical events affecting beach volumes during study period, 1965-1975.

Date	Location	Comments
1965 Spring Apr. 24 May July	Wrightsville Beach Carolina Beach Fort Fisher Beach	Beach fill 1.9-7.0 km; 47-m net excursion Beach fill 22.2-26.5 km; 32-m net excursion Storm; high wind, rain, beach erosion Beach fill and revetment 32.7-33.0 km; 6.5-m net excursion
1966 Spring Spring 10-11 June 9 July Oct.	Wrightsville Beach Masonboro Inlet Wrightsville Beach	Beach fill 3.4-6.1 km; 10-m net excursion Completion of Masonboro jetty Tropical Storm Alma passed offshore Storm; 147-km/h (92 mi/h) winds Beach fill 3.4-4.0 km; 6.5-m excursion
1967 Mar. 15 Mar. 29 May Oct. 24 Nov. 28 Dec.	Carolina Beach Fort Fisher Beach	Beach fill 21.7-23.5 km; 10.5 m net excursion Storm; 71-112 km/h (45-70 mi/h) winds Extratropical cyclone; severe erosion Beach fill 32.7-33.0 km; 6.5-m excursion Storm; 96-km/h (60 mi/h) winds Storm; 122-km/h (76 mi/h) winds
1968 7-12 June Aug. 19-20 Oct.	Carolina Beach	Tropical Storm Abby Beach fill 23.0-23.7 km; 13-m net excursion Hurricane Gladys
1969 1-2 Nov.		Storm; 96-km/h (60 mi/h) winds
1970 Mar.-May	Wrightsville Beach	Beach fill 2.7-4.6 km; approx. 31.5-m net excursion
16-17 Aug. 30-31 Oct. Dec. Dec.	Carolina Beach Carolina Beach Fort Fisher Beach	Storm; 2.5-m (8 ft) waves, riptides; 112-km/h (70 mi/h) winds Storm; beach erosion Beach fill 22.2-23.5 km; 21-m net excursion Completion of rubble-mound seawall Limestone revetment added
1971 26-30 Jan. 13 Feb. 5-7 Apr. Mar.	Carolina Beach	Storm; near hurricane-force winds Storm; near hurricane-force winds Storm; 109-km/h (68 mi/h) winds Beach fill approx. 23.0-26.5 km; 11-m net excursion
16-18 Aug. 27 Aug. Oct.		Storm; 3-m (10 ft) seas Tropical Storm Dora; 96-km/h (60 mi/h) winds, 1.2-m (4 ft) surge Hurricane Ginger; 147-km/h (92 mi/h) winds, 1.2-m (4 ft) surge
1972 24 July		Storm; 83-km/h (52 mi/h) winds
1973 9-10 Feb.		Storm; 80-km/h (50 mi/h) winds, high seas, erosion
22 Mar. Sept.	Carolina Beach	Storm; 3-4-m (10-12 ft) seas, high erosion Extension of rubble-mound seawall
1974 30 Nov.-1 Dec.		Storm; erosion

NOTE: Dates of beach fills, coastal construction, etc. are given only as month or season in which they were completed. Dates of storms are given as calendar date.

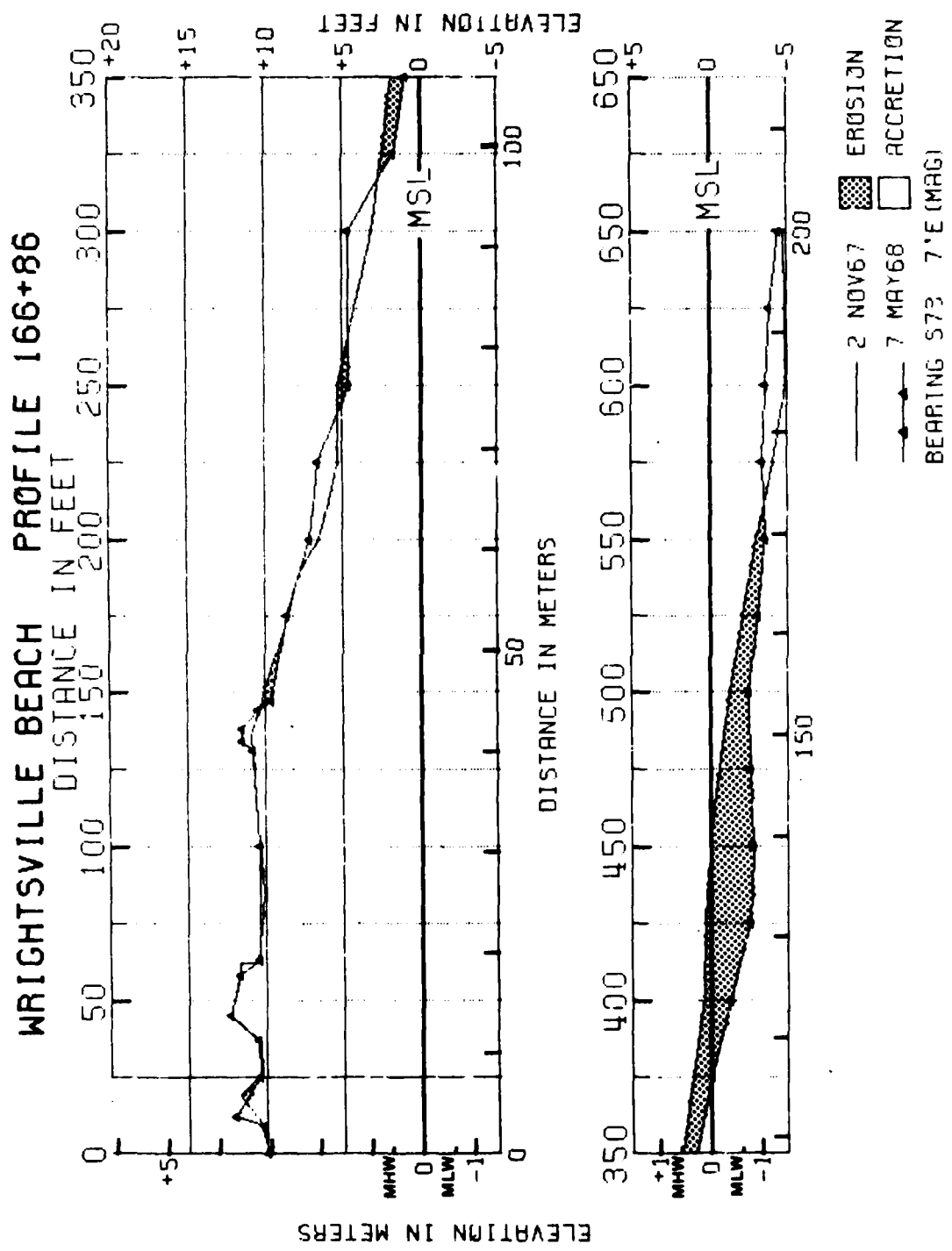


Figure 8. Comparative shore profiles, Wrightsville Beach.

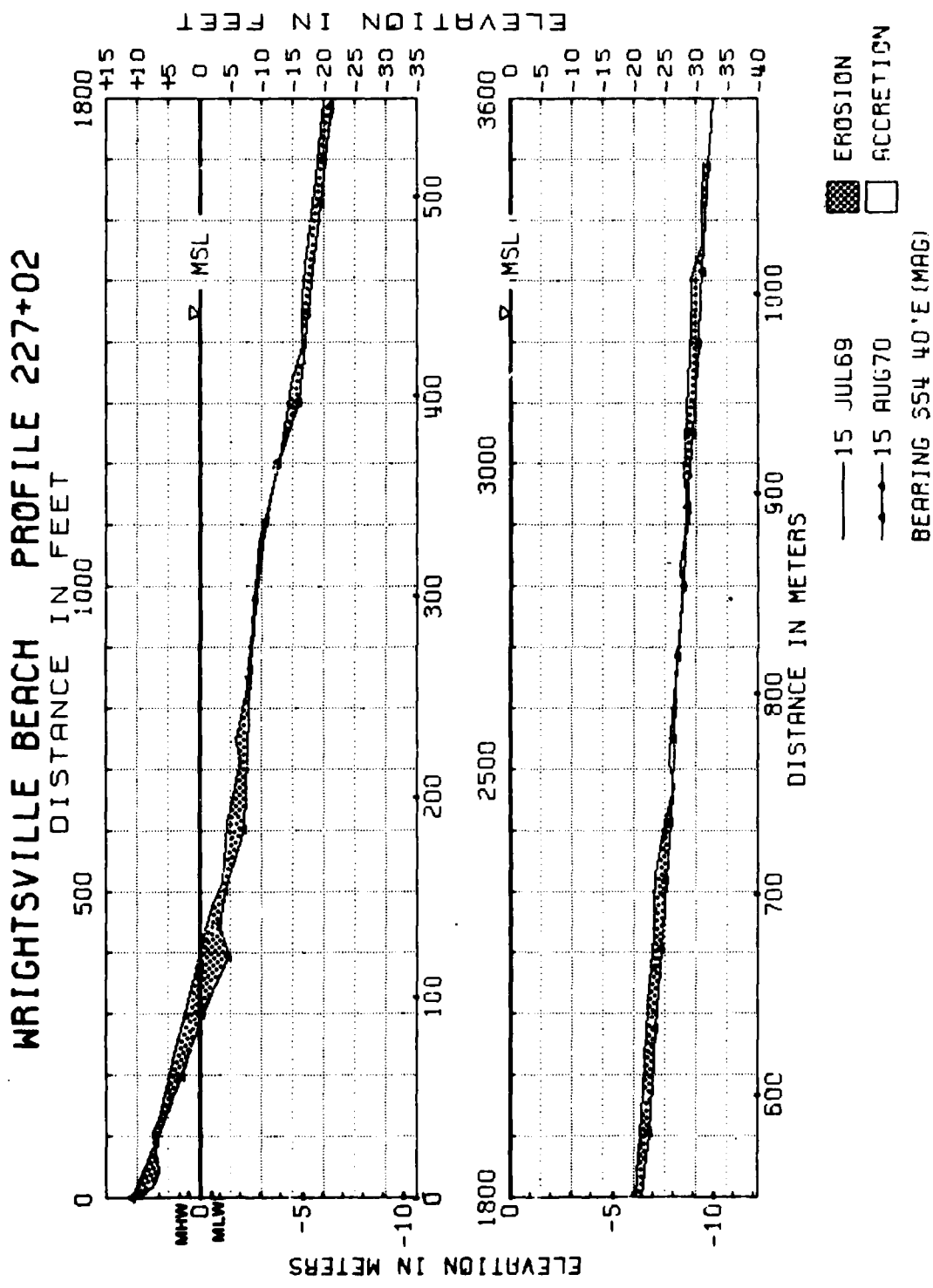


Figure 10. Comparative long profiles, Wrightsville Beach.

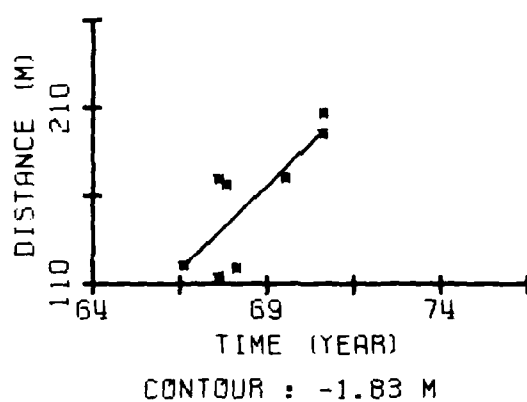
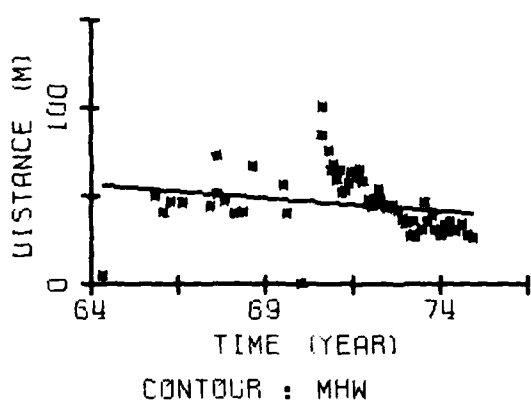
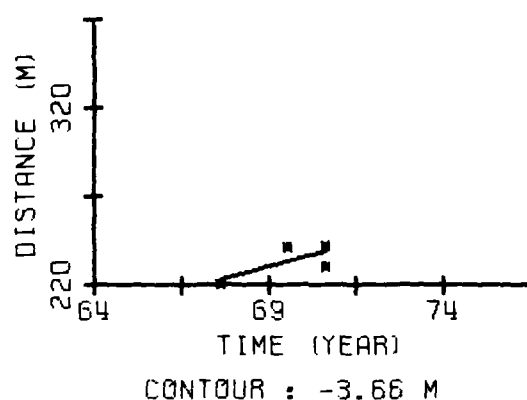
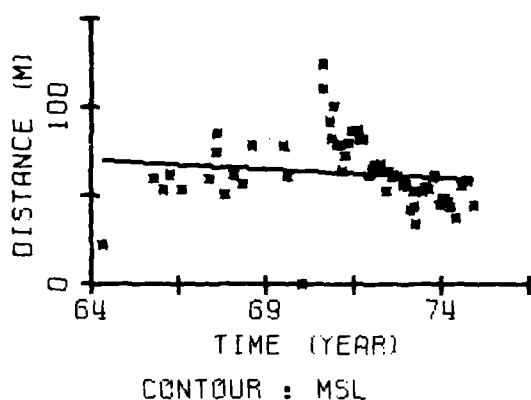
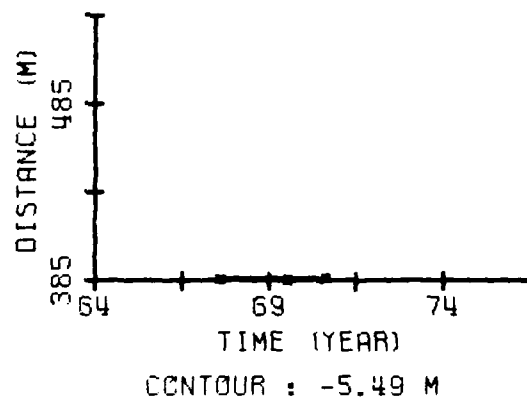
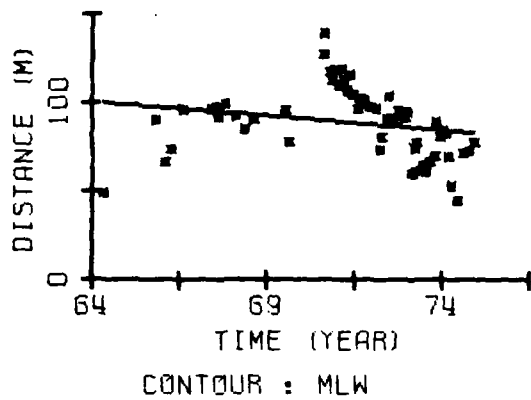
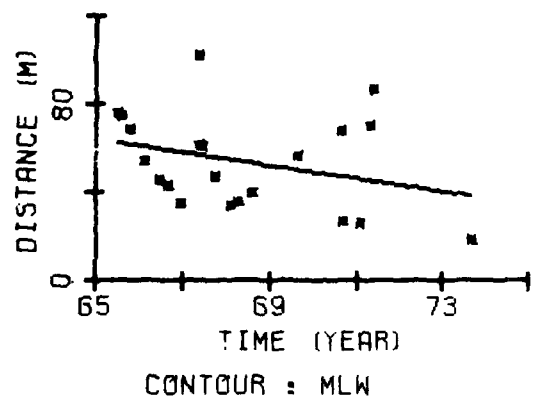
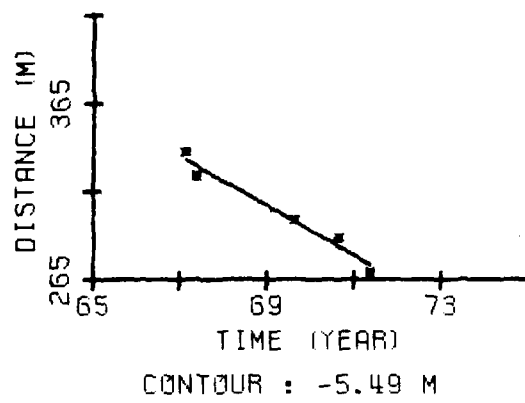


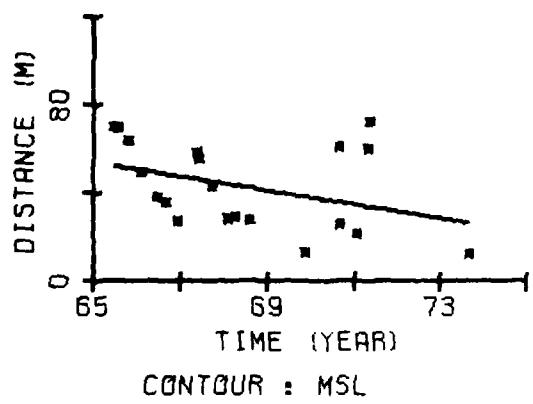
Figure 11. Distance from the base line to stated contours at WB 15.



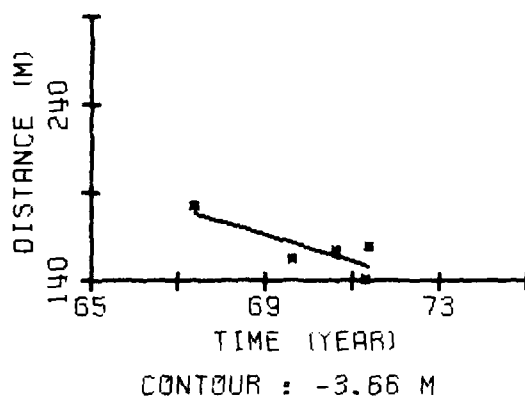
CONTOUR : MLW



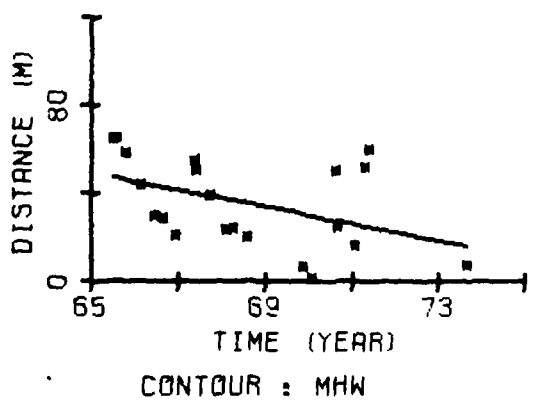
CONTOUR : -5.49 M



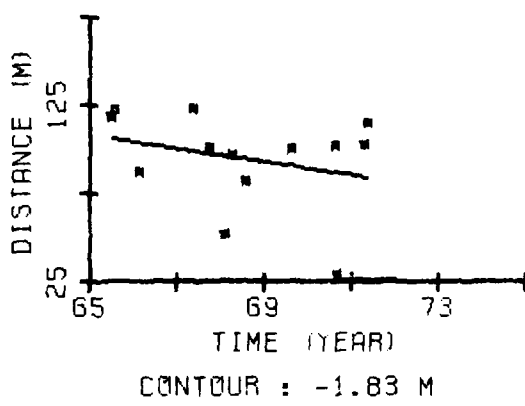
CONTOUR : MSL



CONTOUR : -3.66 M



CONTOUR : MHW



CONTOUR : -1.83 M

Figure 12. Distance from the base line to stated contours at CB 71.

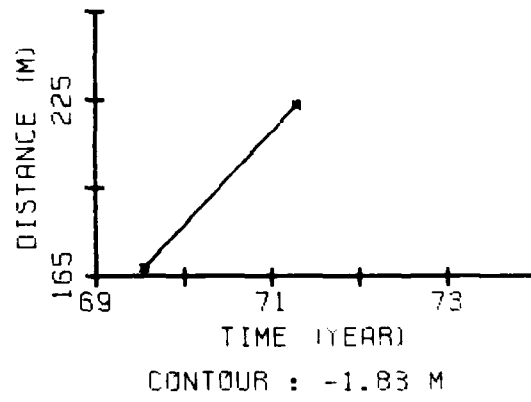
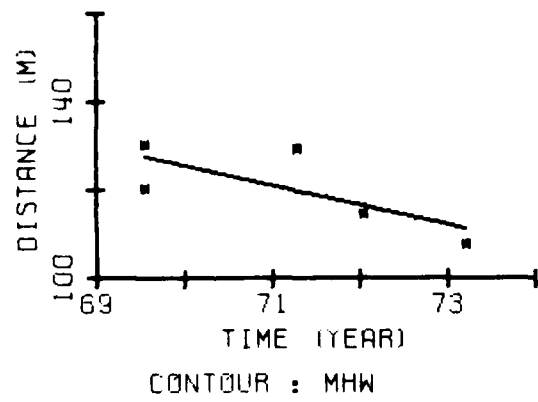
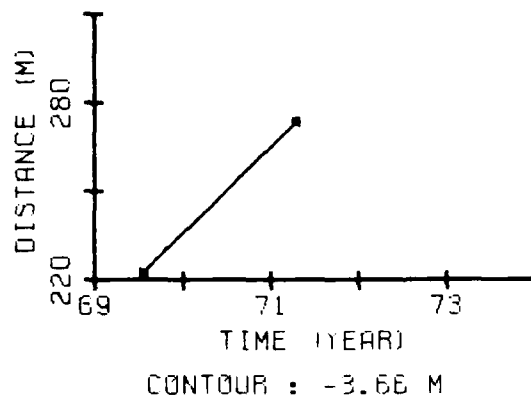
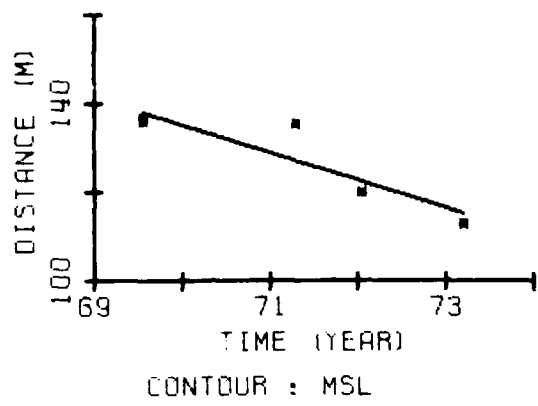
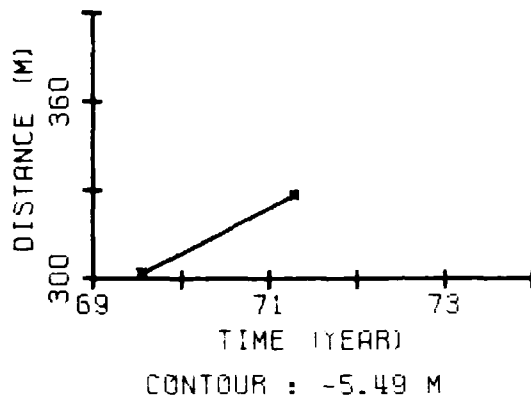
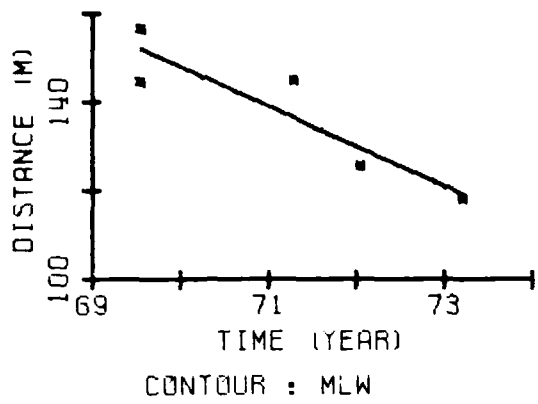


Figure 13. Distance from the base line to stated contours at MB 17.

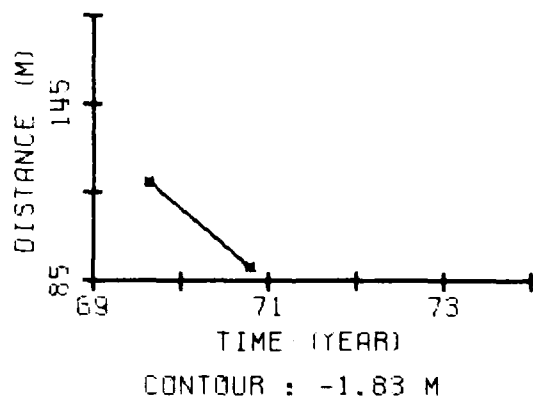
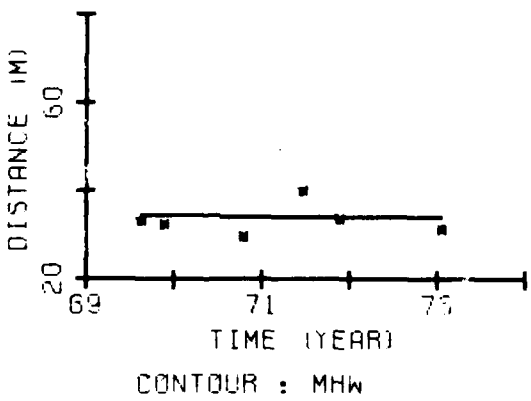
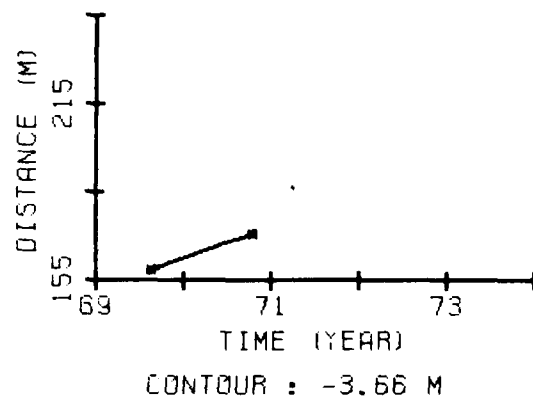
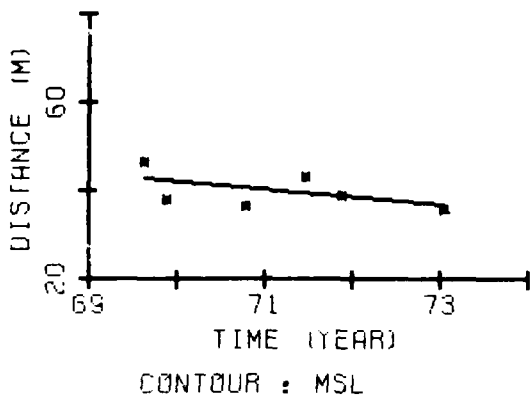
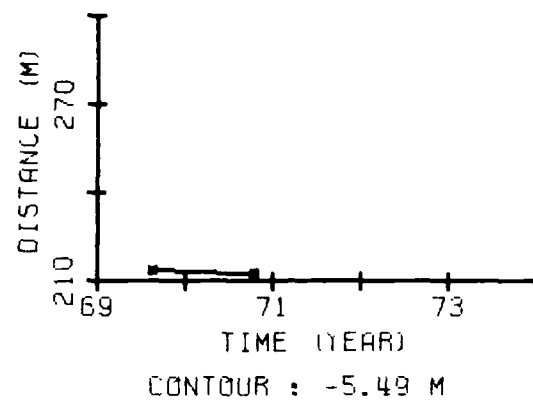
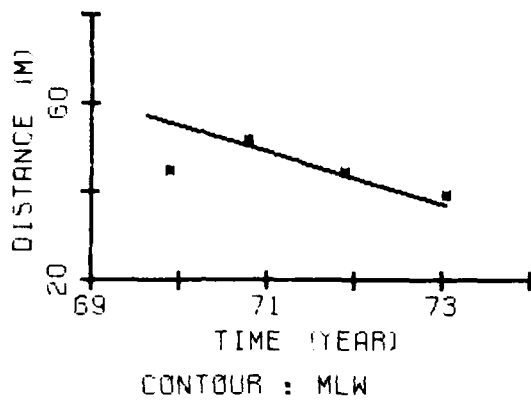


Figure 14. Distance from the base line to stated contours at KB 17.

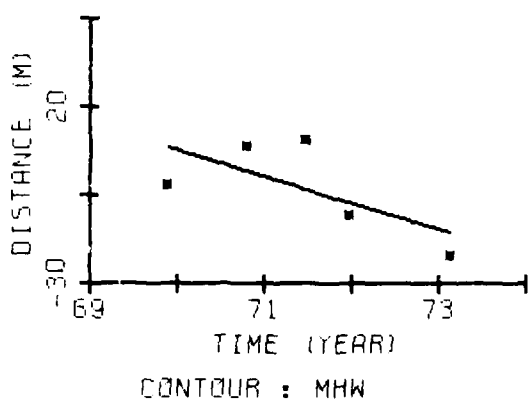
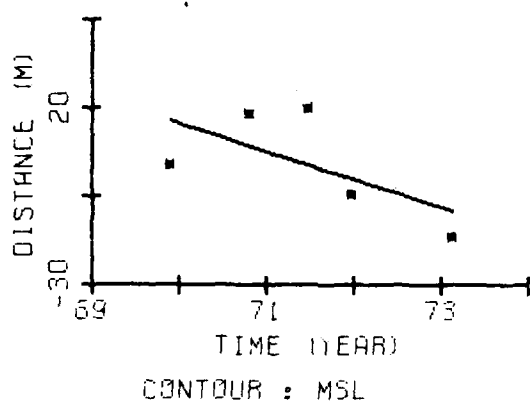
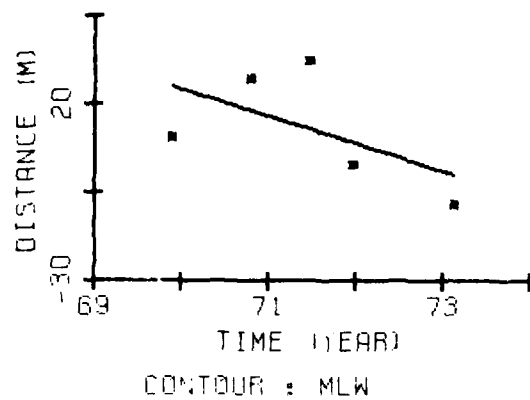


Figure 15. Distance from the base line to stated contours at FB 10.

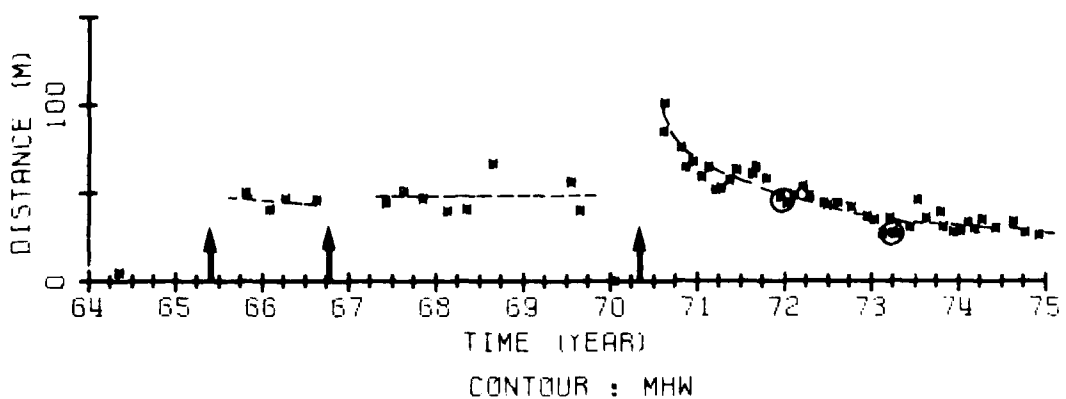
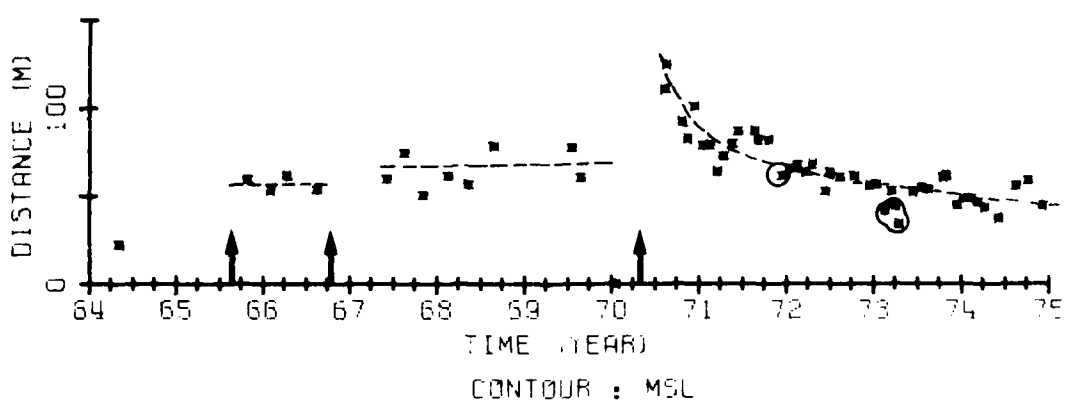
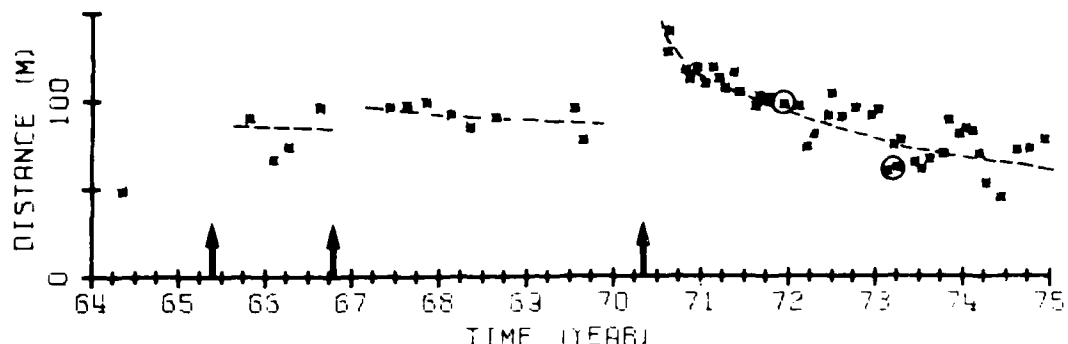
man-influenced excursion rates. The plots (Figs. 11 to 14) are, in one way, atypical of all profile plots taken along each beach because each of these profiles has some data taken below MLW, whereas the majority of profiles along the entire study area do not. This means that analysis of contours below MLW is not worthwhile due to the paucity of data, and that available data can result in misleading or questionable excursion rates. Only Wrightsville and Carolina Beaches have high temporal densities of data points for each MHW, MSL, and MLW contour and, consequently, only plots from these beaches were redrawn at yet a larger scale and analyzed. All large-scale plots for Wrightsville Beach and a representative set from Carolina Beach are contained in Appendixes A and B, respectively; all smaller scaled plots for Masonboro, Kure, and Fort Fisher Beaches are in Appendixes C, D, and E, respectively.

Historic events which may have affected the beach erosion-accretion (excursion distance) are indicated on each excursion distance plot for Wrightsville and Carolina Beaches (Figs. 16 and 17). A circle is placed on a data point measured shortly after localized storm activity (see Table 5), and an arrow is placed at the approximate time beach fills were completed. The same profiles in Figures 11 (WB15) and 12 (CB71) are shown in Figures 16 and 17, respectively, drawn at the larger time scale and with the historic events indicated. Excursion rates between the beach fills (seasonally averaged response shown as a dashline) can now be identified and quantified. Localized storms account for many of the sudden losses in beach volume. However, some erosion (loss of excursion distance) occurs at times other than those indicated in Table 5, possibly due to localized storms of lesser magnitude, but probably due to erosion from swell waves generated from distant storms.

Sequential beach profiles taken between January 1970 and December 1974 for profile WB15 are presented in Appendix F. These profiles are presented to aid the reader in visualizing the postfill response of Wrightsville Beach and thus to help interpret the results shown in Figure 16.

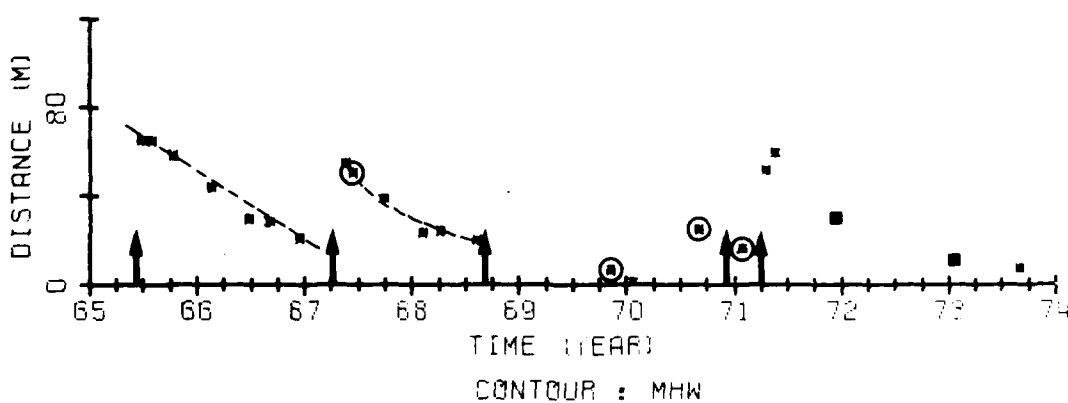
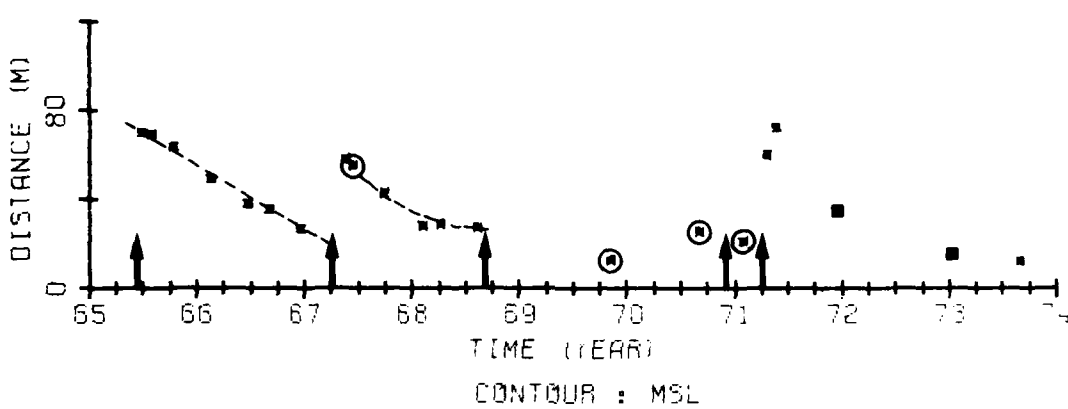
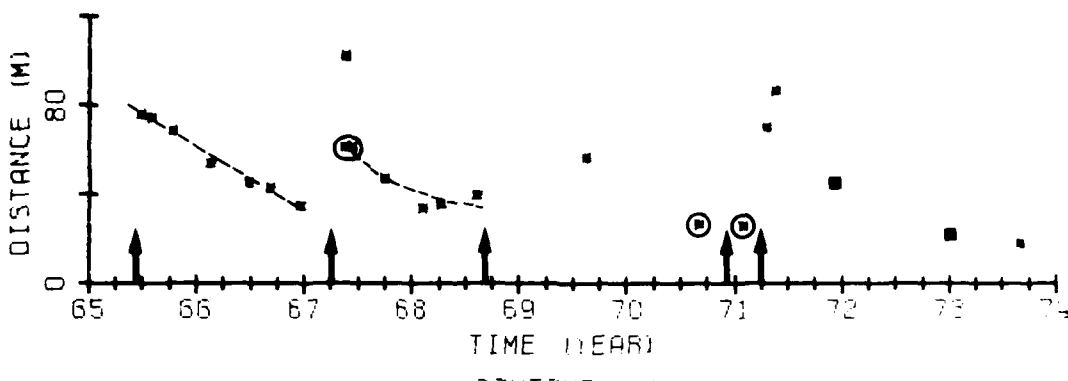
The following discussion outlines the general method of analysis used on all excursion distance plots for Wrightsville and Carolina Beaches. A schematic plot, similar to the MLW excursion distance plot for WB15 (Fig. 16), is used as an example and is shown as Figure 18. Section IV.4 contains a beach-by-beach discussion and quantification detailing the effect of natural and manmade influences on each.

The three most prominent features exhibited by Figures 16 to 18 are: (a) the long-term erosional-accretional trend is approximately constant (linear) between beach-fill periods with minor fluctuations due to seasonal storm-induced erosion and accretion cycles; (b) the placement of a fill results in a sudden positive spike in the excursion distances; and (c) immediately following a significant beach fill, loss of material occurs at a rapid rate which gradually decreases to equal the long-term recession rate.



Note: Circles indicate profiles measured shortly after a local storm.
Arrows indicate the approximate time at which beach fills were placed.

Figure 16. Distance from the base line to stated contours at WB 15.



Note: Circles indicate profiles measured shortly after a local storm.
Arrows indicate the approximate time at which beach fills were placed.

Figure 17. Distance from the base line to stated contours at CB 71.

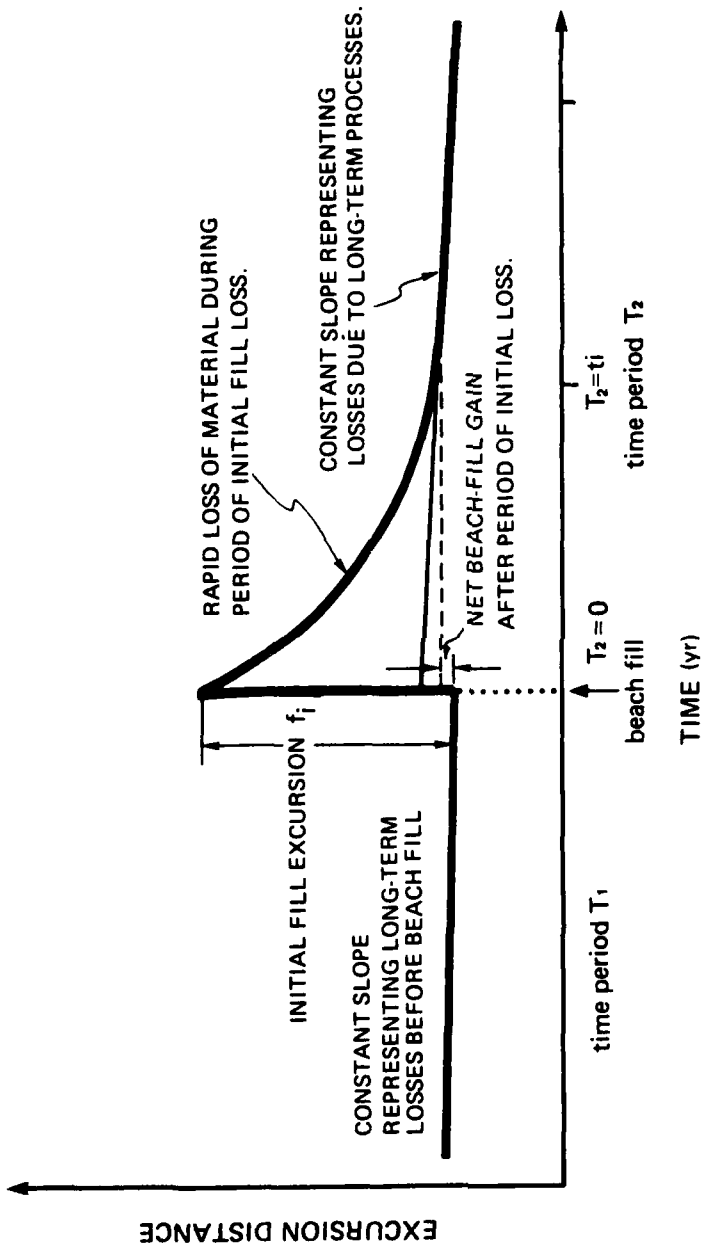


Figure 18. Schematization of beach-fill response.

The long-term change for most beaches in the study is negative, which signifies a long-term erosional trend. This is due primarily to the inability of the beach to return to its original position after a particularly severe winter storm period or after a very severe isolated storm (e.g., a hurricane or tropical storm). During storm activity, sediment is eroded off the upper section of the beach profile and transported either alongshore in the littoral drift or offshore. Particularly severe storms can result in sediment being transported sufficiently far offshore to preclude its return to the beach face under more favorable conditions, thus resulting in a sediment deficit and, hence, erosion. Also important during the erosional phase of beach behavior is the continual exposure of "fresh" beach sediment which may not have the appropriate sediment distribution/characteristics for the dominant wave conditions. This means that under erosional conditions, sorting losses can continually occur (resulting in long-term losses), the magnitude of which is dependent upon the degree of mismatch between the distribution of the exposed sediment to that which is more suitable for the wave conditions. Another cause for the long-term erosional problem is a rise in sea level position. Based on an equilibrium bottom profile, Bruun (1962) quantified the volumetric erosion loss per unit length of shoreline (V) as

$$V = (e + d) (X) \quad (1)$$

where X is the rate of shoreline recession, e is the berm crest MSL, and d is the limiting depth between nearshore and offshore processes.

Limiting depth (d) is approximately -8.2 meters (MSL) based on inspection of long profiles from Wrightsville and Carolina Beach data. Horizontal distances to this depth for the control cells are presented in Table 6. The rate of shoreline recession is expressed by

$$X = \frac{ab}{(e + d)} \quad (2)$$

where a is the rate of local sea level rise, and b is the distance from the initial shoreline to the limiting depth.

Table 6. Volumetric and excursion losses due to rise in MSL.

Littoral Cell	Distance (b) to limiting depth of -8.2 m	Volumetric loss/unit lgth of beach ($m^3/yr/m$)	Excursion rate due to sea level rise (m/yr)
Wrightsville Beach	225	0.83	-0.10
Masonboro Beach	210	0.78	-0.10
Carolina Beach	190	0.70	-0.09
Kure Beach	180	0.67	-0.08
Fort Fisher Beach	220	0.81	-0.10

The rise in MSL during the study period, based on the averaged trends at Portsmouth, Virginia, and Charleston, South Carolina (Hicks, 1972), was approximately 0.37 centimeter per year. The computed annual rate of volumetric and excursion loss due to the rise in sea level for the five beaches is given in Table 6.

The rapid loss of beach material immediately after the placement of a beach fill can be split into two components--a long-term component due to the ongoing long-term processes, and an initial component due to enhanced sorting by slope readjustment. The continual sorting type losses are obviously compounded by beach-fill activity when sediment which has a different distribution to the native beach sediment is used as the fill material. Not only is the magnitude of the sorting losses higher because of the generally greater mismatch between the new distribution and the desired distribution, but also the rate of loss is increased due to the increased exposure rate to wave activity as a result of sediment movement due to slope readjustment.

The long-term component can be represented by the slope of the line of best fit through all data points after time $t=t_i$ (Fig. 18), such that at any time, t ,

$$l_t = at \quad (3)$$

where l_t is the long-term excursion loss (gain) at time t , and a is the slope of the linear section of the excursion distance plot.

Data from this study indicated that after 1 to 2 years following beach-fill completion, the beach face generally eroded back during a winter storm period to its approximate prefill position. Both Figures 16 and 17 show this behavior and subsequent accretion of the beach face during the ensuing summer period. This means that after approximately 2 years most of the beach-fill material has been exposed to the sorting action of wave activity and for this period on (i.e., the time during which the long-term excursion rates were calculated), the enhanced losses due to the sorting of beach-fill material should have been minimal.

To quantify the initial loss component, the long-term component was subtracted from the excursion distances (shown by the dashline in Fig. 19). The time scale was reset to zero at the time of fill ($t=0$), and so the initial loss of beach fill after time t was S_t . Values of S (Fig. 19) for varying time increments up to $t=t_i$ were plotted on semilog paper. Figure 20 shows the results of these plots for the MLW, MSL, and MHW excursion curves of WB15. The results from this profile are typical for all profiles and indicate that the initial loss component due to sorting and beach-slope adjustment can be mathematically represented by an exponential equation of the form

$$S_t = \zeta f_i (1 - 10^{-kt}) \text{ for } 0 < t < t_i \quad (4)$$

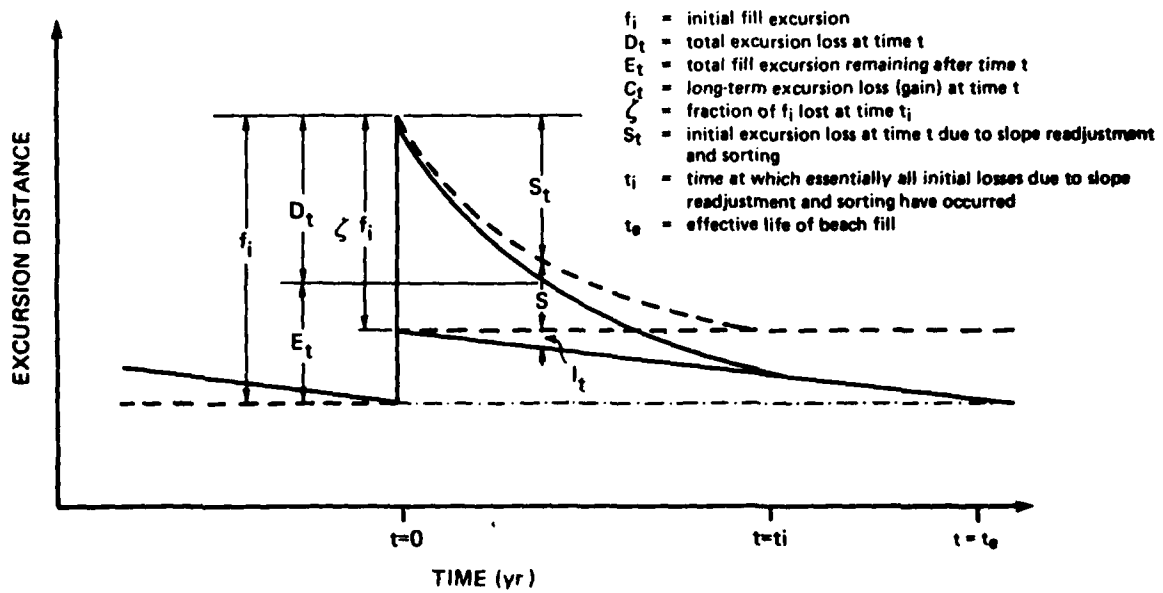


Figure 19. Definition sketch for beach-fill response.

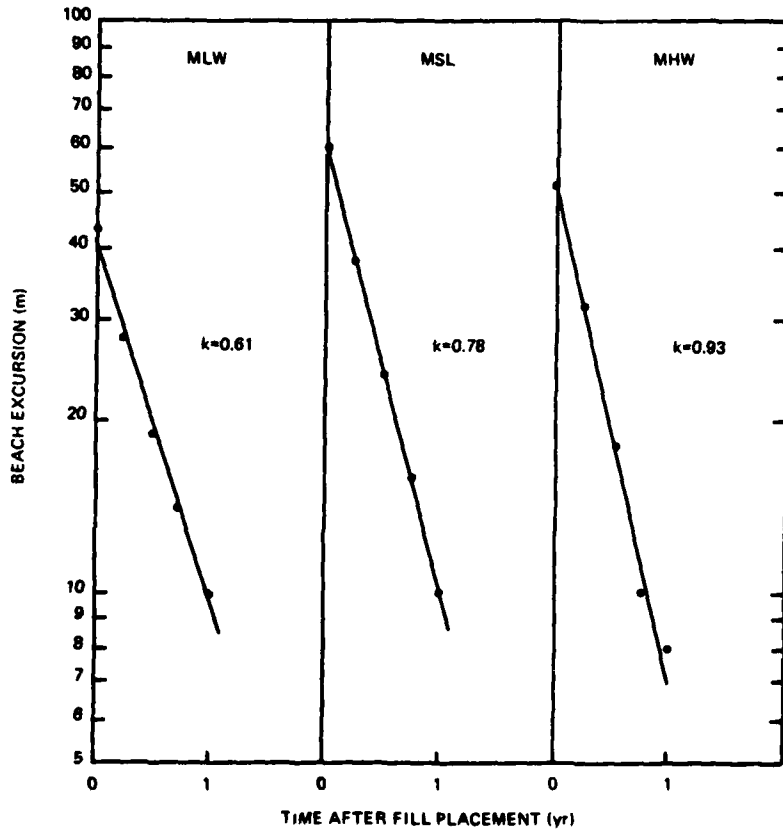


Figure 20. Semilog plots of excursion distance versus time after fill placement for profile WB 15.

where k is the slope of the line of best fit of the semilog plot of S versus t , f_i is the initial fill excursion, ζ is the fraction of f_i lost after initial losses (i.e., at $t=t_i$), and S_t is the excursion loss at time t due to sorting and slope adjustments of a beach fill.

Note that the exponential form of equation (4) implies that the initial losses, although very small, continue indefinitely. However, the excursion plots indicate that after 1 to 2 years the excursion loss due to slope adjustment and initial sorting cannot be separated from the seasonal and long-term losses. Hence, for practical reasons, the initial loss will be mathematically considered complete when 95 percent of ζf_i is lost (i.e., at $t=t_i$).

The total excursion loss, D_t , at time t after fill placement, is the sum of equations (3) and (4).

$$D_t = \zeta f_i (1 - 10^{-kt}) + at \quad (5)$$

or, the total beach excursion relative to the prefill position, E_t , at any time t after a fill, is

$$E_t = f_i \left[1 - \zeta + \zeta 10^{-kt} \right] - at \quad (6)$$

Equation (6) is an important tool which can be used to evaluate historic beach fills and to design future ones. This equation can be used in two ways. First, if a given design lifetime of a fill is required, substituting $E_t=0$ and t equal to the desired design life, then equation (6) is solved to give the initial fill excursion (and volume). Second, for a given volume of fill, or alternatively, for a given initial excursion, the time $t=t_e$ at which the beach returns to its prefill position ($E_t=0$) can be determined (i.e., the "useful life" of the fill can be determined). These calculations can be used to quantify the effectiveness and value of a given beach fill. However, the assumption made within these interpretations of equation (6) is that the beach fill has lost its effectiveness as soon as the beach face between the MLW to MHW contours returns to its initial, prefill position. It must be noted that in addition to providing a horizontal excursion of the beach face, beach fills provide, either directly or indirectly, three other functions which retain their value even when the initial excursion is lost. The direct value is that the elevation of the berm(s) and sometimes dunes is increased during beach-fill operations so that a larger volume of material seaward of the backdune is available to absorb the erosional tendencies of storm waves. This provides an additional degree of protection to the backshore which was not present prior to the fill placement. Indirectly, beach fills result in an increase in sand on downdrift beaches, and produce slight decreases in the nearshore to offshore bathymetry due to the redistribution of beach-fill material offshore as a result of slope readjustment and

sorting. These decreased depths provide an added measure of protection to the beach by forcing waves to break farther offshore. Individual designs of, and the nature of the sediment used in each beach fill, dictate the degree to which these factors benefit the beach area. Consequently, they will not be further addressed in this analysis, but must be kept in mind when dealing with the design or evaluation of a beach fill.

An interesting feature of Figure 20 is the relative magnitude of the k values (the decay rate) of the MLW, MSL, and MHW curves. The greater the k value, the faster the rate of initial loss (erosion). Consequently, the results show that the MHW contour eroded at a faster rate than the MSL contour, which in turn eroded at a faster rate than the MLW contour. In other words, the slope of the beach face readjusted itself and became less steep during the initial loss period.

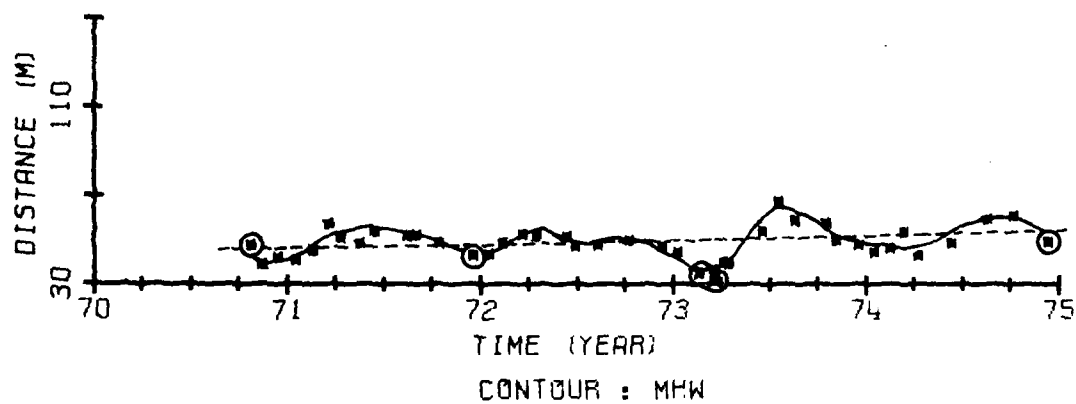
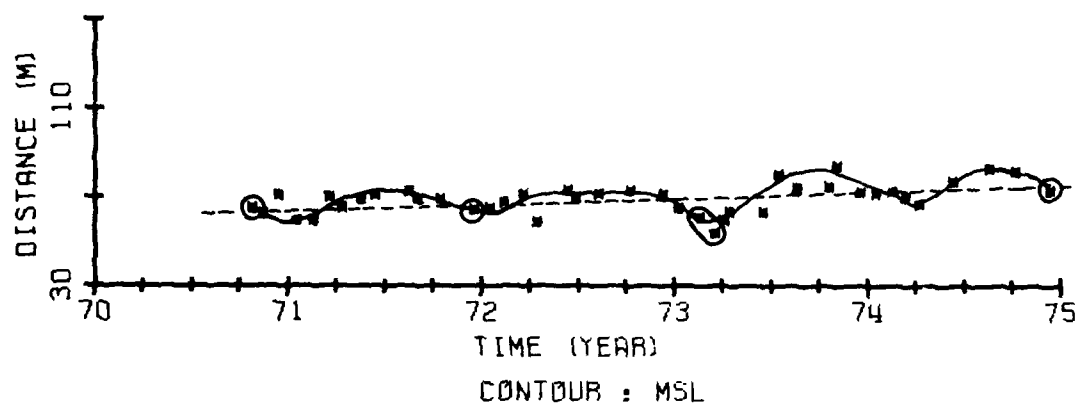
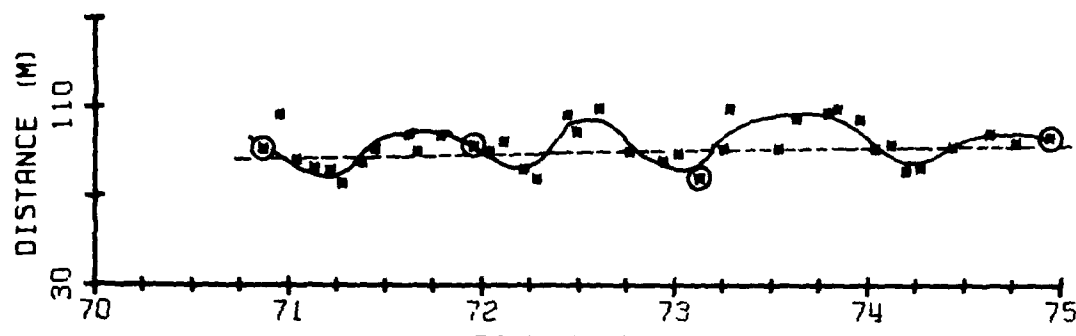
4. Beach Behavior from 1965 to 1975.

(a) Wrightsville Beach. The behavior of Wrightsville Beach in response to coastal processes during the 1965 to 1975 decade is best described by conveniently dividing Wrightsville Beach into three sections--the northern, central, and southern sections.

The northern section can be characterized as a slowly accreting beach with the rate of accretion falling from a maximum of 1.8 meters per year at Mason Inlet to near zero about 1.75 kilometers farther south. Figure 21 shows the excursion plots for WB3, typical of the beach behavior in this northern section. Superimposed upon the average accreting excursion is a seasonal variation of approximately 20 meters. The minimum excursion distances occur during the first three (winter) months of the year and the maximum from July to September. Figure 21 shows that the beach in this section is able to respond to storms, particularly noted are those in February and March of 1973, and to rebuild itself without artificial renourishment.

Between the points 1.75 and 5 kilometers, the central section of Wrightsville Beach has been eroding constantly since 1965. The excursion plots for WB16 (Fig. 22) are typical of the area of maximum erosion experienced around the northern area of the town of Wrightsville Beach. Beach fills in 1965, 1966, and 1970 were placed to protect this town; however, the continued high erosion rate nullified those efforts. The data are too sparse to obtain seasonal variations before 1970, but since that time the seasonal excursion within the central section was approximately 25 meters.

The behavior of the southern 1.5-kilometer section of Wrightsville Beach has been dominated by the construction of the northern jetty on Masonboro Inlet. During the first 4 months in 1966 (prior to the 1966 beach fill), the nearshore zone of the beach immediately north of the nearly completed jetty accreted by up to 40 meters, especially the MSL and MWL contours of profiles WB49 and WB50. This accretion fillet

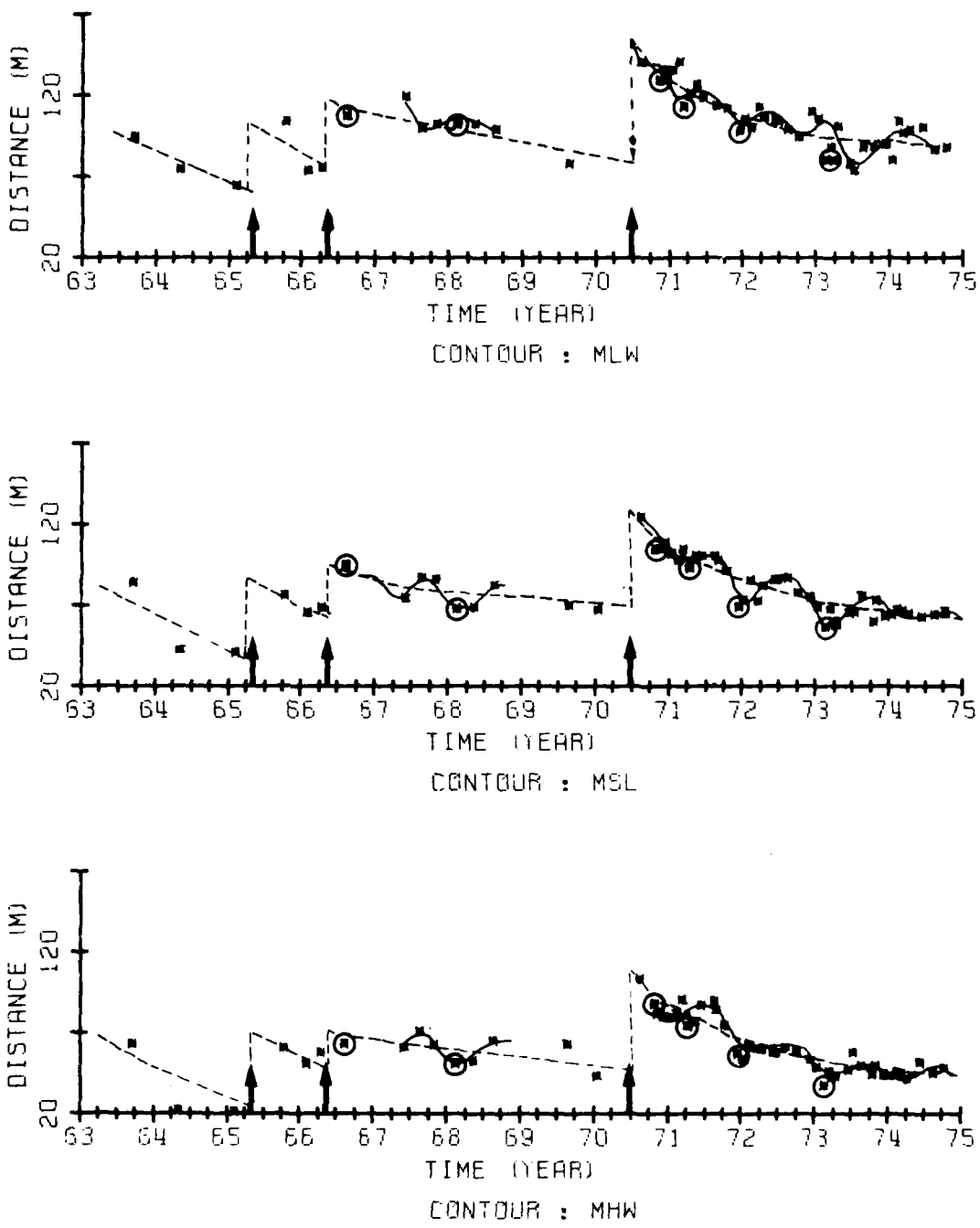


Note: Circles indicate profiles measured shortly after a local storm.

Arrows indicate the approximate time at which beach fills were placed.

Dashline indicates line of best fit of average excursion distance.

Figure 21. Distance from the base line to stated contours at WB 3.



Note: Circles indicate profiles measured shortly after a local storm.
 Arrows indicate the approximate time at which beach fills were placed.
 Dashline indicates line of best fit of average excursion distance.

Figure 22. Distance from the base line to stated contours at WB 16.

extended northwards with time into the area of beach fill and, soon after the completion of the jetty in spring 1966, the southern end of Wrightsville Beach had accreted by approximately 30 to 40 meters. From 1968 until the end of the study period, the accretion fillet underwent only minor changes with seasonal fluctuations of 15 to 25 meters. Figure 23 shows typical excursion plots of WB47.

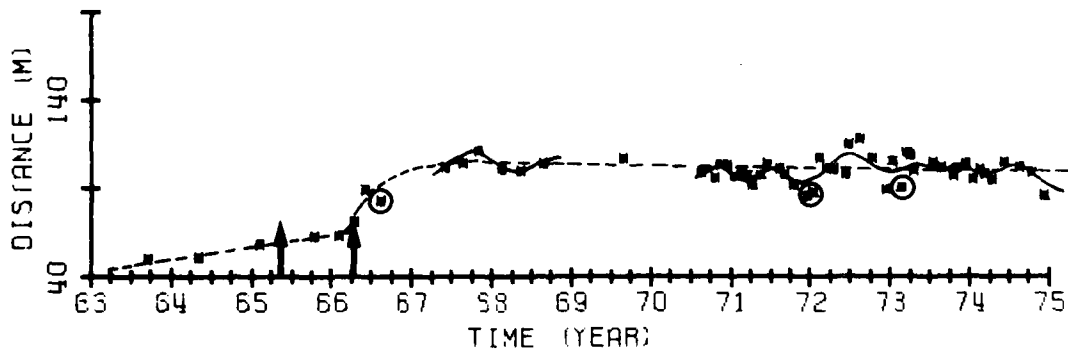
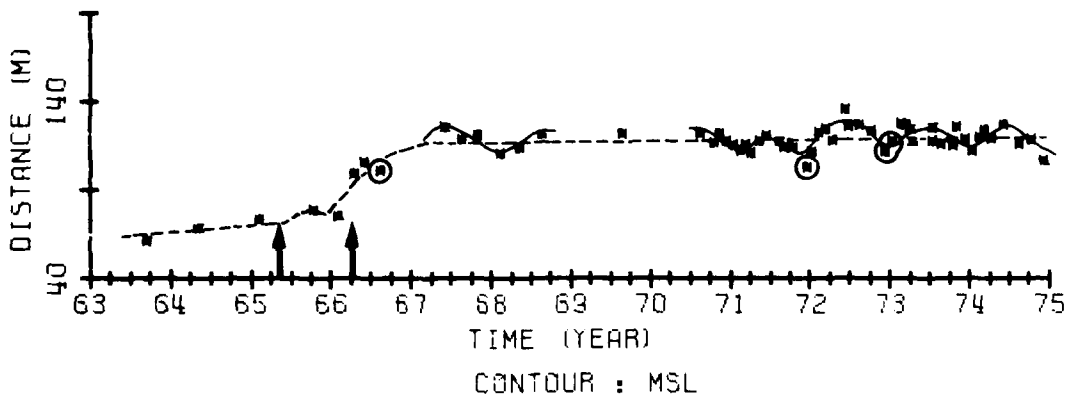
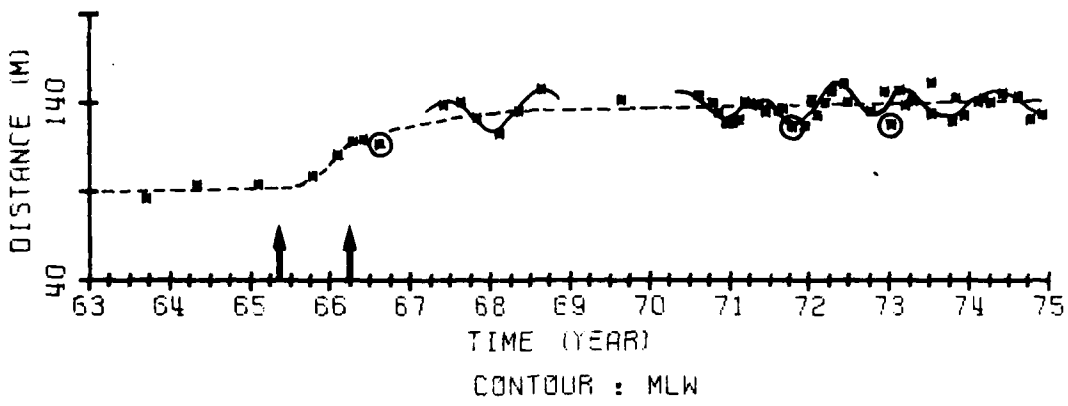
The long-term excursion rate values for the entire beach are shown in Table 7. The average erosion (excursion loss) per year along Wrightsville Beach due to the rise in sea level is 0.10 meter (see Table 6). This value must be subtracted from the measured excursion rates to determine the average annual loss of beach excursion due primarily to longshore processes. These values are shown in Table 7 and are plotted in Figure 24.

The average variation in seasonal excursion remained fairly constant along the entire beach, with a maximum variation occurring at MLW and a minimum at MHW. The difference in the seasonal excursions between MLW-MSL and MHW-MSL gives an indication of the average change in beach-face slope from winter to summer beach profiles. Table 8 gives the average excursion values from 325 observations along Wrightsville Beach; Figure 25 provides a visual interpretation of the relative change in seasonal excursion distances.

There were insufficient data points to quantify the response of Wrightsville Beach to the 1965 and 1966 beach fills. However, Figure 26 shows the semilog plots of the initial excursion loss after the 1970 beach fill. These plots show the combined results from eight profiles and are slightly different from Figure 20. The values of excursion loss at time t after beach-fill placement have been normalized by dividing them by the total initial excursion loss, ζf_i , and hence, the results from many profiles can be combined to compute the average exponential decay constant. Table 9 gives these values for the MLW, MSL, and MHW contours, together with values of ζ , the proportion of the MLW to MHW fill excursion which is lost due to sorting and slope adjustment, the initial fill excursion, and the average long-term loss rate. The relative differences in magnitude of the k values for the three contours (shown in Table 9) indicate that the MSL contour eroded faster, on the average, than either the MLW or MHW contours, thus producing, as expected, a concave beach profile. The average long-term excursion rate of -3.8 meters (erosion) per year for all three contours indicates that once long-term slope readjustments occurred, the average beach slope did not change from year to year.

(b) Carolina Beach. Like Wrightsville Beach, three sections of Carolina Beach (northern end, north-central, and southern half) were affected differently by the action of the coastal processes from 1965 to 1975.

The northern end extends from Carolina Beach Inlet southward for 1.5 kilometers to the 22-kilometer point (measured from the northern



Note: Circles indicate profiles measured shortly after a local storm.
 Arrows indicate the approximate time at which beach fills were placed.
 Dashline indicates line of best fit of average excursion distance.

Figure 23. Distance from the base line to stated contours at WB 47.

Table 7. Average long-term excursion rates along Wrightsville Beach.

Profile station	Distance from north study boundary (km)	Avg excursion rate (m/yr)	Avg excursion rate due to long-shore processes ¹ (m/yr)
WB1 ²	0.00	-1.2	-1.1
WB2	0.55	1.7	1.8
WB3	1.11	1.3	1.4
WB4	1.41	0.6	0.7
WB6	1.74	-0.9	-0.8
WB7	1.80	-1.6	-1.5
WB9	2.01	-1.3	-1.2
WB11	2.32	-5.0	-4.4
WB13	2.61	-4.6	-4.5
WB15	2.91	-5.8	-5.7
WB16	3.22	-5.1	-5.0
WB17	3.24	-4.1	-4.0
WB19	3.52	-4.2	-4.1
WB21	3.82	-4.3	-4.2
WB25	4.12	-1.3	-1.2
WB29	4.42	-2.1	-2.0
WB33	4.72	-4.1	-4.0
WB36	5.01	-0.3	-0.2
WB39	5.32	-0.2	-0.1
WB42	5.62	-0.6	-0.5
WB44	5.91	0.0	0.1
WB47	6.22	-0.5	-0.4
WB49	6.52	-4.1	-4.0
WB50 ²	6.71	-2.7	-2.6

¹Based on a 0.10-meter loss in excursion due to a rise in sea level.

²Profiles within inlet shoals.

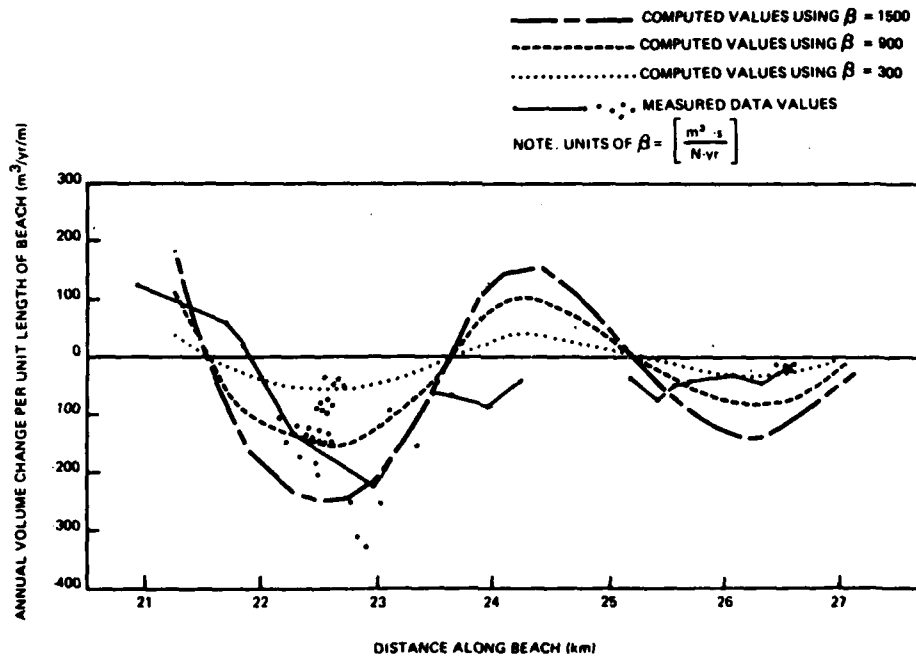


Figure 24. Comparison of measured and computed volumetric change along Carolina Beach.

Table 8. Seasonal variation in MLW, MSL, and MHW position along Wrightsville Beach.

Contour	Avg seasonal excursion (m)	Excursion minus MSL excursion (m)
MLW	28.9	6.6
MSL	22.3	0
MHW	20.6	-1.7
Avg	23.9	

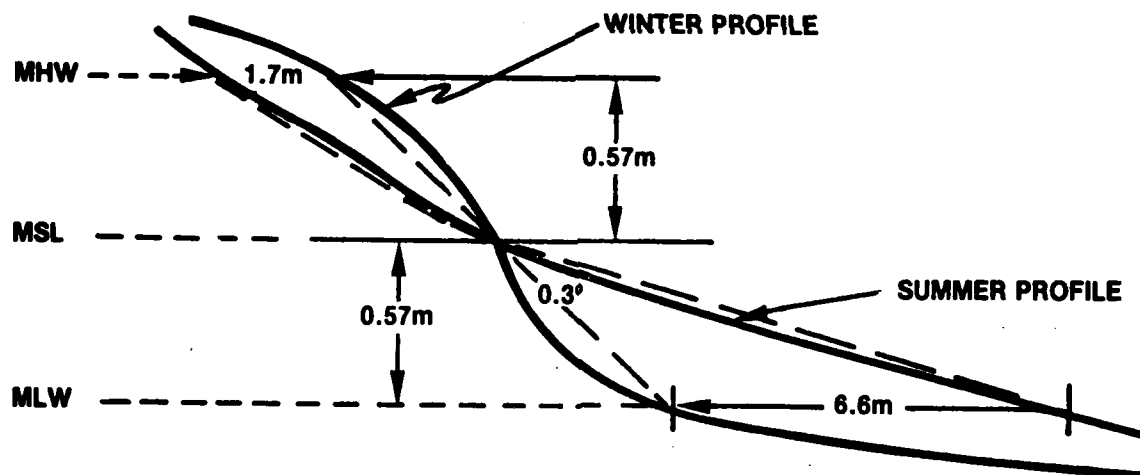


Figure 25. Relative seasonal change in beach slope for Wrightsville Beach .

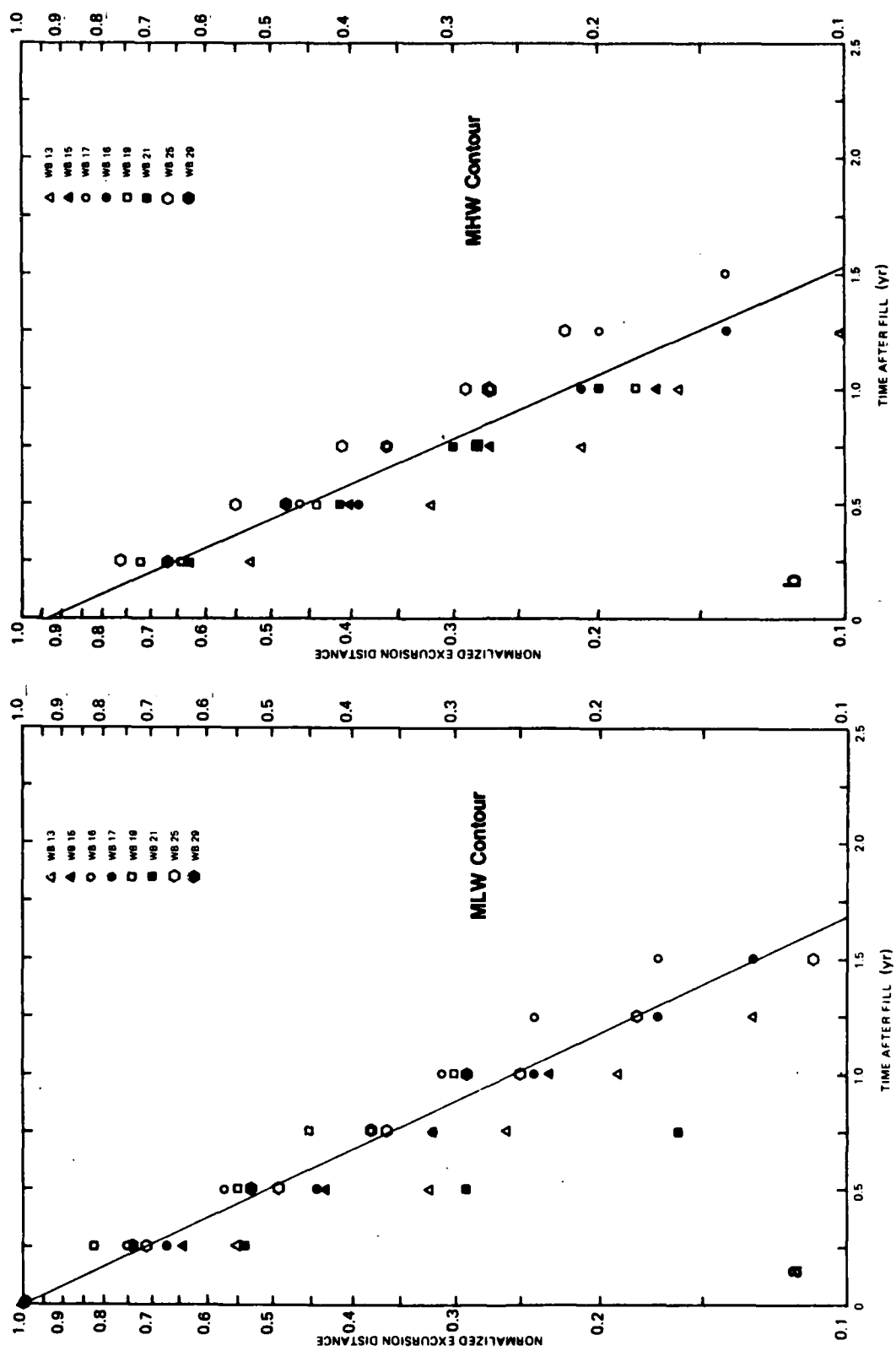


Figure 26. Semilog plots of normalized excursion distance versus time after fill placement for MHW, MLW, and MSL contours (1970 beach fill).

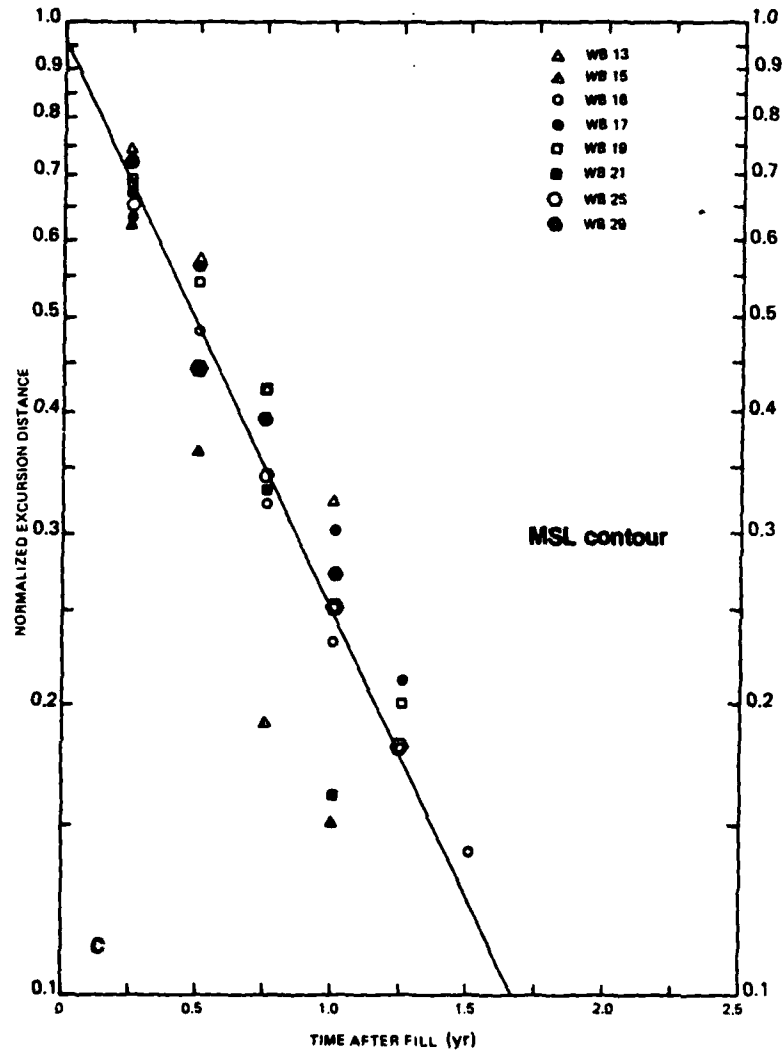


Figure 26. Semilog plots of normalized excursion distance versus time after fill placement for MHW, MLW, and MSL contours (1970 beach fill). --Continued

Table 9. Wrightsville Beach, 1970 beach-fill data.

Contour	Avg exponential decay constant (k)	Avg long-term excursion (m/yr)	Initial beach-fill excursion f_i (m)	ζ
MLW	0.58	-3.8	75.0	0.80
MSL	0.63	-3.8	77.9	0.79
MHW	0.59	-3.8	76.9	0.82

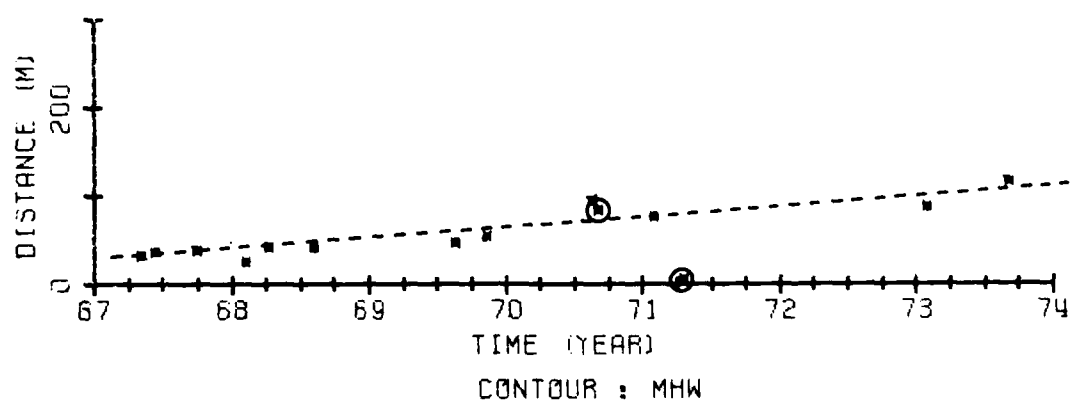
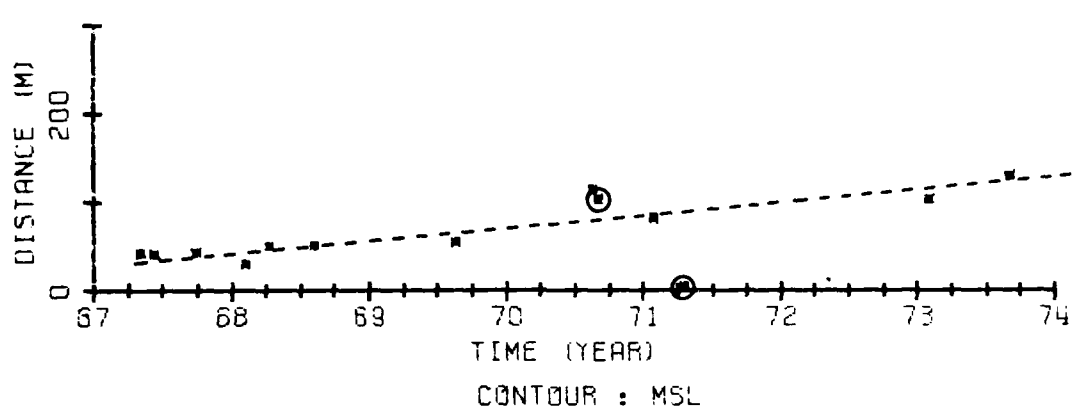
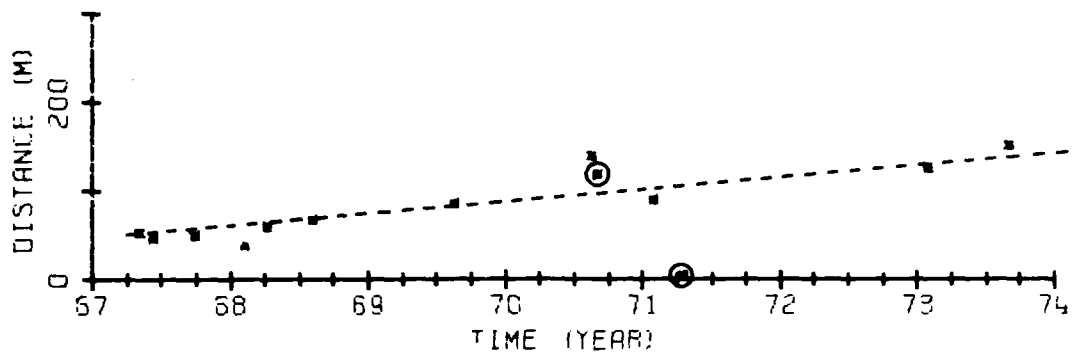
limit of the study area). Similar to the northern end of Wrightsville Beach, this section of Carolina Beach slowly accreted during the study period with a maximum rate of 15 meters per year at the tip decreasing to near zero at 22 kilometers. As shown in Figure 27, this area responded naturally to storm-induced erosion and, consequently, no beach fills were placed during the study period. The average seasonal excursion was 12.8 meters for the northern section.

The north-central section extends from the 22- to 23.5-kilometer points and encompasses both the only significant change in beach orientation along Carolina Beach and the northern end of the town of Carolina Beach. This section suffered the highest measured annual erosion rate of the entire study area, and estimates of that rate vary between 5 to 40 meters per year. The range is large, and errors in the estimation of the excursion rates from the excursion distance plots probably account for some of the scatter in the rate values. Because of the high erosion rates, and since the northern end of the town of Carolina Beach is exposed to this erosion (see Fig. 4), six beach fills were placed in this section between 1965 and 1971, three of which were connected with the experimental deposition basin in the throat of Carolina Beach Inlet. The excursion distance plots for CB64 (Fig. 28) reveal rapid erosion after each beach fill and the continued loss of beach material despite the beach-fill activities. The seasonal excursion distance within this area is about 19.5 meters.

The southern half of Carolina Beach experienced mild erosion rates of approximately 5 meters per year. Beach fills in 1965 and 1971 provided protection to the southern end of the Carolina Beach township because the net excursion in 1974 was still positive; i.e., more sand was placed on the beach by the beach-fill projects than was eroded away during the 1965-74 period. Figure 29 shows an example of the excess in excursion distance for CB119 and also shows that the average seasonal variation along this section is relatively small with a mean value of approximately 7.6 meters.

The long-term excursion rates for the entire beach are shown in Table 10. The representative value of average annual excursion loss along Carolina Beach due to the rise in sea level is 0.09 meter (see Table 6). This value must be subtracted from the measured excursion rates to determine the annual excursion loss due to longshore processes. Representative values are given in Table 10, and a complete set along Carolina Beach is plotted in Figure 30.

Table 11 shows the average MLW, MSL, and MHW seasonal excursion values for the entire beach and the relative differences in seasonal variation between these contours. The average change in beach slope at MSL from a summer profile to a winter profile was 0.2° , i.e., 1 on 286. Figures 31 and 32 show the semilog plots of the normalized initial excursion loss values versus time after fill placement for the 1965 and 1971 beach fills, respectively. Since there is a lack of data for the 1971 fill, all MLW, MSL, and MHW values from profile CB93 were combined

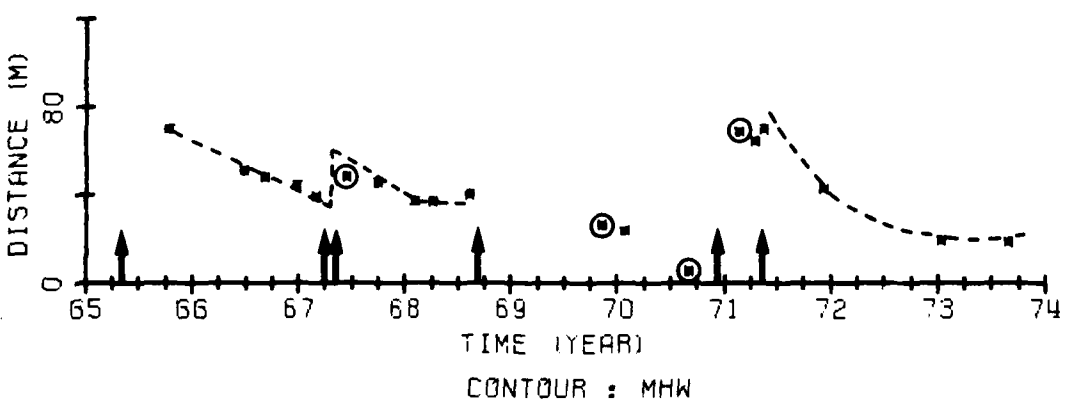
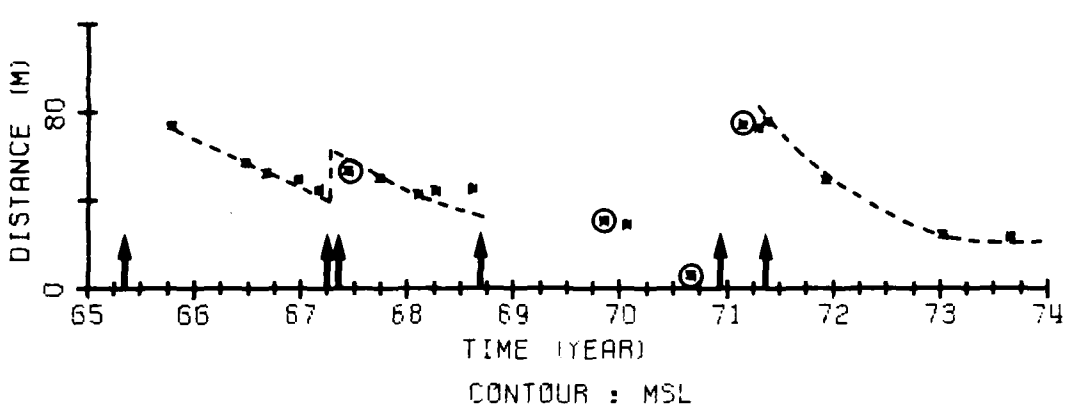
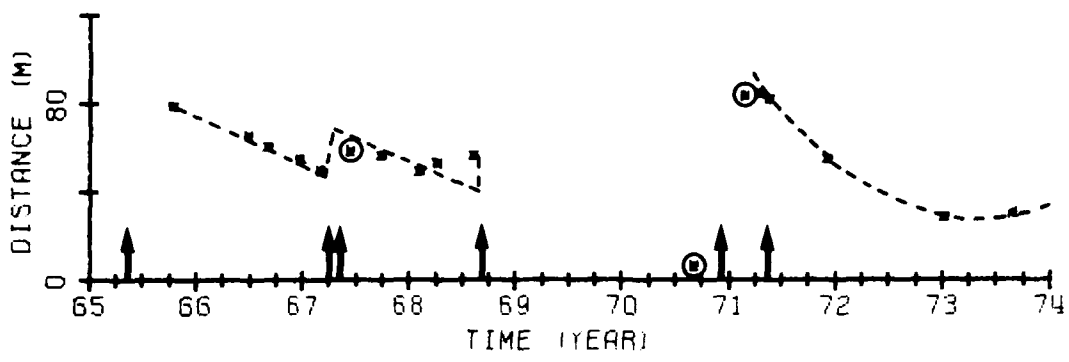


Note: Circles indicate profiles measured shortly after a local storm.

Arrows indicate the approximate time at which beach fills were placed.

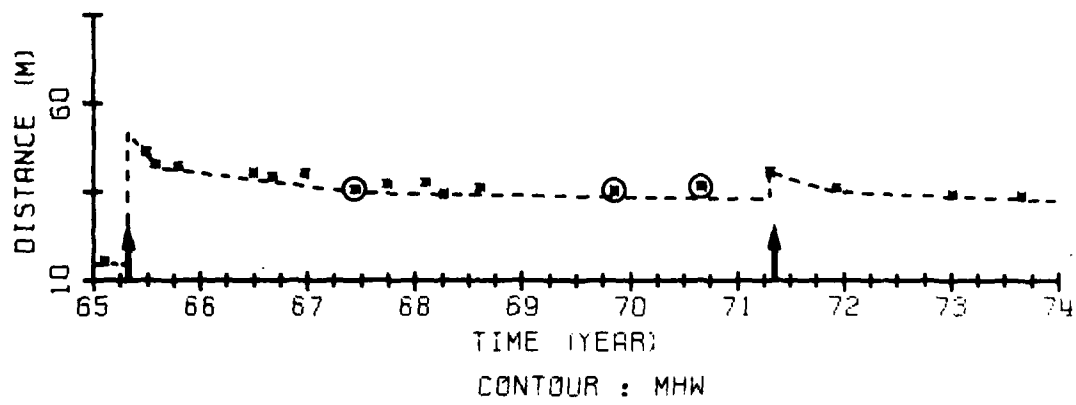
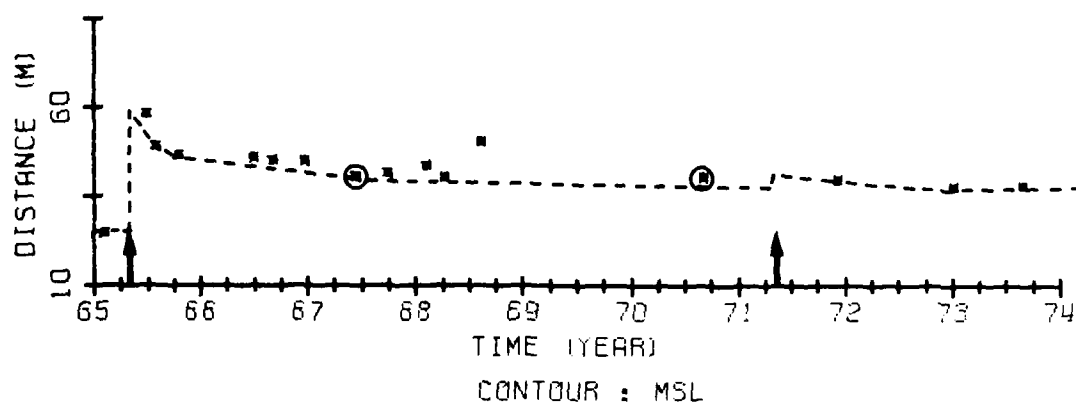
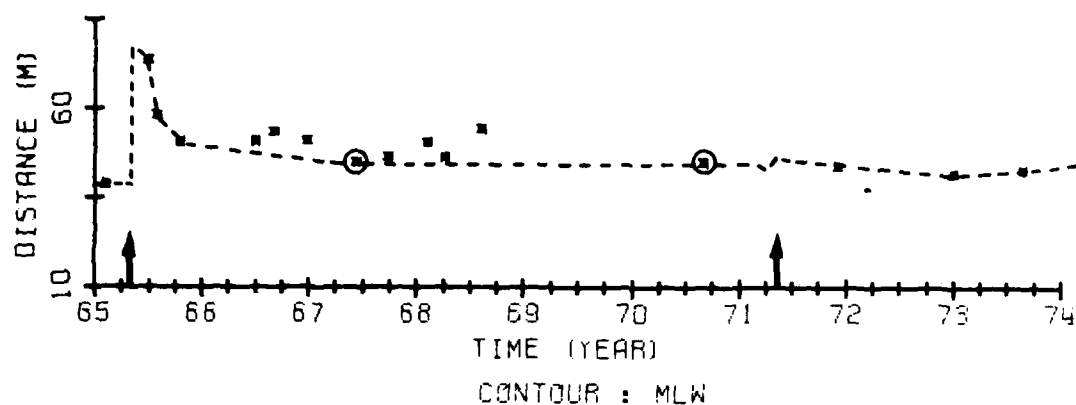
Dashline indicates line of best fit of average excursion distance.

Figure 27. Distance from the base line to stated contours at CB 2.



Note: Circles indicate profiles measured shortly after a local storm.
 Arrows indicate the approximate time at which beach fills were placed.
 Dashline indicates line of best fit of average excursion distance.

Figure 28. Distance from the base line to stated contours at CB 64.



Note: Circles indicate profiles measured shortly after a local storm.
 Arrows indicate the approximate time at which beach fills were placed.
 Dashline indicates line of best fit of average excursion distance.

Figure 29. Distance from the base line to stated contours at CB 119.

Table 10. Average long-term excursion rates along Carolina Beach.

Profile station	Distance from north study boundary (km)	Avg excursion rate (m/yr)	Avg excursion rate due to long-shore processes ¹ (m/yr)
CB1 ²	20.64	9.0	9.1
CB2	20.94	15.0	15.1
CB10	21.70	6.0	6.1
CB15	22.15	-12.9	-12.8
CB16	22.23	-17.9	-17.8
CB21	22.35	-20.9	-20.8
CB32	22.48	-22.5	-22.4
CB40	22.53	-10.4	10.3
CB44	22.54	-5.3	-5.2
CB53	22.59	-18.5	-18.4
CB61	22.72	-5.8	-5.7
CB71	23.03	-27.4	-27.3
CB84	23.36	-19.2	-19.1
CB93	23.64	-9.2	-9.1
CB96	24.24	-5.8	-5.7
CB99	25.20	-4.9	-4.8
CB106	26.07	-3.4	-3.3
CB117	26.56	-1.0	-0.9
CB119	26.68	-0.8	-0.7

¹Based on a 0.09-meter loss in excursion due to a rise in sea level.

²Profiles within inlet shoals.

..... COMPUTED VALUES USING $\beta = 400$
 - - - - - COMPUTED VALUES USING $\beta = 300$
 - - - - - COMPUTED VALUES USING $\beta = 200$
 - - - - - MEASURED DATA VALUES

NOTE: UNITS OF β ARE $\left[\frac{m^3 \cdot s}{N \cdot yr} \right]$

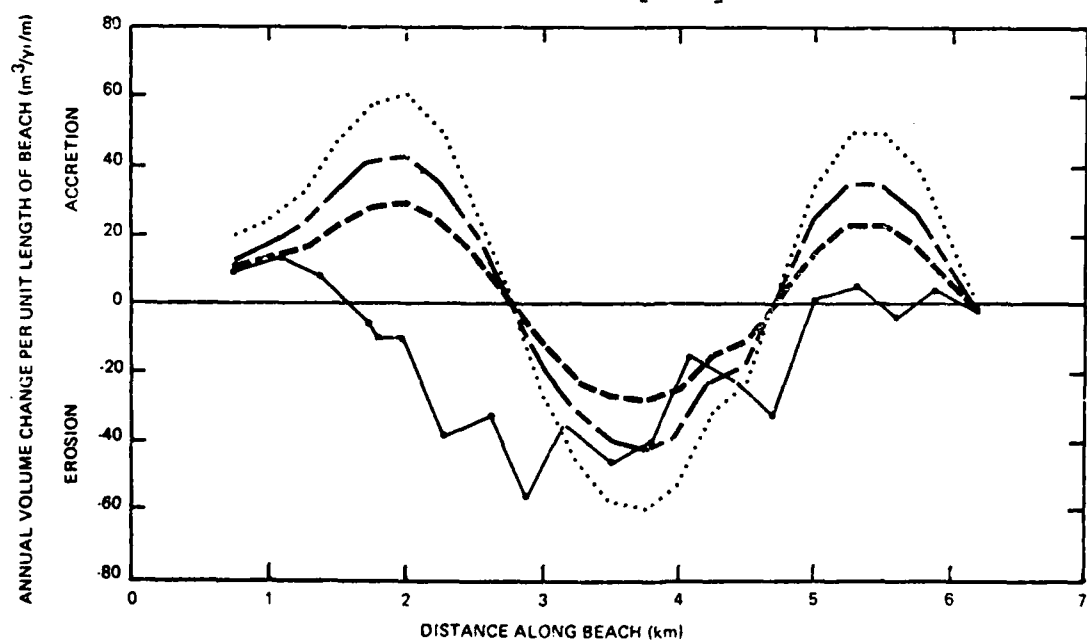


Figure 30. Comparison of measured and computed volumetric change along Wrightsville Beach.

Table 11. Seasonal variation in MLW, MSL, and MHW positions, Carolina Beach.

Contour	Avg seasonal excursion (m)	Excursion minus MSL excursion (m)
MLW	18.2	0.4
MSL	17.8	0
MHW	16.4	-1.4

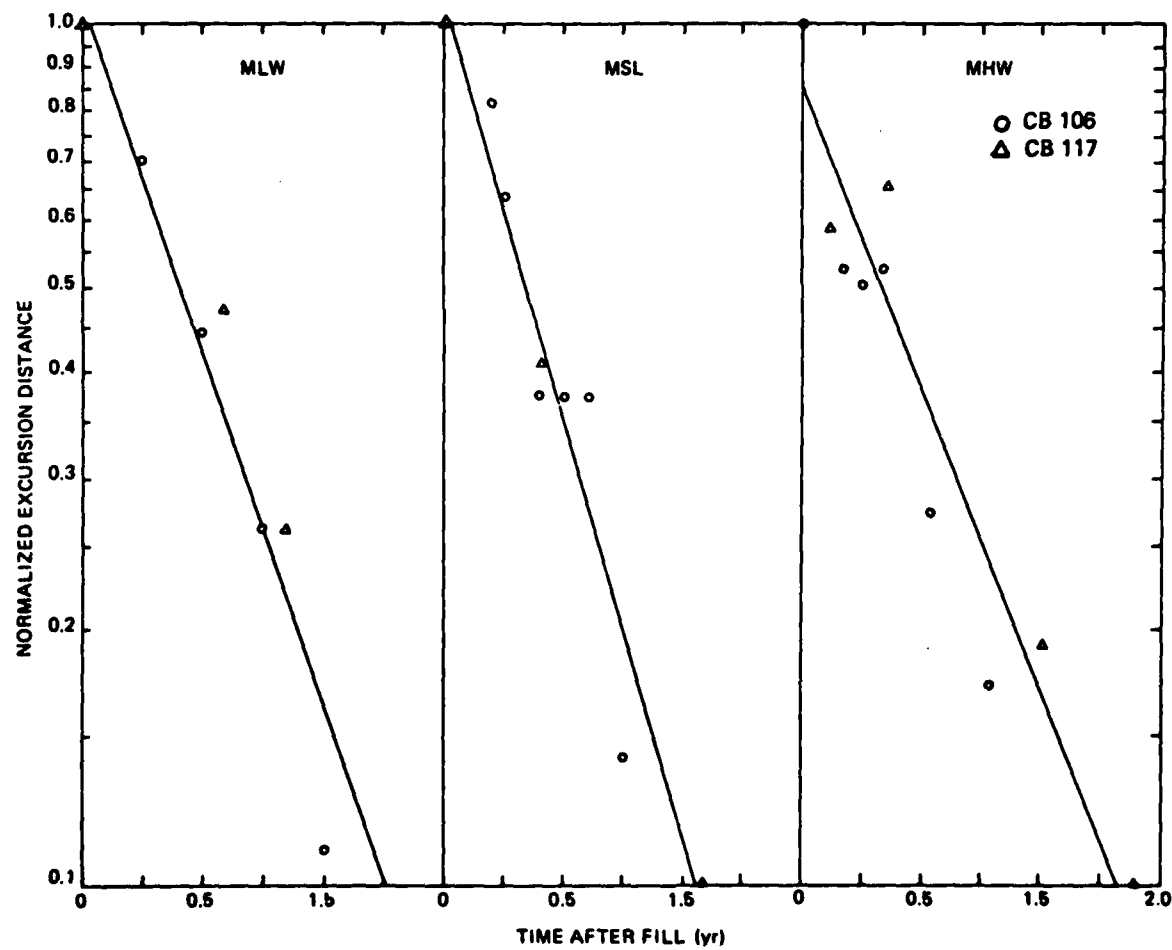


Figure 31. Semilog plots of normalized excursion distance versus time after fill placement for 1985 beach fill.

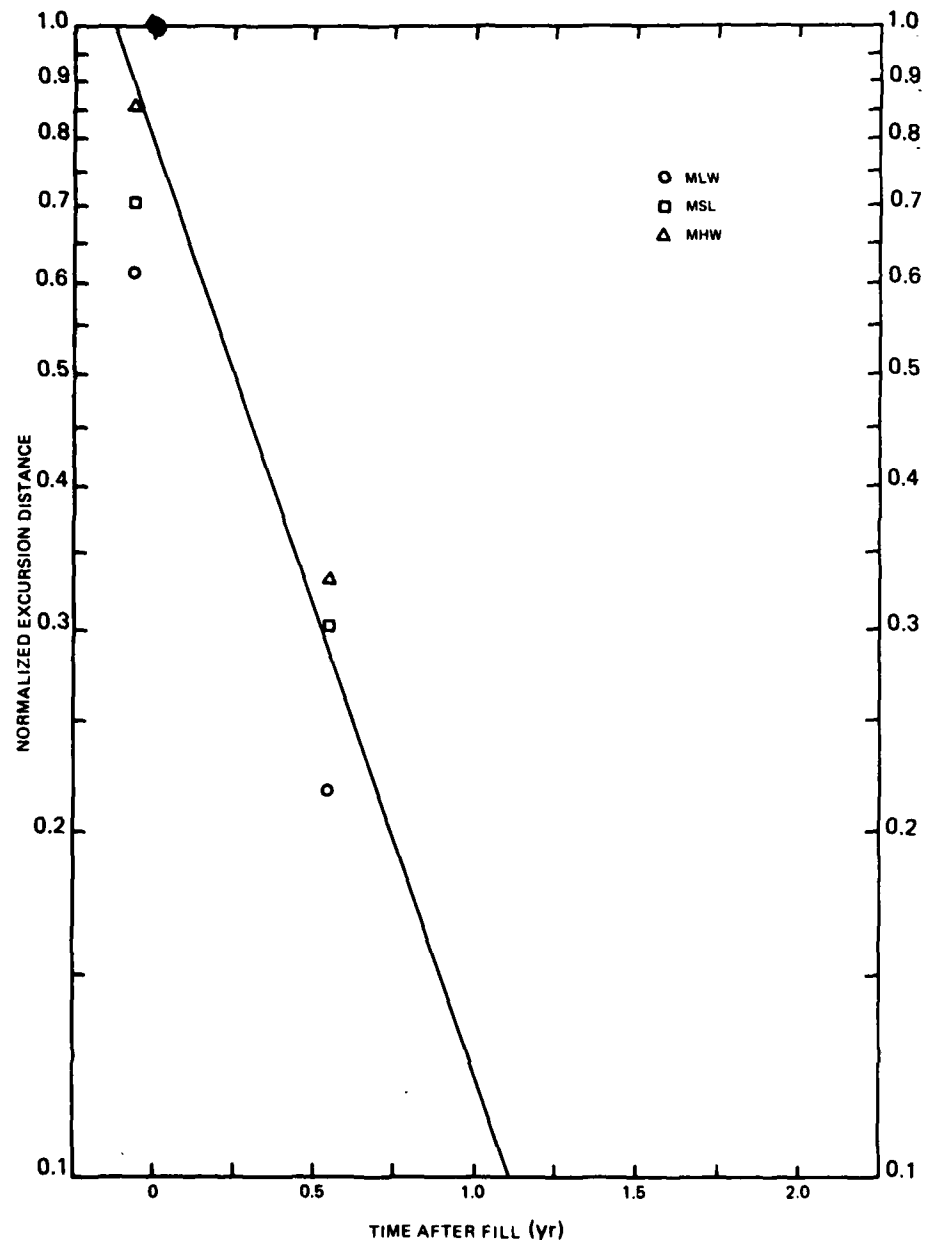


Figure 32. Semilog plots of normalized excursion distance versus time after fill placement for 1971 beach fill.

to calculate the exponential decay constant for the sorting and slope adjustment losses. Table 12 contains all relevant data for the 1965 and 1971 beach fills that could be confidently extracted from the excursion distance plots.

Table 12. 1965 to 1971 beach-fill data, Carolina Beach.

Beach fill	Avg exponential decay count (k)				Avg initial fill excursion (m)	Avg long-term excursion (m/yr)
	MLW	MSL	MHW	Avg		
1965	0.83	0.98	0.70	0.84	25	-2.2
1971	--	--	--	0.83	45	-4.2

(c) Masonboro, Kure, and Fort Fisher Beaches. Because of insufficient and nonconsistent temporal distribution of excursion distance data, beach response in terms of long-term erosional-accretionary rates, beach fills, and storm events cannot be described for Masonboro, Kure, or Fort Fisher Beaches. Therefore, only a brief statement concerning the relative difference in excursion distance between the first and final data points can be made; however, because of seasonal variation and possible poststorm excursions, even this may be misleading.

From 1966 to 1973, the erosional loss at Masonboro Beach was generally 10 to 30 meters. However, two profiles (MB2 and MB5), which are located in the vicinity of the only significant change in beach angle along Masonboro Beach, show losses of 80 to 100 meters. The excursion differences for most profiles fall within the possible range of seasonal or poststorm excursion ranges and, consequently, the actual long-term loss on Masonboro Beach may not be reflected by the above values.

The availability of excursion distance data for Kure Beach and Fort Fisher Beach is even less than that for Masonboro Beach, with data collected only from late 1969 to early 1973. Differences in excursion positions between those dates for both beaches vary from +5 to -20 meters, but again, estimated seasonal variation from two profiles of 10 to 15 meters makes any conclusion on the long-term response of these beaches impossible.

V. LONGSHORE SEDIMENT TRANSPORT ANALYSIS

1. Introduction.

The procedure to mathematically predict the volume of sediment in the littoral drift requires knowledge of the magnitude and direction of the energy flux due to waves breaking along the study area beaches. To determine this quantity, a wave climate representative of the annual wave conditions measured or experienced in offshore waters must be established. The wave climate, in this case in the form of a set of wave heights with different periods and directions, must be "routed" towards shore by a wave refraction model until the waves break on or near the beach. Information on their breaking angles (relative to the beach orientation), breaking wave heights, and wave speed at breaking are determined and used to establish the longshore components of the energy flux for both the northerly and southerly directions.

The quantity of sediment carried by the littoral drift in each direction is found by multiplying the magnitude of the energy flux by a conversion factor (U.S. Army, Corps of Engineers, Coastal Engineering Research Center, 1977). However, uncertainty exists in the exact value of that factor (Vitale, 1980), and therefore, it will be recalculated for this study area by comparing the known time rate of volumetric change at Wrightsville Beach and Carolina Beach to the predicted values of the energy flux at those beaches. The recomputed conversion factors will be used to estimate the annual northerly and southerly longshore transport quantities and the volume of material lost into the adjacent inlets.

2. Wave Refraction Analysis.

(a) Wave Climate. Wave climate was determined from a joint probability evaluation of wave gage data at Johnnie Mercer's Pier and wave observation data from Wrightsville Beach. The directional distribution of wave height and wave period, calculated from the wave observation data, was assumed to hold for the Johnnie Mercer's Pier data. Consequently, wave angles at the gage were statistically correlated to the wave observation data observations. The SSMO and Frying Pan Shoals wave data were not used due to a lack of confidence in data recording (Harris, 1972).

Under random sea conditions, the distribution of the values for wave height, period, and direction is continuous. However, to perform the wave refraction analysis, a representative set of wave height, period, and direction conditions was needed. Consequently, the distribution of wave height was divided into three ranges and the period into six groups with midrange values of 3, 6.5, 8.5, 10.5, 12.5, and 16 seconds. The angles of wave approach were also divided into four sectors (northeast,

east, southeast, and south), with the wave statistics from the intermediate directions (north-northeast, east-northeast, etc.) being incorporated proportionately into the four primary directions. Figure 33 shows these approach angles relative to the shoreline orientation.

The distribution of wave height was converted to an equivalent distribution of wave energy (wave height squared) and divided into three ranges. The wave height corresponding to each of the midrange values of wave energy was then determined. The offshore wave height and approach angle corresponding to each of the three nearshore wave heights were calculated for each period and nearshore angle condition. Both the offshore wave direction and refraction coefficients were determined by using Snell's Law, and the shoaling coefficients were calculated by the ratio of nearshore and offshore depths. The offshore wave heights corresponding to each of the three nearshore wave heights were calculated by dividing the nearshore height by the product of the refraction, shoaling, and friction coefficients. Explanation of the development of the friction coefficient is detailed later in Section (c). The three offshore wave heights used in the analysis were 0.52, 1.40, and 2.47 meters.

The probability of occurrence (expressed as a percentage) of a wave approaching the study area from each of the four directions, with a wave height and period falling within one of the three height ranges and six period ranges (i.e., 72 different cases), was calculated from the data sets for each season; i.e., winter (December, January, and February), spring (March, April, and May), summer (June, July, and August), and fall (September, October, and November). This information is presented in Table 13.

The percentage of occurrence of many of the wave height-period-direction combinations is less than one. To reduce excessive and unnecessary analysis costs, it was decided that satisfactory results could be achieved by using only enough wave combinations so that, for each season, 95 percent of occurrence by wave energy of all possible combinations of height, period, and direction was modeled. Selection of seasonal wave types was based on the summation of percentage of occurrence by wave energy of those wave conditions with the highest percentage until the 95-percent criterion was satisfied. Summation to 95 percent by wave energy resulted in a representation of the wave climate by approximately 98 percent of the observed wave types. Table 14 shows the offshore wave climate chosen to represent the average seasonal conditions measured along the study area. The average annual climate is represented by the arithmetic average of the seasonal values for each combination of wave height, period, and direction.

The final step in the selection of the wave climate data was a calibration check using the wave refraction model. The annual wave climate sets were refracted toward shore and combined according to their percentage of occurrence (see Section V, 3). The directional distribution of the wave energy at Wrightsville Beach was compared to

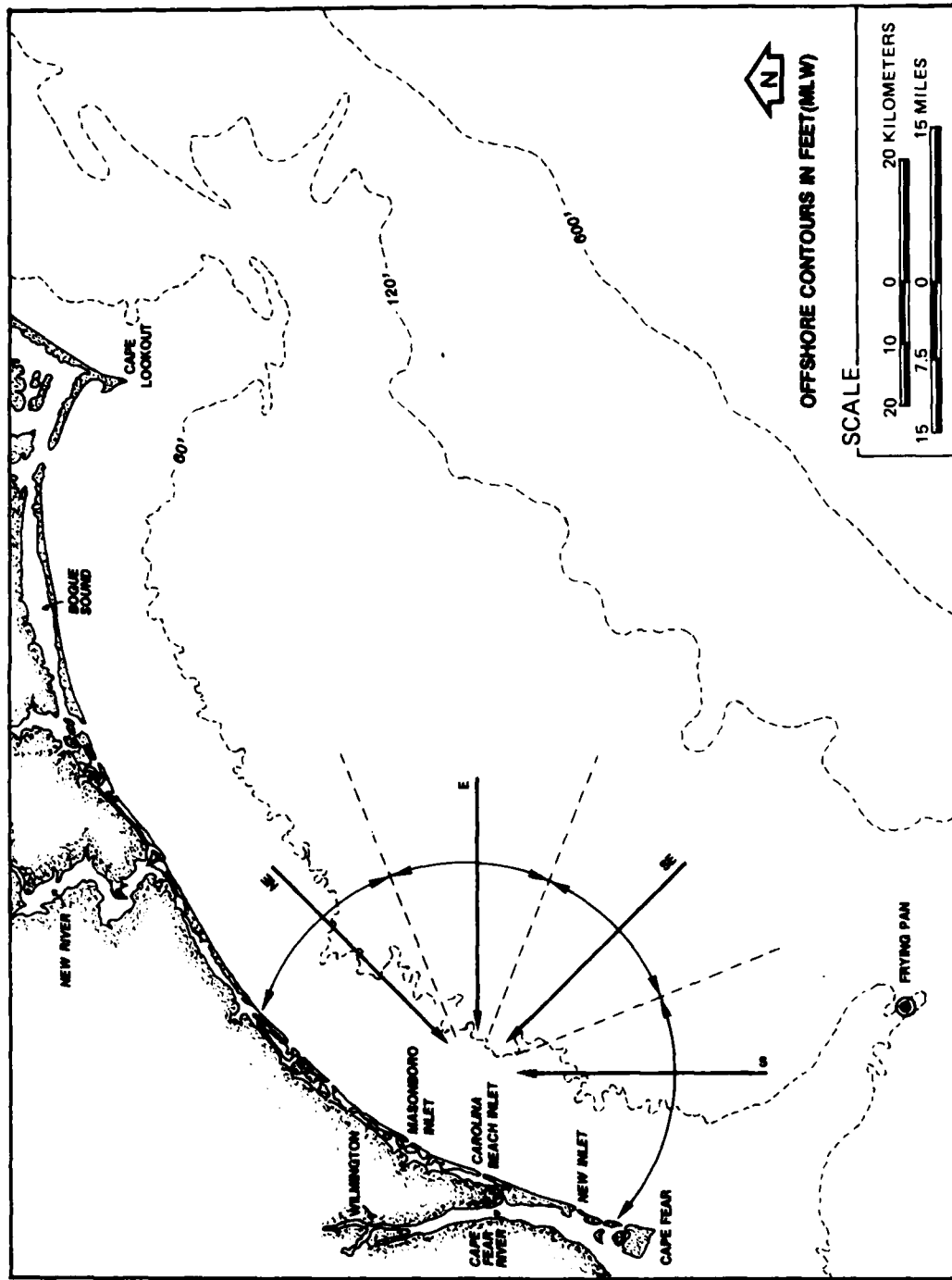


Figure 33. Wave directions used in refraction analysis.

Table 13. Statistical wave climate parameters for the study area.

T (s)	1	Northeast			Southeast			South		
		Wave height (m)	Σ							
		0.52	1.40	2.47	0.52	1.40	2.47	0.52	1.40	2.47
Spring										
3.0	6.34	3.52	0.04	9.90	10.8	6.00	0.06	16.87	0.90	0.50
6.5	5.39	2.68	0.15	8.22	9.19	4.58	0.26	14.03	0.76	0.38
8.5	10.26	2.63	0.21	13.10	17.50	4.47	0.36	22.33	1.45	0.37
10.5	1.82	0.23	—	2.05	3.10	0.38	—	3.48	0.26	0.03
12.5	0.76	0.31	—	1.07	1.29	0.53	—	1.82	0.11	0.04
16.0	0.60	0.20	—	0.80	1.03	0.34	—	1.37	0.08	0.02
Σ	25.17	9.57	0.40	35.14	42.92	16.30	0.68	59.90	3.56	1.34
Summer										
3.0	0.55	0.27	—	0.82	6.57	3.16	—	9.73	10.36	4.99
6.5	0.76	0.14	0.02	0.92	9.02	1.70	0.20	10.92	14.22	2.68
8.5	1.06	0.19	—	1.25	12.66	2.20	—	14.86	19.98	3.47
10.5	0.05	—	0.01	0.06	0.64	—	0.14	0.78	1.00	—
12.5	0.06	—	—	0.06	0.73	—	—	0.73	1.14	—
16.0	0.04	0.01	—	0.05	0.49	0.07	—	0.56	0.77	0.11
Σ	2.52	0.61	0.03	3.16	30.11	7.13	0.34	37.58	47.47	11.25
Fall										
3.0	0.74	0.45	—	1.19	8.62	5.24	—	13.86	7.01	4.26
6.5	0.77	0.24	0.01	1.02	9.01	2.73	0.07	11.81	7.32	2.22
8.5	1.22	0.25	0.02	1.49	14.17	2.89	0.26	17.32	11.50	2.35
10.5	0.31	0.05	—	0.36	3.63	0.63	—	4.26	2.96	0.51
12.5	0.29	0.05	—	0.34	3.40	0.56	—	3.96	2.76	0.46
16.0	0.11	0.01	—	0.12	1.32	0.14	—	1.46	1.07	0.12
Σ	3.44	1.05	0.03	4.52	40.15	12.19	0.33	52.6	32.62	9.92
Winter										
3.0	8.36	6.37	0.22	14.95	4.60	3.90	0.12	8.22	0.01	—
6.5	7.36	6.41	0.51	14.28	4.05	3.53	0.28	7.86	0.01	—
8.5	18.33	6.52	0.69	25.54	10.09	3.59	0.38	16.06	0.01	—
10.5	4.64	1.15	—	5.79	2.55	0.63	—	3.18	—	—
12.5	2.20	0.06	—	2.26	1.21	0.04	—	1.25	—	—
16.0	0.99	0.67	—	1.66	0.55	0.37	—	0.92	—	—
Σ	41.88	21.18	1.42	64.48	23.05	11.66	0.78	35.49	0.02	0.01

1 Wave period in seconds.

2 Summation of the seasonal percent of occurrence for that specific wave condition.

Table 14. Selected seasonal wave parameters used in the wave refraction analysis.

T (s)	Northeast			South				
	1	Wave height (m)	1.40	2.47	0.52	1.40	2.47	
3.0								
6.5								
8.5								
10.5								
12.5								
16.0								
East								
Wave height (m)								
0.52	1.40	2.47	0.52	1.40	2.47	0.52	1.40	2.47
Southeast								
Wave height (m)								
6.34	3.52	0.04	10.8	6.00	0.50	0.90	0.50	0.02
5.39	2.68	0.15	9.19	4.58	0.26	0.76	0.38	0.03
10.26	2.63	0.21	17.50	4.47	0.36	1.45	0.37	
1.82	0.23		3.10	0.38				
0.76	0.31		1.29	0.53				
	0.20			0.34				
Spring								
Summer								
6.57	3.16	0.04	10.36	4.99	0.32	14.22	2.68	0.32
9.02	1.70	0.20	19.98	3.47				
12.66	2.20	0.14	1.00	—				
0.64			1.14	0.11				
0.73	0.07							
Fall								
8.62	5.24	0.07	7.01	4.26	0.06	7.32	2.22	0.21
9.01	2.73	0.07	11.50	2.35				
14.17	2.89	0.26	3.63	0.63				
3.63			3.40	0.56				
3.40	0.56		0.14	0.12				
Winter								
8.36	6.37	0.22	4.60	3.50	0.28	4.05	3.53	0.38
7.36	6.41	0.51	10.99	3.59		2.55	0.63	
18.33	6.52	0.69	2.20	0.06		1.21	0.04	0.37
4.64	1.15		0.67					
2.20								

¹Wave period in seconds.

the measured distribution calculated from the wave observation data. Considering the errors inherent in the visual data collection method, in the data analyses techniques, and errors resulting from presenting the continuous distribution of wave approach angles as approach sectors, Table 15 shows a favorable comparison.

Table 15. Predicted and measured distribution of wave energy at Wrightsville Beach.

Sector	Sector bisector (rel. to North)	Pct wave energy	
		Predicted	Measured
1	60°	0.8	1.4
2	103.5°	28.0	31.2
3	120°	36.0	38.7
4	137.5°	35.0	28.2
5	180°	0.2	0.8

(b) Bathymetric Data. The wave refraction model requires knowledge of the general bathymetry offshore from the study area to accurately refract the approaching wave sets. The bathymetric data was provided on a 150-meter (500-foot) square-grid spacing which extended from the MLW position of the shoreline to a depth of approximatley 20 meters (65 feet), 15 kilometers (9.4 miles) offshore. The nearshore depths were interpolated from the long beach profiles and the greater offshore depths were measured from 1978 National Ocean Survey (NOS) nautical charts.

The offshore bathymetry of the study area is quite irregular and a qualitative graphical representation of it is shown in Figure 34. This figure is a three-dimensional line drawing display of the data generated by a computer graphics program, and consequently the offshore representation is quite accurate. However, the interpolation scheme used by this program distorted the shoreline position, and a dot screen pattern has been included to alleviate this visual distraction.

(c) Wave Refraction Model. The numerical model used for the wave refraction analysis is a modified version of the wave refraction model developed by Dobson (1967). Dobson's model requires the wave ray to originate in deep water, a condition which is not always practical (or economical relative to computer costs) for long-period waves. Therefore, a subroutine was added to account for the refraction and shoaling of the wave ray which occurs in the deeper offshore regions. This routine assumes that bathymetry in the offshore region has straight and parallel contours. Snell's law is used to compute the refraction coefficient and the change in the wave angle at an economically more reasonable "offshore" boundary for the model. The partially refracted wave ray is then used as the starting condition for Dobson's numerical model which integrates the wave ray through shallower regions toward the



Figure 34. A three-dimensional line drawing representation of the offshore bathymetry (view looking onshore from southeast).

MSL shoreline. For this study, the numerical model offshore boundary extended to about the 20-meter (65-foot) depth contour (MSL), about 15 kilometers (9.4 miles) offshore.

A second modification to the original program was the addition of a subroutine to account for energy losses due to friction. The wave height, H , at any point along the wave ray can be represented by

$$H = H_0 \cdot K_r \cdot K_s \cdot K_f \quad (7)$$

where H_0 is the deepwater wave height, K_r is the refraction coefficient, K_s is the shoaling coefficient, and K_f is the friction coefficient.

Dobson's (1967) original model calculated both the refraction and shoaling coefficients. The additional subroutine calculates the friction coefficient by integrating an expression developed by Skovgaard, Jonsson, and Bertelson (1975) along the wave ray from deep water to the point of interest (optionally the point of wave breaking). The integration is carried out using a trapezoidal integration scheme. The local bottom friction factor is calculated from the local wave conditions by a numerical algorithm developed by Fritsch, Shafer, and Crowley (1973). The expression for the wave friction coefficient, as given by Skovgaard, Jonsson, and Bertelsen, further requires a value for the equivalent (Nikuradse) bottom roughness. A field observation on a sandy coast by Iwagaki and Kakinuma (1963) found that the bottom roughness ranged from 1 to 2 centimeters. For this study, the value of equivalent bottom roughness was determined from the calibration of offshore SSMO wave height (wave energy) data which had been routed inshore to wave height (wave energy) data measured at Johnnie Mercer's Pier gage. Although some uncertainty exists with the SSMO data, as noted in Section 2(a), it was used here in a simple test to determine whether or not the literature values for bottom roughness were applicable on this part of the coast. A value of 1.5 centimeters gave the best results for the comparison of computed and measured wave energy at the beach, and this value falls within Iwagaki and Kakinuma's range of values.

The effect of including bottom friction in the wave refraction model is a reduction in the wave height and, therefore, wave energy as the wave ray progresses into shallow water. It has no effect, within the limits of the linear theory used by Dobson (1967), on the direction of wave propagation; however, reduction of the wave height does affect breaking conditions, as a wave with a reduced height can propagate closer to shore before breaking. For waves in shallow water, solitary wave theory defines the breaking condition

$$\frac{H}{d} = 0.78 \quad (8)$$

where H is the local wave height, and d is the local water depth.

The third modification to Dobson's model was a routine to stop integration of the wave ray when the ratio of wave height to local water

depth exceeds 0.78. To determine the depth at any point along the wave ray, the model uses an algorithm which fits a polynomial to the depth of the surrounding square of eight grid points (relative to that wave ray). Under the rapidly varying bathymetric conditions which exist within the study area, the algorithm often computed nonrepresentative depth values which in turn resulted in offshore wave breaking and caustic (wave crossing) conditions. To help alleviate this problem, the depth grid spacing was increased from 150 meters (500 feet) to 300 meters (1,000 feet), and this modification resulted in a significant reduction in the number of offshore caustics and wave breaking. In addition to this problem, diffraction (i.e., the lateral spreading of energy along the crest of a wave), an important process in "smoothing-out" peaks in wave energy (and height), is ignored by Dobson's model.

Figures 35 and 36 are two computer-generated wave refraction diagrams for a wave approaching from the east with an offshore wave height of 1.4 meters and a period of 10.5 seconds. Figure 35 shows that many of the wave rays cross before reaching the beach or break offshore. Since each wave ray is propagated independently toward the shoreline, the model is "unaware" of the possibility that any two or more wave rays may cross. Linear wave theory is not valid under these conditions; therefore, all wave rays which crossed before reaching breaking condition must be eliminated from the analysis. Figure 36 shows the same wave propagation as in Figure 35; however, all crossed wave rays have been eliminated. The energy, and therefore, wave properties like height, celerity, and angle along a wave crest between two adjacent noncaustic rays, was assumed to be proportional to the energy values of these noncaustic rays. Hence, breaking wave conditions at all locations along the beach were found by linearly interpolating the values between adjacent noncaustic wave-ray locations.

Another shortcoming of Dobson's (1967) model is that the influence of tidal jets and currents near inlets on wave refraction is not considered. Together with the fact that bathymetric changes are rapid in the vicinity of inlets, the resulting values of wave height, angle, and celerity at those locations must be considered with some skepticism.

Computer plots showing the results of the refraction analysis for 1.4-meter waves for each wave period and for all four wave approach angles are contained in Appendix G. The difference between the results of waves having the same period and approach direction, but differing in height, is simply a slight difference in the breaking position of the wave along the same wave-ray path.

3. Energy Flux Computation.

The longshore component of wave energy flux, P_1 , is defined as (U.S. Army, Corps of Engineers, Coastal Engineering Research Center, 1977; Vitale, 1980)

$$P_1 = \frac{\rho g}{16} H^2 C_g \sin 2\alpha \quad (9)$$

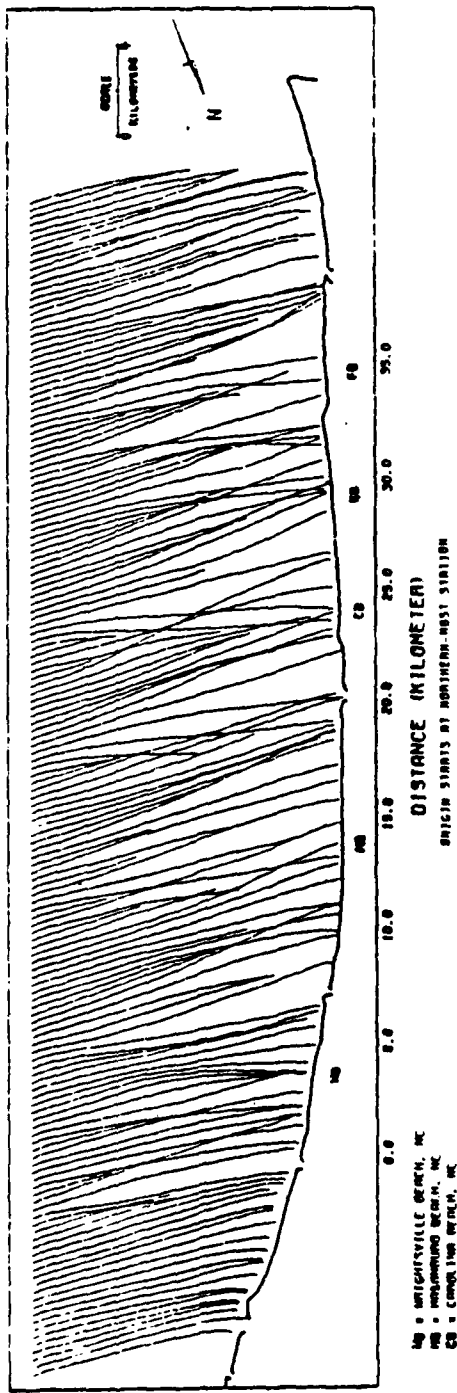


Figure 35. Wave refraction diagram for a medium period wave ($T = 10.5$ seconds; $H = 1.40$ meters from the east).

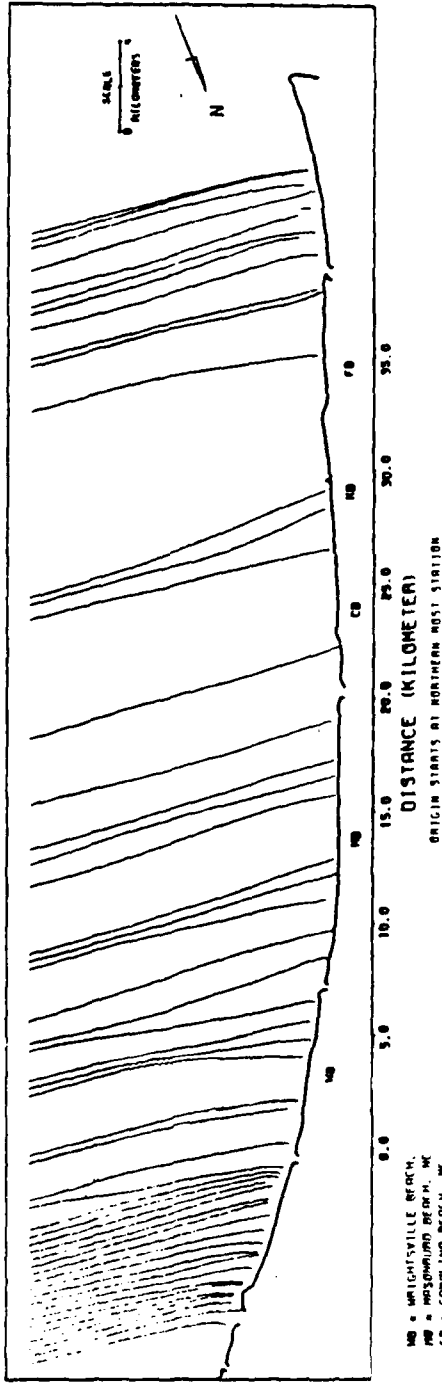


Figure 36. Wave refraction diagram for a medium period wave ($T = 10.5$ seconds; $H = 1.40$ meters from the east) with crossed wave waves eliminated.

where H is the wave height, C_g is the wave group velocity, and α is the angle the wave crest makes with the shoreline. Usually the breaking wave characteristics (H_b , C_{gb} , and α_b) are used to represent the wave energy flux entering the surf zone.

Each wave type was refracted toward shore by the refraction model. The breaking wave values of H_b , C_g , and approach angle, α_b were determined at each breaking wave-ray location, and then interpolated at beach stations every 250 meters along the study area. The shoreline (plan) angle at each of these 250-meter locations was measured from aerial photos and the value of α then determined. The longshore component of wave energy flux at breaking was calculated using equation (9) at each 250-meter beach station, and was then multiplied by that wave type's percent occurrence. A positive value of P_1 represented a component of wave energy flux in a southerly direction and a negative value represented a component in the northerly direction.

As each wave type was refracted toward shore, and the longshore component of wave energy flux was calculated, the percent contribution to either the northerly or southerly components of the annual longshore flux was summed, by direction, with the contribution from the other wave types. The resulting totals at each 250-meter beach station represent the northerly and southerly longshore components of the annual wave energy flux.

The spatial variation of these totals was significant, and the sudden changes in magnitude were not representative of the actual energy flux conditions. Several factors which contributed to this problem were:

- (a) The refraction model used a static representation of shoreline conditions and bathymetry. As soon as a concentration of wave energy in shallow water occurs in the prototype, erosion results and bathymetry changes to reduce the energy concentration; i.e., nature tends to smooth out sudden changes in concentrations of wave energy, but the model cannot.
- (b) The resolution of the computational grid cells close to the beach were not fine enough to allow for the rapid changes in bathymetry and beach planform.
- (c) The energy flux values are proportional to the product of the sine and cosine values of the wave approach angle relative to the beach shoreline. Consequently, subtle errors in offshore angles can result in significant errors in the energy flux computation at the beach face.
- (d) Diffraction effects and the influence of tidal currents were not included.

To overcome these problems, i.e., to remove the rapid fluctuations without significantly altering the longer term trends, a nine-point running filter was applied to the results of the energy flux computations. The running filter averages the values from nine points (in this case, nine 250-meter points are equivalent to averaging over a 2-kilometer stretch of beach) and assigns that average to the middle point. The filter is then moved to the next (middle) point and averages its value with the four values on either side, etc.

Figure 37 shows the filtered results of the northerly and southerly components of the annual longshore energy flux; Figure 38 combines both components and shows the net annual longshore energy flux acting along the study area.

4. Longshore Sediment Transport Model.

The accepted practice for computing the longshore sediment transport rate has been to use an empirical relationship between the longshore component of the energy flux entering the surf zone and the volume of sand moved. This dimensional relationship is given in the Shore Protection Manual (SPM) (U.S. Army, Corps of Engineers, Coastal Engineering Research Center, 1977) and can be expressed as

$$Q \left[\frac{M^3}{yr} \right] = 1,288 \left[\frac{M^3-s}{N-yr} \right] P_{ls} \left[\frac{N-M}{s-M} \right] \quad (10a)$$

or

$$Q \left[\frac{yd^3}{yr} \right] = 7,500 \left[\frac{yd^3-s}{lb-yr} \right] P_{ls} \left[\frac{ft-lb}{ft-s} \right] \quad (10b)$$

where P_{ls} is the energy flux factor and Q is the longshore sediment transport rate. This equation was developed from field observations in which wave height characteristics were represented by only one value--the significant wave height.

In this study, actual longshore energy flux components were calculated for a set of wave types which were subsequently summed together according to their percent occurrence. Consequently, this calculation of the longshore energy flux is not compatible with equation (10) above; hence, the dimensional constants given in the SPM cannot be directly applied or compared. Jarrett (1977) performed a refraction analysis similar to that performed in this study and found a value for the constant by correlating measured volumetric changes along Wrightsville Beach to computed energy flux values at each end of the beach. Jarrett's successful results showed that the same type of relationship which is given in the SPM exists between the computed values of the longshore energy flux and the sediment transport rates. Therefore, that relationship is used in this study and is expressed by

$$Q \left[\frac{L^3}{T} \right] = \beta \left[\frac{L^3}{F} \right] \sum_{i=1}^n (P_{li} P_i)_b \left[\frac{LF}{TL} \right] \quad (11)$$

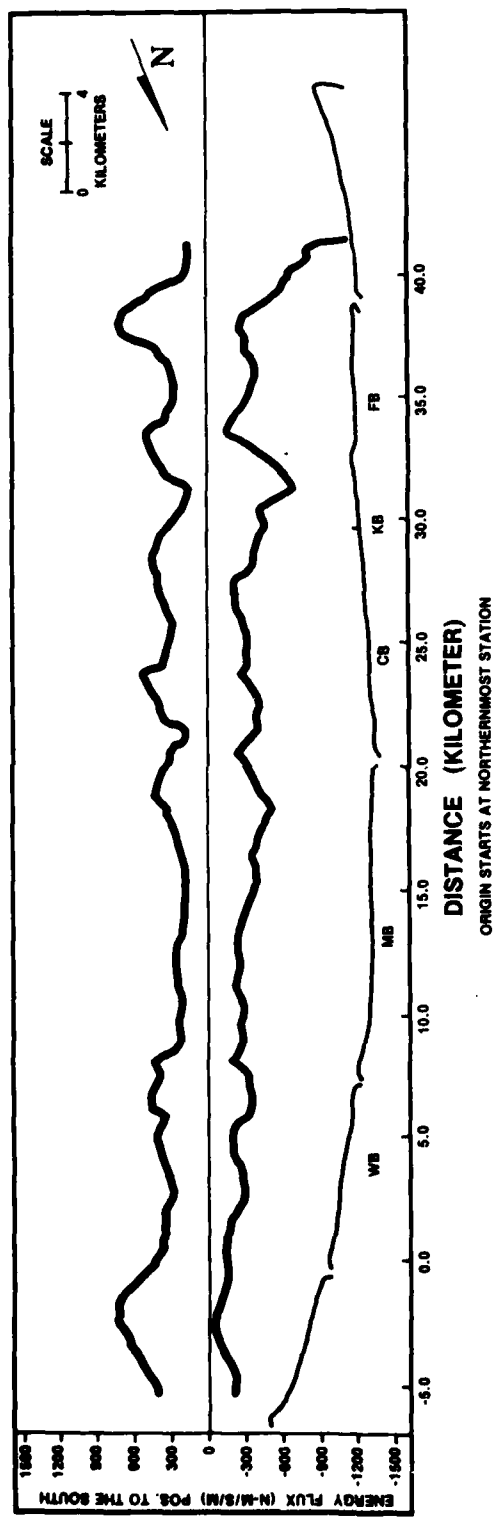


Figure 37. Northerly and southerly components of longshore energy flux along study area.

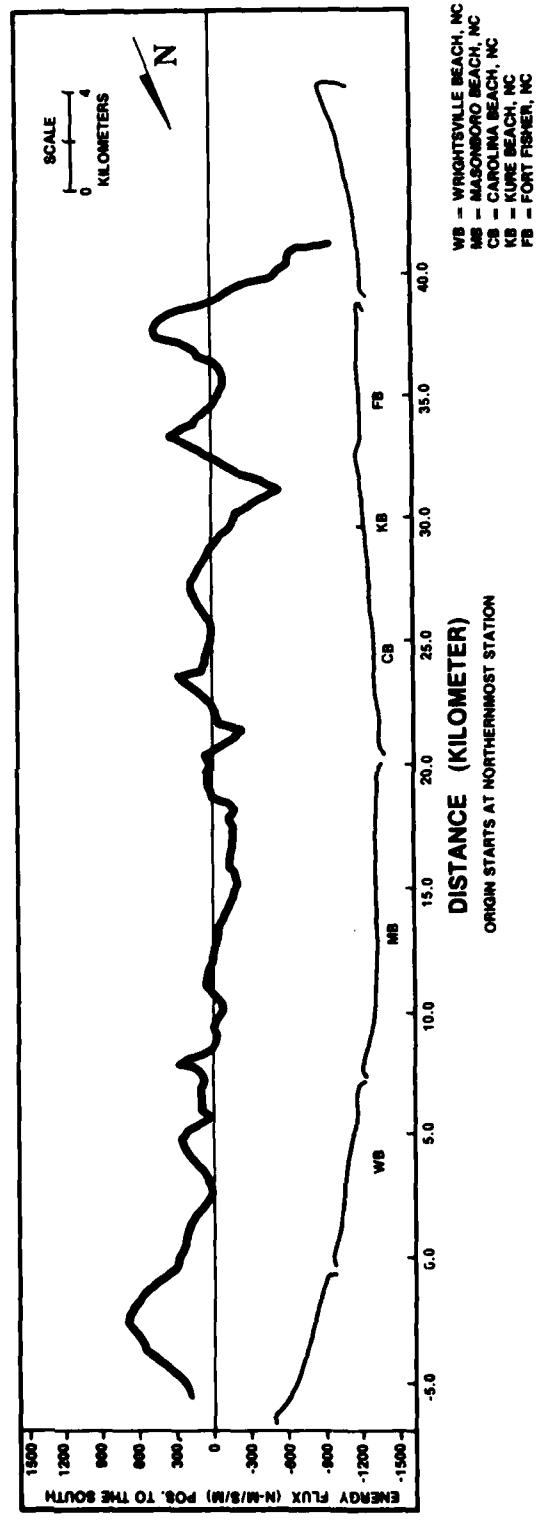
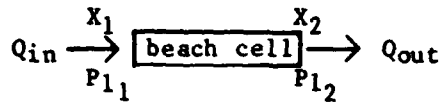


Figure 38. Net annual longshore energy flux along study area.

where n is the number of wave types used to represent the seasonal or annual wave climate, P_{1i} is the longshore component of wave energy flux (at breaking), p_i is the percent occurrence of that wave type, Q is the long-term longshore sediment transport rate, and β is the dimensional constant (found from correlation) relating Q to P_{1b} . The dimensions of each term are shown in brackets.

A sediment budget approach can be used for the correlation of Q and P_1 . For a beach cell, as shown below, Q_{in} represents all long-term sources of sediment supplied into the cell-per-unit time and Q_{out} all long-term losses from the cell-per-unit time. The difference, $Q_{out}-Q_{in}$, represents the long-term change in beach volume for that cell.

The longshore components of wave energy flux, as calculated in Section V,3, are P_{11} and P_{12} and their respective beach coordinates are X_1 and X_2 .



From equation (11), $Q_{out}-Q_{in} = \beta [P_{12}-P_{11}]$. Let q_L be the long-term erosion or accretion rate per unit length of beach, then

$$q_L = \frac{Q_{out}-Q_{in}}{X_2-X_1}$$

and hence,

$$q_L = \beta \left[\frac{P_{12}-P_{11}}{X_2-X_1} \right]$$

or

$$q_L = \beta \frac{\Delta P_1}{\Delta X}$$

In the limit, as $\Delta X \rightarrow 0$

$$q_L = \beta \frac{dP_1}{dX} \quad (12)$$

At any point along the beach, β can be determined from the ratio of the long-term erosion-accretion rate to the spatial gradient of the longshore component of wave energy flux.

Values of measured q_L were taken from all profiles along the beaches away from the immediate area of inlet influence. Unfortunately, due to the insufficient temporal and spatial distribution of profile data, volumetric change data for Masonboro, Kure, and Fort Fisher Beaches were not calculated. Only values for Wrightsville and Carolina Beaches, in Tables 7 and 10, were compared to predicted values. A plot of q_L and β (dP_1/dX), versus beach distance X , was drawn by choosing a value of β which produced the best correlation between the two lines. To eliminate sudden computational fluctuations before comparison with measured q_L values, the $\beta dP_1/dX$ values were filtered to produce smoothly varying distribution.

Figures 39 and 40 show the results of these comparisons for Wrightsville Beach and Carolina Beach, respectively. Although considerable scatter in the values of q_L is obvious, especially along the northern Carolina Beach region, the general trends of both the computed and measured volumetric change values are similar along each beach.

Within the limitations of the analysis, it appears that a value of $\beta = 300 \text{ m}^3\text{-s/N-yr}$ provides the best fit for Wrightsville Beach with a data scatter of +33 percent. For Carolina Beach, the best-fit value is $\beta = 900 \text{ m}^3\text{-s/N-yr}$ with a data scatter of +66 percent. These results as summarized in Table 16, show a large possible range in values of β . Assuming that equation (11) is a valid representation of the relationship between the longshore sediment transport rate and the longshore component of wave energy flux, then two possible conclusions can be made. First, the value of β is highly localized and strongly dependent on the local physical characteristics of the beach and sediment properties. Table 3 shows that the sediment characteristics do change along these beaches, and differences in offshore beach slopes between Wrightsville Beach and Carolina Beach were discussed in Section II. The second possible conclusion, and probably the more dominant one for this study, is that the value of β is very sensitive to the method of computation of the variables in the rates $q_L/(dP_1/dX)$. In particular, errors inherent within the refraction analysis technique can result in significant spatial variation of the energy flux and hence in the dP_1/dX values. This variation is then reflected in the spatial variation of the β values.

Table 16. Values of β for Wrightsville and Carolina Beaches.

Beach	Values of β in units of $\text{m}^3\text{-s/N-yr}$		
	Best fit	Lower bound	Upper bound
Wrightsville	300	200	400
Carolina	900	300	1,500

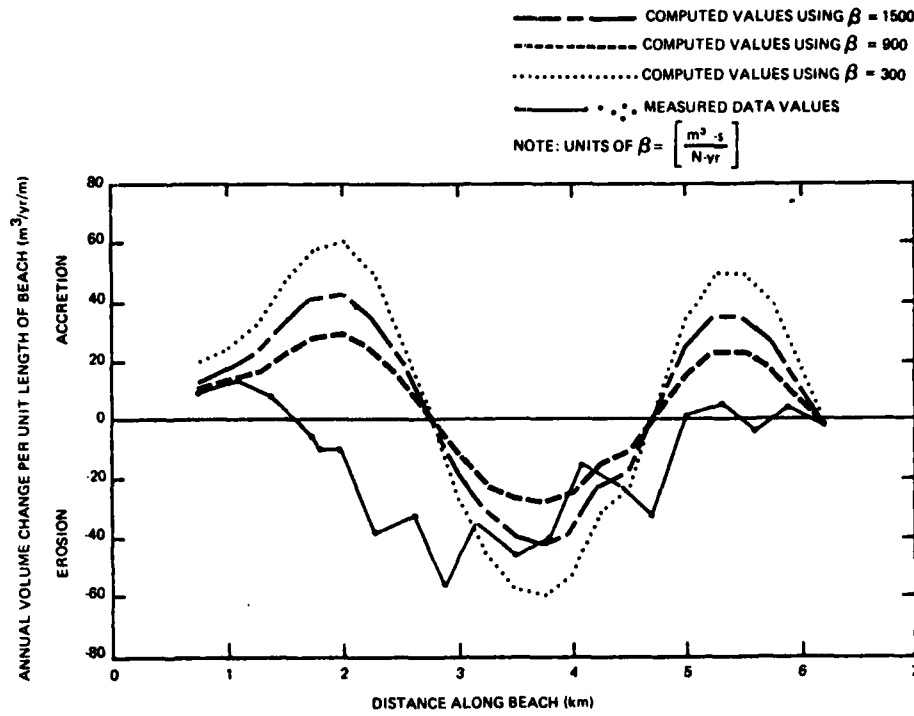


Figure 39. Comparison of measured and computed volumetric change along Wrightsville Beach.

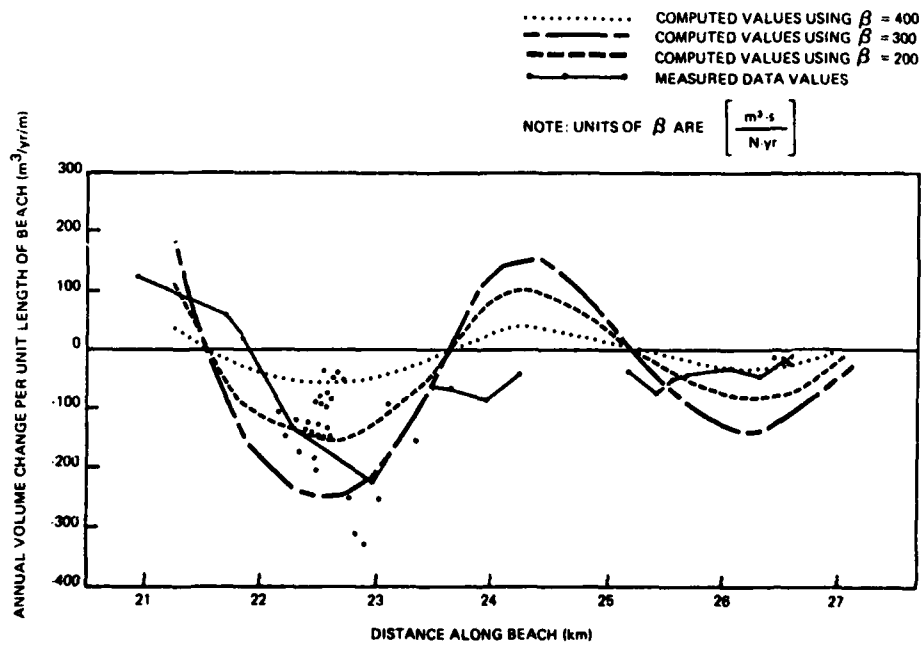


Figure 40. Comparison of measured and computed volumetric change along Carolina Beach.

Comparison of the results of this study with those of Jarrett's (1977) are encouraging. Although Jarret calculated his β value based only on the midsection of Wrightsville Beach, his value of $\beta = 418 \text{ m}^3 \cdot \text{s} / \text{N} \cdot \text{yr}$ is approximately equal to the upper limit of the value of β for Wrightsville Beach as predicted by this study.

5. Sediment Budget.

To illustrate the application of the sediment transport model in estimating the northerly and southerly longshore transport rates and the quantity of material lost into the adjacent inlets, sediment budgets using littoral cells of finite length along Wrightsville and Carolina Beaches were performed. Each beach was divided into the three cells which, as described in Section IV, 4, best represent the long-term volumetric changes along those beaches. Losses from the active profile due to a rise in sea level, losses from the beach due to inlet trapping, and losses or gains in each cell due to longshore sediment transport were all considered. The long-term excursion rates which were used to determine the annual volumetric beach change for each cell were calculated by eliminating identified excursions, both within the project boundaries and along downdrift beaches, due to the placement and subsequent initial erosion of beach fills. Consequently, the contributions to, and the commensurate offshore losses from, the overall sediment budget due to beach-fill operations were addressed and do not need to be further incorporated into the sediment budget equations. Aeolian losses were considered inconsequential (U.S. Army Engineer District, Wilmington, 1977) and also were not included. An inherent assumption within this approach to developing a sediment budget is that offshore losses due to ongoing sorting of freshly exposed beach face is minimal. This assumption is addressed later in Section VI and was found to be valid.

Based on the concept of maintenance of an equilibrium profile under rising sea conditions (Bruun, 1962), the annual volumetric loss of sediment due to a sea level rise is shown in Tables 6 and 17. Losses due to wave overtopping occurred only along the northern section of Carolina Beach. Aerial photos taken in May 1964 and November 1974 were used to estimate the bayward excursion of the bayside shoreline. Results from that analysis indicated that approximately $4,600 \text{ m}^3/\text{yr}$ was lost from the oceanside of Carolina Beach (U.S. Army Engineer District, Wilmington, 1977).

Table 17. Annual volumetric changes in beach-cell volume and losses due to sea level rise and wave overtopping.

Beach cell	Change in beach-cell volume (m^3/yr)	Loss due to sea level rise (m^3/yr)	Loss due to wave overtopping (m^3/yr)
Wrightsville (north)	-24,430	2,289	--
Wrightsville (central)	-7,530	1,873	--
Wrightsville (south)	-12,370	1,457	--
Carolina (north)	+104,500	700	4,600
Carolina (central)	-269,750	1,582	--
Carolina (south)	-107,970	2,285	--

The sediment budget equations for a typical beach cell (see Fig. 41) are:

Sediment sources: $Q_{n-1,n} + Q_{n+1,n}$

Sediment losses: $Q_{n,n-1} + Q_{n,n+1} + SL_n + OT_n$

Annual volumetric beach change:

$$V_n = Q_{n-1,n} + Q_{n+1,n} - Q_{n,n-1} - Q_{n,n+1} - SL_n - OT_n \quad (13)$$

where n , $n-1$, and $n+1$ are individual beach cells, SL_n is the annual sediment loss from cell n due to the rise in sea level, OT_n is the annual sediment loss from cell n due to wave overtopping, and $Q_{n,n+1}$ is the annual longshore sediment transport from cell n into cell $n+1$.

Equation (11) is used to predict the quantity Q between littoral cells located on a continuous beach; however, a problem with this formulation arises when a cell boundary borders an inlet, weir jetty, headland, etc. In these situations, the actual quantity of sediment moving in the littoral drift may be less than that predicted by equation (11) and so a modification must be incorporated into the sediment budget equations. The actual longshore sediment transport rate, Q_a , is related to the potential longshore sediment transport rate by the "efficiency factor," α , such that

$$Q_a = \alpha (\beta P_1) \quad (14)$$

Along straight and continuous beaches, the value of α must be unity; however, at inlets and other sediment traps, its value is less than or equal to one. In extreme cases of total sediment removal, the value of α is zero. The solution of all sediment budget equations for a set of littoral cells defines the values of α at each cell boundary.

The sediment budget schematizations for Wrightsville and Carolina Beaches are shown in Figure 42. The values of the northerly and southerly components of the longshore energy flux at each littoral cell boundary are shown in Table 18. The values of β used in the longshore sediment transport equations were $\beta=300$ for Wrightsville Beach and $\beta=900$ for Carolina Beach. The measured volumetric change within each cell, the annual volumetric loss due to sea level rise, and the loss due to wave overtopping are shown in Table 17.

The sets of α values at each inlet boundary (i.e., $\alpha_{1,2}$ and $\alpha_{2,1}$; $\alpha_{4,5}$ and $\alpha_{5,4}$; and $\alpha_{7,8}$ and $\alpha_{8,7}$) cannot be uniquely determined (there are more unknowns than equations) and therefore, the values of one efficiency factor of each pair must be assumed. For an unimproved inlet (i.e., no jetties, weirs, etc.), it was assumed that all sediment contained within the littoral drift system entered the inlet cell. In this case, the northerly longshore transport from the northern ends of Wrightsville and Carolina Beaches was assumed to enter Mason and Carolina Beach Inlets, respectively. Consequently, $\alpha_{2,1}$ and $\alpha_{8,7}$ were set equal to one and the sediment budget equations solved resulting in the values of $\alpha_{1,2}=0.09$ and $\alpha_{7,8}=0.31$.

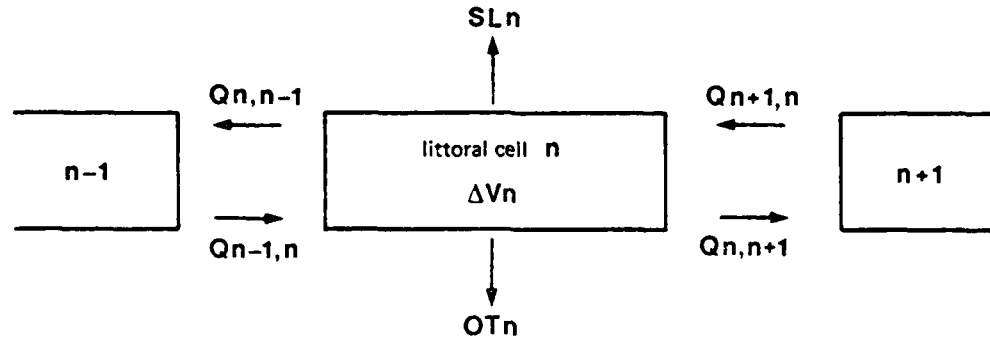
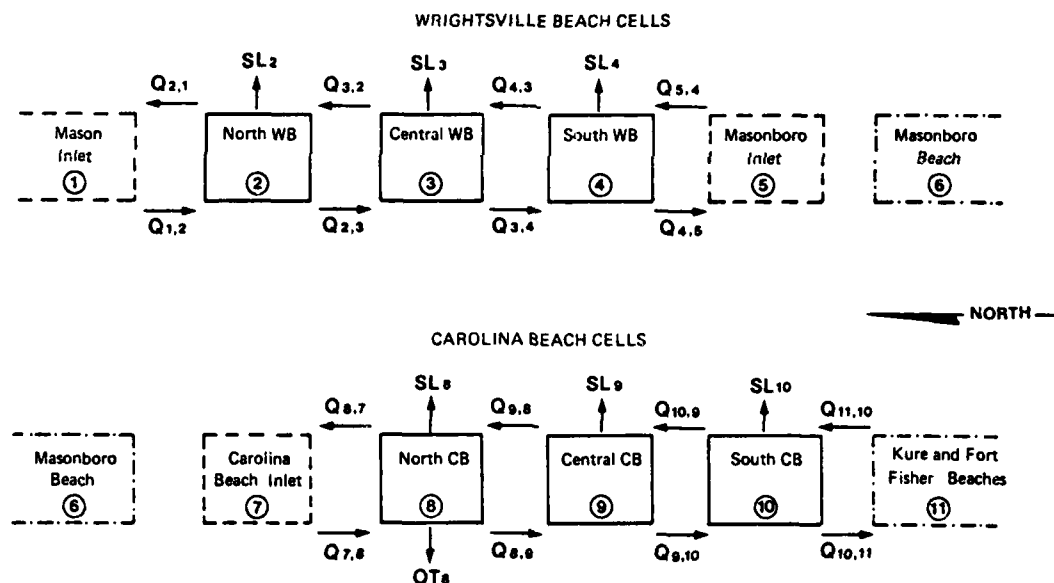


Figure 41. Beach-cell schematization.



Note: Arrows indicate direction of sediment movement.

Figure 42. Sediment budget schematics for Wrightsville Beach and Carolina Beach.

Table 18. Energy flux values at cell boundaries.

Beach cell	Cell No.	Cell boundaries (km)	Gross northerly flux		Gross southerly flux	
			Notation	Magnitude (N-m/s/m)	Notation	Magnitude (N-m/s/m)
Northern boundary (Mason Inlet)	1	0.0	—	—	P _{1,2}	421.5
Wrightsville (north)	2	0.0-2.5	P _{2,1}	115.8	P _{2,3}	287.6
Wrightsville (central)	3	2.5-4.8	P _{3,2}	290.0	P _{3,4}	424.3
Wrightsville (south)	4	4.8-6.7	P _{4,3}	175.3	P _{4,5}	446.3
Masonboro Inlet	5	6.7-7.2	P _{5,4}	352.8	—	—
Carolina Beach Inlet	7	19.7-20.5	—	—	P _{7,8}	310.2
Carolina (north)	8	20.5-21.5	P _{8,7}	226.7	P _{8,9}	165.6
Carolina (central)	9	21.5-24.3	P _{9,8}	418.6	P _{9,10}	350.0
Carolina (south)	10	24.3-27.3	P _{10,9}	305.0	P _{10,11}	386.5
Kure and Fort Fisher	11	27.3-42.0	P _{11,10}	224.2	—	—

These values indicate that approximately 90 percent of the potential southerly longshore sediment transport remained trapped in Mason Inlet and 70 percent remained in Carolina Beach Inlet.

The north jetty at Masonboro Inlet was completed in spring 1966 and consists of a rubble-mound outer section and a low concrete sheet-pile inner or weir section. The design of this weir jetty and the dredging of material from the deposition basin on the inlet side of the weir have caused a reduction in the northward sediment bypassing to near zero (U.S. Army Engineer District, Wilmington, 1977). Therefore, $\alpha_{5,4}$ was set equal to zero and the solution of the sediment budget equations gave $\alpha_{4,5}=0.64$. This means that approximately two-thirds of the potential littoral drift passes over or around the weir jetty into Masonboro Inlet and one-third remains trapped on the southern end of Wrightsville Beach, providing a source of material for northerly transport. Table 19 gives the α values for the Wrightsville Beach and Carolina Beach sediment budgets.

Table 19. Efficiency factors α for Wrightsville and Carolina Beach sediment budgets.

Beach cell	Cell No.	Northerly transport		Southerly transport	
		Notation	Factor	Notation	Factor
Mason Inlet	1	—	—	1,2	0.09
Wrightsville (north)	2	2,1	1.0	2,3	1.0
Wrightsville (central)	3	3,2	1.0	3,4	1.0
Wrightsville (south)	4	4,3	1.0	4,5	0.64
Masonboro Inlet	5	5,4	0.0	—	—
Carolina Beach Inlet	7	—	—	7,8	0.31
Carolina (north)	8	8,7	1.0	8,9	1.0
Carolina (central)	9	9,8	1.0	9,10	1.0
Carolina (south)	10	10,9	1.0	10,11	1.0
Kure and Fort Fisher	11	11,10	1.0	—	—

Analyses were performed to include Masonboro, Kure, and Fort Fisher Beaches into one continuous sediment budget analysis; however, the lack of reliable long-term volumetric change data along those beaches meant that large and somewhat arbitrary changes in either the volumetric excursion rates, energy flux values, or β values were needed to balance all sediment budget equations. Because of these changes, the results were not meaningful and are not presented.

VI. BEACH-FILL PERFORMANCE

All beach fills placed along the study area between 1965 and 1975 were discussed in Section II; Table 4 and Figure 8 of Section IV show additional detailed information on their location and time of placement. The beach fills are also discussed in Vallianos (1970), U.S. Army Engineer District, Wilmington (1970, 1974, 1977), and Jarrett (1977). Information presented in this section is based on the quantitative interpretation of the excursion distance analyses of the 1970 beach fill on Wrightsville Beach and of the 1965 and 1971 beach fills on Carolina Beach. There was insufficient repetitive profile information for the other fills to allow excursion analysis and subsequent fill performance evaluation.

The 1970 beach fill along the central part of Wrightsville Beach was the best documented (in terms of repetitive beach surveys before and after placement of fill material) beach-fill project, and the excursion distance plots of profiles WB13 to WB29 (App. A) show the response of the beach to this fill. Sequential profiles showing the post-fill behavior at profile WB-15 are presented in Appendix F. All relevant data from all of these plots are summarized in Figure 43 which shows the spatial variation along the beach of the initial fill excursion, the percent total initial losses, the net excursion after initial losses, the long-term erosion rate, and the value of the exponential decay constant, k . All values in the figure are averaged from the MLW, MSL, and MHW excursion distance plot of each profile located along the central section of Wrightsville Beach.

The average initial fill excursion, as defined by the first measurements taken after fill placement, was 76.6 meters, and the distribution of the fill along the beach was almost triangular. The maximum initial excursion was approximately 125 meters in the middle and the excursion at the project boundaries was approximately 50 meters. Figure 43 shows that beach excursions were measurable along the beaches on either side of the project boundaries soon after the initial fill placement. These edge excursions indicate that some of the material placed within the project limits of the fill quickly spread laterally to the adjacent beaches. The average fill excursion remaining on the beach face, after all initial losses had occurred (approximately 2 years), was 15.5 meters with a maximum retention of 29 meters in the middle of the fill. This means that 80 percent of the initial fill was lost due to sorting, slope readjustment, and lateral spreading. The southern end of the fill experienced the highest initial loss of 90 percent where only 5 meters of fill still remained after approximately 1.5 years.

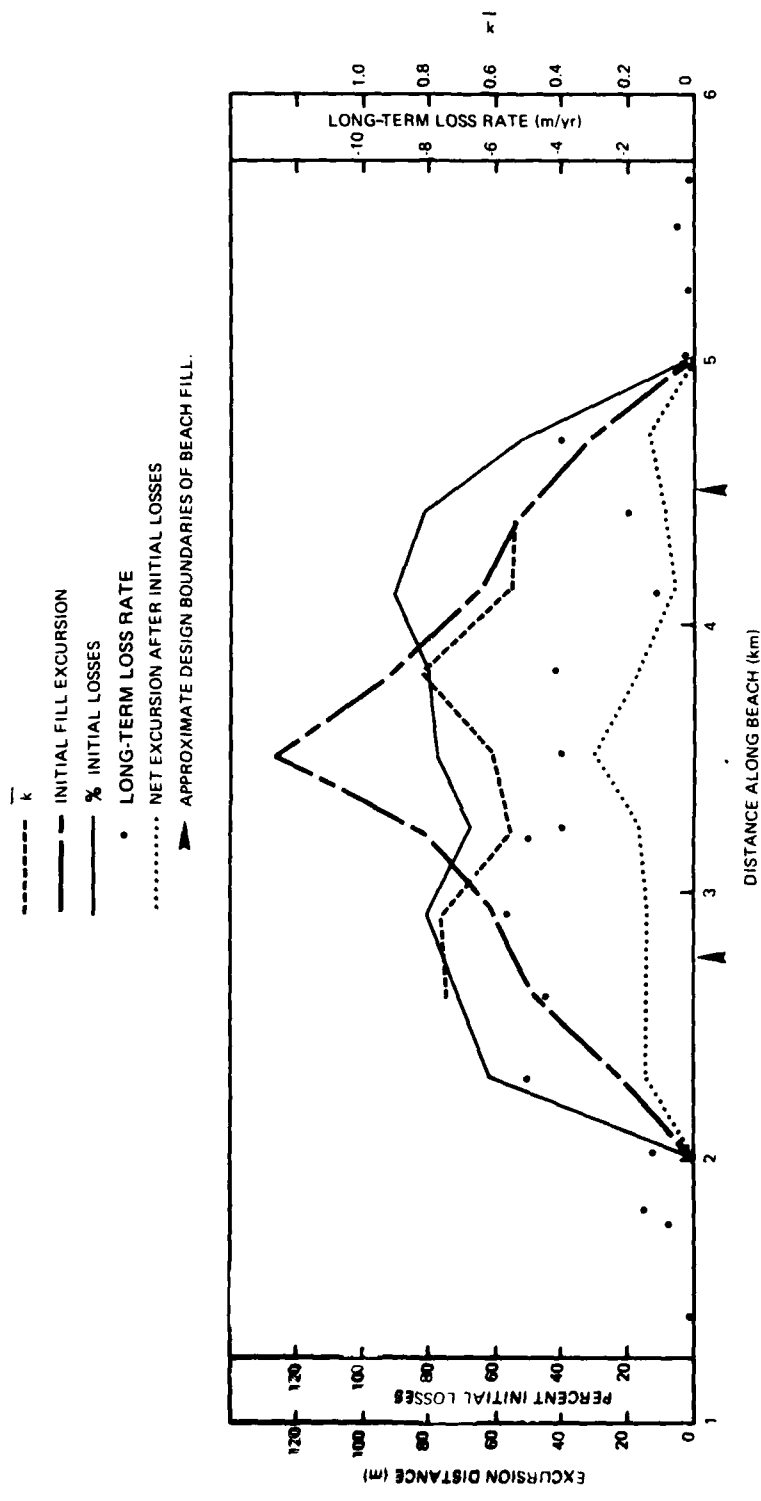


Figure 43. Wrightsville Beach 1970 beach fill.

During the calculation of volumetric change between two subsequent profiles, based upon the application of the volumetric equivalent factor to the MLW-MHW contour excursions of those profiles, an assumption of self similarity in profile shape was employed. In other words, volumetric changes were assumed to occur only as a result of horizontal displacement of the profile and not to the redistribution of material from the upper beach face offshore, a phenomenon which occurs during the slope readjustment phase of the beach-fill response. Consequently, the total initial volumetric loss for the fill may be slightly less than the 80 percent value; however, the average initial loss in beach face position is still 80 percent of the fill excursion.

The adjustment during the design phase of the project for the expected sorting losses was accomplished by applying a factor known as the critical ratio (or beach-fill factor) to the required volume of beach fill. The critical ratio is simply an estimate of the quantity of borrow material required to yield 1 cubic meter of beach material having granulometric characteristics similar to the native beach. The value calculated for the Banks Channel borrow site, and which was applied to the Shell Island borrow material, was 2.5 (U.S. Army Engineer District, Wilmington 1977). This means that 2.5 cubic meters of fill material was required to produce 1 cubic meter of fill material on the beach after sorting; i.e., a 60-percent sorting loss was expected.

A modification to the original fill-factor formulation was developed by James (1965) and has now been incorporated into modern beach-fill design practices (U.S. Army, Corps of Engineers, Coastal Engineering Research Center, 1977). Granulometric data from profiles taken in July 1969 just before the fill and samples taken from profiles along the fill just after placement are shown in Table 20. These values were used to calculate the adjusted fill factor, R_A , from Figure 5.3 of the SPM. The value of the adjusted fill factor was $R_A=3.0$, which implies that 66 percent of the initial fill was lost to sorting. The new adjusted fill factor predicted larger sorting losses than did the older formulation; however, both methods predicted losses that were lower than that measured. Assuming that these formulations are correct, then losses in addition to sorting (slope readjustment, lateral spreading, etc.), are significant and must be included in the beach-fill design.

Table 20. Granulometric data for Wrightsville Beach 1970 beach fill.

Granulometric conditions	Date	Profile	Composite mean grain size μ (in phi units)	Composite standard deviation ζ (in phi units)
Before fill	July 1969	WB16 WB29	1.53 1.52 1.52	0.41 0.83 0.87
Prefill composite values				
After fill	Aug. 1970	WB13 WB19 WB25	2.23 1.64 1.78 1.88	0.49 0.76 0.83 0.69
Prefill composite values				

The values in Table 20 were also used to calculate James' (1974) renourishment factor, $R_j=1.9$. This factor expresses the ratio of the retreat rate of the beach after fill placement to the retreat rate before beach-fill operations. However, in its derivation, James (1974) assumed that the postfill retreat rate was linear and not exponential. Therefore, its value cannot be compared to the results of this study.

The relative changes in the upper beach-face angle (from MHW to MLW) after fill placement were measured for profile WB17. Figure 44 shows that immediately after placement the average beach face angle was 1 on 57, which was flatter than the prefill angle of 1 on 35. The beach angle changed fairly rapidly during the first 6 months after placement, and after 9 to 12 months, the difference in the average beach angle at that time and the long-term beach face angle was less than the expected difference due to seasonal fluctuations. It is apparent that a significant proportion of the upper beach slope adjustments and sorting losses occurred during the first 9 to 12 months. After that period, the upper beach face retreated with a fairly constant slope.

The value of the exponential decay constant, determined from the average of the individual k values for each of the MLW, MSL, and MHW excursion plots from each profile, was $k=0.66$. Substituting this value into equation (4), together with $\zeta=0.8$ and $S_t=0.95\zeta f_i$, gave $t_1=1.8$ years; i.e., effectively all initial losses due to sorting, slope adjustment, and lateral spreading occurred during the first 1.8 years after fill completion. Substituting $k=0.66$, $\zeta=0.8$, and $E_t=0$ into equation (6) produces $t=4.06$ years. This means that the beach face eroded back to its original prefill position 4.06 years after fill completion, and that the beach-fill project effectively "bought" this time for the beach segment within the project boundaries by artificially placing sand on the beach. This is in agreement with observed behavior. Between October 1970 and December 1974, an estimated 91 percent of the initial beach fill was lost (U.S. Army Engineer District, Wilmington, 1977), and the sequential beach profiles in Appendix F show that by April 1974 the location of profile WB15 was approximately in its pre-1970 beach-fill position. Only a few percent of the initial fill was retained above the MHW contour after 4 years and, unfortunately, little information is available to describe the changes in offshore bathymetry. Downdrift beaches benefited from the fill due to alongshore transport away from the fill site. However, quantification of this benefit was not possible due to the masking effect of the seasonal variations in beach position.

Assuming that only slope and sorting adjustments occurred during the first 9 to 12 months, then solving equation (4) for S_t at $t_1=0.75$ and $t_2=1.0$ indicates that 54 to 62 percent of the total initial fill volume was lost to sorting and slope adjustment. This range compares favorably with the values of 60 to 66 percent sorting loss estimated by the adjusted fill factor and critical ratio techniques, respectively.

The rate of initial loss of beach material was not constant along the length of the beach-fill project. The k values calculated for

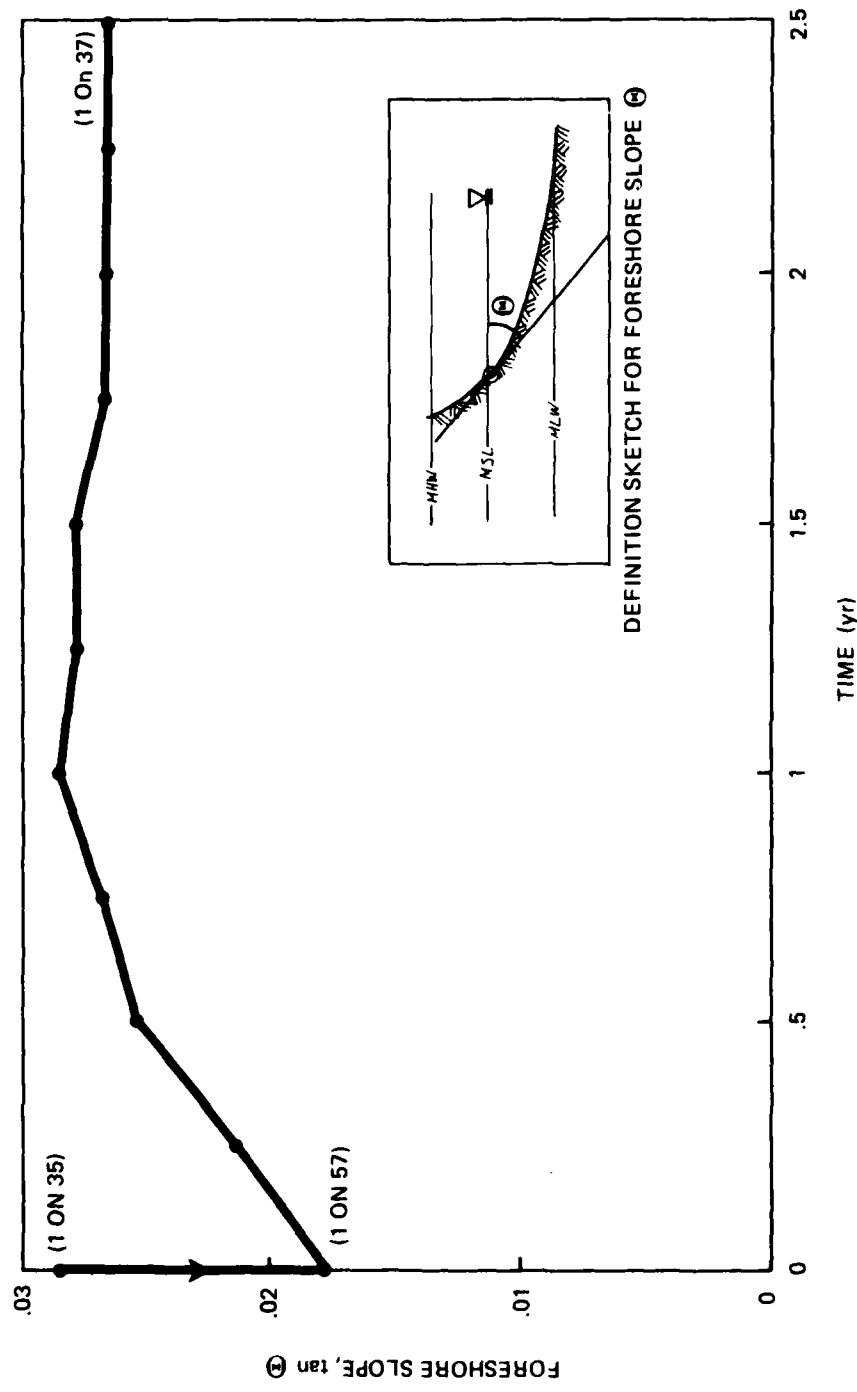


Figure 44. Response of foreshore slope after Wrightsville Beach 1970 beach fill.

profiles near the ends of the fill tended to be slightly higher than those for profiles located in the middle. This implies that the ends of the fill eroded at a slightly faster rate than did the center, which can be expected since the relative changes in beach angle and nearshore bathymetry at the ends are greater than the relative changes in the center, and thus cause greater concentration of wave energy and sediment transport. Together with the fact that 20- to 30-meter excursions occurred on either side of the fill soon after placement, this information supports the concept that significant quantities of fill material spread laterally from the fill ends. It should be noted, however, that nonhomogeneity in the fill material properties may have been the real cause of the variation in the rate of initial loss along the project length. Approximately 70 percent of the fill material was obtained from a shoal in the Banks Channel, and the balance which was extremely fine sand of poor beach-fill quality was obtained from the sound area behind Shell Island (U.S. Army Engineer District, Wilmington, 1977).

The most significant feature of the variation in long-term excursion rate along central Wrightsville Beach is that the rate calculated for the 1965 to 1975 decade (i.e., 5 years before and 5 years after fill placement) was significantly higher in the vicinity of the fill than along adjacent beach sections. This means that the reason for the high erosion rates, which existed before and probably resulted in the need of the 1970 fill, still existed after 1970 and caused high annual sediment losses to the fill.

There are two possible causes for these localized higher erosion rates. In 1965, the north jetty of Masonboro Inlet was completed and effectively cut all northward sand transfer from Masonboro Island to Wrightsville Beach. Consequently, Wrightsville Beach suffered higher erosional losses since 1965 due to the partial lack of sediment supply. South of the fill the growth of the accretion fillet may have offset the increased erosional trends; however, the same is not true for the area adjacent to the north fill boundary.

An oblique aerial photo of Wrightsville Beach taken between 1968 and 1969 (Fig. 45), shows a significant deviation in the present-day shoreline alignment near the center of the island. The uniform-width dark band between the beach and the seawardmost houses is the grassed part of the constructed dune of the 1965 beach-fill project. The misalignment of the north end of the Wrightsville Beach fill, relative to the present tendency of the shoreline, resulted from Moore Inlet which, prior to its artificial closure in 1965 as part of the overall beach nourishment plan, was located just north of arrow A. The closure of Moore Inlet eliminated the interaction between tidal and littoral forces in this area, which had existed since 1887 and which had combined to form a seaward concavity in the shoreline alignment immediately south of the inlet. Erosion prior to the 1965 beach fill exposed the northern building line of the township of Wrightsville Beach and so the alignment of the 1965 beach fill was forced to follow this line, thus causing a bulge in the resulting beach planform. Arrow B points to profile

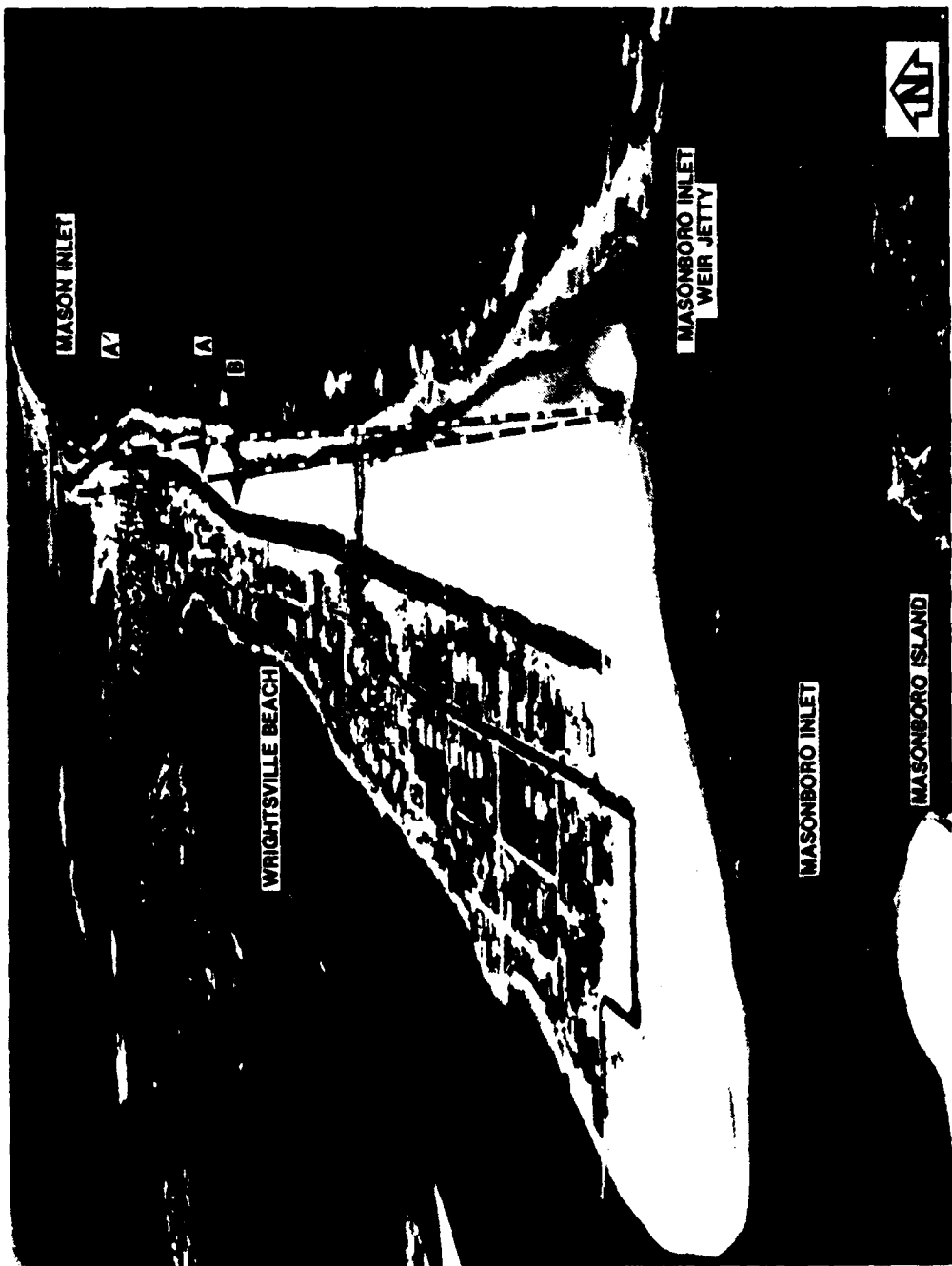


Figure 45. View of Wrightsville Beach looking north-northeast.

WB36, the approximate start of the alinement problem. Between 1965 and 1970, the beach on the north side of the Masonboro Inlet jetty accreted, however, the central island bulge and alinement problem remained. The 1970 beach fill was placed approximately between arrows A and A', thus reinforcing the beach alinement problems. The greater relative change in beach planform and nearshore bathymetry in the central section of the island from 1965 to 1975 resulted in higher wave activity and erosional trends.

Natural beach processes tend to focus on and smooth out irregularities, thus creating a smoothly curving beach as is idealized by the dashline in Figure 45. The high rates of erosion and initial losses associated with the 1970 beach fill may not be typical of all beach fills, but may have been partly caused by the exposure to increased wave attack due to the misalignment of the beach planform. The resulting implication means that if improvement in performance of a future beach fill located in the same area is desired, then additional fill should be placed along the adjacent beaches, as shown by the dot-dash line in Figure 45, to remove the alinement problem. This, however, may not be an economically feasible solution.

Information obtained from the postfill beach response was used to examine the assumption in the sediment budget analysis that offshore losses due to sorting of freshly exposed beach material were minor. Equation (6) showed that 4.06 years after the fill placement, the beach returned to its prefill position and with approximately the same nearshore profile (Fig. 44). This means that whatever came into the fill area during the 4.06-year period was transported out by the end of that time.

The sources of sediment include longshore transport into the fill region, material placed during the beach-fill operations, and material brought ashore by seasonal onshore transport. Losses of sediment include longshore transport out of the fill region, losses due to sorting of the beach fill, seasonal losses due to offshore transport, losses due to the rising sea level, overwash, and aeolian processes. Since the pre- and end-of-period profiles had approximately the same shape, the net volumetric changes due to slope readjustment were zero. Over an even 4-year period, seasonal changes should approximately balance out, and so within the limits of accuracy of this study, the net on/offshore contribution was set to zero. Volumetric gains from the beach fill (BF) were determined from surveys, and associated sorting losses (sorting) were calculated using the adjusted fill factor (R_A). Losses due to sea level (SL) were calculated by use of Bruun's (1962) formulation. Aeolian and washover losses were near zero. Since the net volume change at the end of the 4.06-year period was zero, then the net volumetric change due to alongshore transport of the boundaries ($Q_{in} - Q_{out}$) must equal the difference between these identified sources and sinks since the fill area was away from active inlets, jetties, etc.; i.e.,

$$Q_{in} - Q_{out} + BF - \text{sorting} - SL = 0$$

or

$$Q_{in} - Q_{out} + BF/R_A - SL = 0$$

Substituting in values from Tables 4 and 6 and with $R_A=3$, the annual volumetric change due to alongshore transport was

$$Q_{in} - Q_{out} = -86,125 \text{ m}^3/\text{yr}$$

From equation (11)

$$Q_{in} - Q_{out} = \beta (P_{lin} - P_{lout})$$

and from Figure 38

$$P_{lin} - P_{lout} = -300 \text{ N-M/S-M}$$

and hence

$$\beta = 287 \text{ m}^3\text{-s/Nyr}$$

Within the limits of accuracy of both the data and technical analyses, this simple postfill sediment budget determination, where all contributions to the sediment budget were quantified, produced a value of β which was very close to that calculated earlier (mean value of $\beta = 300$) when using long-term beach response characteristics and where the losses due to sorting of "freshly" exposed native beach material by ongoing erosion was assumed to be small. Since the calculated values of β are similar and they come from analyses of two distinct phases of beach response, these results support the contention that ongoing sorting losses during the long-term response phase are minimal.

Analysis of the spatial variation of the beach response to the 1965 and 1971 beach fills along Carolina Beach was not possible because of insufficient profile information. Results for the 1965 fill, as shown by the beach photos in Figure 46, were determined from MLW, MSL, and MHW excursion distance plots for profiles CB106 and CB107 which were less than 0.5 kilometer apart. Consecutive profiles at CB97 were used to determine the response to the 1971 beach fill. The average exponential decay constant, the average initial fill excursion, and the average long-term erosional rate are given in Table 12. Substituting these values into equation (4) indicates that most initial losses occurred during the first 1.5 to 2 years following both fills, in agreement with observed behavior (U.S. Army Engineer District, Wilmington, 1970). Using the values contained in Table 12 and assuming $\zeta=0.8$, equation (6) predicts that 2.4 years and 2.25 years after the 1965 and 1971 fill projects, respectively, the beach face eroded to approximately its original prefill position. These values are in reasonable agreement with recorded observations on the loss of beach fill during the 2 years following each fill (U.S. Army Engineer District, Wilmington, 1977).

Granulometric data taken immediately after fill placement in 1965, and taken again 2 years later, are shown in Table 21. These data were used to calculate a critical ratio of 2.1 for the fill material, and thus an expected 55 percent volumetric loss due to sorting (U.S. Army Engineer District, Wilmington, 1970). Results from profile 'B106 tend to show that 50 percent of the initial excursion was lost during the first 1.5 to 2 years, close to the design value. The adjusted fill factor and James' (1975) renourishment factor were evaluated from the same data and were found to be $R_A=1.02$ and $R_j=0.25$, respectively. For the 1965 Carolina beach-fill data, the adjusted fill-factor techniques predicted a value of expected sorting loss significantly lower than both



Before restoration (1964)



After restoration (1965)

Figure 46. Views of Carolina Beach shoreline before and after construction of 1965 beach-fill project.

Table 21. Average granulometric data for Carolina Beach 1965 beach fill.

Granulometric conditions (date)	Composite mean grain size μ (in phi units)	Composite standard deviation ζ (in phi units)
Spring 1965 (time of fill)	0.96	1.23
May 1967 (2 years after fill)	1.69	0.91

the value calculated by the critical ratio technique and the actual measured loss from one profile. Granulometric data were not available for the 1970 Carolina beach fill.

With only data from two beach fills, a relationship between the exponential decay constant k and granulometric properties of the beach fills was not investigated.

VII. SUMMARY AND CONCLUSIONS

During the period from 1964 to 1975, 2,952 repetitive beach profiles were recorded at 241 stations between Wrightsville Beach and Fort Fisher Beach. The total length of Wrightsville and Carolina Beaches represented only 32 percent of the total length of the study area, but nearly 70 percent of all beach profile stations and 89 percent of the total number of recorded profiles were located along these two beaches. Of the nearly 3,000 profiles, only 4 percent extended beyond the MLW position to approximatley the -10 meter contour. As a consequence, volumetric changes representative of actual changes occurring between successive surveys could not be calculated by simply measuring the change in area under the measured profile curves because significant changes occur below the low water line.

The positions of the MHW, MSL, MLW, -1.83 meters (-6 feet), -3.66 meters (-12 feet), and -5.49 meters (-18 feet) contours were plotted relative to a fixed base line, for all profiles. The excursion distance of each contour between successive profiles is indicative of volumetric change, the magnitude of which is found by applying a volumetric equivalent factor, calculated from changes in area under some profiles which repetitively extended out into deeper water, to the mean excursion distance value. Due to the poor spatial and temporal distribution of profiles along Masonboro, Kure, and Fort Fisher Beaches, only profiles from Wrightsville and Carolina Beaches were used in the analysis of beach response and volumetric changes associated with storms and manmade influences. The results indicate that the average seasonal changes along Wrightsville and Carolina Beaches, measured 24 and 17 meters, respectively, were significantly larger than the long-term loss (erosion) rate for 1 year. In addition, the response of these beaches to storm-induced erosion or beach-fill placement was, in many instances, very short in duration and therefore difficult to identify in many of the excursion plots which had poor temporal resolution.

Most of the beach profile data are not a result of one coordinated and well-planned study, but rather from several independent and overlapping studies. The following recommendations on the distribution of beach profile surveys are based on comparison of adjacent profiles and are made so that the most efficient use of manpower and money can be incorporated into future beach studies.

The spatial separation of profiles should be in the range of 0.5 to 1.0 kilometers, if possible, along straight or smoothly varying stretches of beach. Profiles should be spaced closer in areas of abrupt changes in beach planform (e.g., inlets, headlands, etc.) or in areas where historic observations indicate large relative changes in beach position.

The profiles must be measured with sufficient frequency so that seasonal fluctuations and longer term trends can be identified and separated. To accomplish this, some stations (e.g., every fourth) must be surveyed frequently, no more than 1 or 2 months apart, and the intermediate stations should be profiled at least twice a year (surveyed at the same times each year).

Some of the profiles which are surveyed frequently must be surveyed out beyond the MLW position to approximately the position of the -10 meter contour. These long profiles are necessary to establish the actual volumetric changes for the entire active profile, and hence, used to calculate the volumetric equivalent factor applied to the intermediate profiles.

If the seasonal variation in beach excursion is larger than the long-term trends, then profile data must be collected for a minimum of 2 to 3 years for both processes to be quantified. Greater variability in the data necessitates longer collection periods.

For projects with tight budget constraints, a few profiles located in key positions and surveyed frequently will provide a better data base than more profiles surveyed infrequently.

Wave gage data collected at Johnnie Mercer's Pier and LEO data from Wrightsville Beach were combined to develop a wave climate representative of the wave conditions found along the study area. This data was refracted in to shore and the breaking wave conditions were used to calculate both the northerly and southerly components of longshore energy flux. The spatial gradient of these values along Wrightsville and Carolina Beaches were compared with the long-term (nonseasonal) volumetric changes, and the empirical factor, β , which relates the longshore sediment transport rate to the longshore component of energy flux was calculated. By choosing a best-fit value of $\beta = 300$ and $\beta = 900 \text{ m}^3\text{-s/N-yr}$ for Wrightsville and Carolina Beaches, respectively, plots of predicted and measured volumetric change due to longshore sediment transport along each beach showed similar trends, although the absolute magnitude at any beach location was different.

To improve the accuracy of the energy flux computation in future studies, the following recommendations on desirable refraction model characteristics should be utilized or developed.

- (a) Variable grid cell spacing should be used to allow coarse-sized computational cells in deep water and finer cells in the nearshore region where greater relative changes in bathymetry can cause instability problems.
- (b) The effects of diffraction and tidal currents on wave propagation should be included.
- (c) The dynamic interrelationship between both the nearshore bathymetry and shoreline planform, and the sediment transport potential of the incoming waves should be incorporated. The present static boundary condition representation of the shoreline, used in refraction analysis programs, does not allow for any change in shape in the shoreline due to increased sediment transport capabilities as a result of increased (focused) wave activity. Thus changes in refraction patterns and beach approach angles due to beach response between different sets of wave types used to represent seasonal or annual conditions should be included.

Until these improvements can be incorporated, the results of this study indicate that the additional expenses incurred due to the use of a large number of wave rays and high resolution in the bathymetric data cannot be justified.

Sediment budgets were developed for Wrightsville and Carolina Beaches. These two beaches were each divided into three littoral cells in which the response of the beach to all natural and man-influenced changes was fairly similar. Long-term volumetric changes were assumed to be the result of differences in longshore sediment transport rates, sediment loss to wave overtopping, and to sea level rise. Losses due to ongoing sorting of beach sediment were considered minor. Values of wave energy flux at each cell boundary were multiplied by the empirical factor β which relates the longshore transport potential to the longshore component of wave energy flux. An additional efficiency factor, α which relates the actual volume of sediment transported to the potential amount as predicted from the energy flux analysis, was included in the sediment budget equations. The value of α along a smooth and uninterrupted coastline was assumed to be one and at positions where a coastal structure (e.g., the north jetty weir at Masonboro Inlet) or where geologic control (availability of sediment supply) prohibit transport, the value of α was assumed to be zero. The solution of the sediment transport equations resulted in α values which indicated that only two-thirds of the gross southerly transport along Wrightsville Beach spills over the north jetty weir into Masonboro Inlet and one-third is either trapped along the southern end of Wrightsville Beach or locally transported northward by wave energy reversals. At the northern ends of Wrightsville and Carolina Beaches, only 10 and 31 percent of the potential volume of sediment is transported out of Mason and Carolina Beach Inlets, respectively. If better volumetric change data had been available for Masonboro Beach, then the influence of Masonboro and Carolina Beach Inlets in terms of their inlet trapping potential on the supply and storage of sand have been determined.

Analyses of the beach profiles taken along Wrightsville Beach after the 1970 beach fill indicate several components of beach response. The first component was a long-term loss rate of -3.8 meters per year which was approximately equal to the long-term loss rate during the 5-year period prior to the 1970 fill operations. This rate was much higher in the immediate vicinity of the fill than along adjacent beaches both during the prefill and postfill periods, and indicated that the fill placement did not reduce or eliminate the problem which resulted in the need for a fill, but rather provided recreational opportunity and "bought-time" for the properties behind the project boundaries.

In addition to the long-term component, an exponential loss of beach-fill volume was recorded during the first 1.5 to 2 years. Excursion plot analysis showed that about 80 percent of the total initial fill was eroded during this period of rapid initial loss, and that severe storm erosion was not the primary cause for the very high initial loss rate.

The first set of profile measurements taken after fill completion indicated that the fill material was placed at a beach angle shallower

AD-A103 168

ENVIRONMENTAL SCIENCE AND ENGINEERING INC GAINESVILLE FL F/6 8/10
ANALYSIS OF COASTAL SEDIMENT TRANSPORT PROCESSES FROM WRIGHTSVI--ETC(U)
JUN 81 T C WINTON, I B CHOU, G M POWELL DACW72-79-C-0001

UNCLASSIFIED

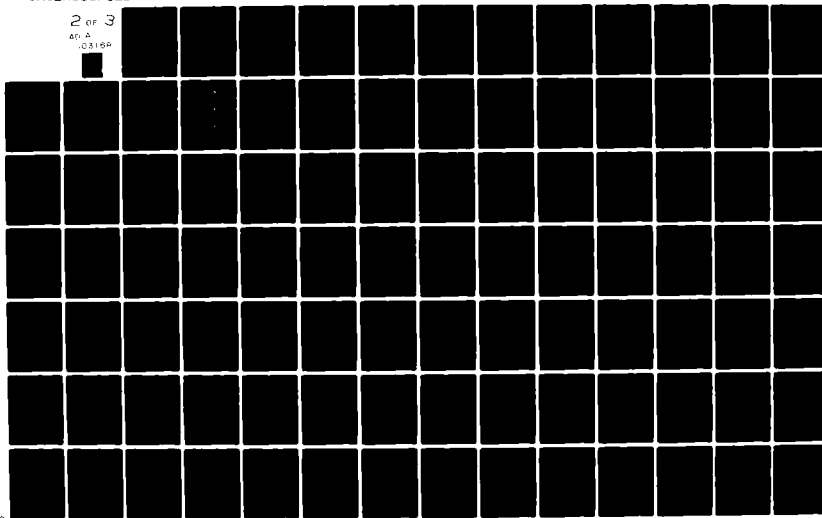
CERC-MR-81-6

NL

2 OF 3

60 A

0315P



than the existing 1970 prefill beach slope. During the first 9 to 12 months the MHW-MLW beach slope steepened (and retreated) in response to the seaward sorting of fine sand grains and to the readjustment of the profile slope to the prevailing wave conditions. After this period, the upper beach face retreated with only minor changes in beach slope due to seasonal wave climate influences.

Sediment characteristics of the fill and native beach material were used to calculate a value for the adjusted fill factor of $R_A=3.0$. This value indicates that 66 percent of the fill material can be expected to be lost due to sorting; however, comparison with measured results indicates that this calculation underestimates the initial loss percentage. In addition to the sorting and slope readjustment losses, significant quantities of fill material were lost due to the lateral spreading of material onto adjacent beaches.

An oblique aerial photo taken before the 1970 beach fill showed that the placement of the fill could only have reinforced the beach alignment problem along Wrightsville Beach. Since 1965, the beach section which suffered the localized and high erosion rates protruded from the generally smooth, curving beach planform. It was concluded that the relative change in beach planform and nearshore bathymetry resulted in an increase in localized wave activity, sediment transport potential, and erosional trends, and that this phenomena would continue until the relative change in beach shape is eliminated. Therefore, it appears that the continual renourishment of this section perpetuated the problem of increased localized wave activity.

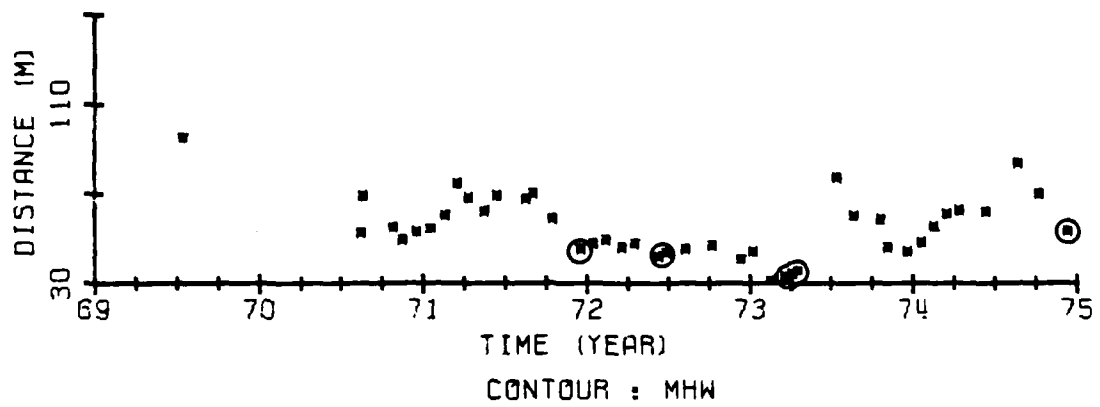
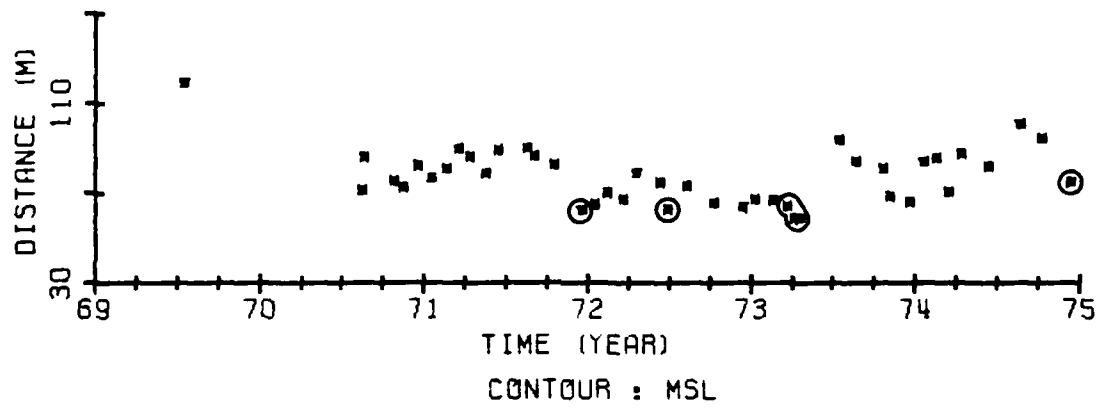
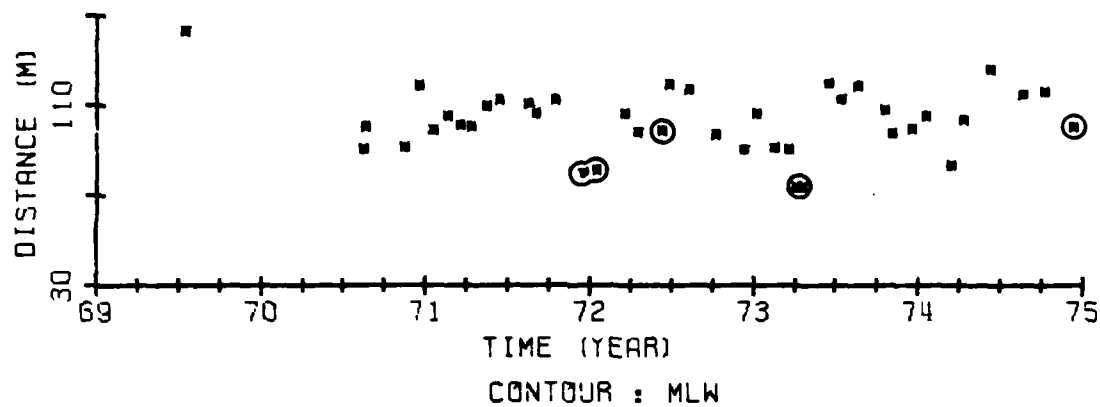
This study showed that beach losses in addition to the expected losses due to sorting and slope readjustment occurred during the initial 1.5- to 2-year response phase. It appeared that lateral spreading of the fill material onto adjacent beaches, due to the forced protrusion of the beach fill out beyond the general beach alignment, resulted in these additional significant losses.

LITERATURE CITED

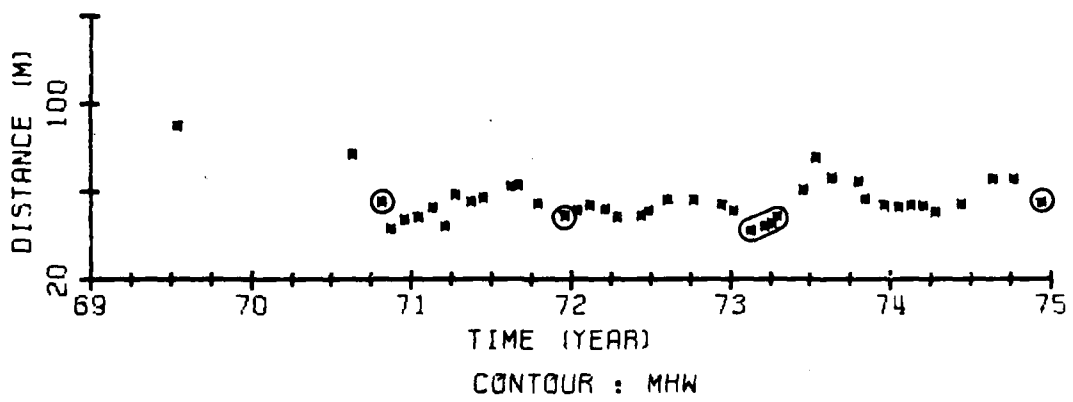
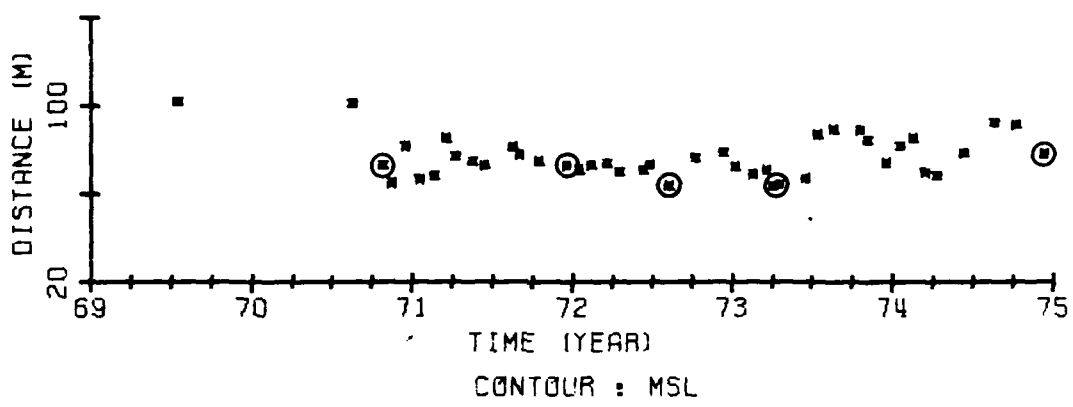
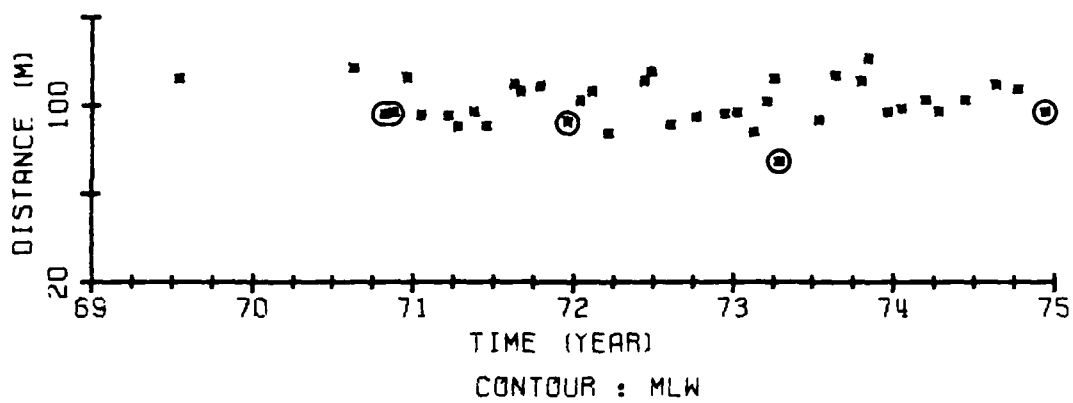
- BRUUN, P., "Sea Level Rise as a Cause of Shore Erosion," *Journal of the Waterways and Harbors Division*, Feb. 1962.
- DOBSON, R.S., "Some Applications of a Digital Computer to Hydraulic Engineering Problems," TR-80, Office of Naval Research, June 1967.
- FRITSCH, F.N., SHAFFER, R.E., and CROWLEY, W.P., "Algorithm 443, Solution of the Transcendental Equation $w e^w = x$," *Communications of the Association for Computing Machinery*, Vol. 16, No. 2, 1973, pp. 123-124; errata, EINARSSON, B., "Remark on Algorithm 442," *Communications of the Association for Computing Machinery*, Vol. 17, No. 4, 1974.
- HARRIS, D.L., "Characteristics of Wave Records in the Coastal Zone," R 2-73, U.S. Army, Corps of Engineers, Coastal Engineering Research Center, Fort Belvoir, Va., Oct. 1973.
- HICKS, S.D., and SHOFONOS, W., "Yearly Sea Level Variations for the United States," *Journal of the Hydraulics Division*, Sept. 1965.
- IWAGAKI, Y., and KAKINUMA, T., "On the Bottom Friction Factor of the Akita Coast," *Coastal Engineering in Japan*, Vol. 6, 1963, pp. 83-91.
- JAMES, W.R., "Techniques in Evaluating Suitability of Borrow Material for Beach Nourishment," TM-60, U.S. Army, Corps of Engineers, Coastal Engineering Research Center, Fort Belvoir, Va., 1975.
- JAMES, W.R., "Borrow Material Texture and Beach Fill Stability," *Proceedings of the 14th International Conference on Coastal Engineering*, American Society of Civil Engineers, Vol. II, 1974, pp. 1334-1344.
- JARRETT, J.T., "Sediment Budget Analysis, Wrightsville Beach to Kure Beach, North Carolina," *Coastal Sediments*, American Society of Civil Engineers, New York, Nov. 1977, pp. 986-1005.
- KOMAR, P.D., *Beach Processes and Sedimentation*, Prentice-Hall, Englewood Cliffs, N.J., 1976.
- LANGFELDER, L.J., "Coastal Erosion in North Carolina," *Proceedings of the Coastal Processes and Shore Protection Seminar*, Mar. 1970.
- MOGEL, T.R., and STREET, R.L., "Computation of Longshore Energy and Littoral Transport," *Proceedings of the 12th Conference on Coastal Engineering*, Vol. 2, 1970, pp. 899-917.
- PIERCE, J.W., "Holocene Evolution of Portions of the Carolina Coast," *Bulletin of the Geologic Society of America*, Vol. 81, Dec. 1970.
- SKOVGAARD, O., JONSSON, I.G., and BERTELSEN, J.A., "Computation of Wave Heights due to Refraction and Friction," *Journal of the Waterways and Harbors Division*, New York, Vol. 101, WWI, 1975, pp. 15-32.
- THOMPSON, E.F., "Wave Climate at Selected Locations Along U.S. Coasts," TR 77-1, U.S. Army, Corps of Engineers, Coastal Engineering Research Center, Fort Belvoir, Va., Jan. 1977.

- U.S. ARMY, CORPS OF ENGINEERS, COASTAL ENGINEERING RESEARCH CENTER,
"Documentation of CERC Beach Evaluation Program Beach Profile--Line
Locations at Wrightsville Beach, North Carolina," Fort Belvoir, Va., 1973.
- U.S. ARMY, CORPS OF ENGINEERS, COASTAL ENGINEERING RESEARCH CENTER, *Shore
Protection Manual*, 3d ed., Vols. I, II, and III, Stock No. 008-022-00113-1,
U.S. Government Printing Office, Washington, D.C., 1977, 1,262 pp.
- U.S. ARMY CORPS OF ENGINEERS, "Carolina Beach and Vicinity, North Carolina,"
letter from the Acting Chief of Engineers, Department of Administration,
Washington, D.C., Oct. 1961.
- U.S. ARMY CORPS OF ENGINEERS, "Wrightsville Beach, North Carolina," letter
from Secretary of the Army, Washington, D.C., Mar. 1962.
- U.S. ARMY ENGINEER DISTRICT, WILMINGTON, "Beach Erosion Control and Hurricane
Wave Protection, Wrightsville Beach, North Carolina," Design Memorandum,
Wilmington, N.C., July 1964.
- U.S. ARMY ENGINEER DISTRICT, WILMINGTON, "Masonboro Inlet, North Carolina--
North Jetty," Design Memorandum, Wilmington, N.C., 1965.
- U.S. ARMY ENGINEER DISTRICT, WILMINGTON, "Carolina Beach Harbor, North
Carolina, Survey Report," Wilmington, N.C., Jan. 1966.
- U.S. ARMY ENGINEER DISTRICT, WILMINGTON, "Investigation of Beach Erosion,
Carolina Beach, North Carolina," Wilmington, N.C., 1970.
- U.S. ARMY ENGINEER DISTRICT, WILMINGTON, "Fort Fisher and Vicinity, North
Carolina, Feasibility Report of Beach Erosion Control," Wilmington, N.C.,
July 1974.
- U.S. ARMY ENGINEER DISTRICT, WILMINGTON, "Carolina Beach Inlet, North
Carolina, Draft Feasibility Report on Improvement of Navigation,"
Wilmington, N.C., 1976.
- U.S. ARMY ENGINEER DISTRICT, WILMINGTON, "The Masonboro Inlet, North Carolina
South Jetty General Design Memorandum," Wilmington, N.C., Oct. 1977.
- U.S. ARMY ENGINEER DISTRICT, WILMINGTON, "Specifications for Dredging Depos-
ition Basin, Carolina Beach Inlet, North Carolina," Wilmington, N.C., 1967.
- U.S. ARMY ENGINEER DIVISION, SOUTH ATLANTIC, "National Shoreline Study--
Regional Inventory Report," South Atlantic-Gulf Region, Atlanta, Ga., Aug.
1971.
- U.S. NAVAL WEATHER SERVICE COMMAND, "Summary of Synoptic Meteorological Obser-
vations, Atlantic and Gulf Coasts," Vol. 3, 1975.
- VALLIANOS, L., "Recent History of Erosion at Carolina Beach, North Carolina,"
Proceedings of the 12th Conference on Coastal Engineering, Vol. 2, 1970,
pp. 1223-1242.
- VITALE, P., "A Guide for Estimating Longshore Transport Rate Using Four SPM
Methods," CETA 80-6, U.S. Army, Corps of Engineers, Coastal Engineering
Research Center, Fort Belvoir, Va., Apr. 1980.

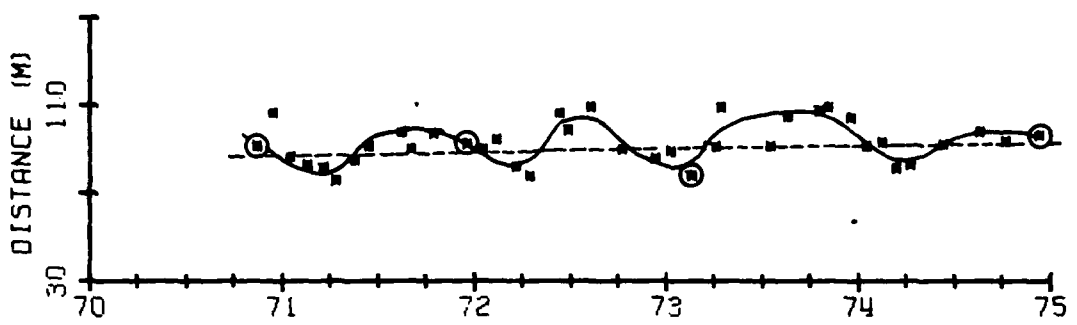
APPENDIX A
WRIGHTSVILLE BEACH EXCURSION DISTANCE PLOTS



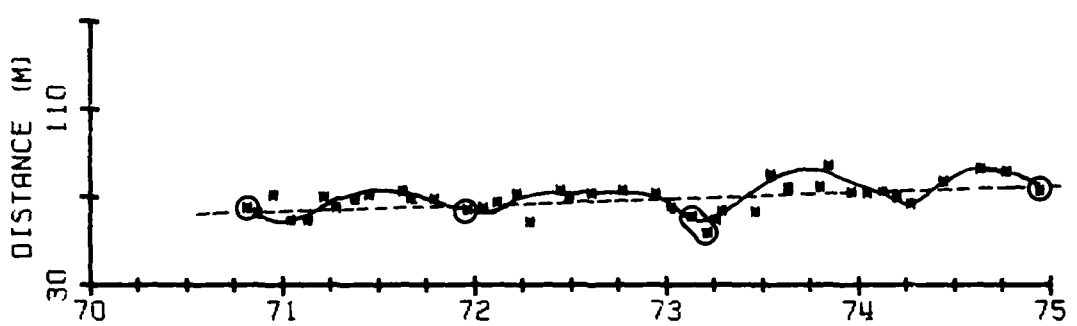
DISTANCE FROM THE BASE LINE TO STATED CONTOURS AT WB 1



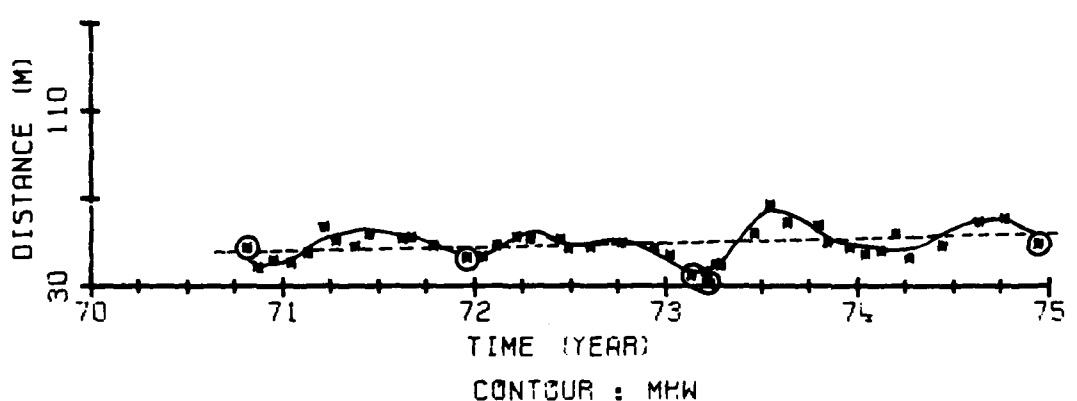
DISTANCE FROM THE BASE LINE TO STATED CONTOURS AT WB 2



CONTOUR • MI W

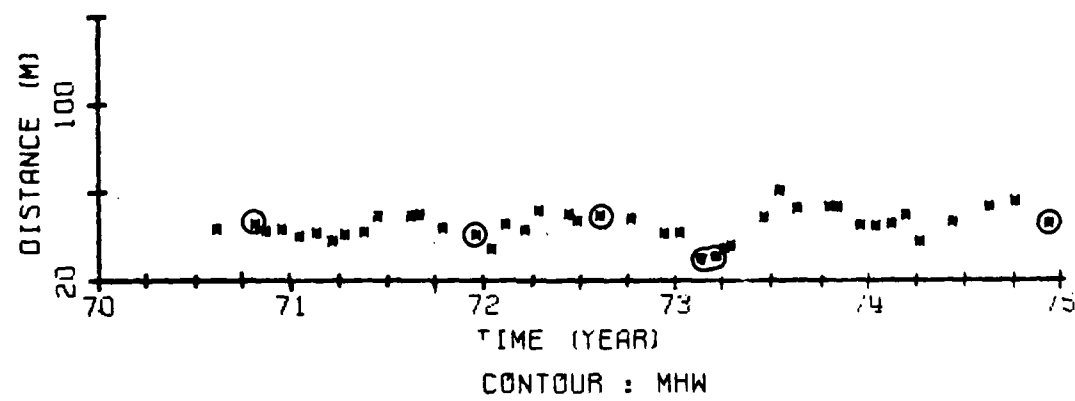
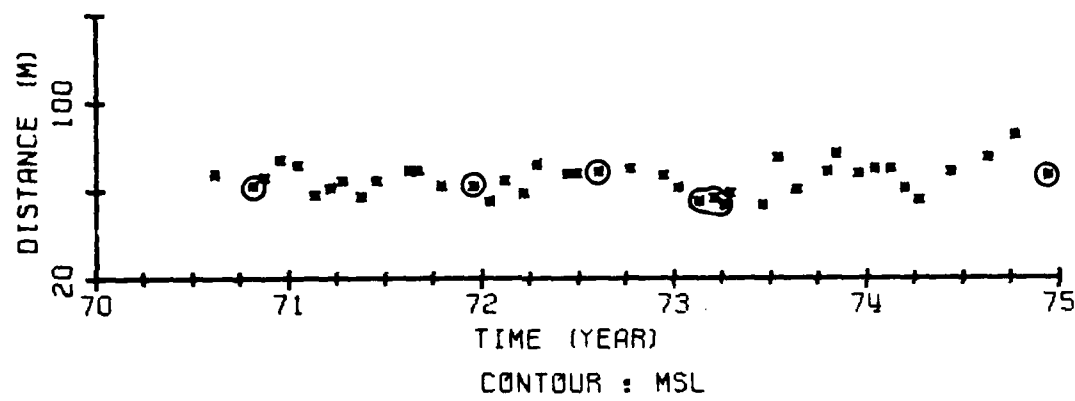
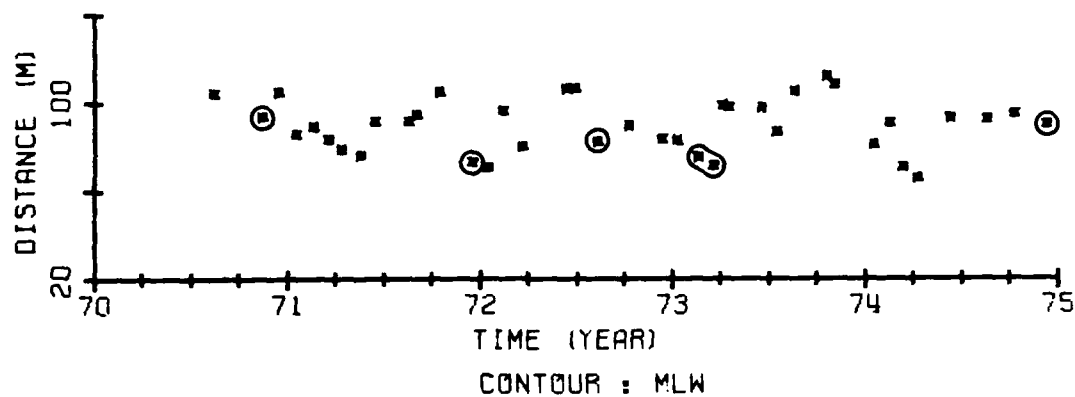


CONTINUE • MSI

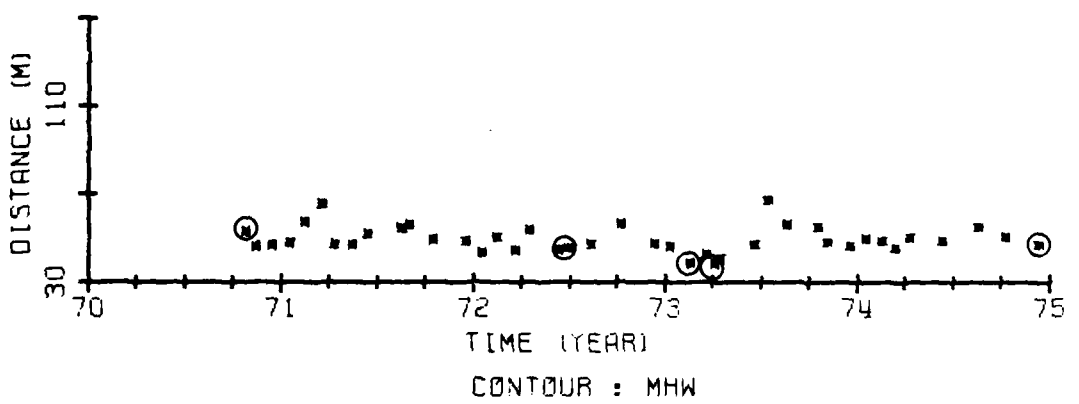
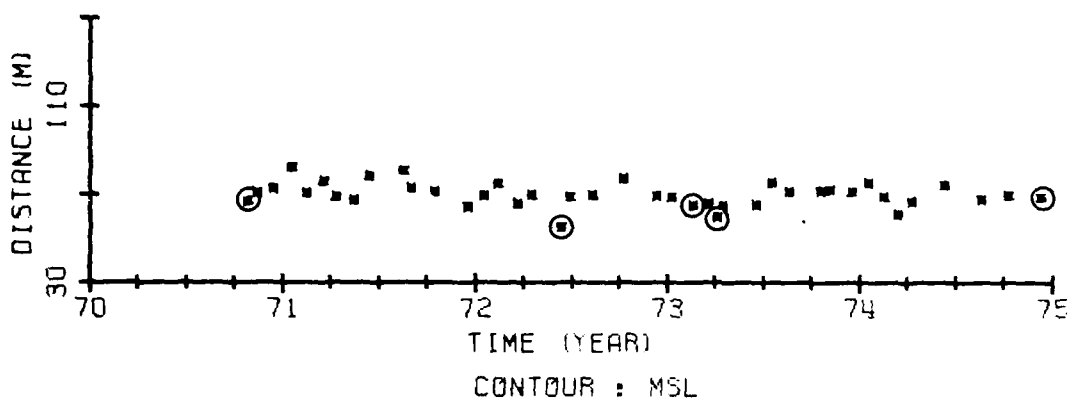
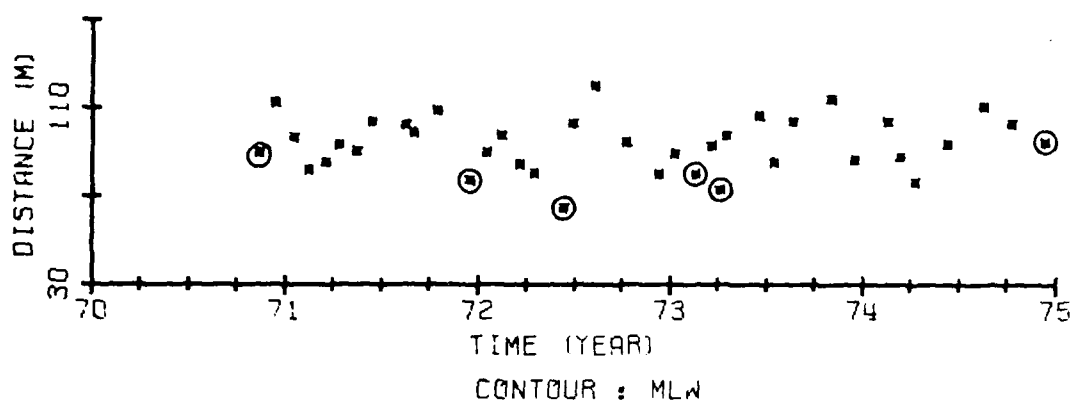


Note: Circles indicate profiles measured shortly after a local storm.
Arrows indicate the approximate time at which beach fills were placed.

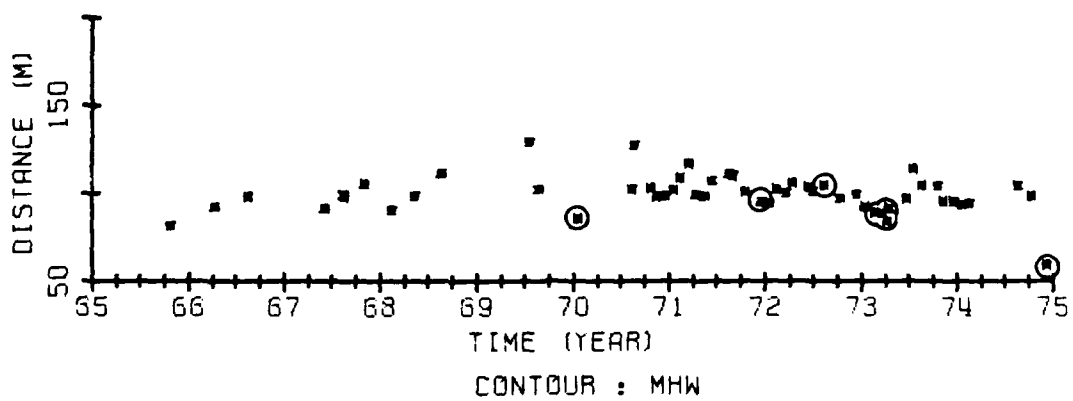
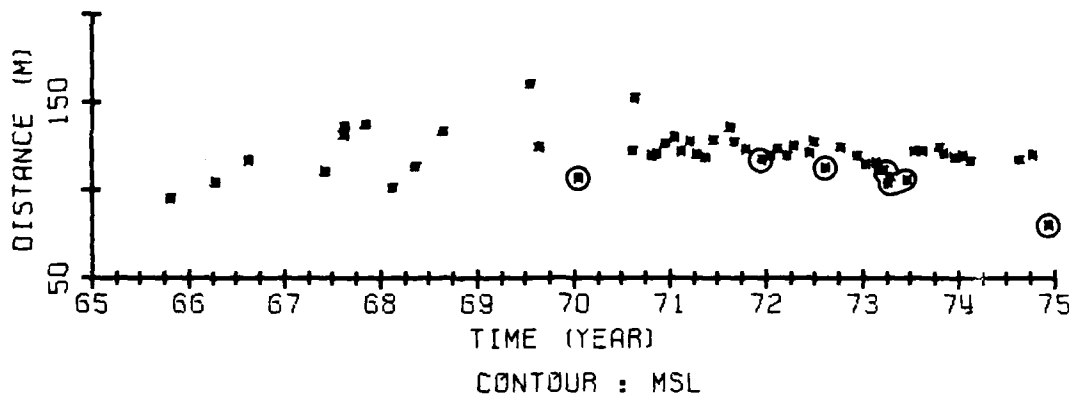
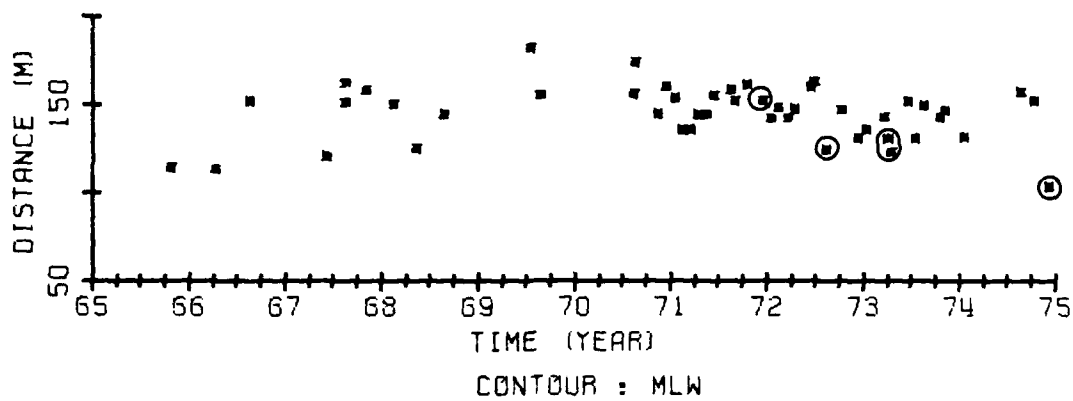
DISTANCE FROM THE BASE LINE TO STATED CONTOURS AT WB 3



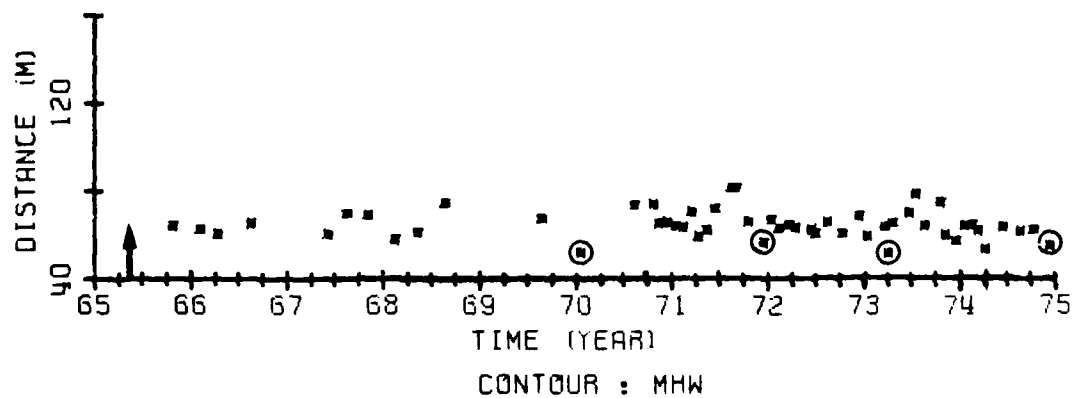
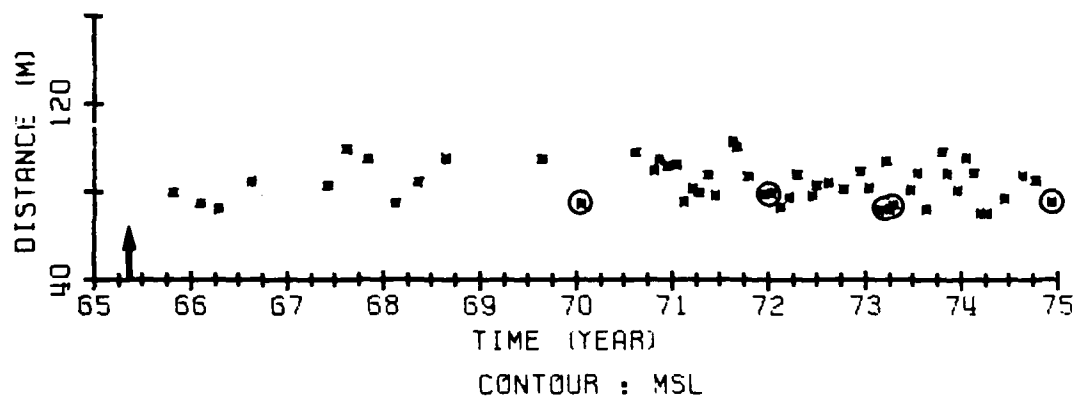
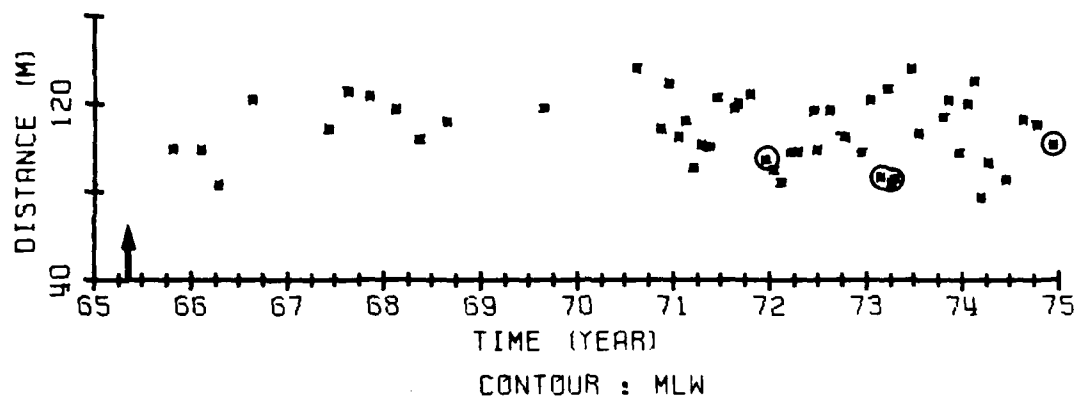
DISTANCE FROM THE BASE LINE TO STATED CONTOURS AT WB 4



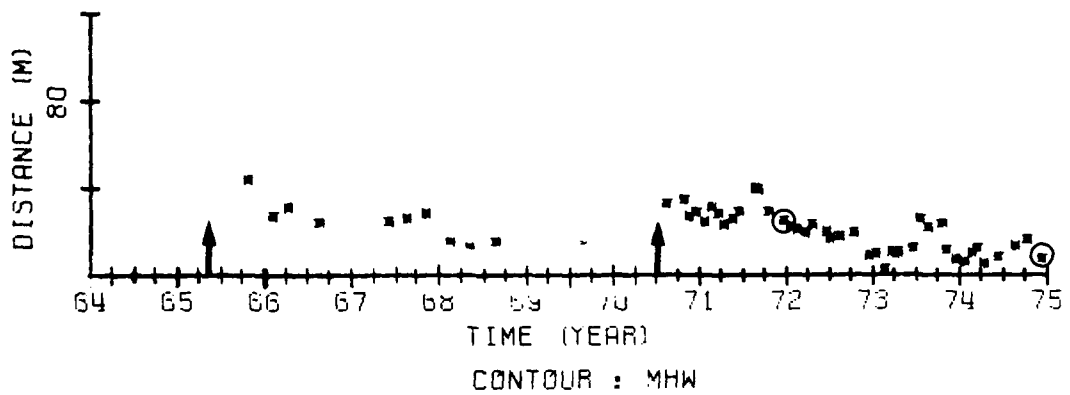
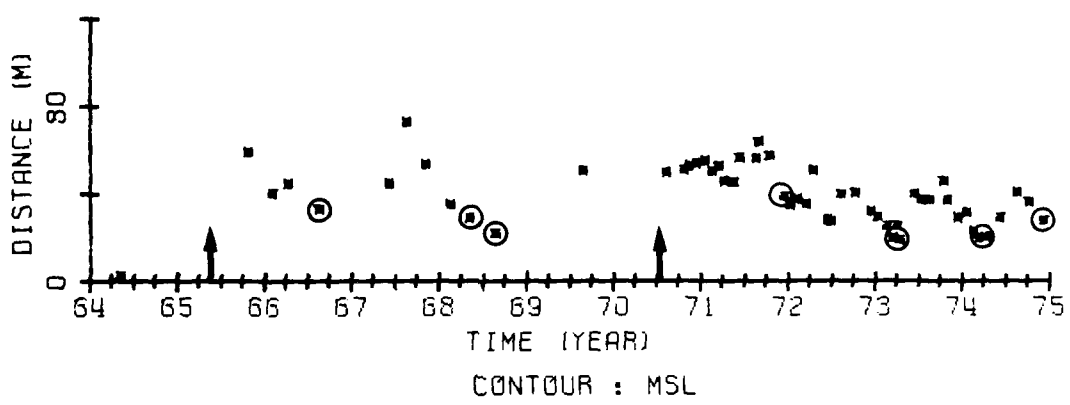
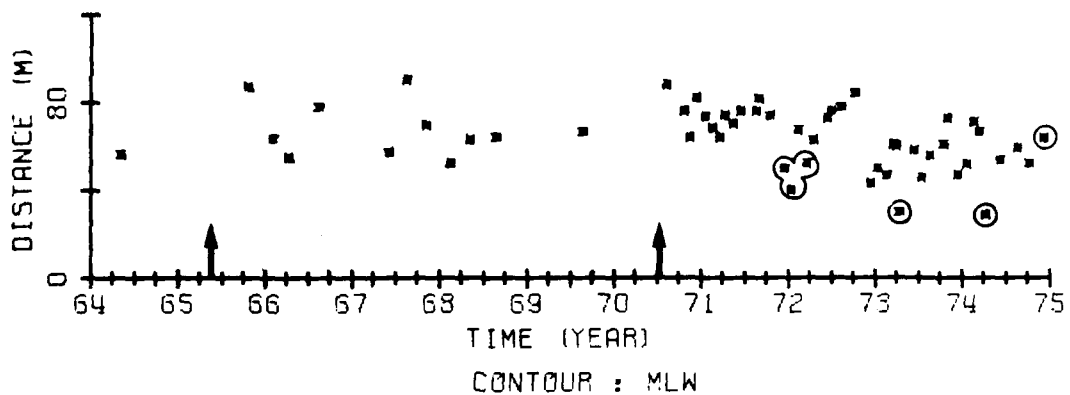
DISTANCE FROM THE BASE LINE TO STATED CONTOURS AT WB 6



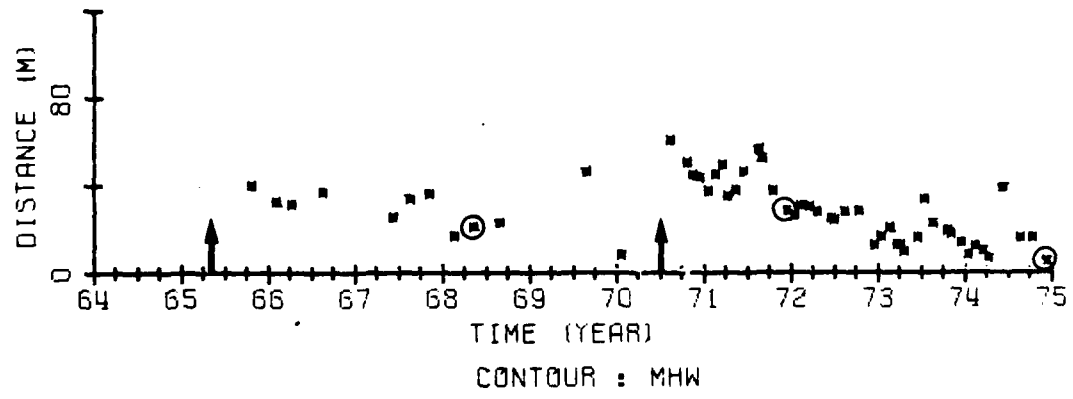
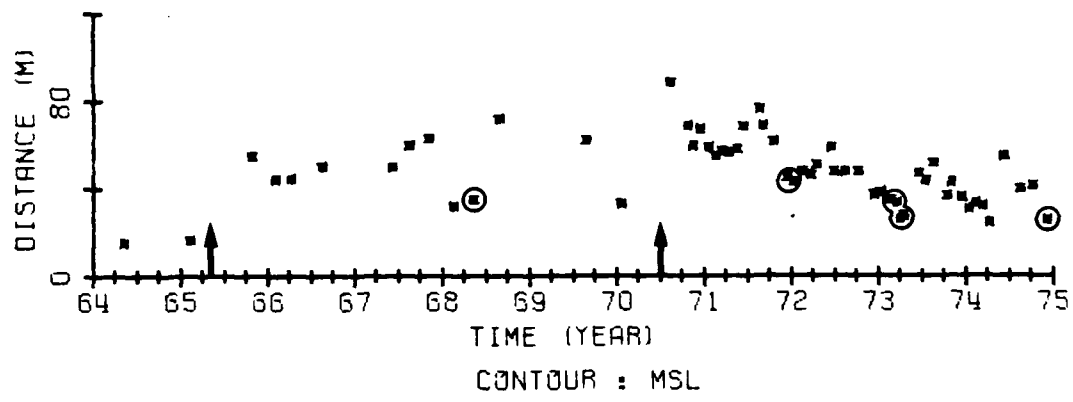
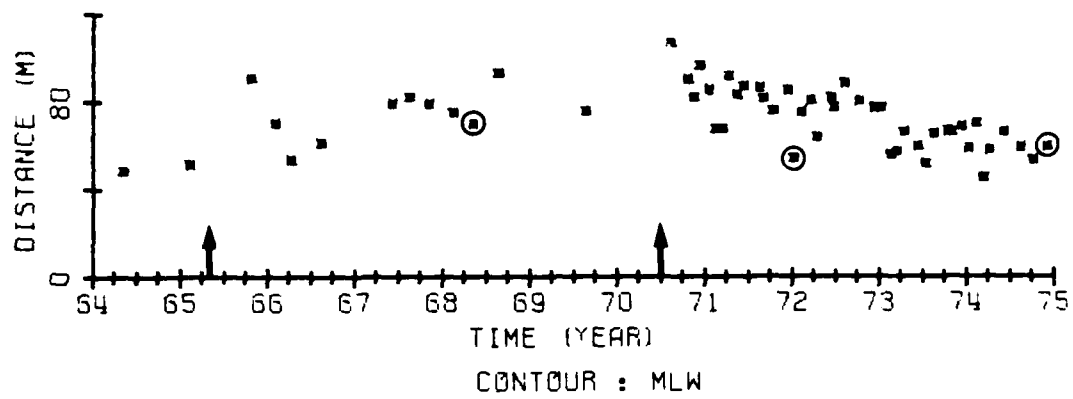
DISTANCE FROM THE BASE LINE TO STATED CONTOURS AT WB 7



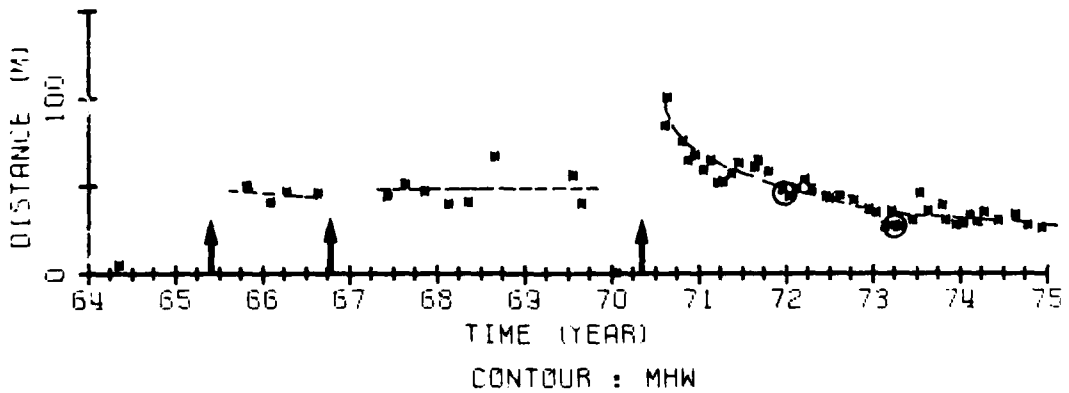
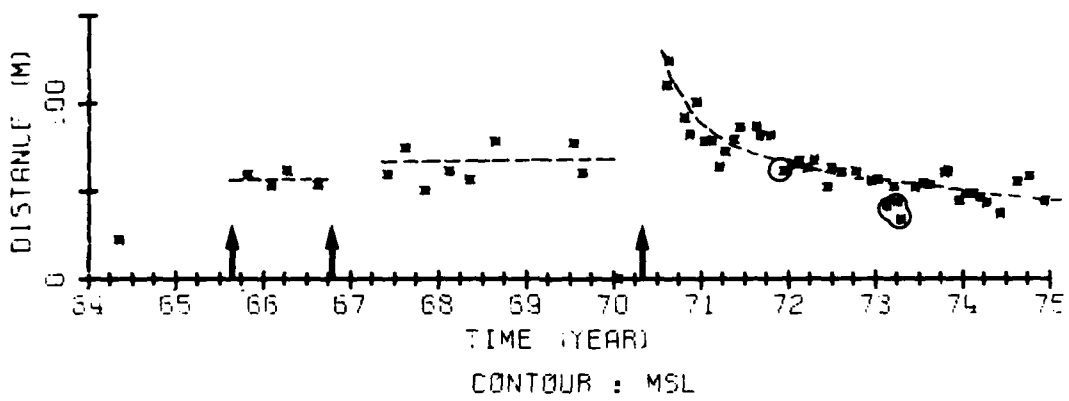
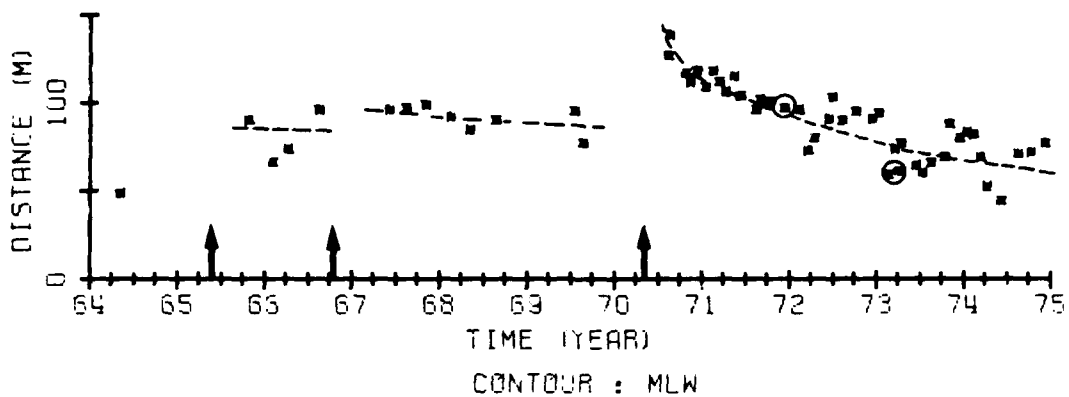
DISTANCE FROM THE BASE LINE TO STATED CONTOURS AT WB 9



DISTANCE FROM THE BASE LINE TO STATED CONTOURS AT WB 11

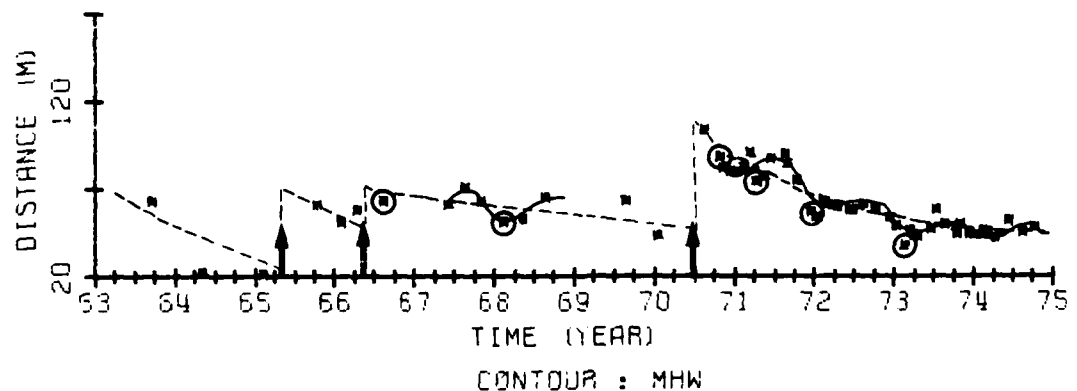
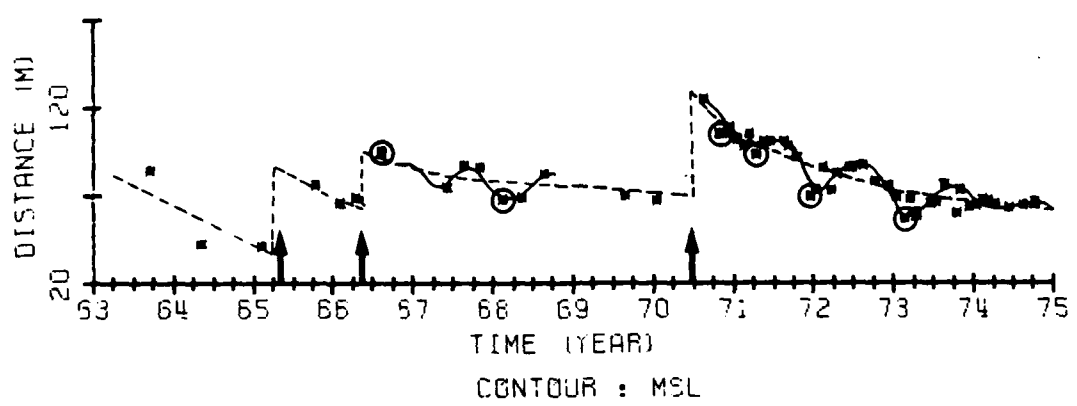
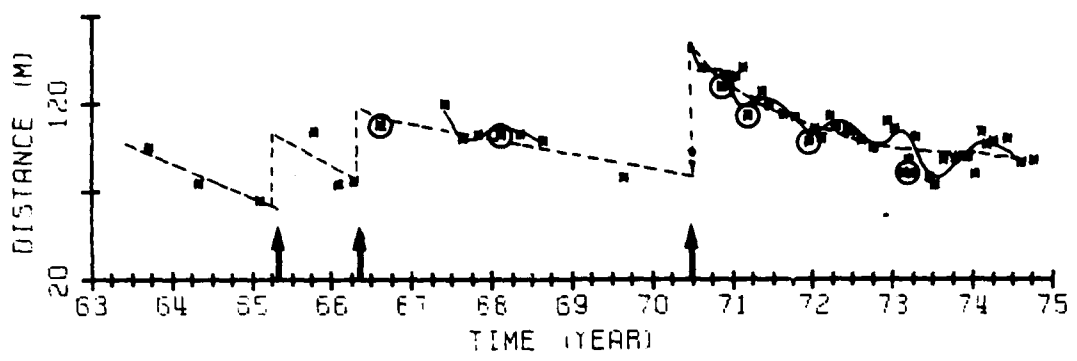


DISTANCE FROM THE BASE LINE TO STATED CONTOURS AT WB 13



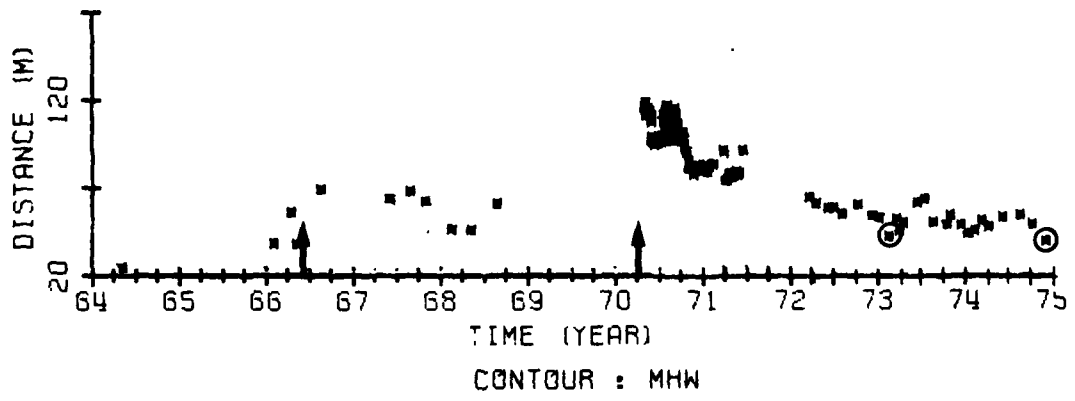
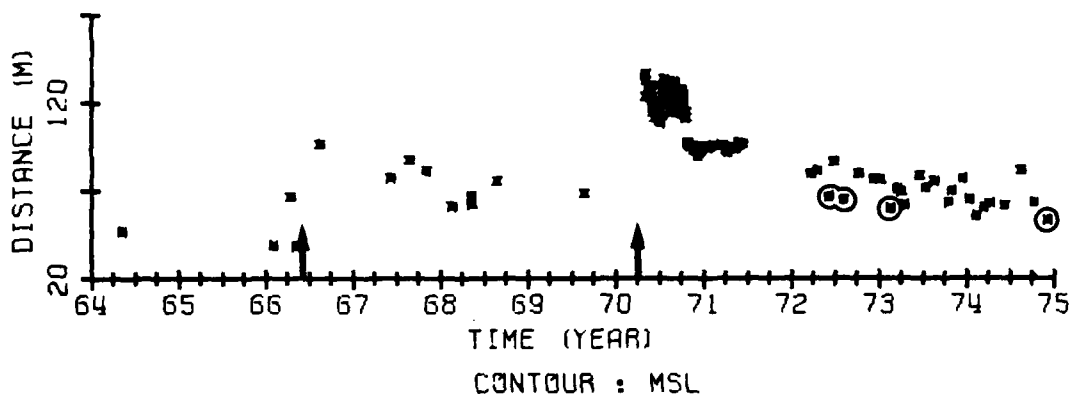
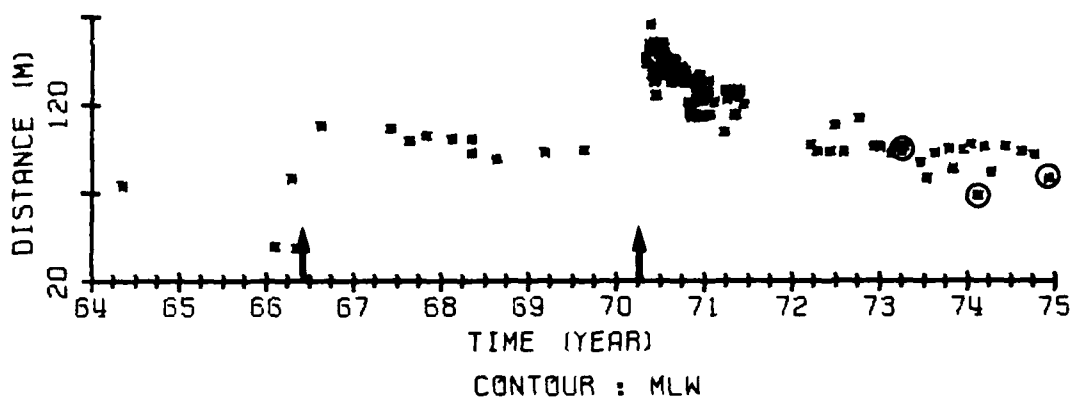
Note: Circles indicate profiles measured shortly after a local storm.
Arrows indicate the approximate time at which beach fills were placed.

DISTANCE FROM THE BASE LINE TO STATED CONTOURS AT WB 15

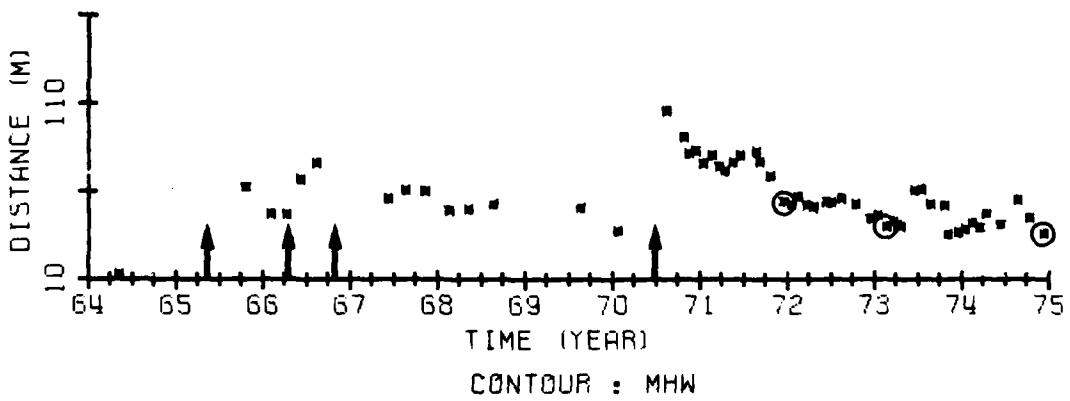
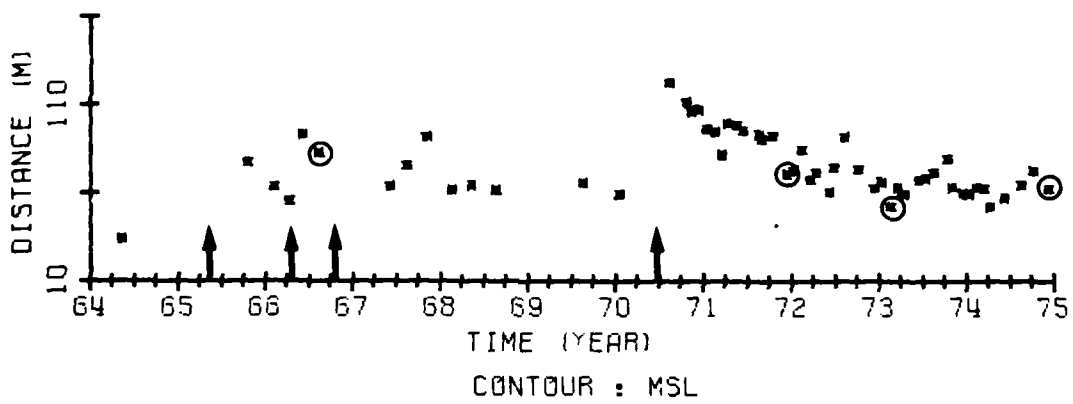
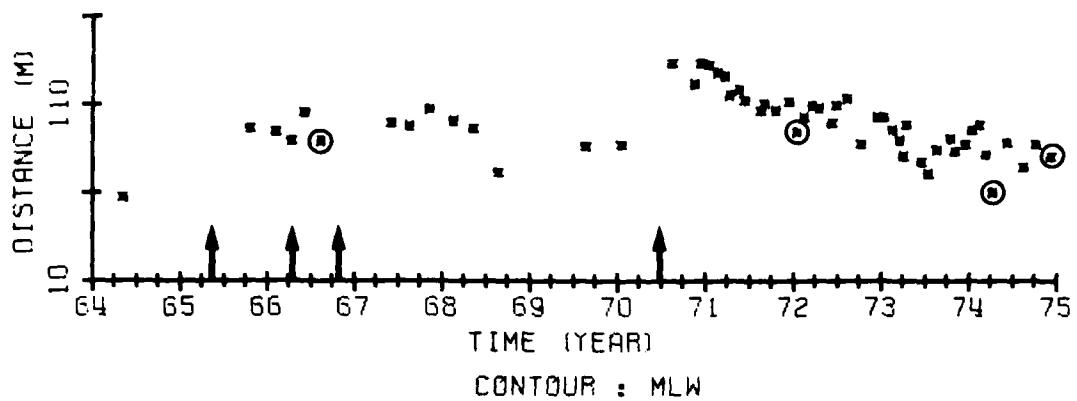


Note: Circles indicate profiles measured shortly after a local storm
 Arrows indicate the approximate time at which beach fills
 were placed.

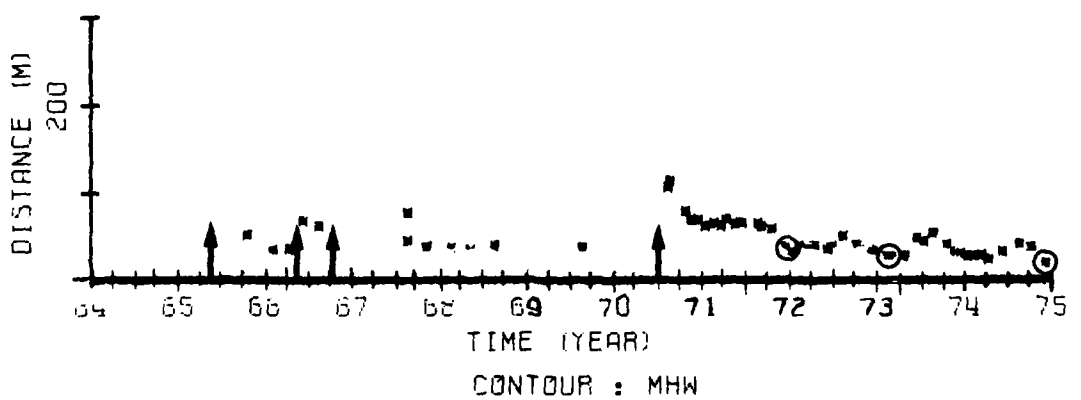
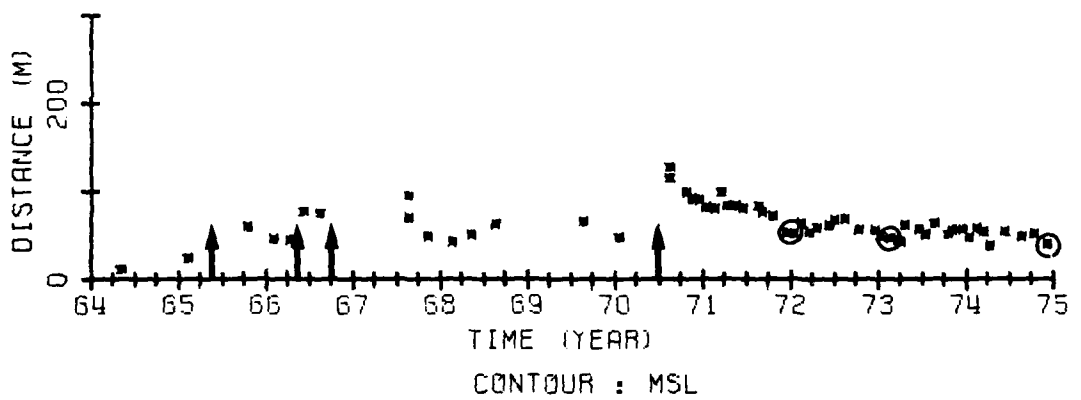
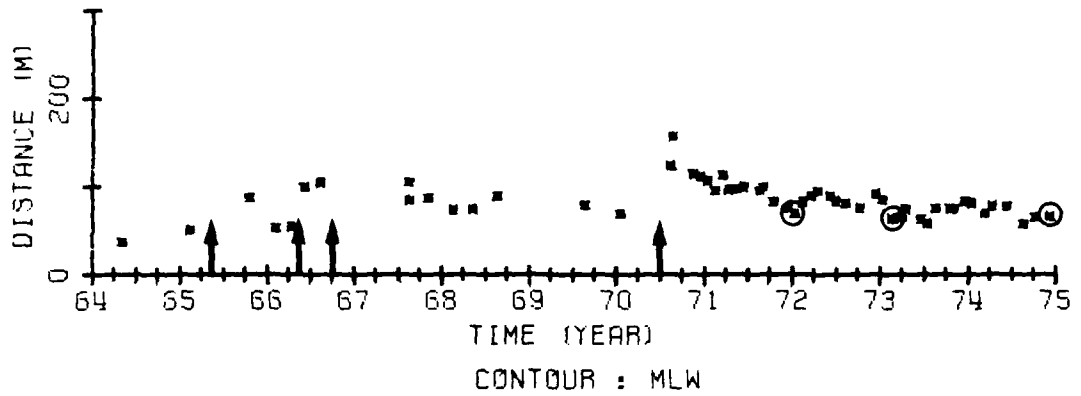
DISTANCE FROM THE BASE LINE TO STATED CONTOURS AT WB 16



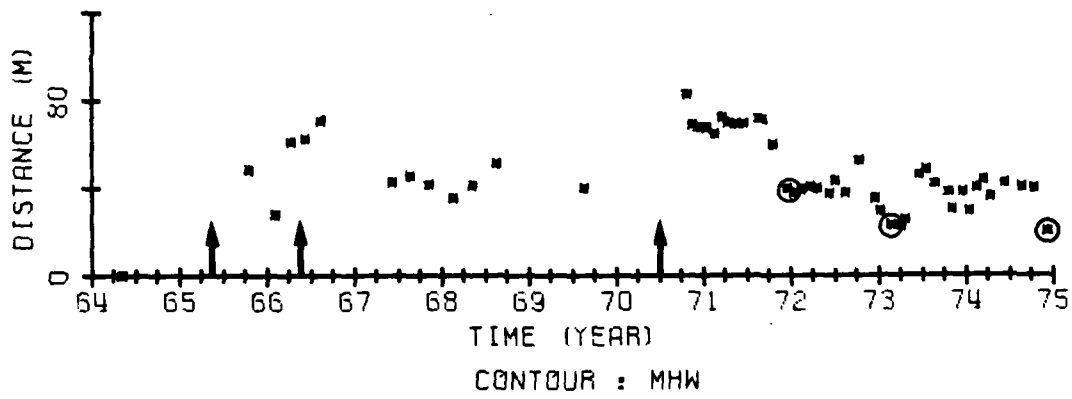
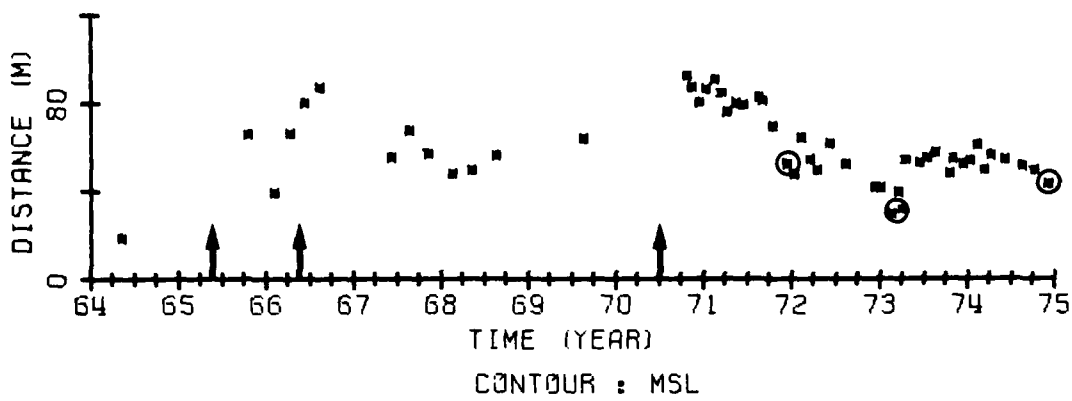
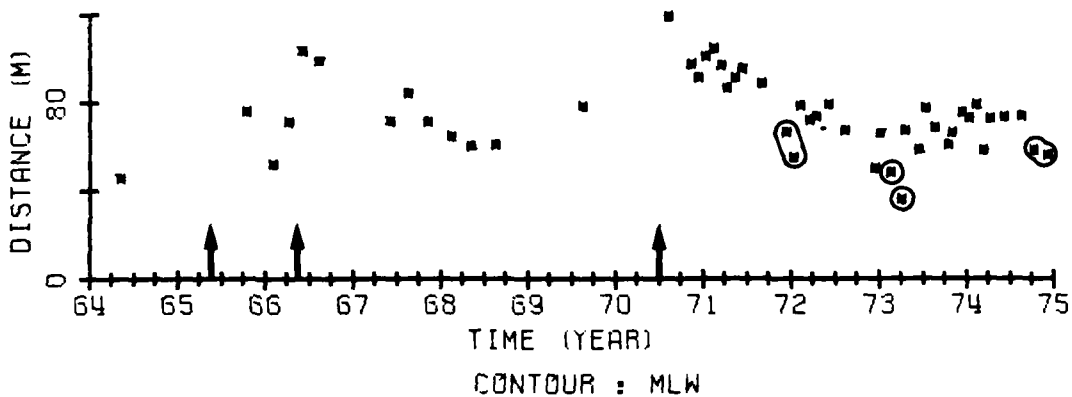
DISTANCE FROM THE BASE LINE TO STATED CONTOURS AT WB 17



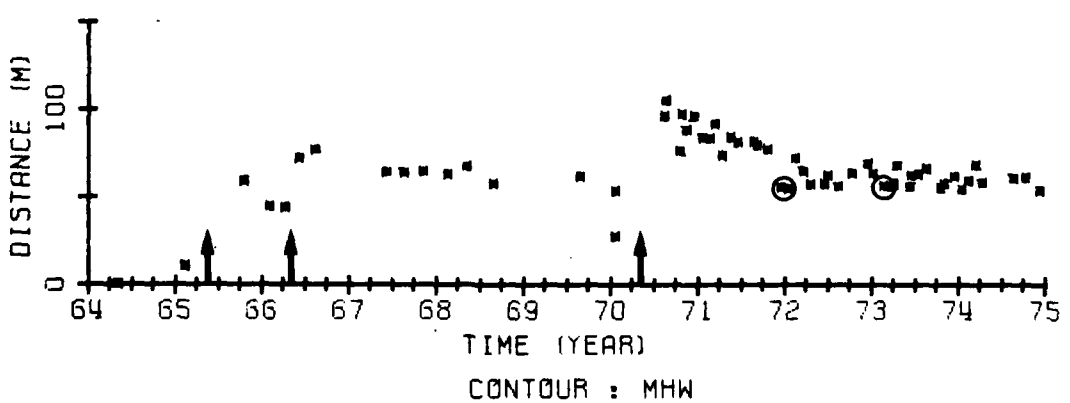
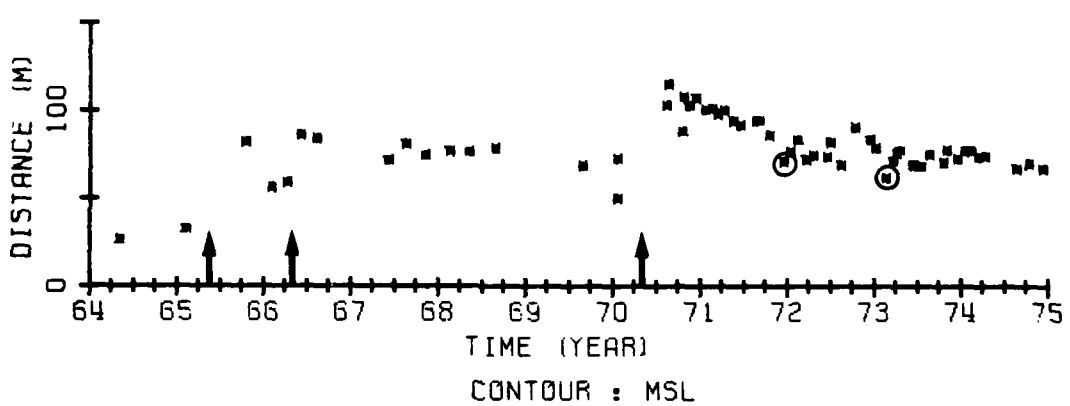
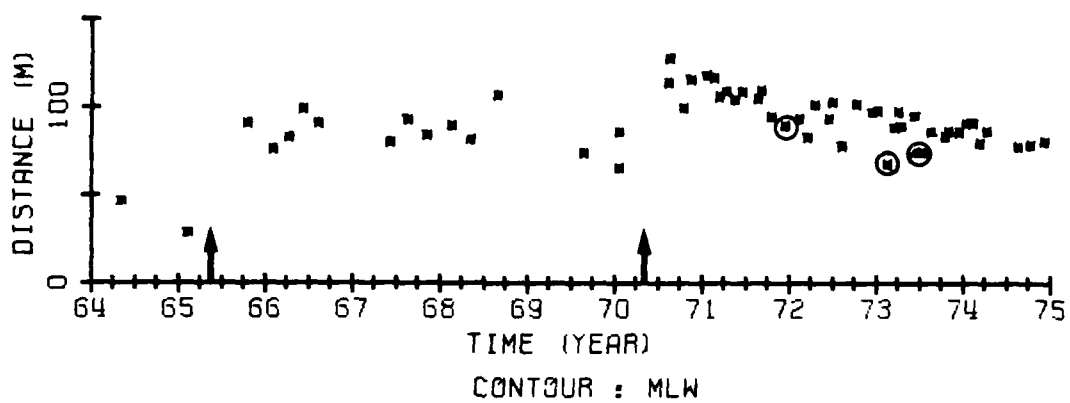
DISTANCE FROM THE BASE LINE TO STATED CONTOURS AT WB 19



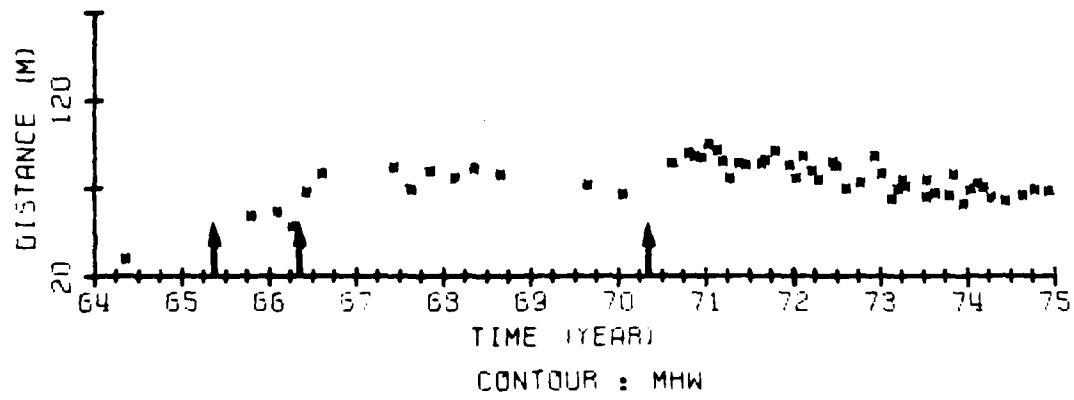
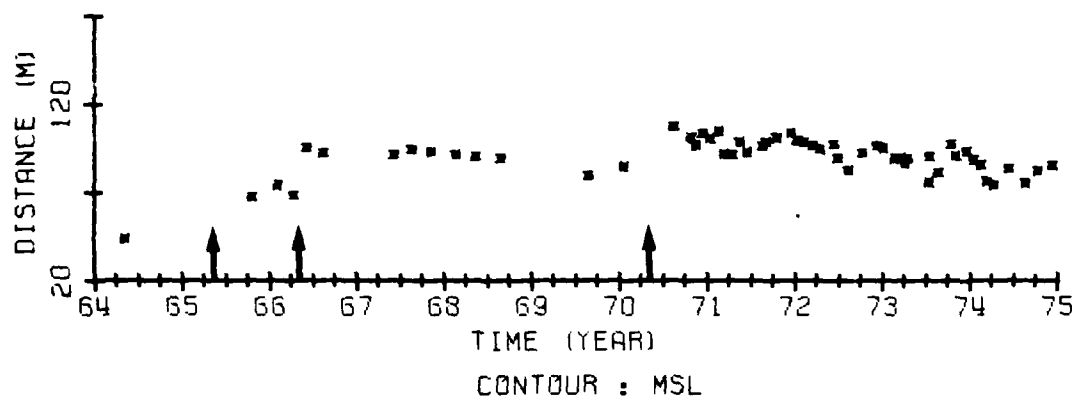
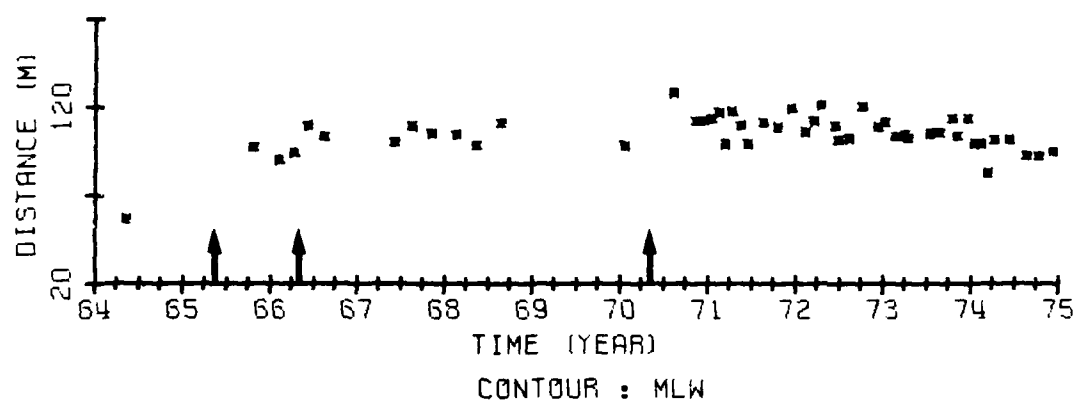
DISTANCE FROM THE BASE LINE TO STATED CONTOURS AT WB 21



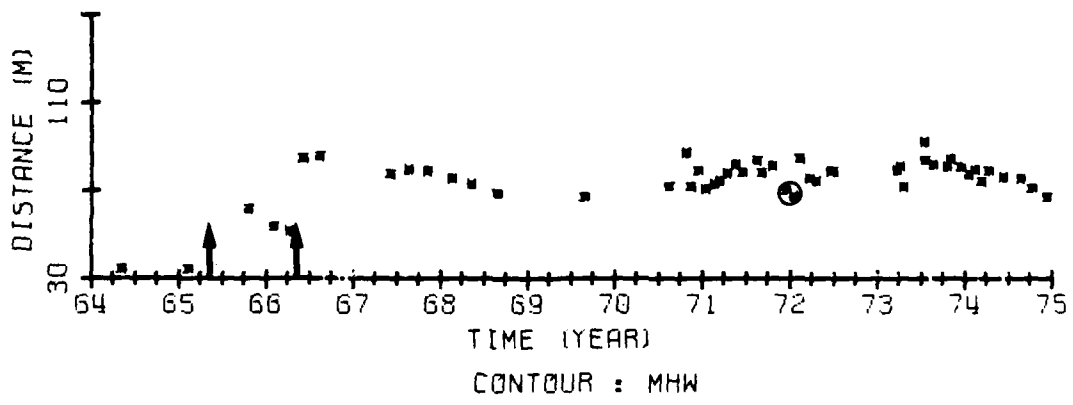
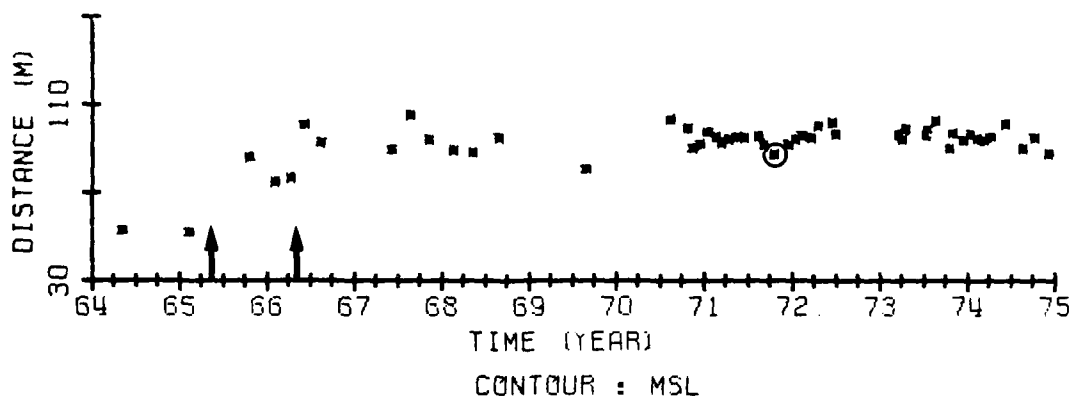
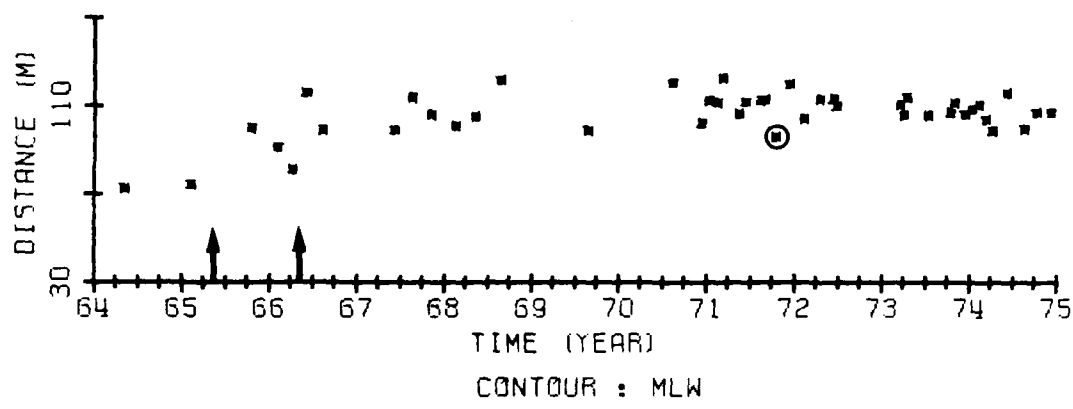
DISTANCE FROM THE BASE LINE TO STATED CONTOURS AT WB 25



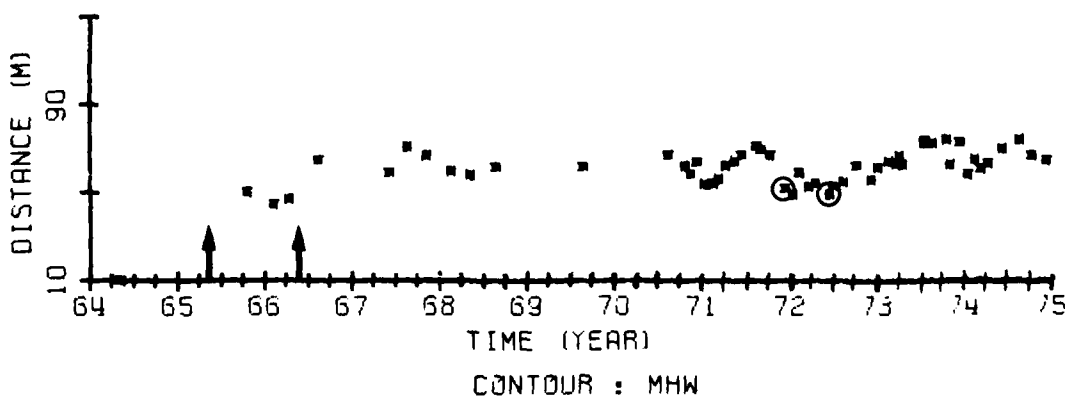
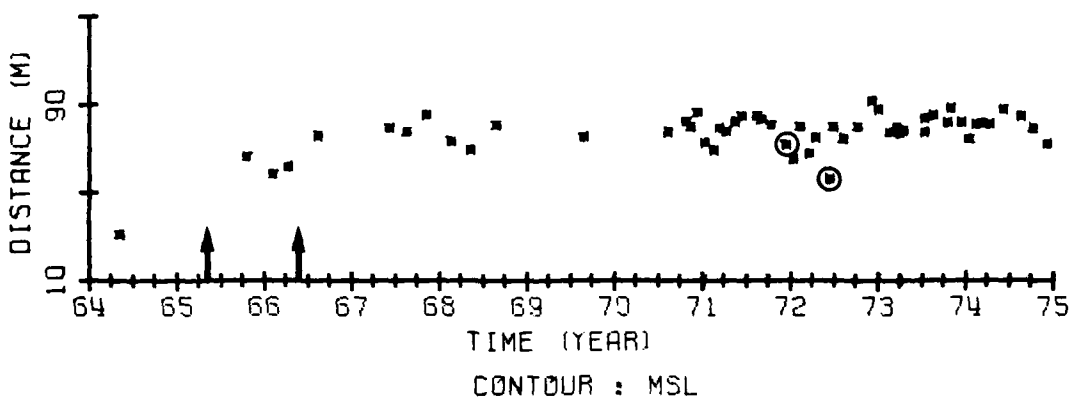
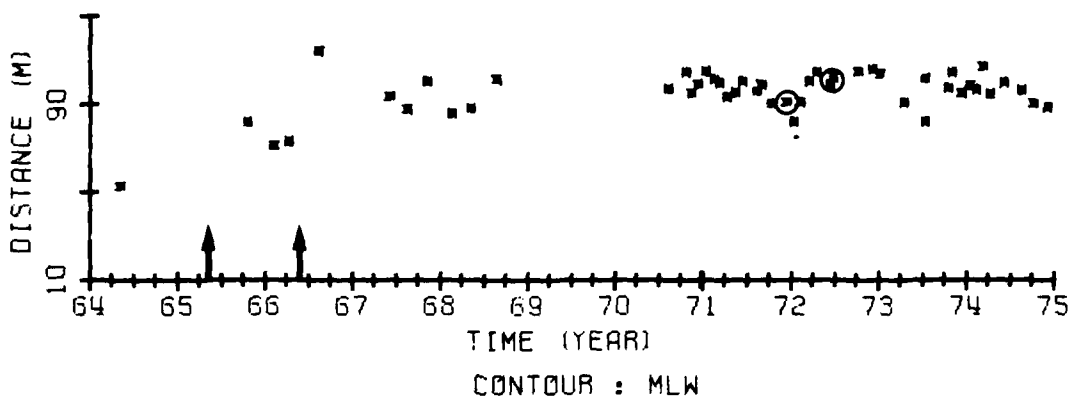
DISTANCE FROM THE BASE LINE TO STATED CONTOURS AT WB 29



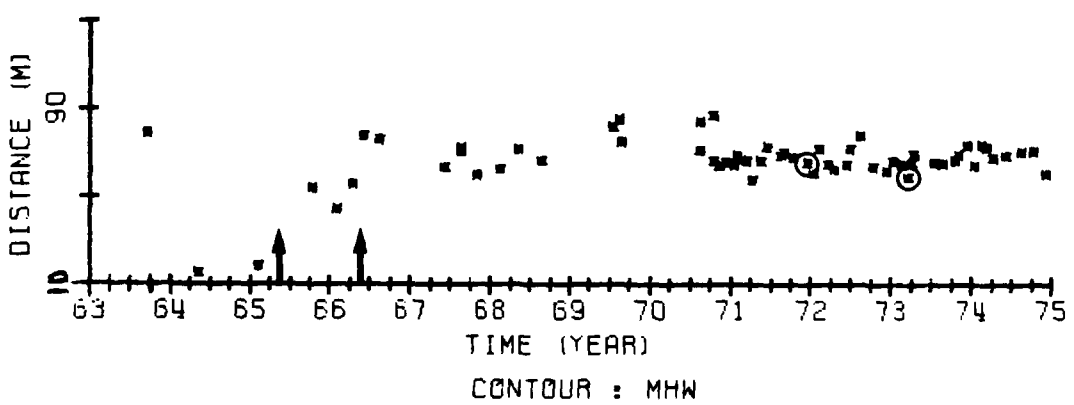
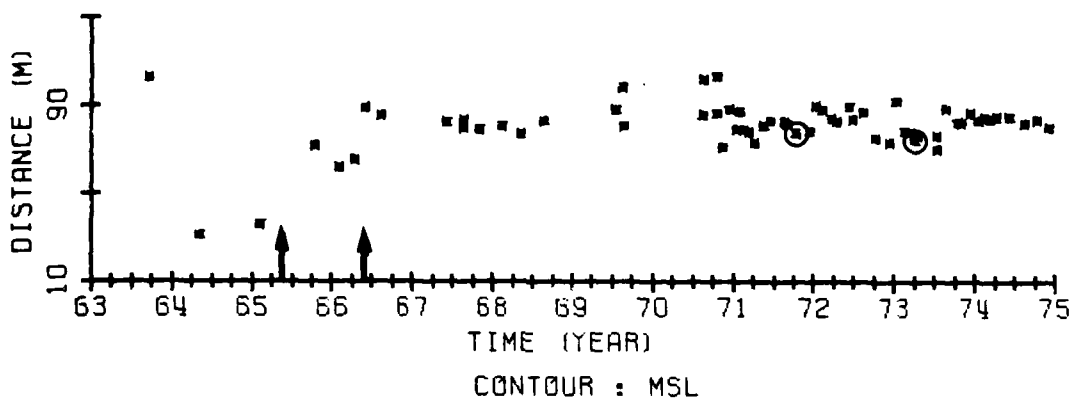
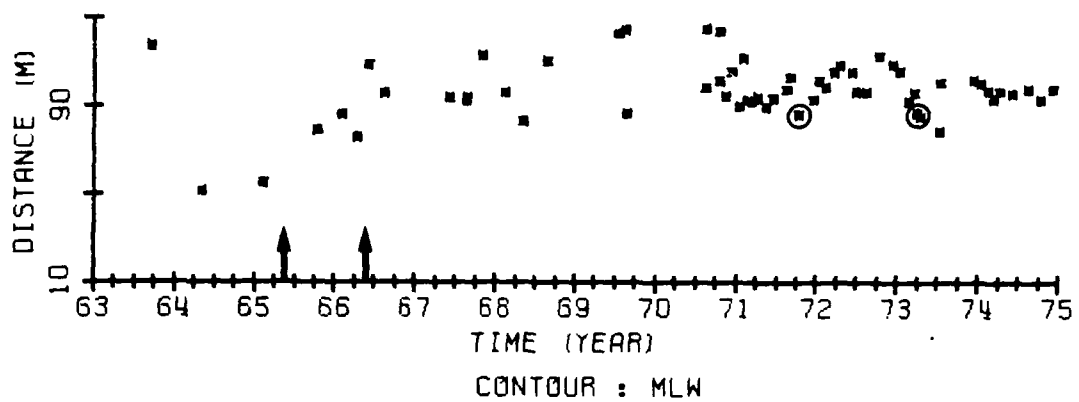
DISTANCE FROM THE BASE LINE TO STATED CONTOURS AT WB 33



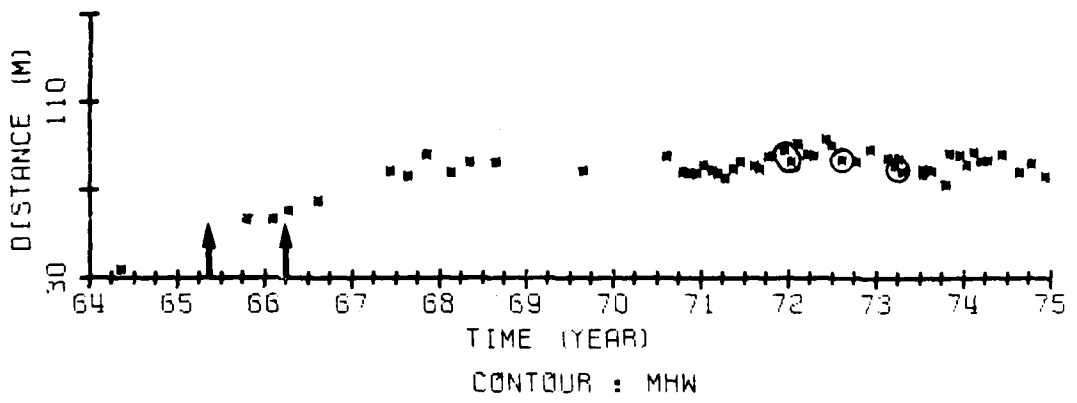
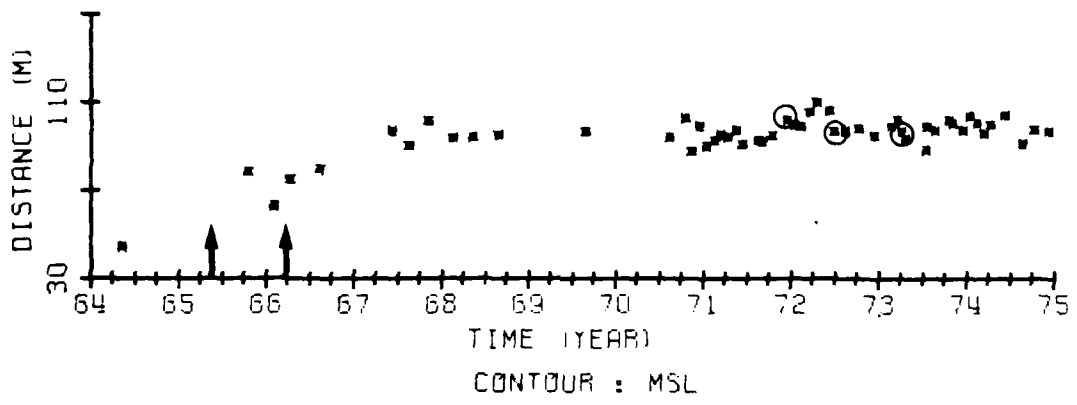
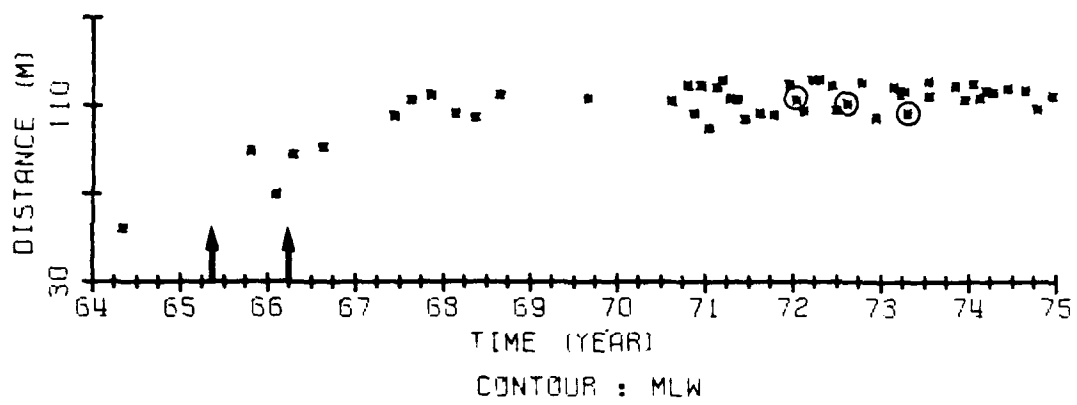
DISTANCE FROM THE BASE LINE TO STATED CONTOURS AT WB 36



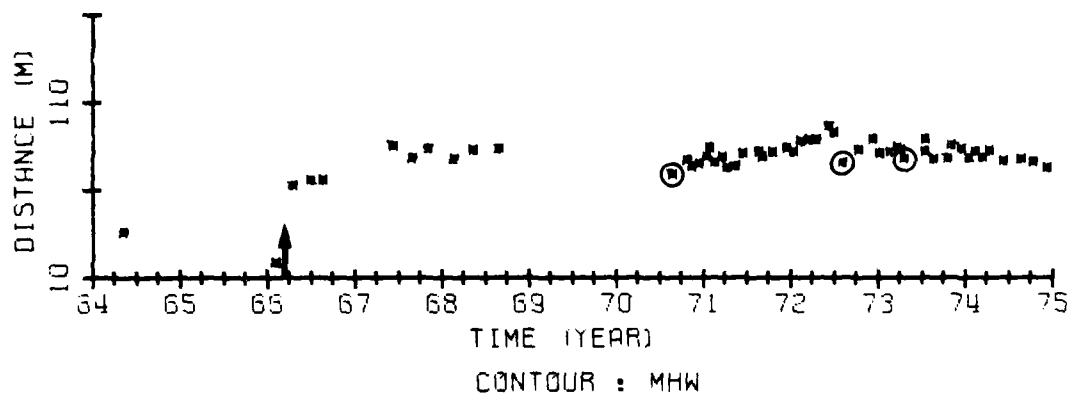
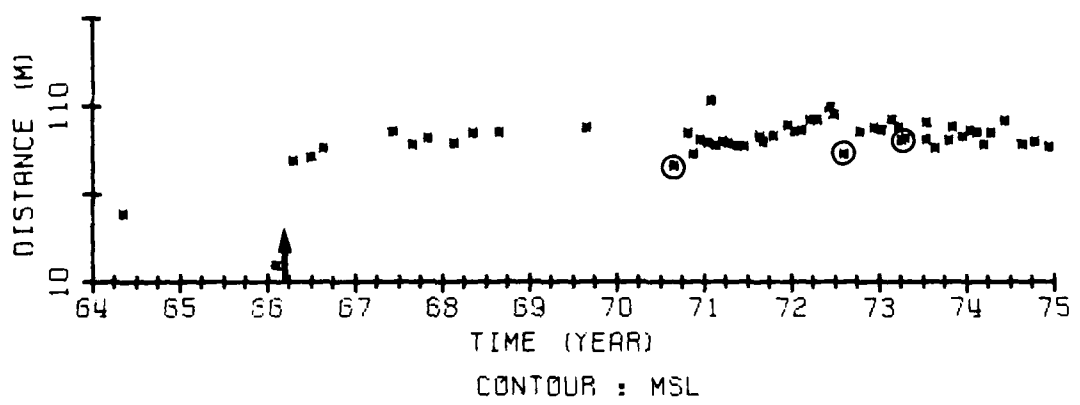
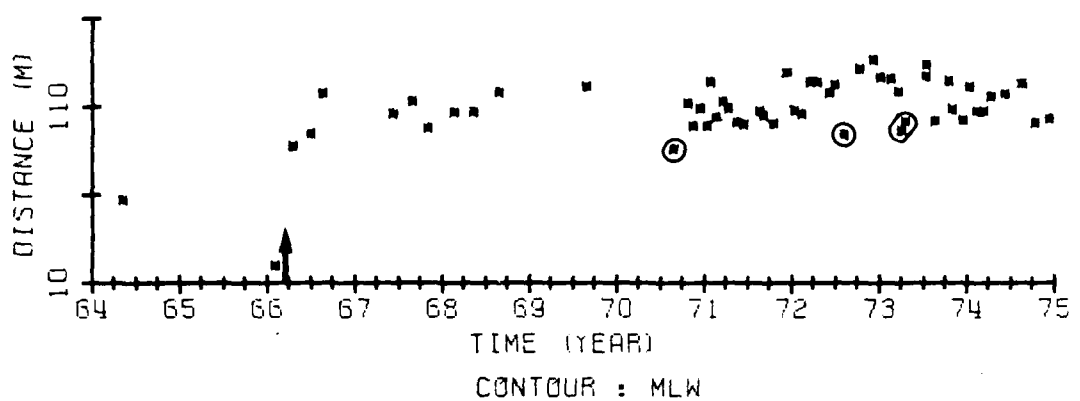
DISTANCE FROM THE BASE LINE TO STATED CONTOURS AT WB 39



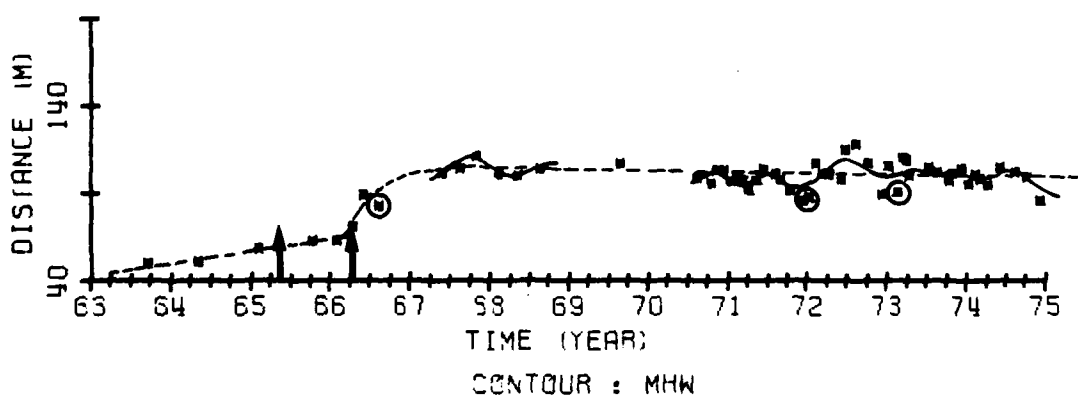
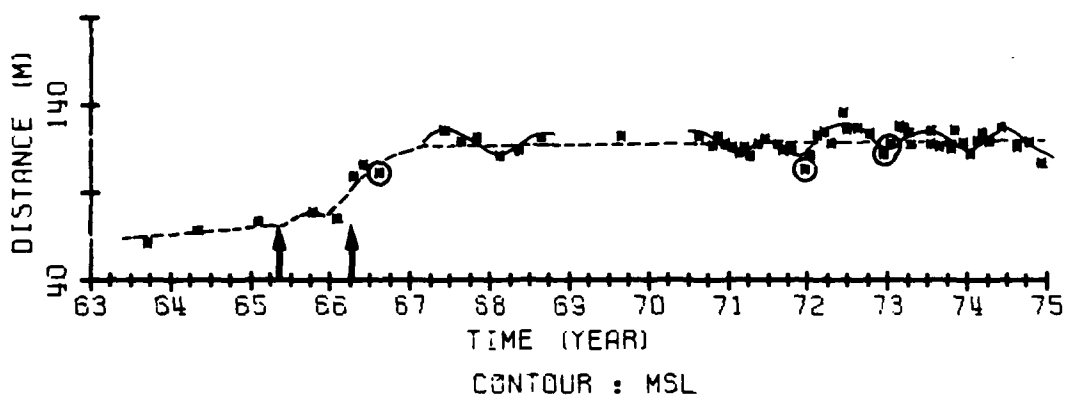
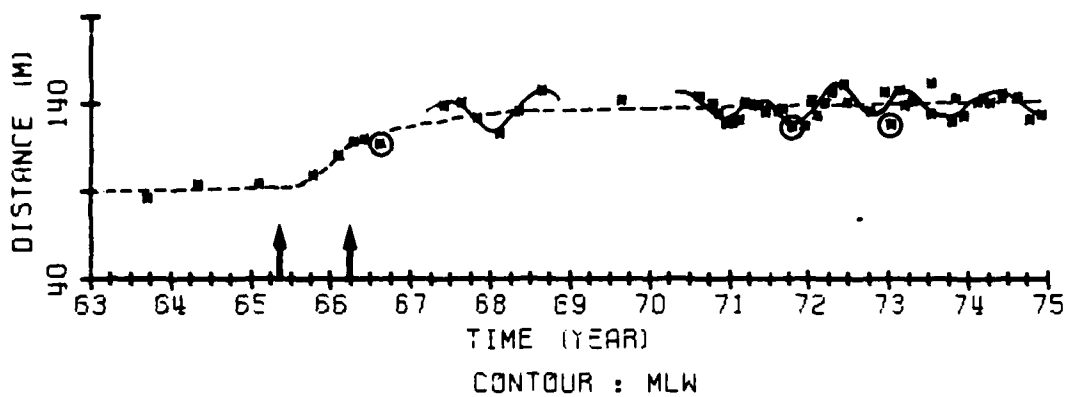
DISTANCE FROM THE BASE LINE TO STATED CONTOURS AT WB 42



DISTANCE FROM THE BASE LINE TO STATED CONTOURS AT WB 44

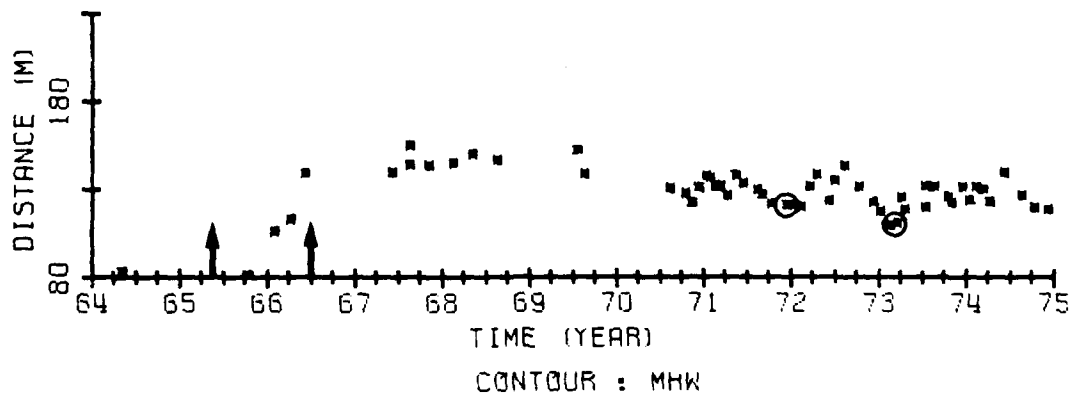
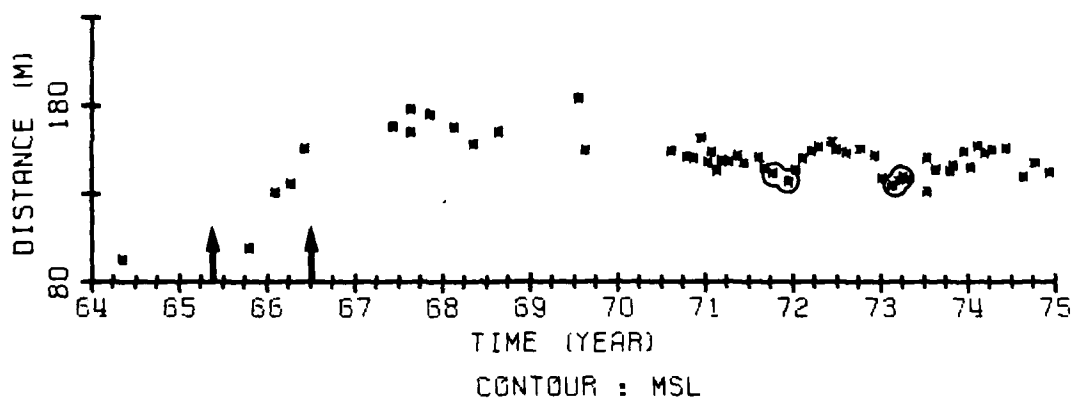
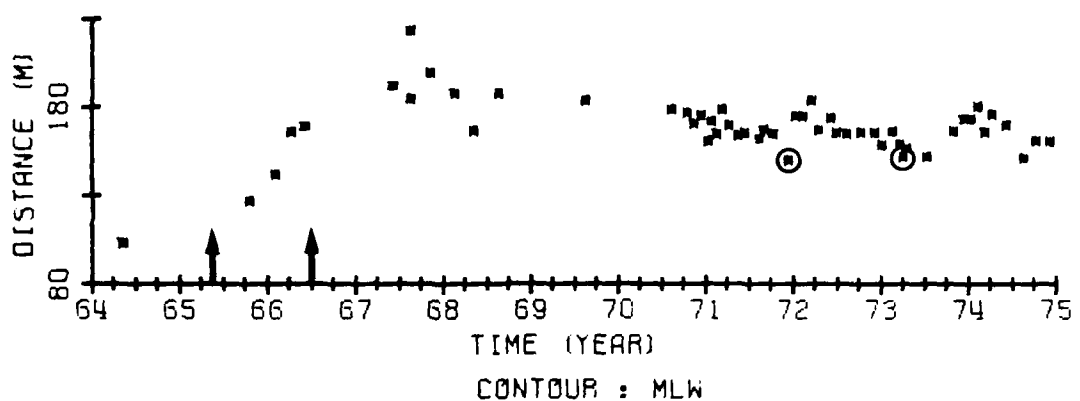


DISTANCE FROM THE BASE LINE TO STATED CONTOURS AT WB 45

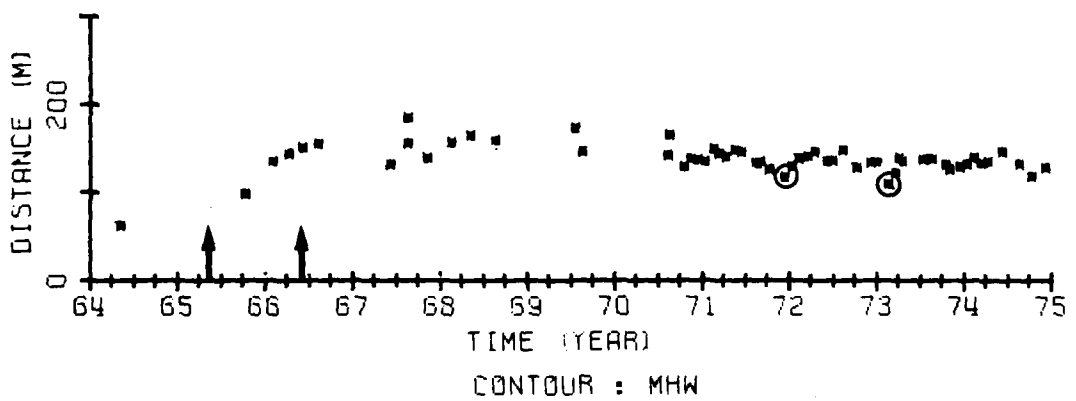
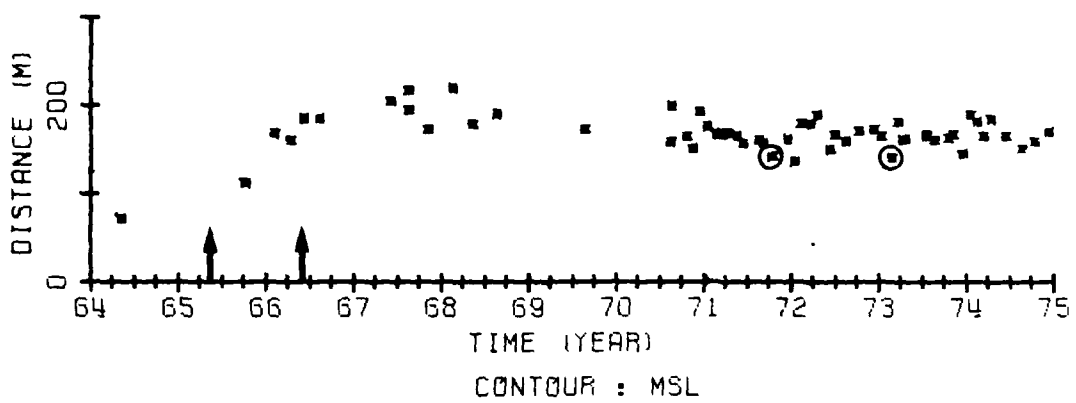
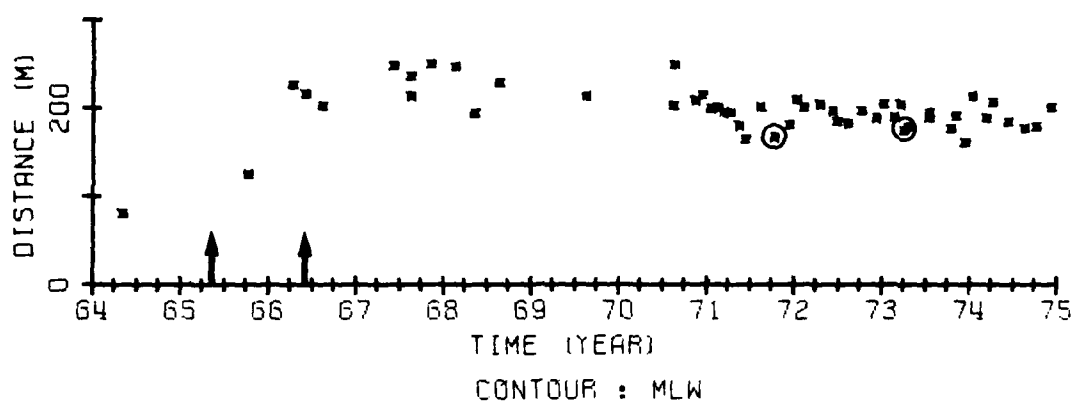


Note: Circles Indicate profiles measured shortly after a local storm.
 Arrows Indicate the approximate time at which beach fills were placed.

DISTANCE FROM THE BASE LINE TO STATED CONTOURS AT WB 47

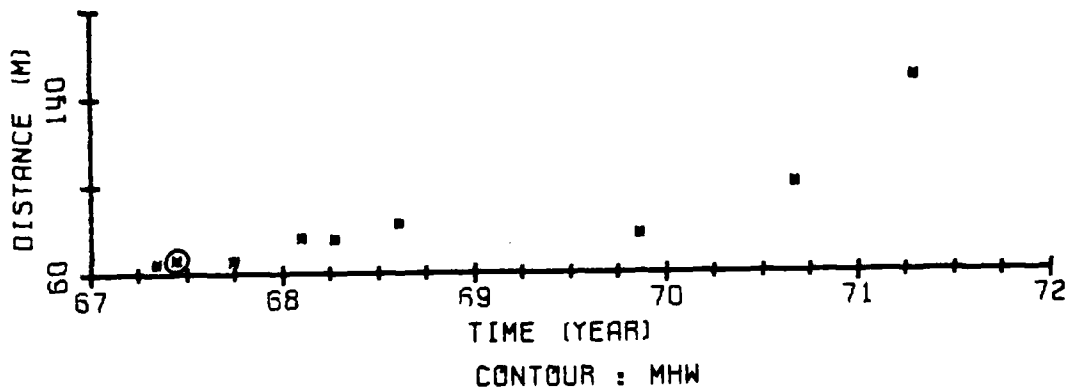
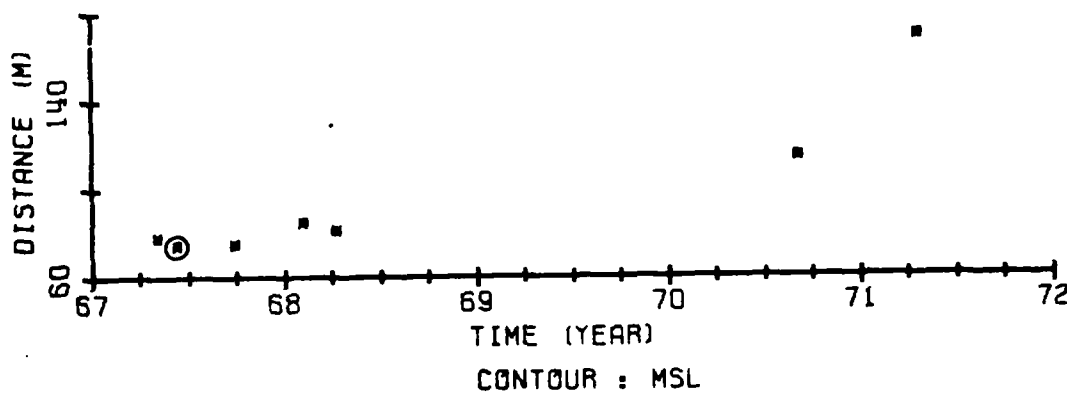
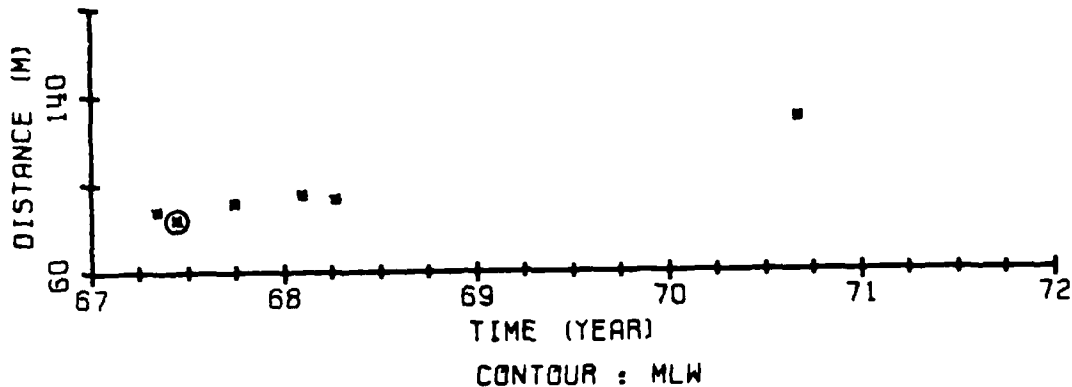


DISTANCE FROM THE BASE LINE TO STATED CONTOURS AT WB 49

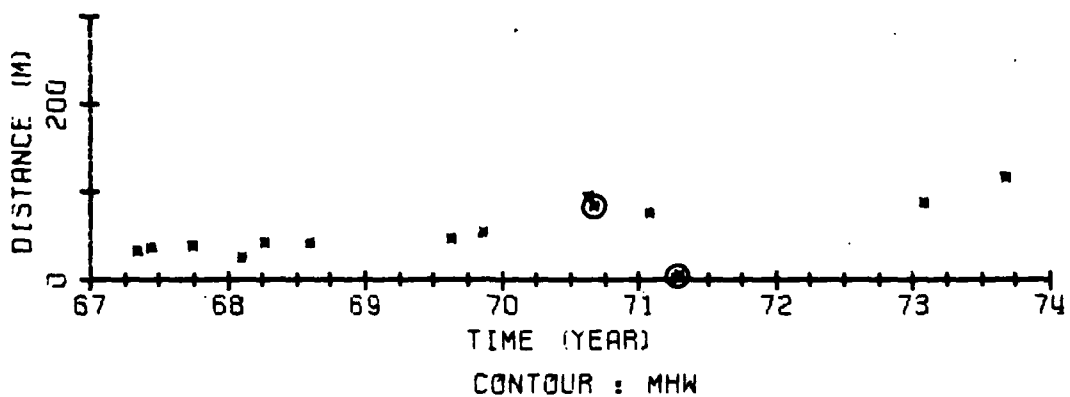
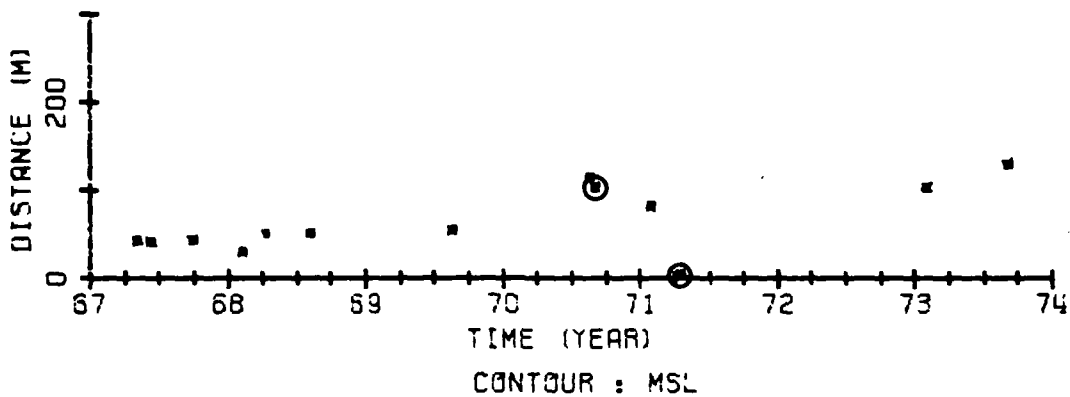
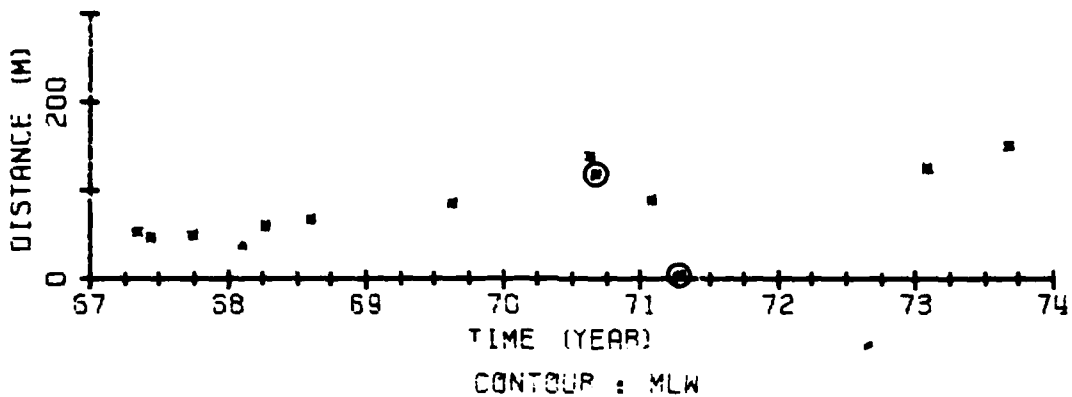


DISTANCE FROM THE BASE LINE TO STATED CONTOURS AT WB 50

APPENDIX B
CAROLINA BEACH EXCURSION DISTANCE PLOTS

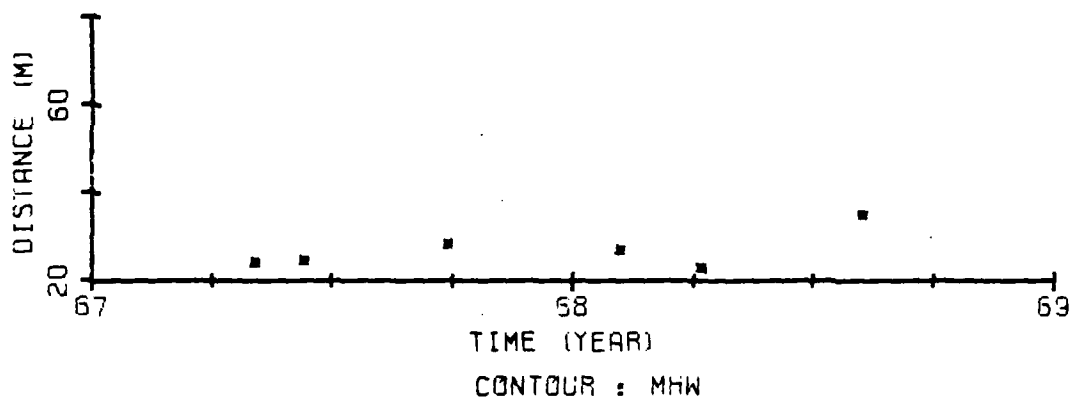
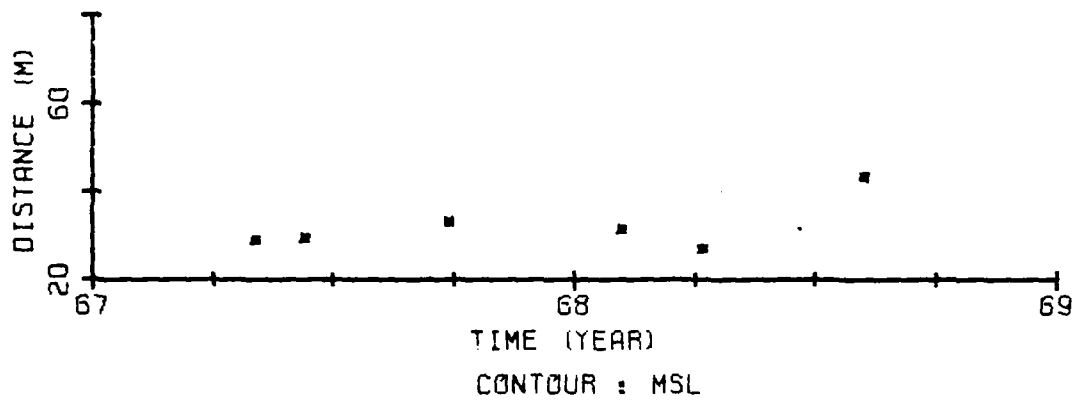
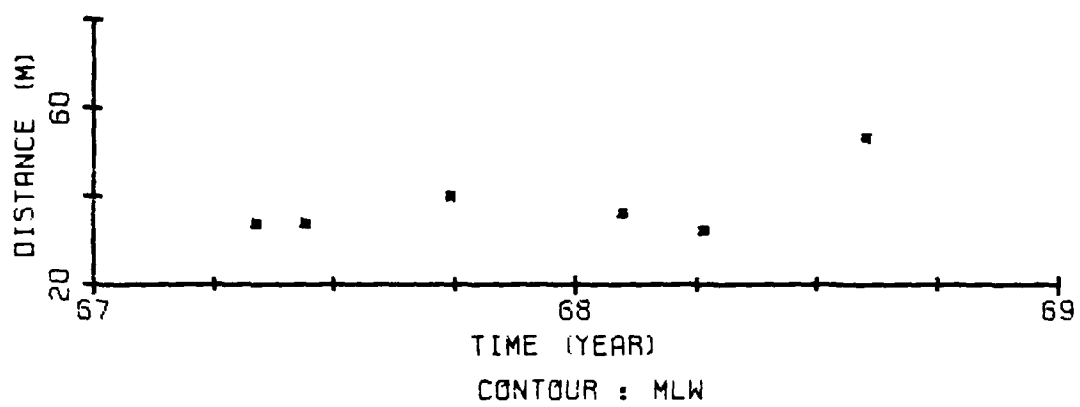


DISTANCE FROM THE BASE LINE TO STATED CONTOURS AT CB 1

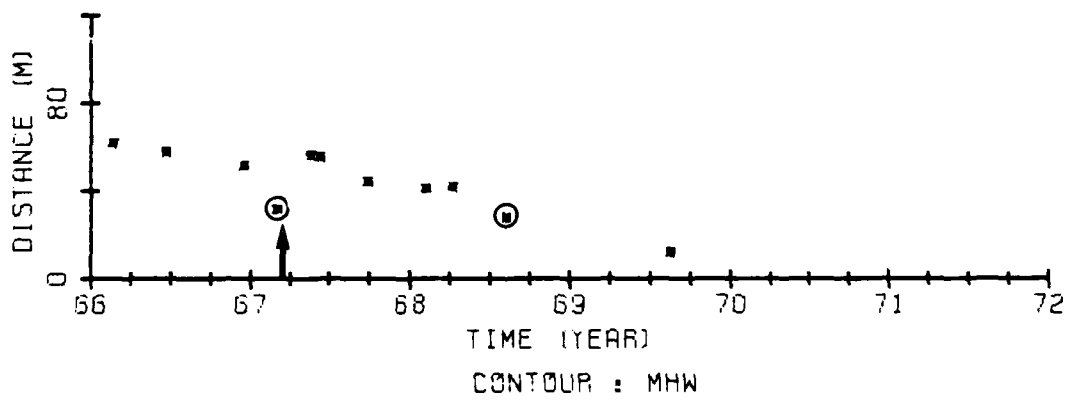
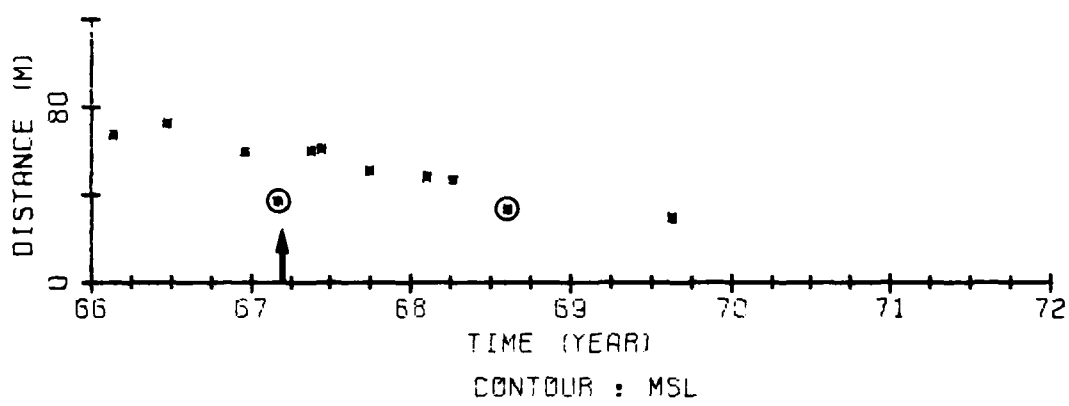
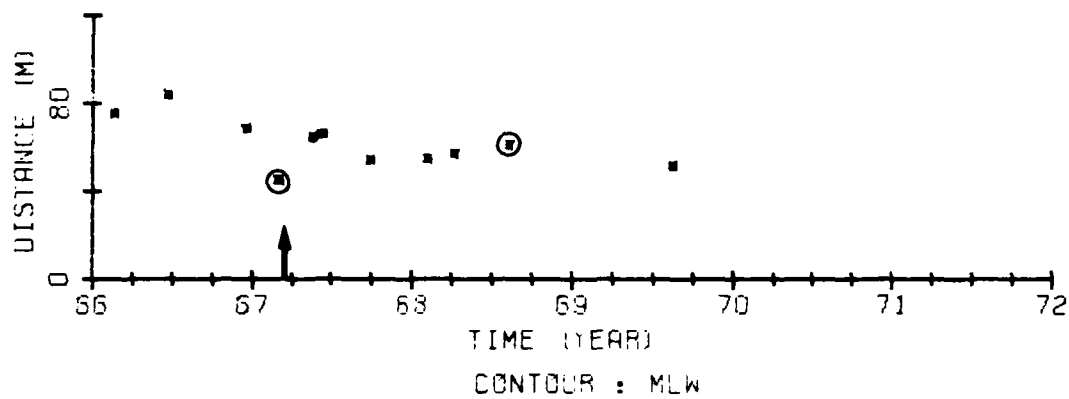


Note: Circles indicate profiles measured shortly after a local storm.
Arrows indicate the approximate time at which beach fills were placed.

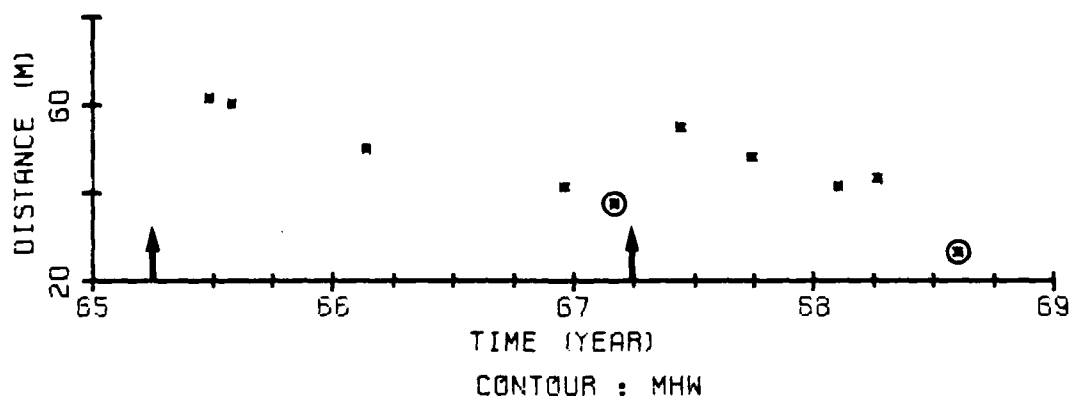
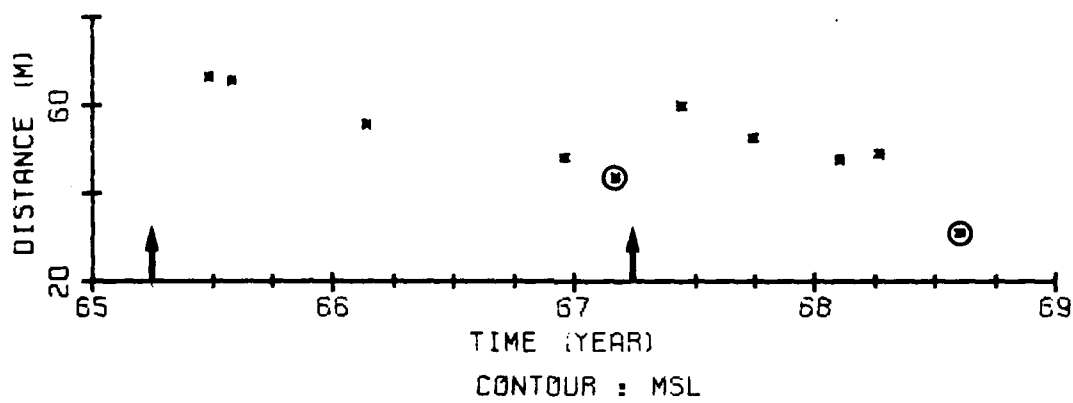
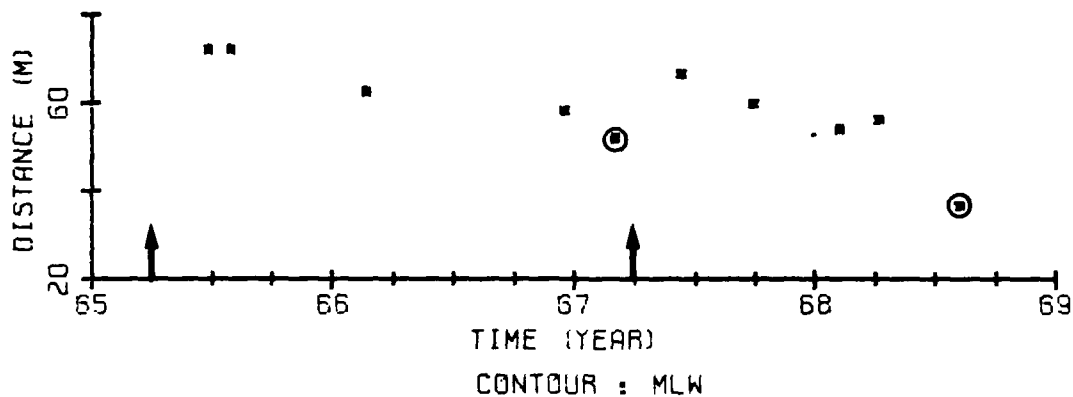
DISTANCE FROM THE BASE LINE TO STATED CONTOURS AT CB 2



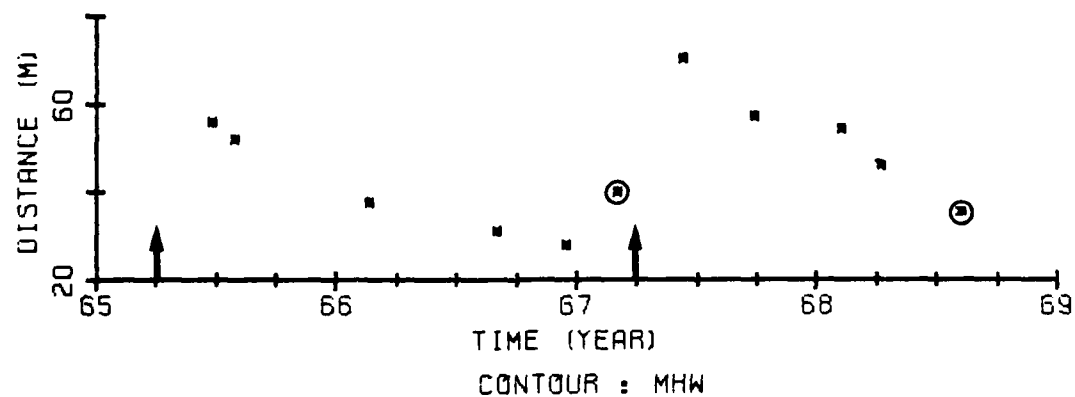
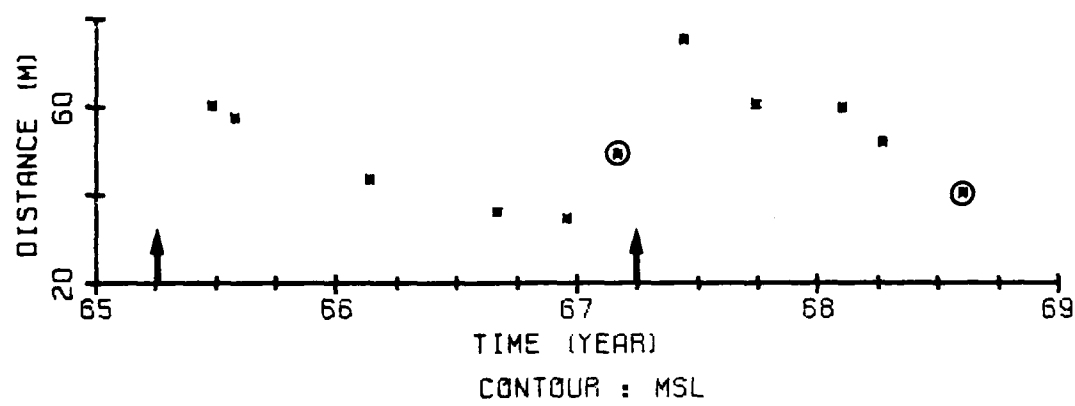
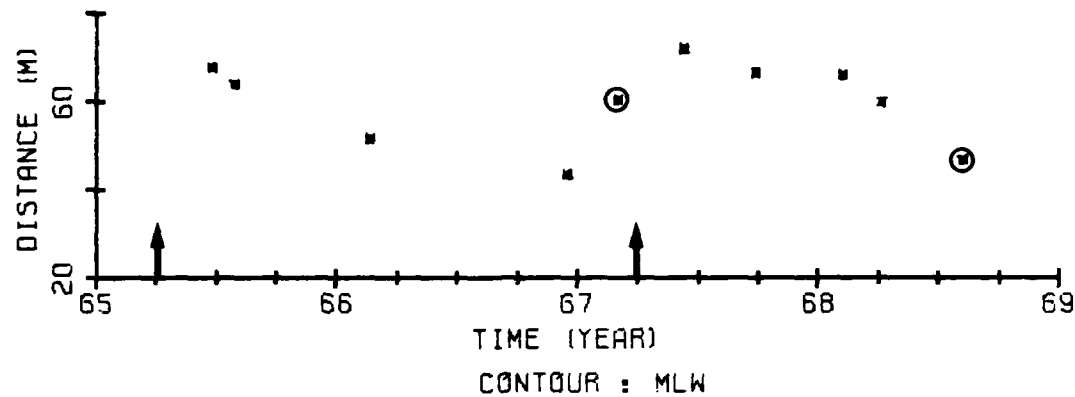
DISTANCE FROM THE BASE LINE TO STATED CONTOURS AT CB 10



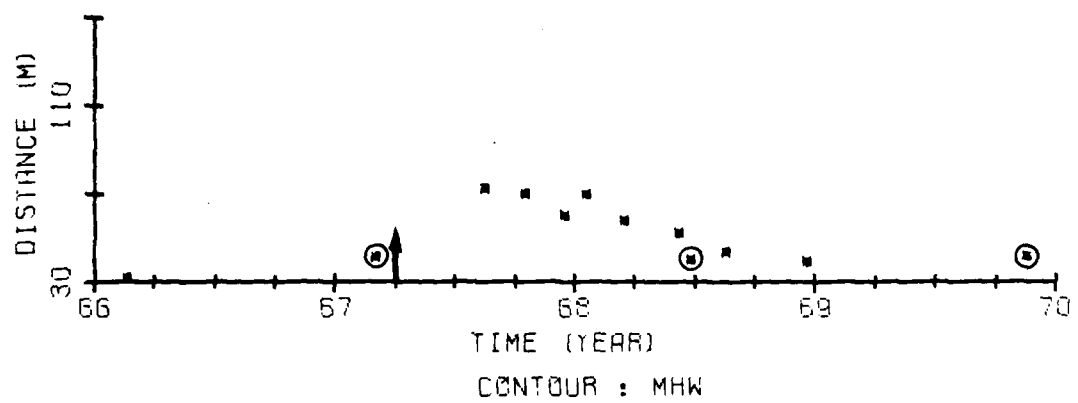
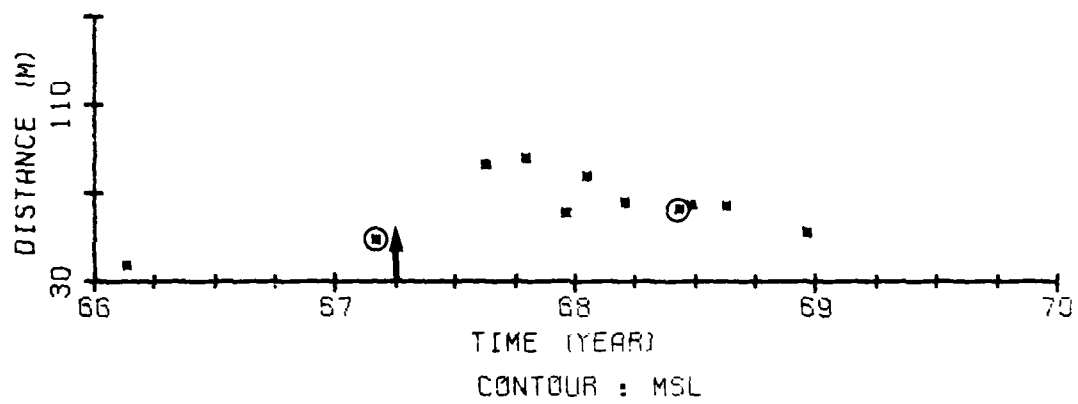
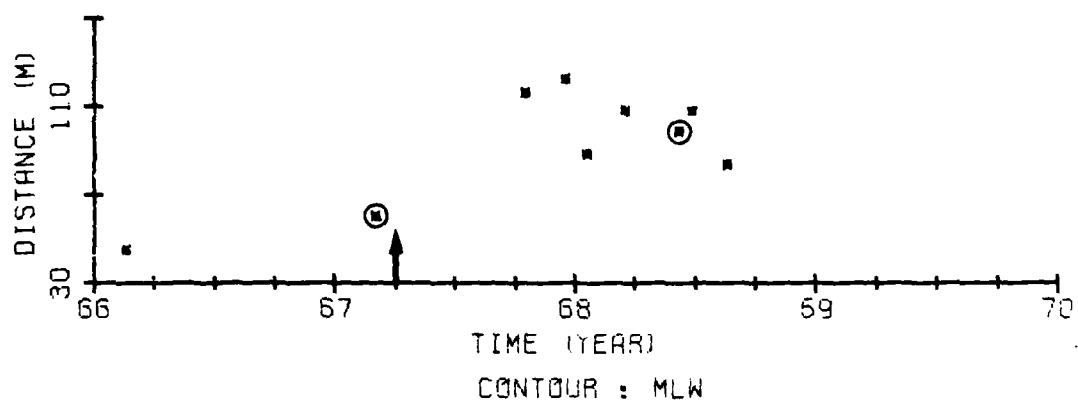
DISTANCE FROM THE BASE LINE TO STATED CONTOURS AT CB 15



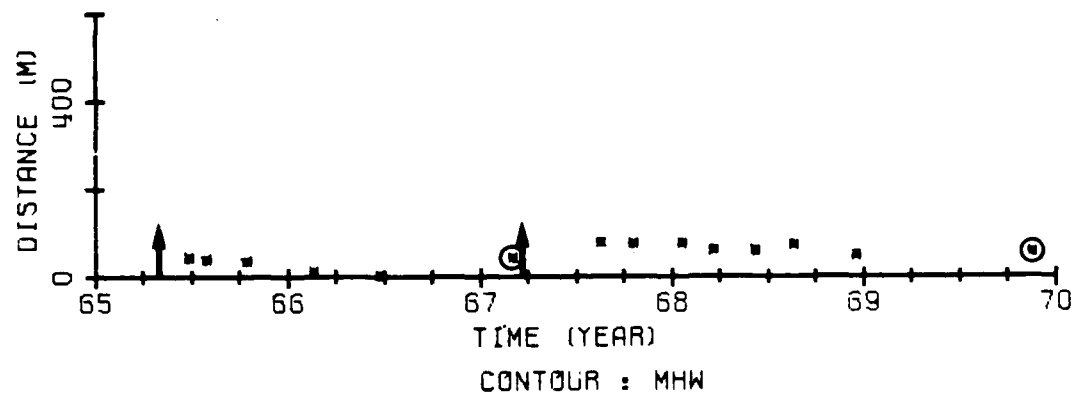
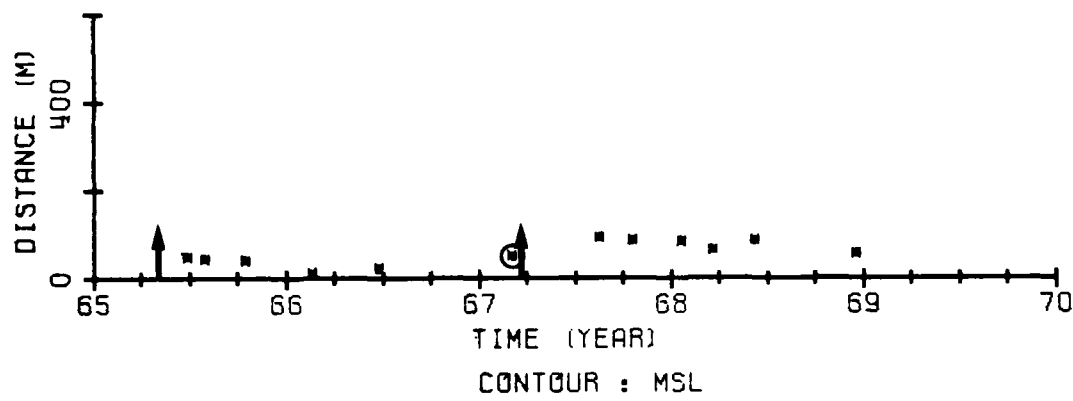
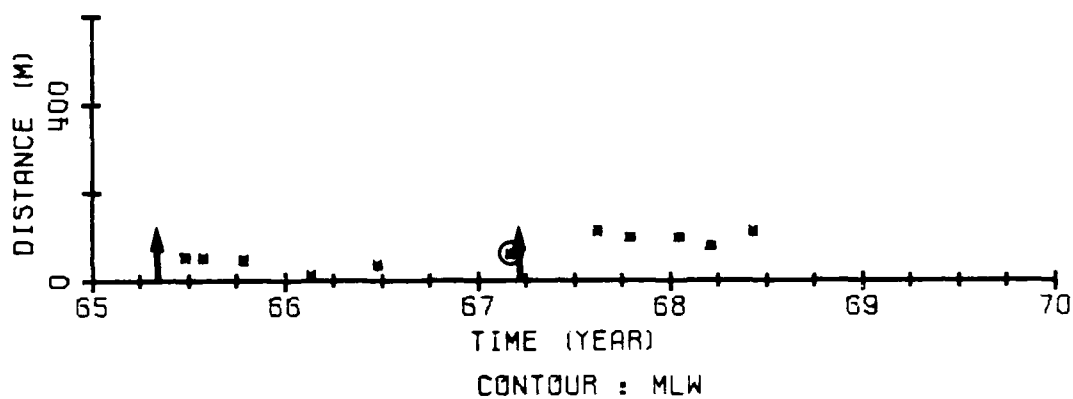
DISTANCE FROM THE BASE LINE TO STATED CONTOURS AT CB 1E



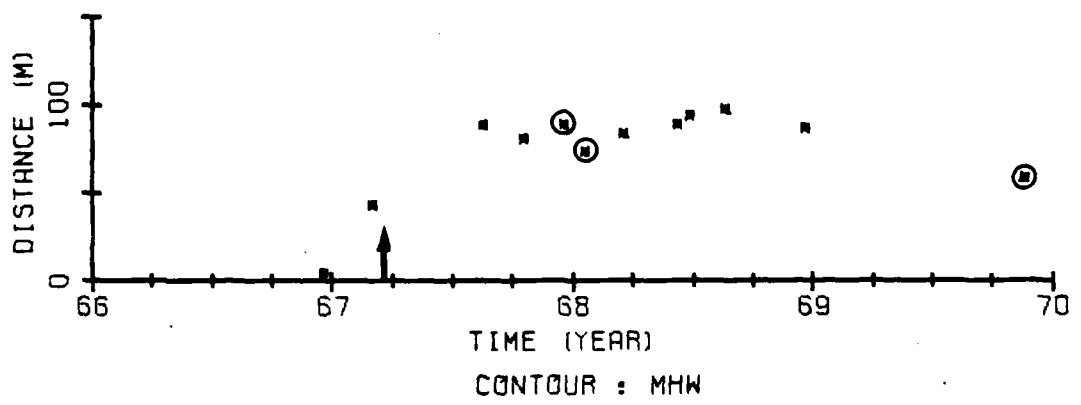
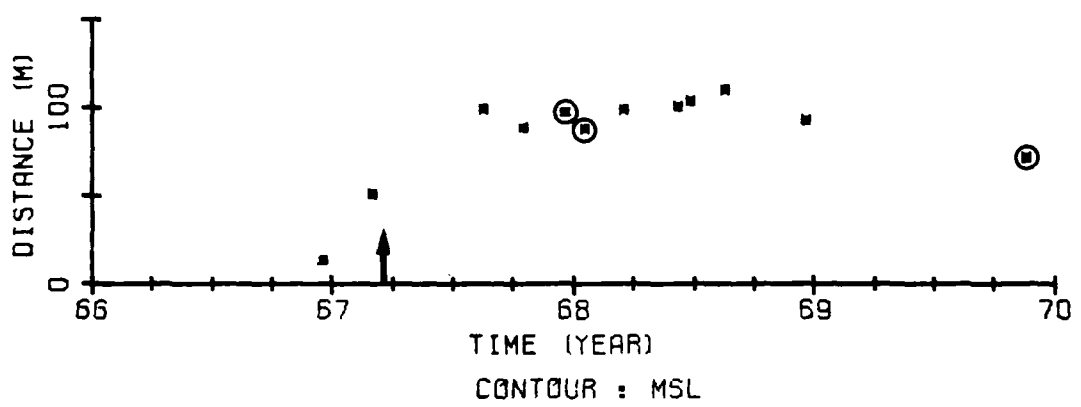
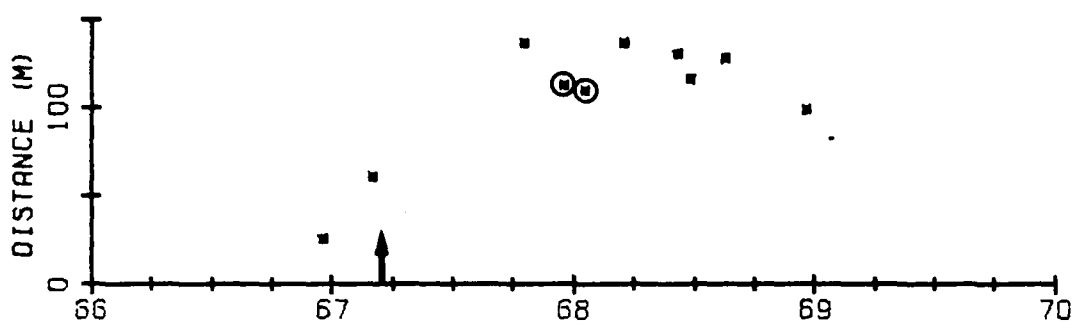
DISTANCE FROM THE BASE LINE TO STATED CONTOURS AT CB 21



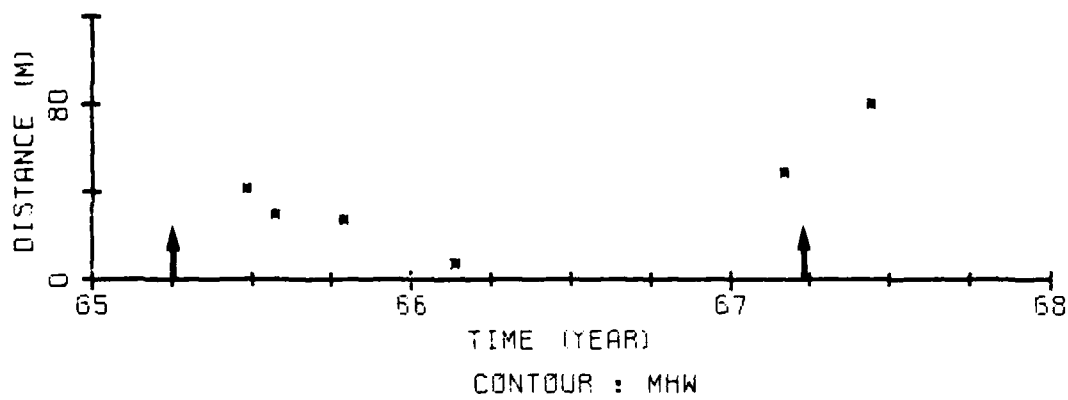
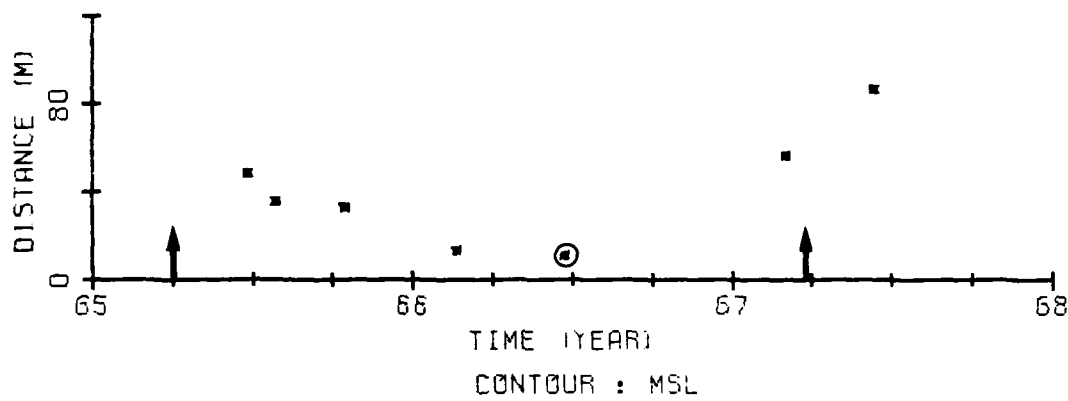
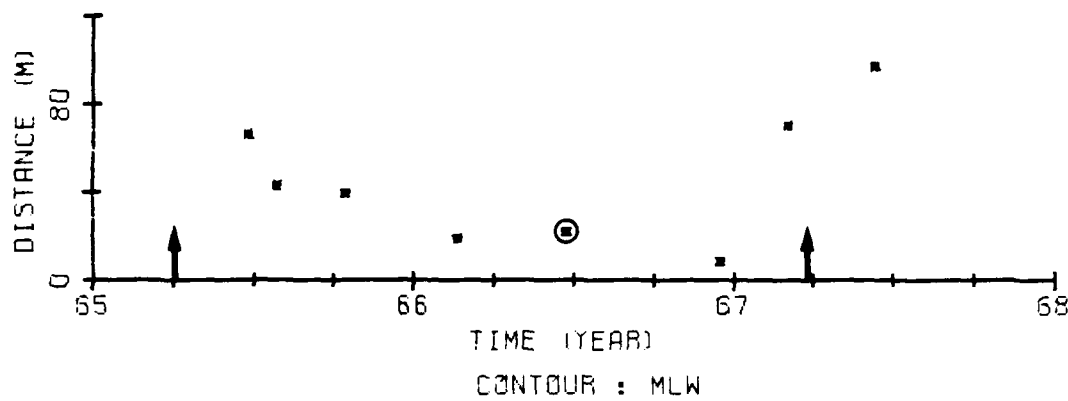
DISTANCE FROM THE BASE LINE TO STATED CONTOURS AT CB 32



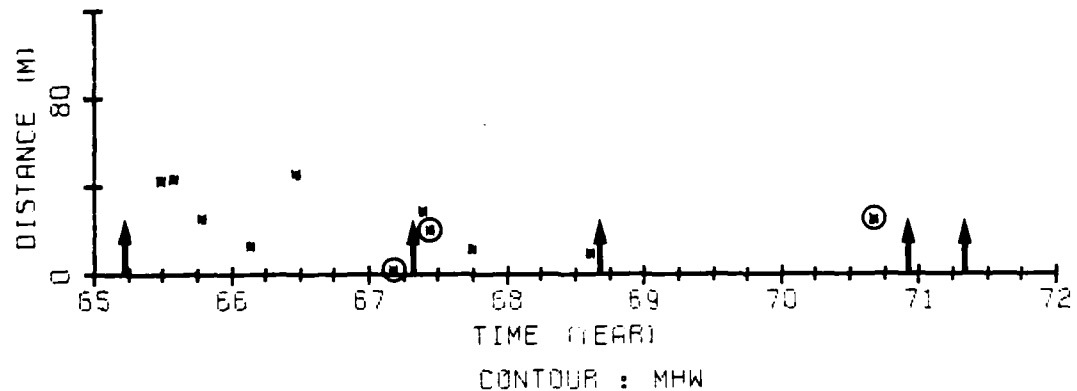
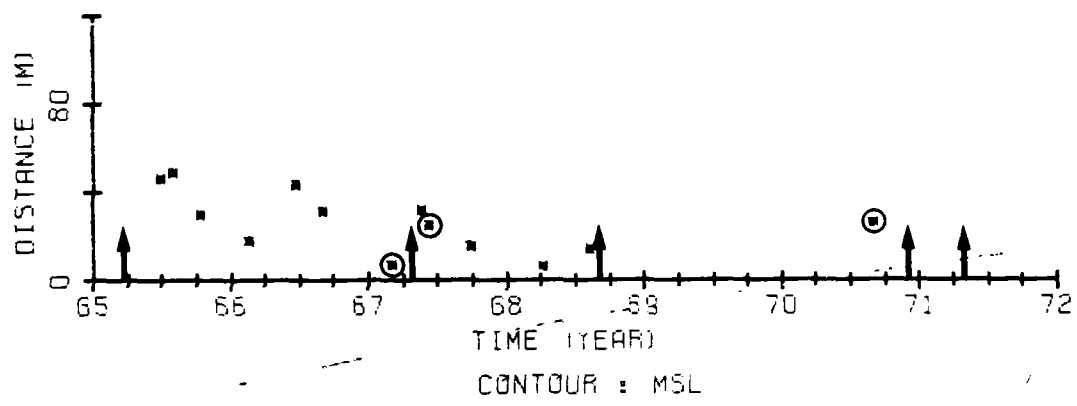
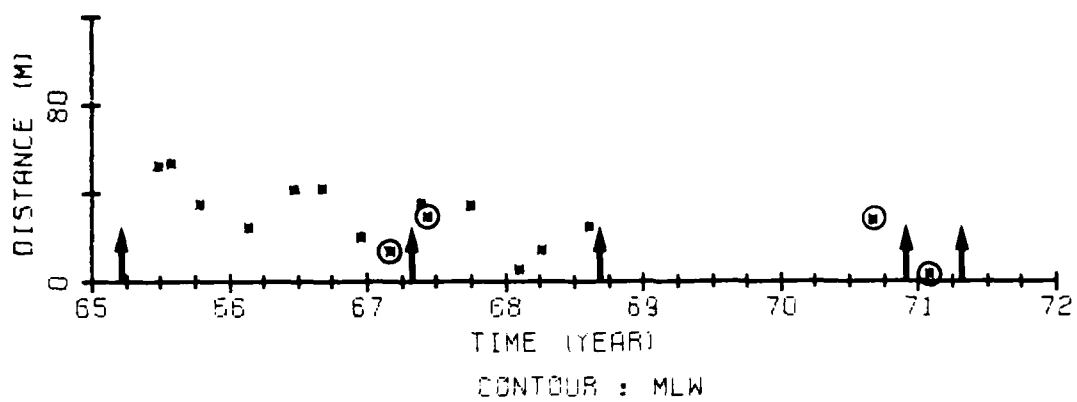
DISTANCE FROM THE BASE LINE TO STATED CONTOURS AT CB 40



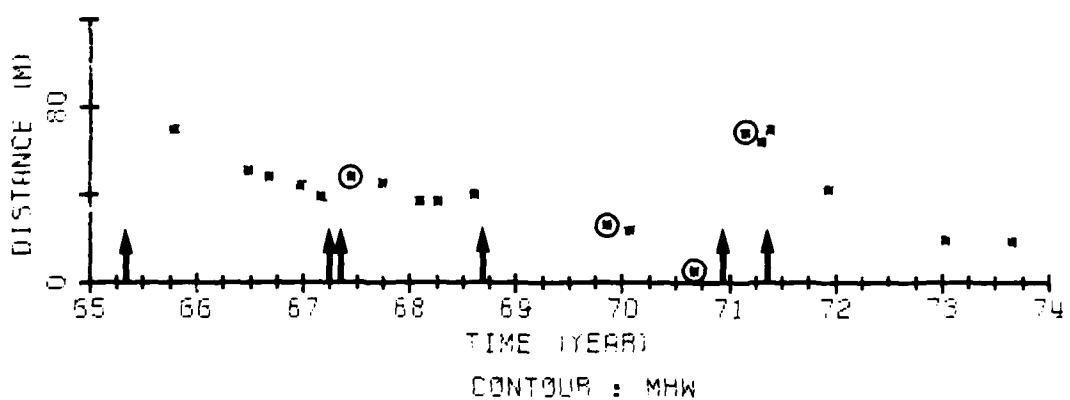
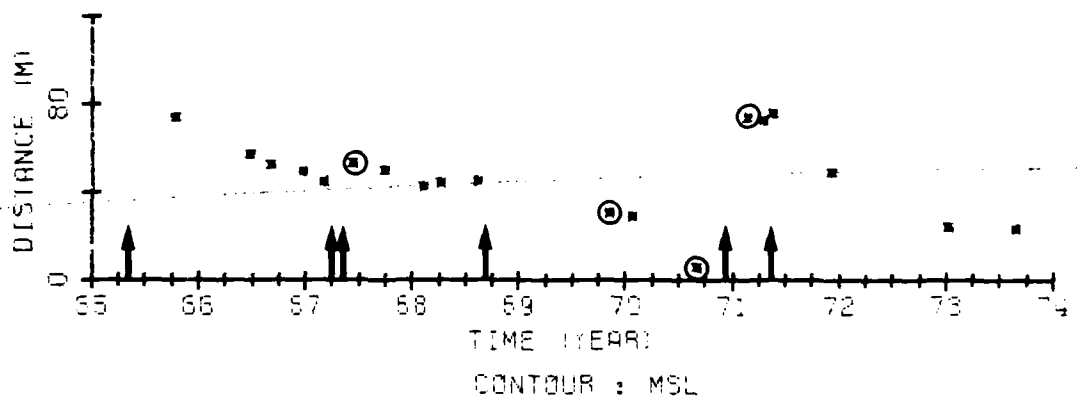
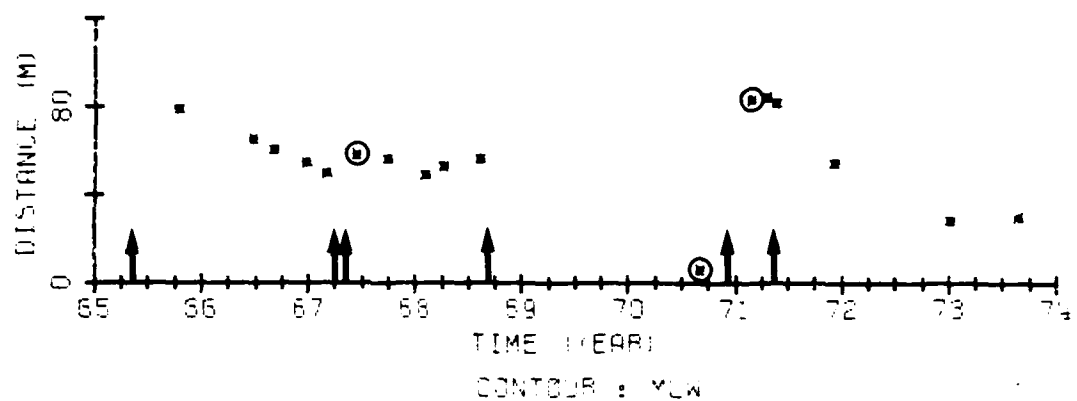
DISTANCE FROM THE BASE LINE TO STATED CONTOURS AT CB 44



DISTANCE FROM THE BASE LINE TO STATED CONTOURS AT CB 53

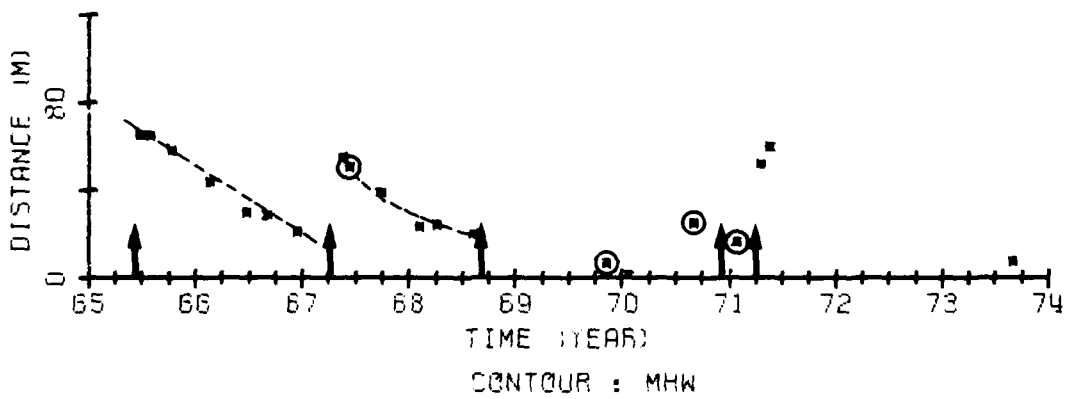
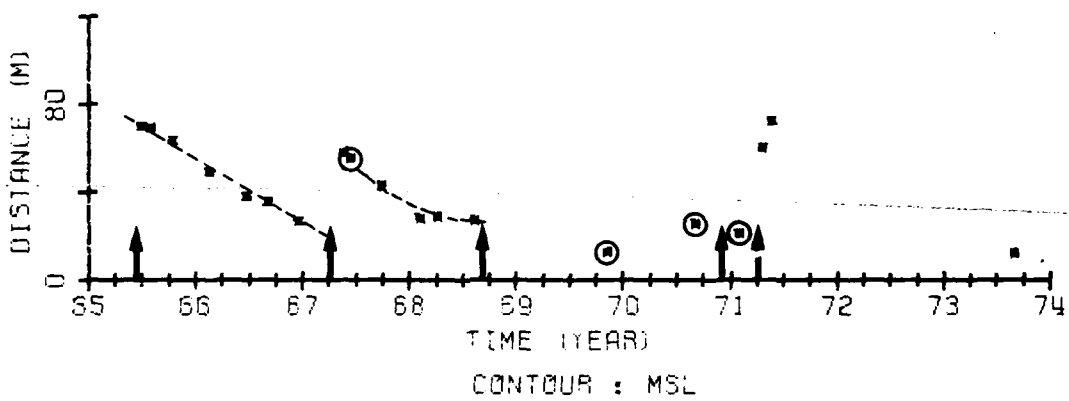
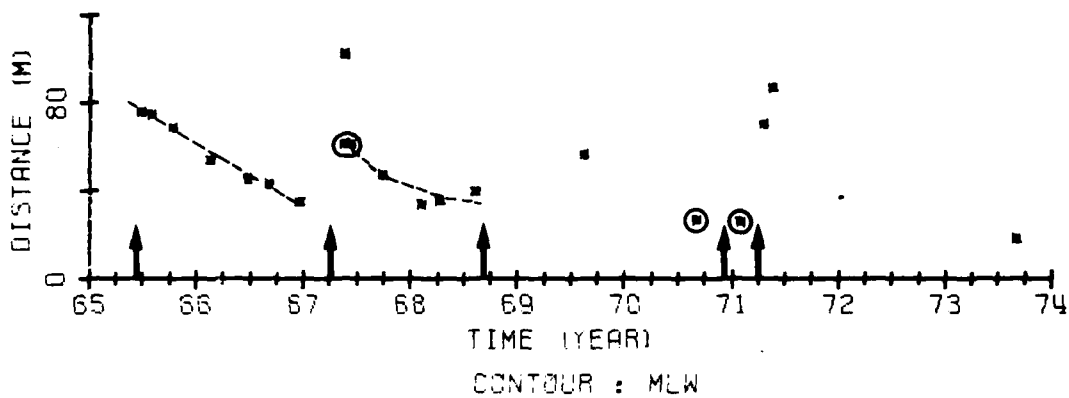


DISTANCE FROM THE BASE LINE TO STATED CONTOURS AT CB 61



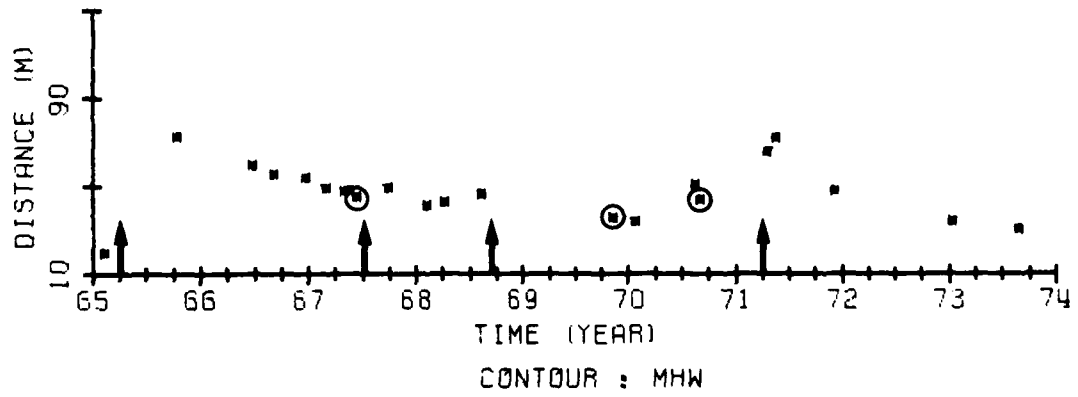
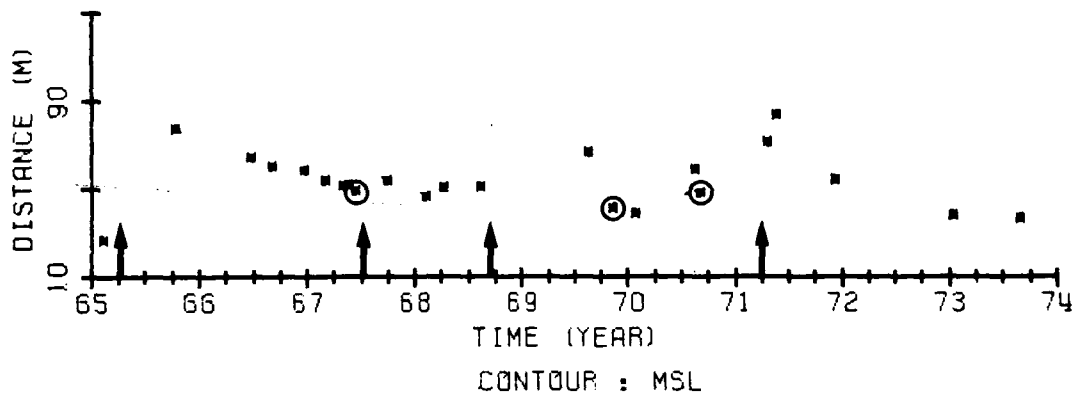
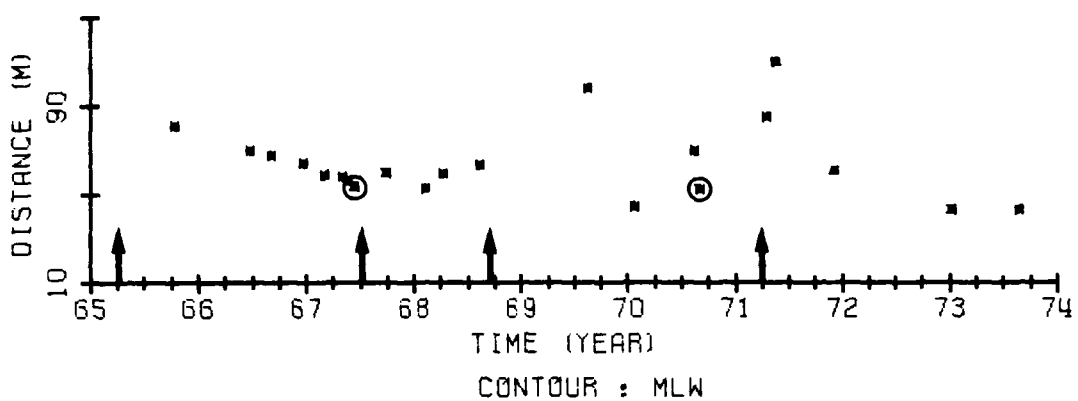
Note: Circles indicate profiles measured shortly after a local storm.
Arrows indicate the approximate time at which beach files were placed.

DISTANCE FROM THE BASE LINE TO STATED CONTOURS AT CB 64

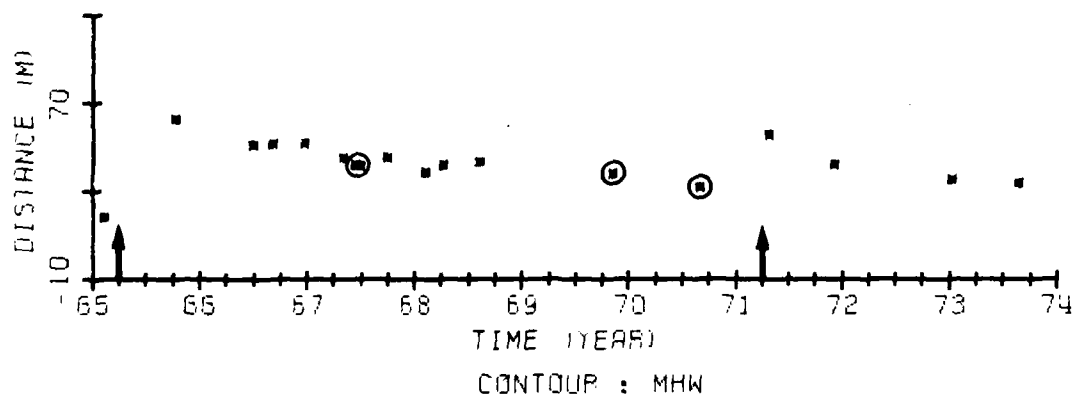
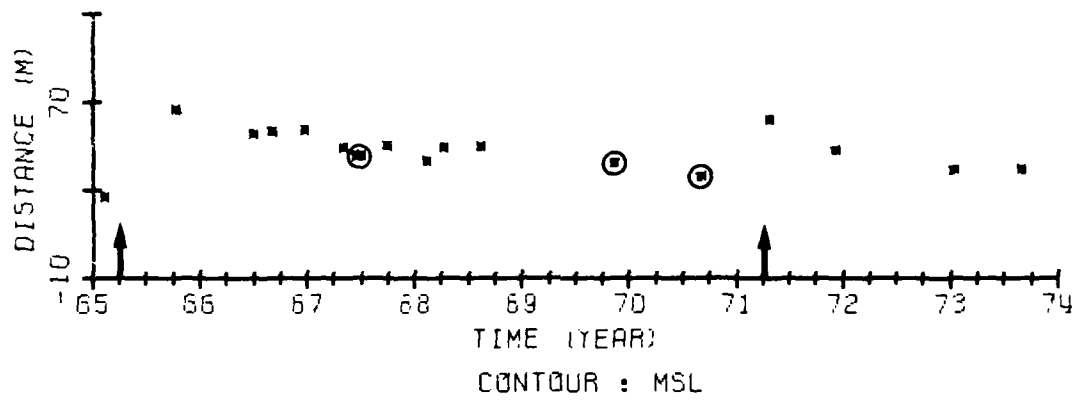
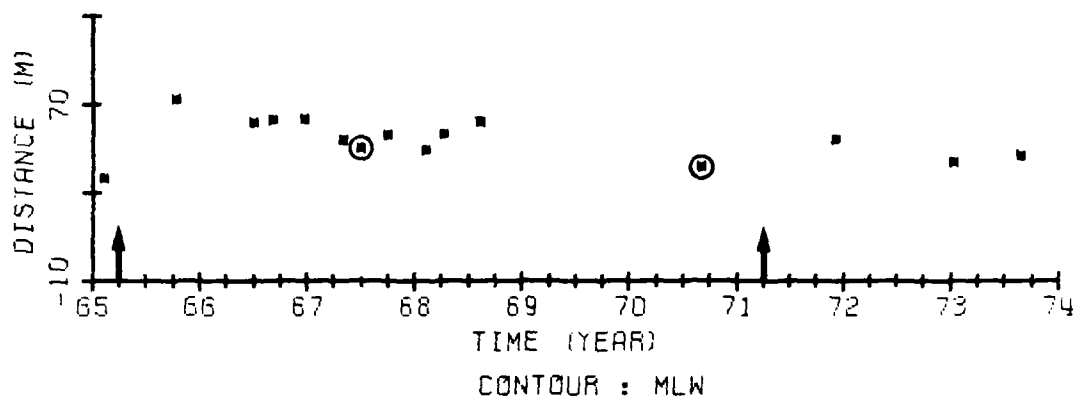


Note: Circles indicate profiles measured shortly after a local storm.
Arrows indicate the approximate time at which beach fills were placed.

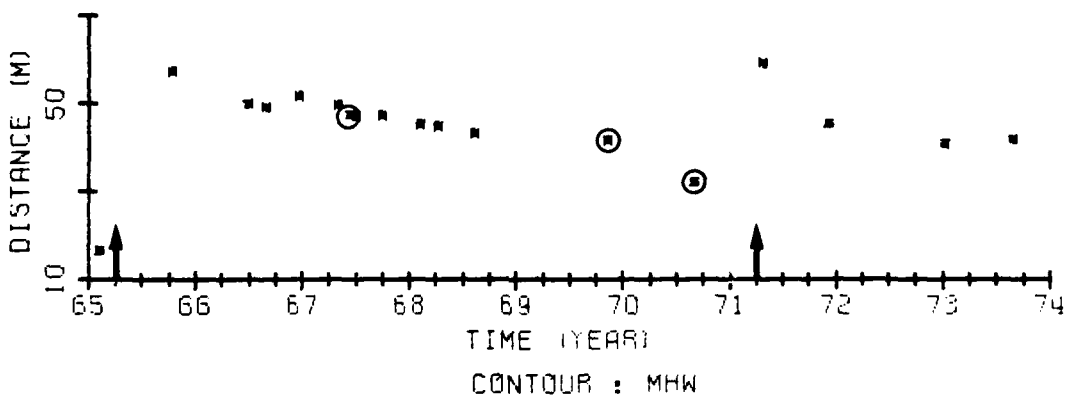
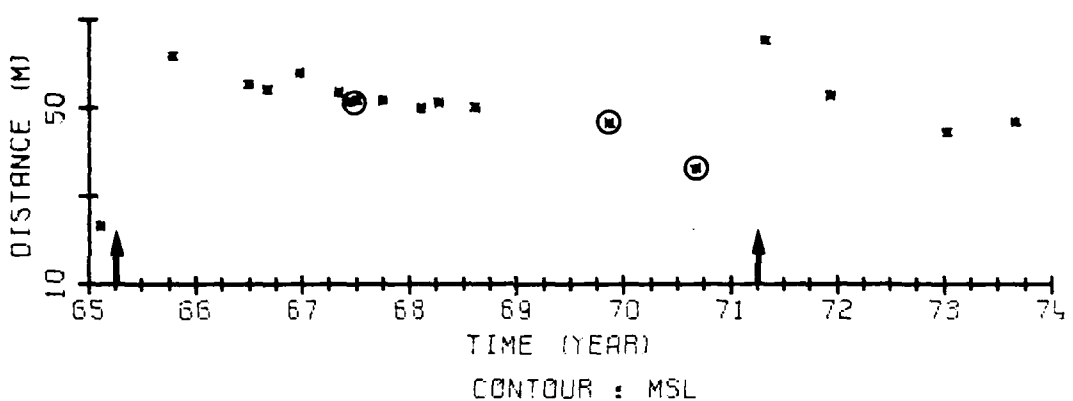
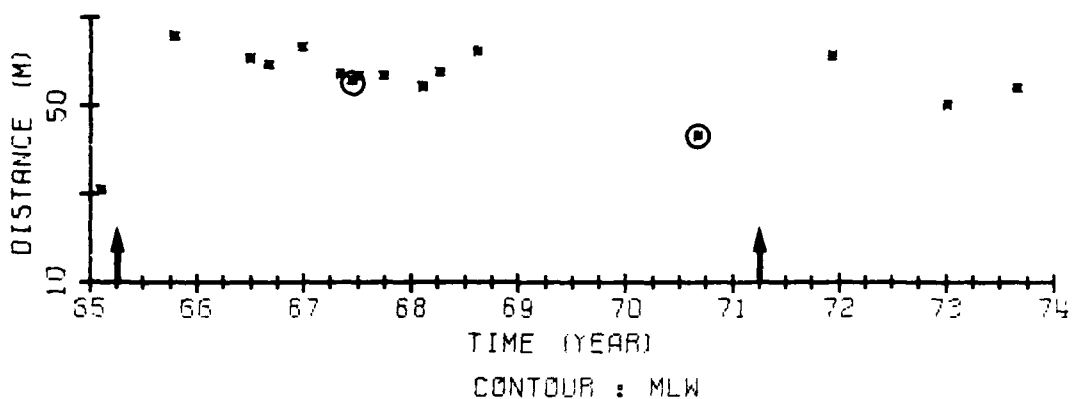
DISTANCE FROM THE BASE LINE TO STATED CONTOURS AT CB 71



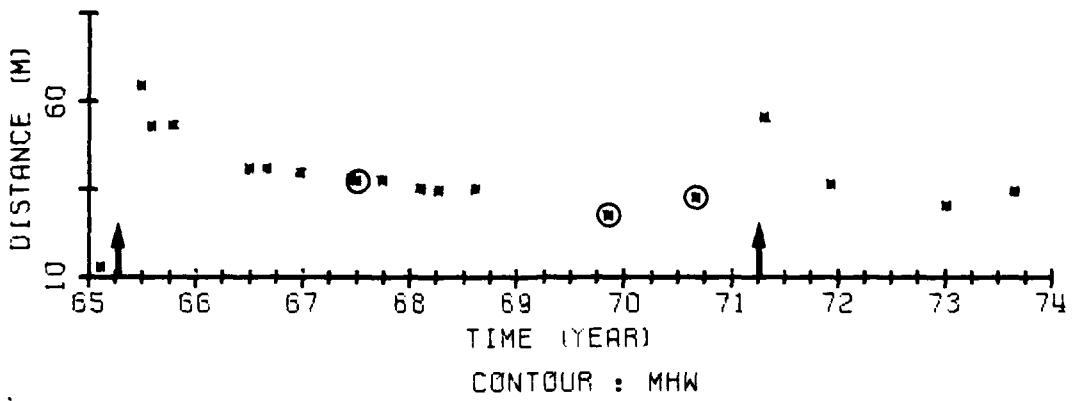
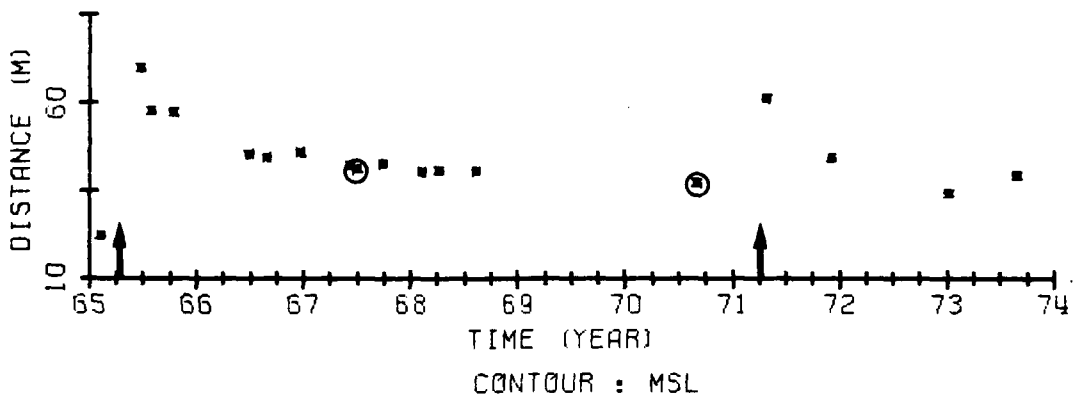
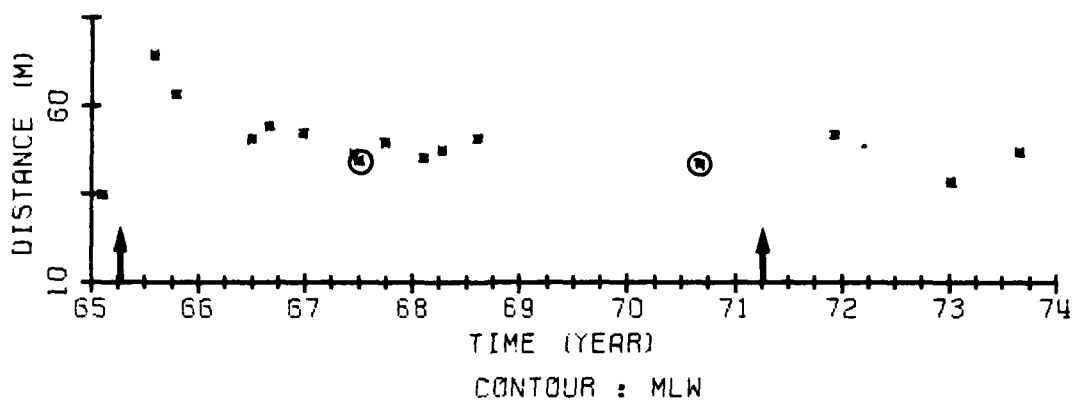
DISTANCE FROM THE BASE LINE TO STATED CONTOURS AT CB 83



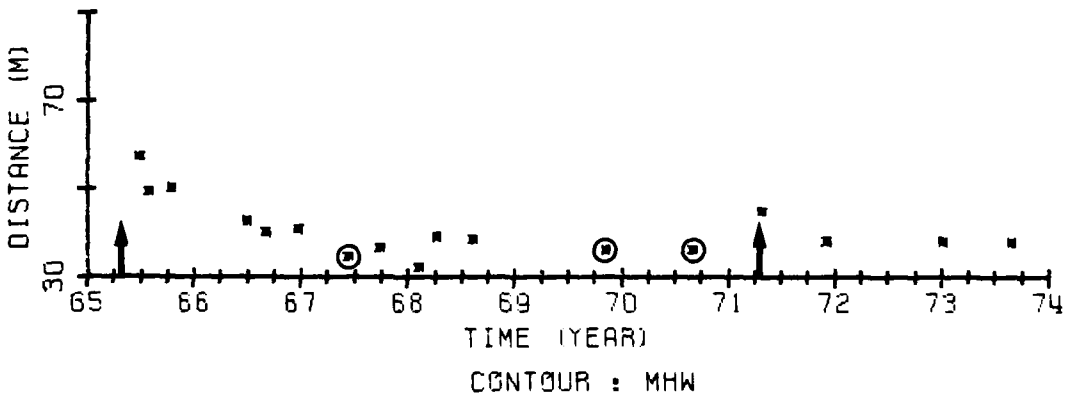
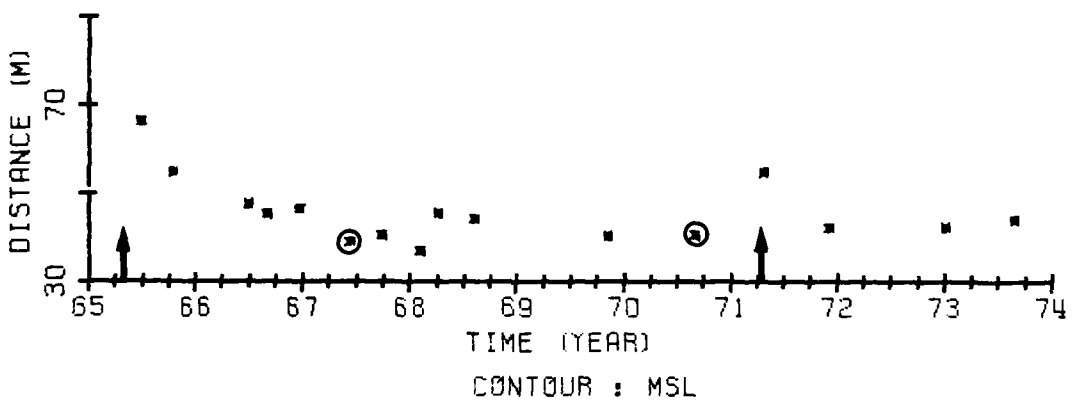
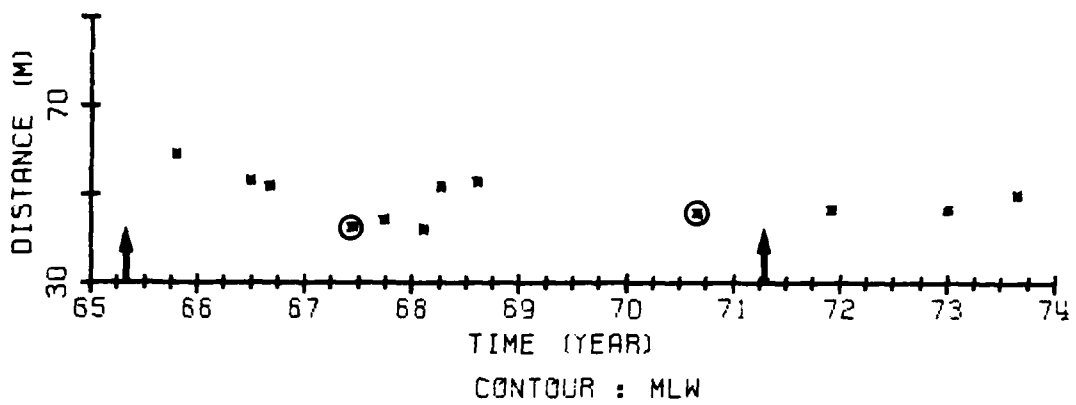
DISTANCE FROM THE BASE LINE TO STATED CONTOURS AT CB 96



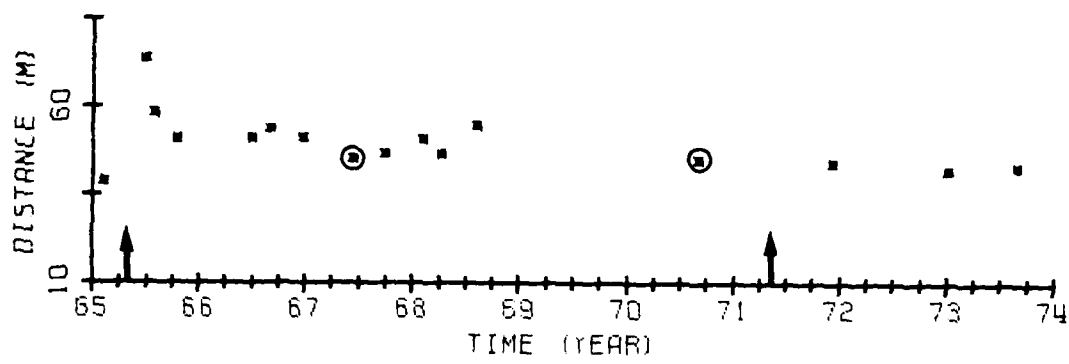
DISTANCE FROM THE BASE LINE TO STATED CONTOURS AT CB 99



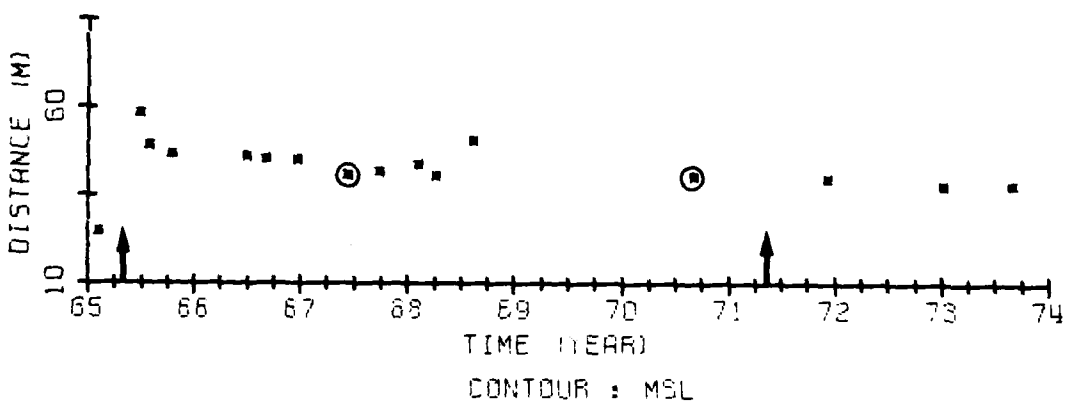
DISTANCE FROM THE BASE LINE TO STATED CONTOURS AT CB 106



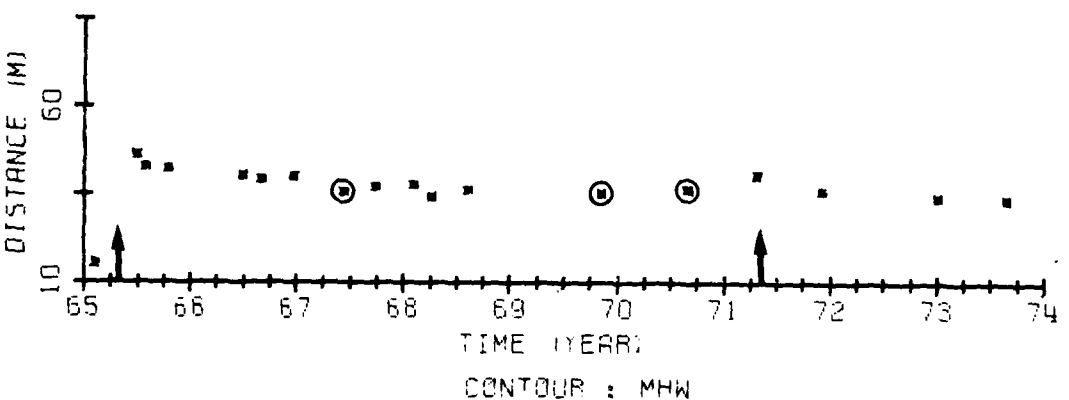
DISTANCE FROM THE BASE LINE TO STATED CONTOURS AT CB 117



CONTOUR : MLW



CONTOUR : MSL

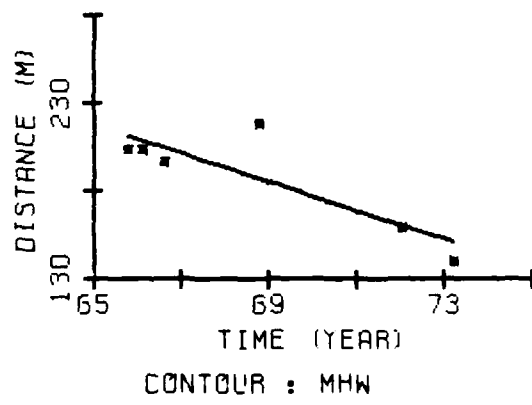
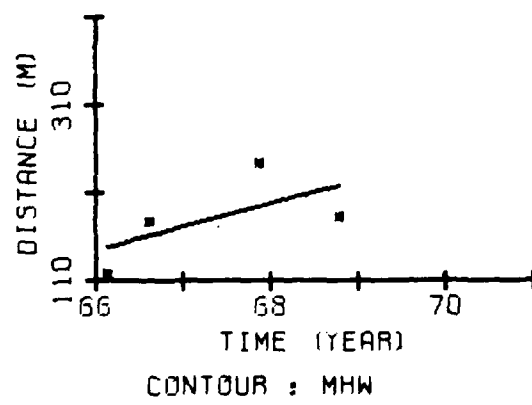
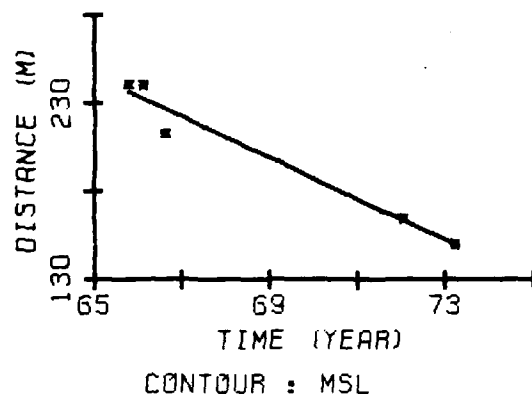
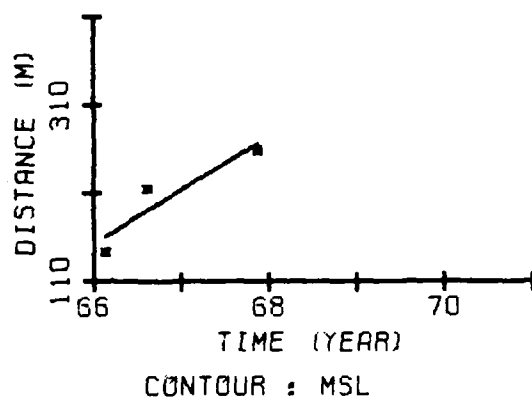
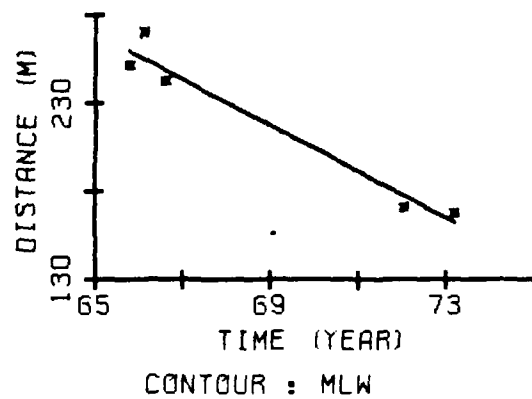
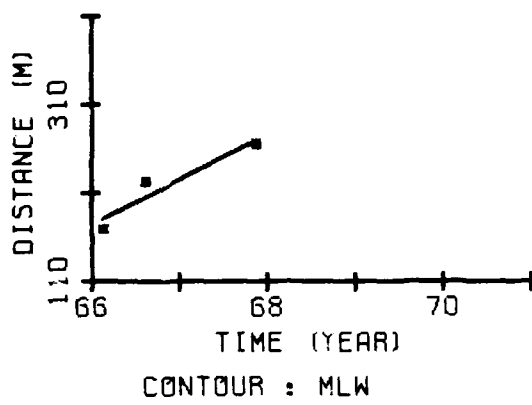


CONTOUR : MHW

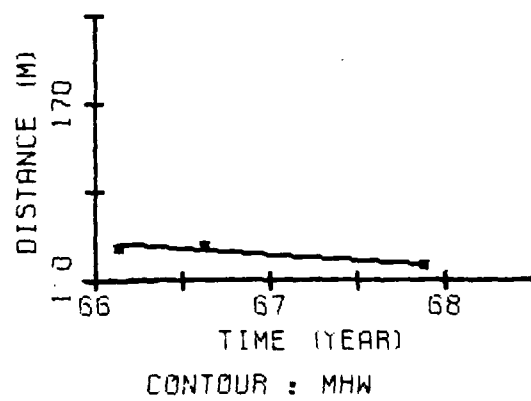
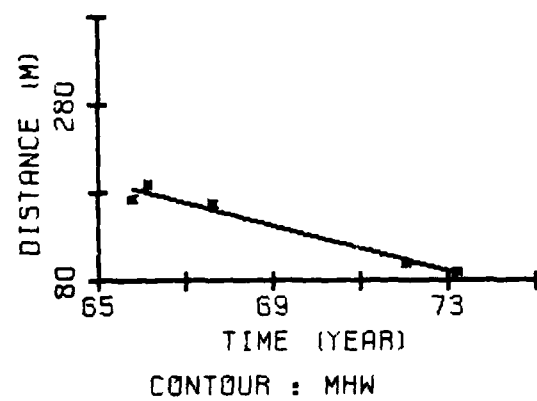
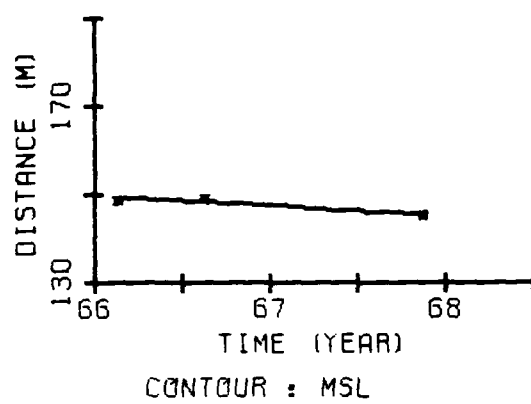
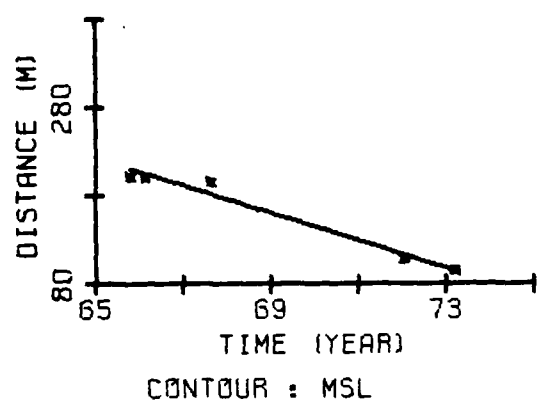
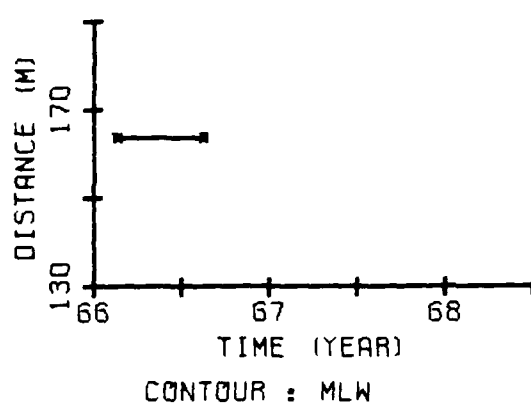
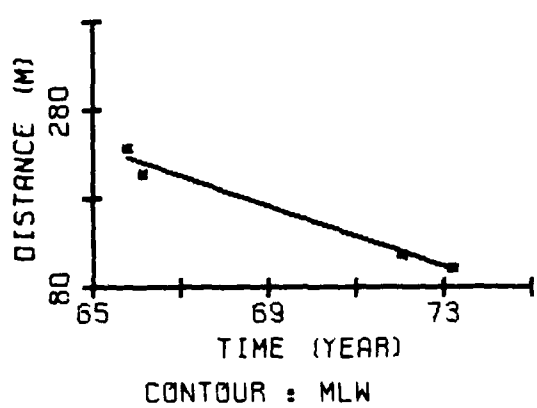
Note: Circles indicate profiles measured shortly after a local storm.
Arrows indicate the approximate time at which beach fills were placed.

DISTANCE FROM THE BASE LINE TO STATED CONTOURS AT CB 119

APPENDIX C
MASONBORO BEACH EXCURSION DISTANCE PLOTS



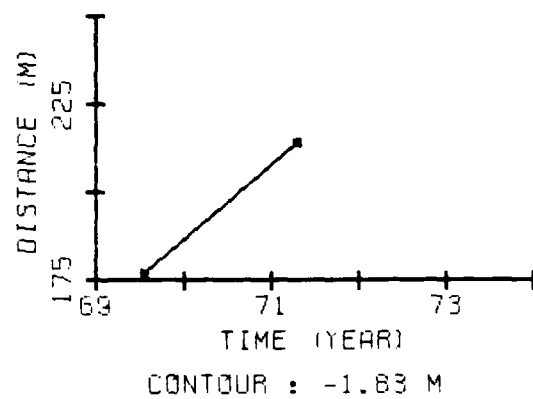
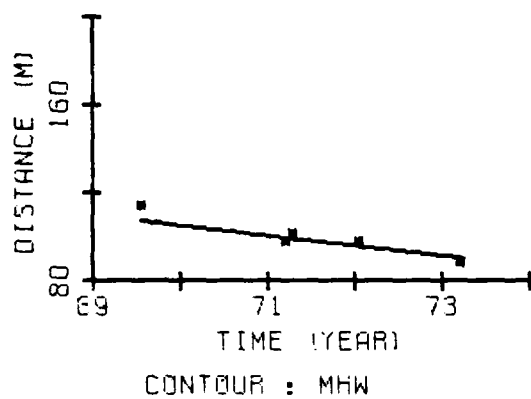
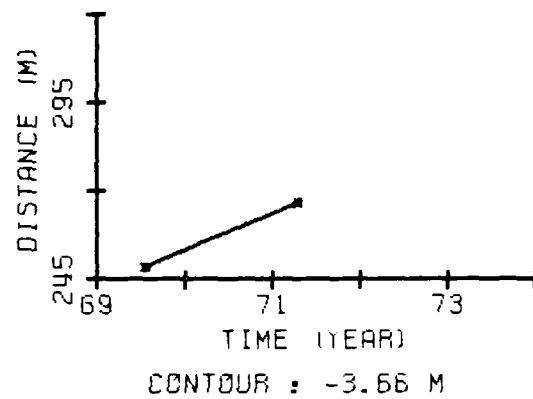
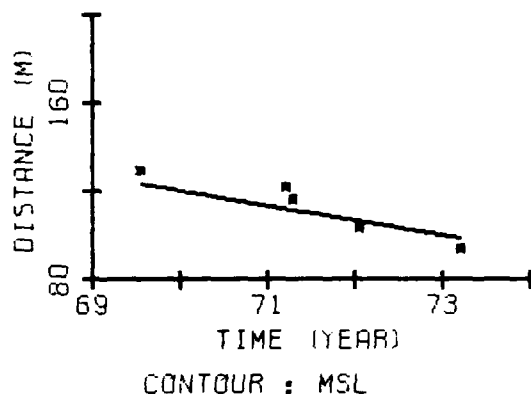
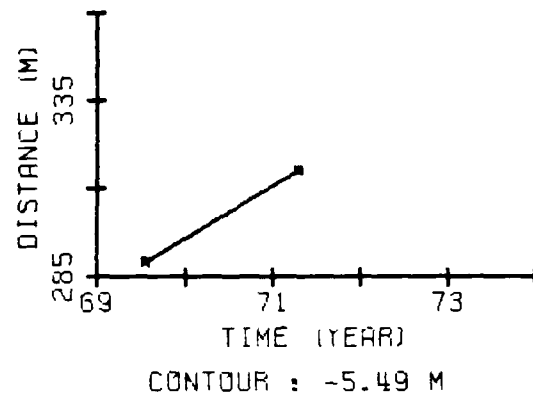
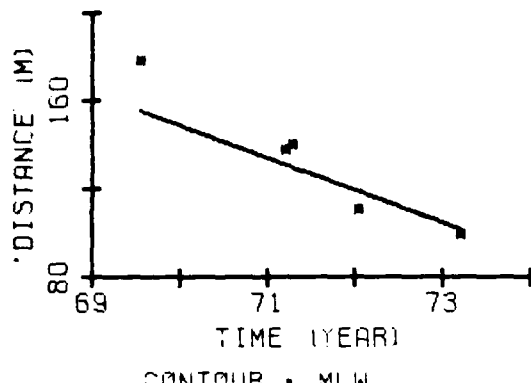
DISTANCE FROM THE BASE LINE TO STATED CONTOURS



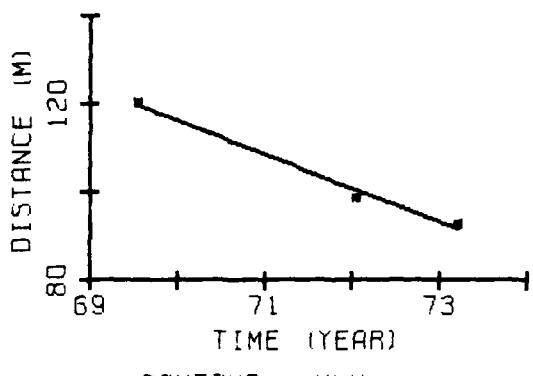
MB 5

MB 7

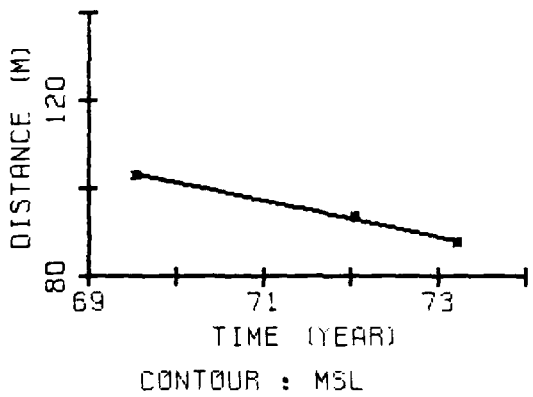
DISTANCE FROM THE BASE LINE TO STATED CONTOURS



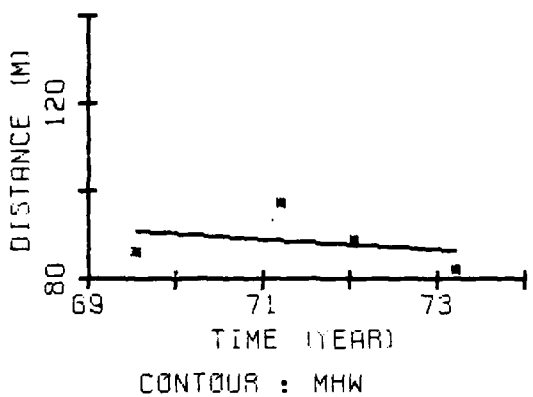
DISTANCE FROM THE BASELINE TO STATED CONTOURS AT MB 14



CONTOUR : MLW

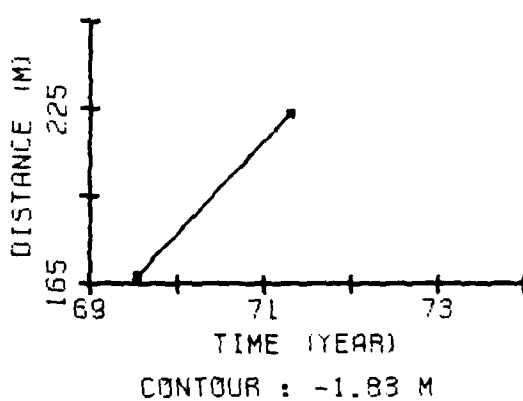
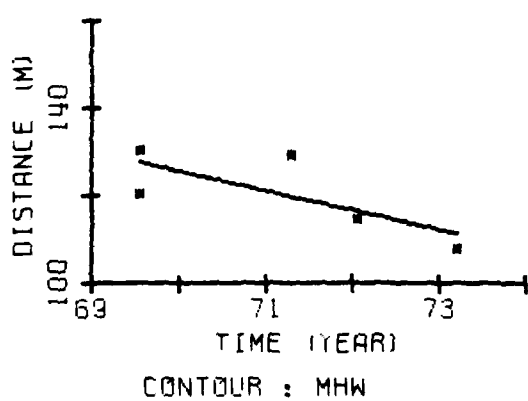
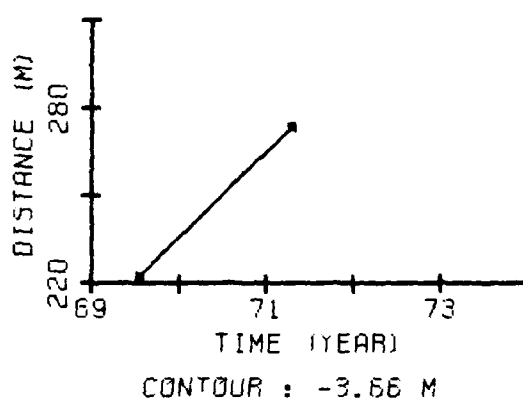
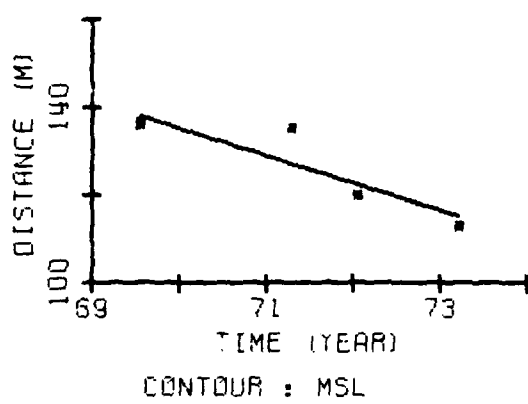
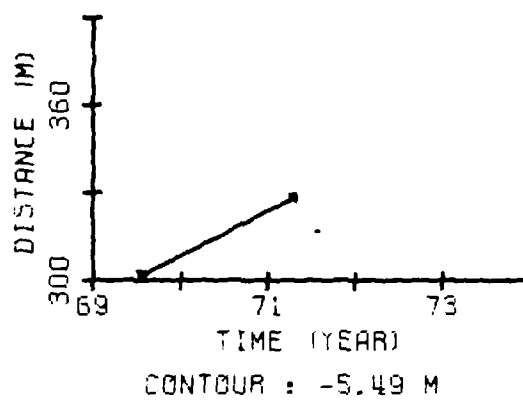
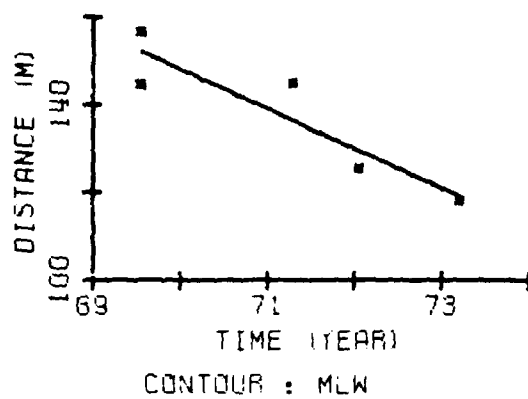


CONTOUR : MSL

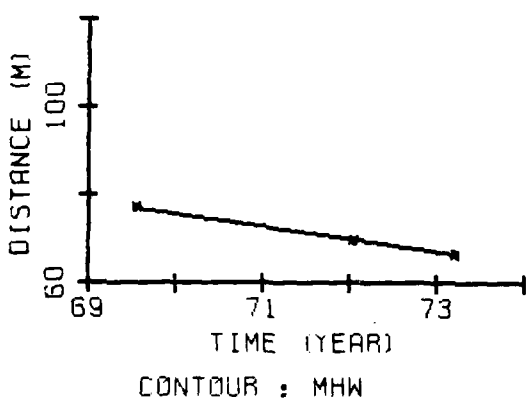
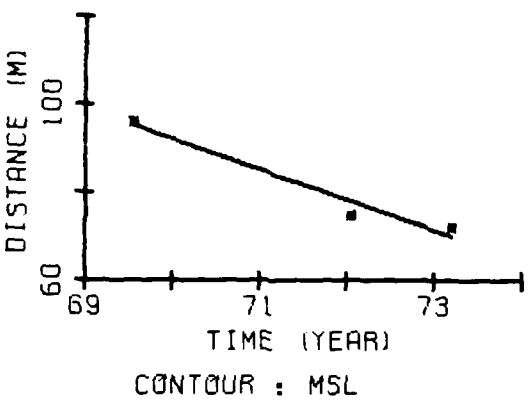
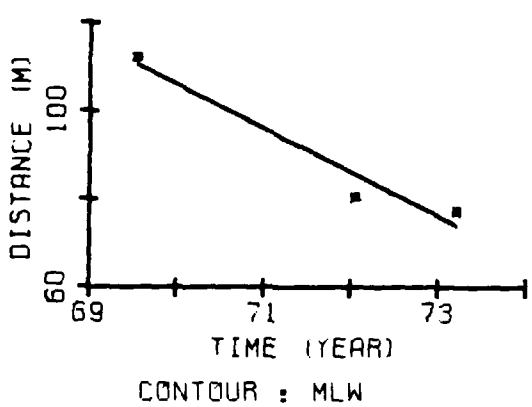


CONTOUR : MHW

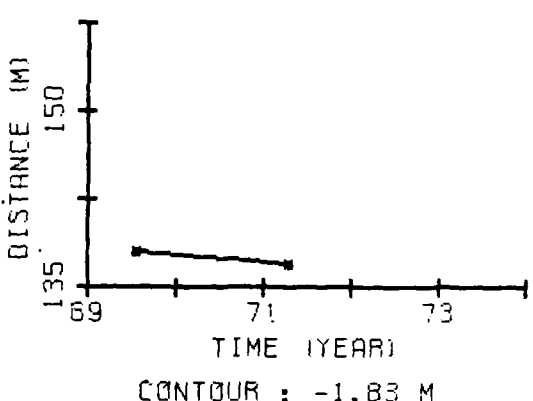
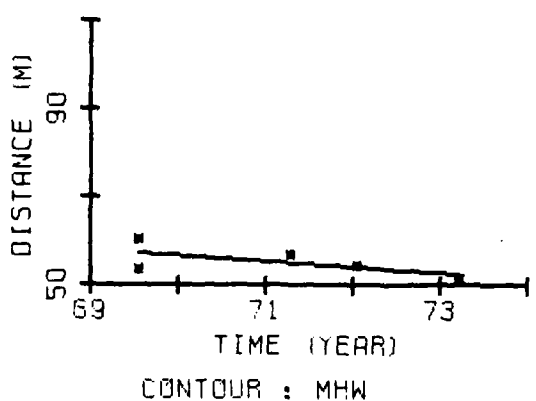
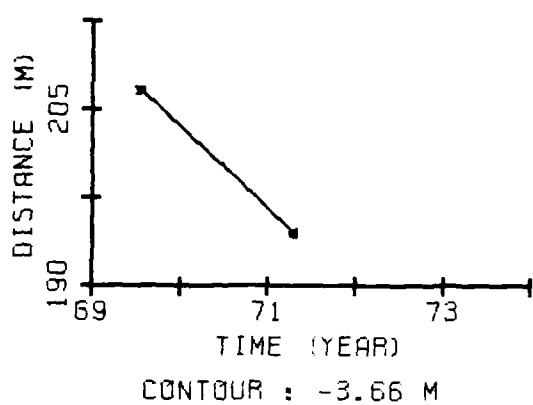
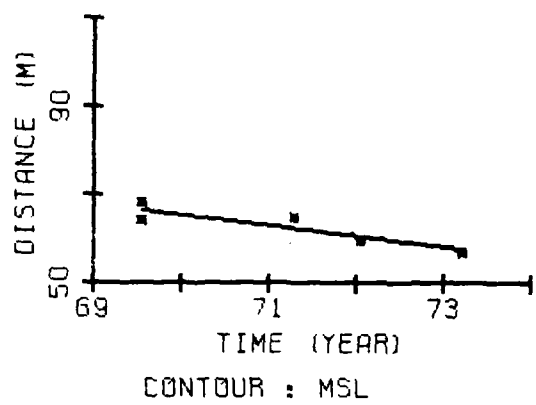
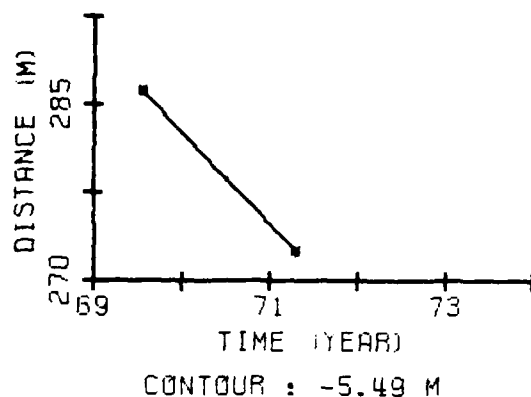
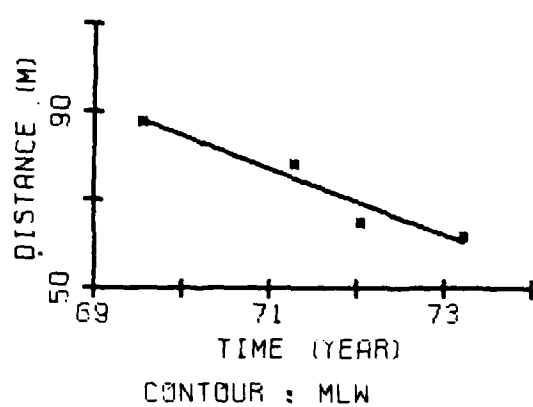
DISTANCE FROM THE BASE LINE TO STATED CONTOURS AT MB 16



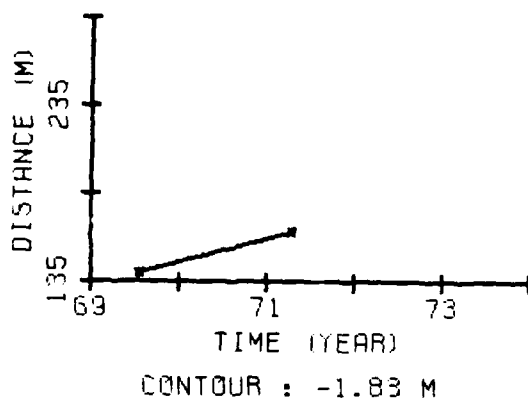
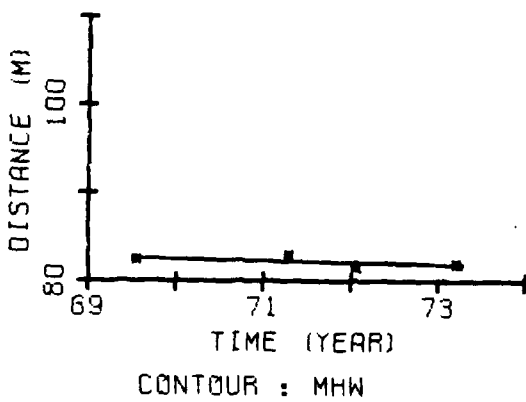
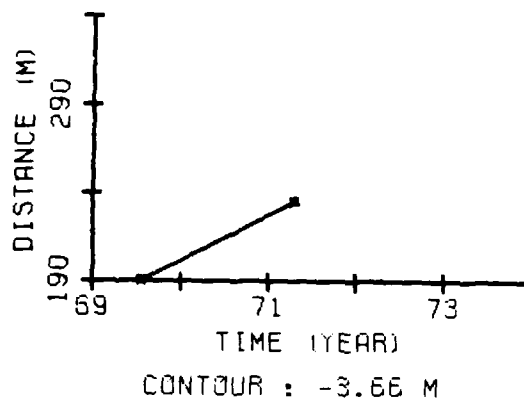
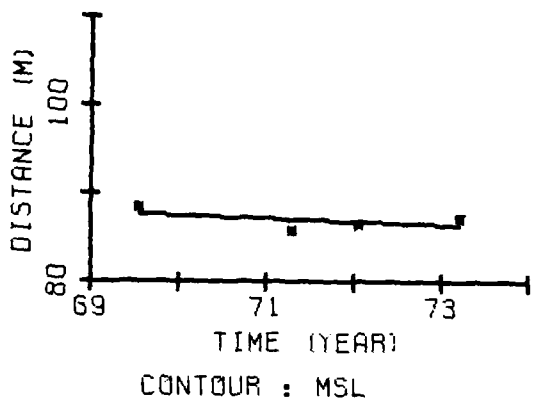
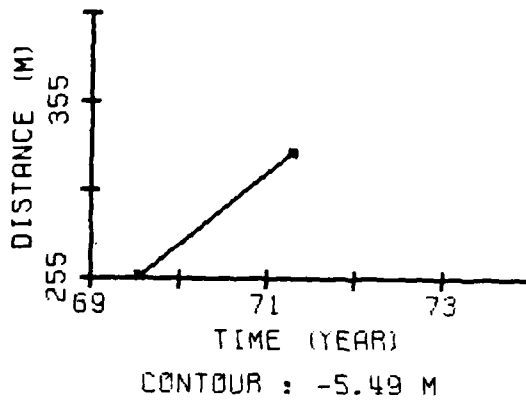
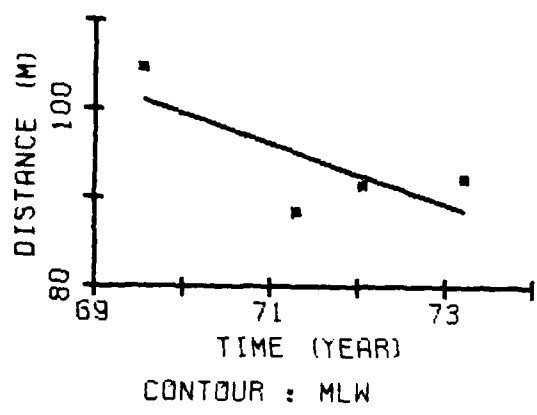
DISTANCE FROM THE BASE LINE TO STATED CONTOURS AT MB 17



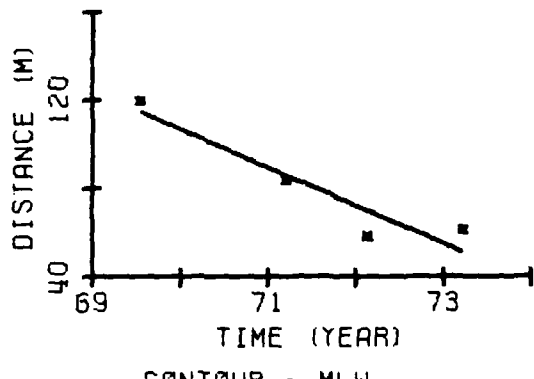
DISTANCE FROM THE BASE LINE TO STATED CONTOURS AT MB 19



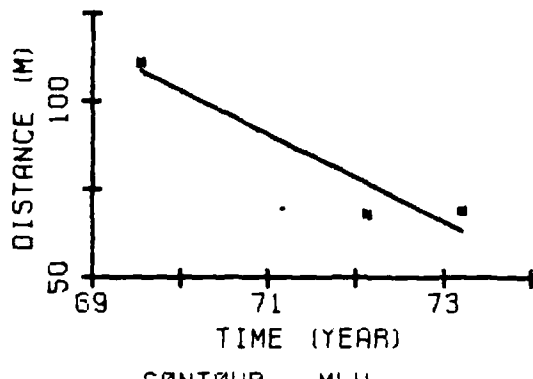
DISTANCE FROM THE BASE LINE TO STATED CONTOURS AT MB 20



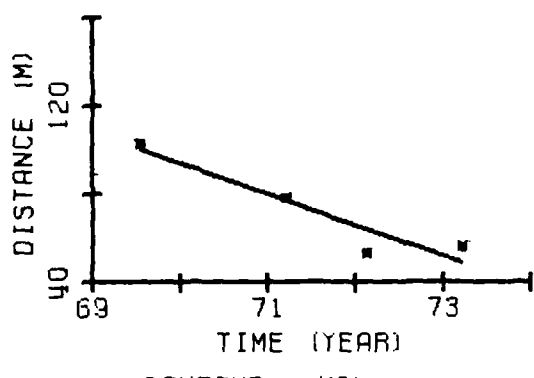
DISTANCE FROM THE BASE LINE TO STATED CONTOURS AT MB 23



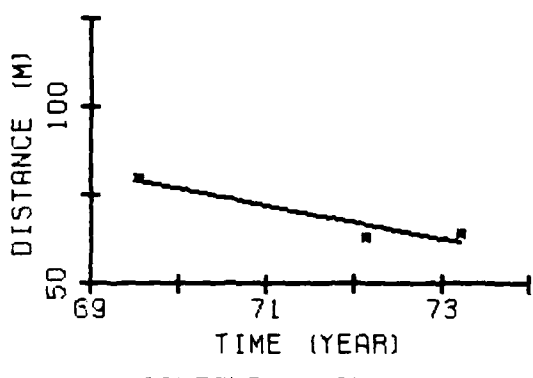
CONTOUR : MLW



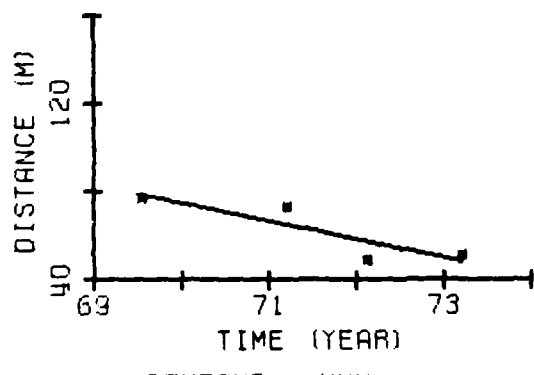
CONTOUR : MLW



CONTOUR : MSL

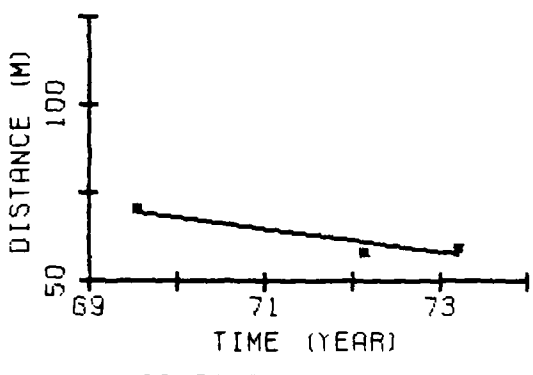


CONTOUR : MSL



CONTOUR : MHW

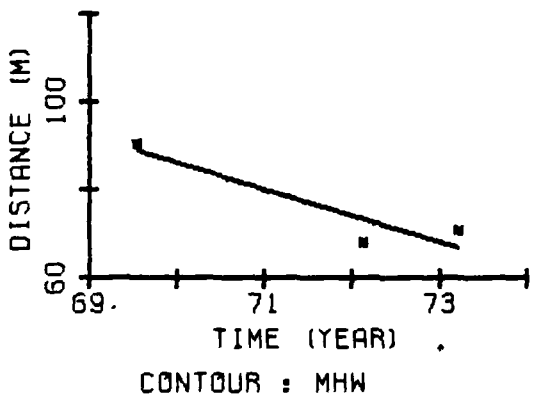
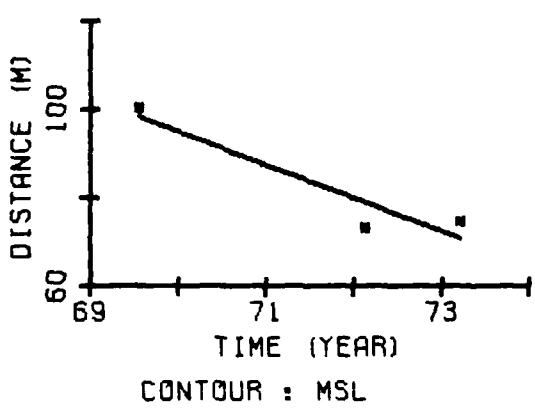
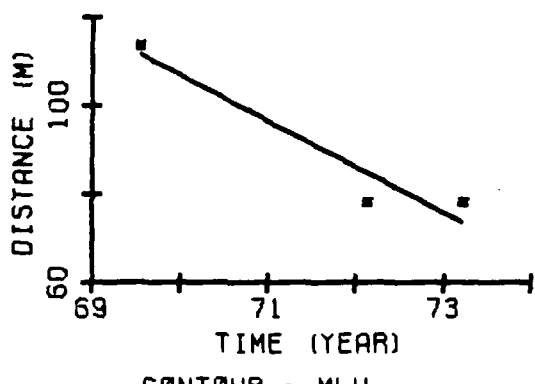
MB 25



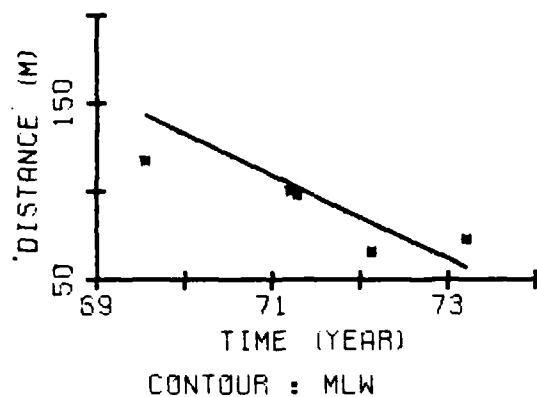
CONTOUR : MHW

MB 27

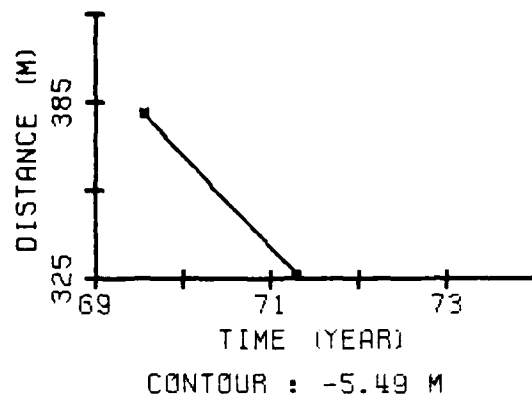
DISTANCE FROM THE BASE LINE TO STATED CONTOURS



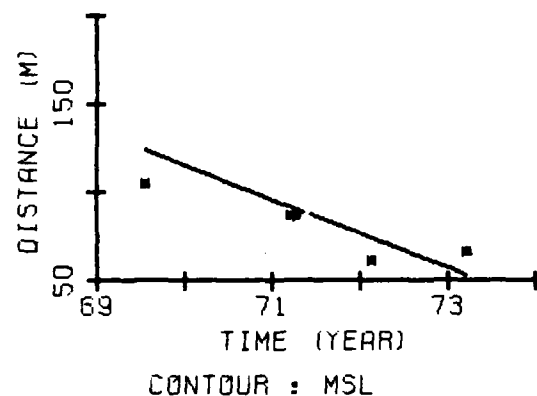
DISTANCE FROM THE BASE LINE TO STATED CONTOURS AT MB 28



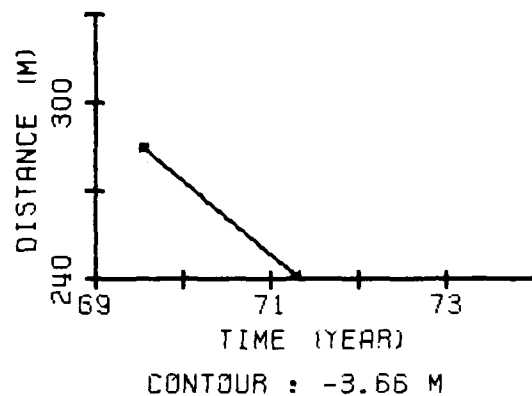
CONTOUR : MLW



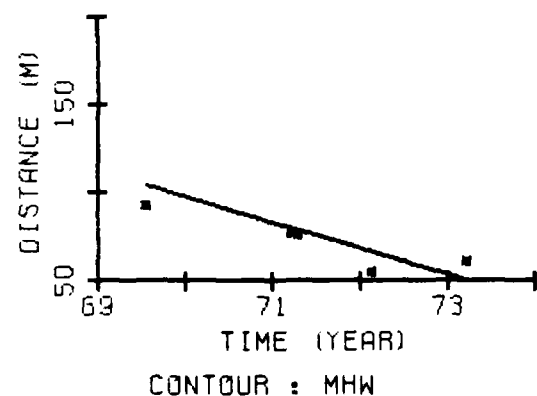
CONTOUR : -5.49 M



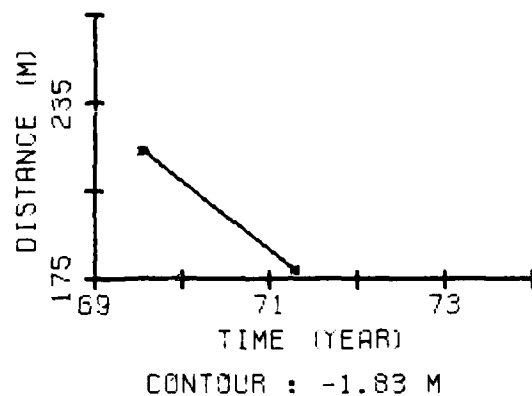
CONTOUR : MSL



CONTOUR : -3.66 M

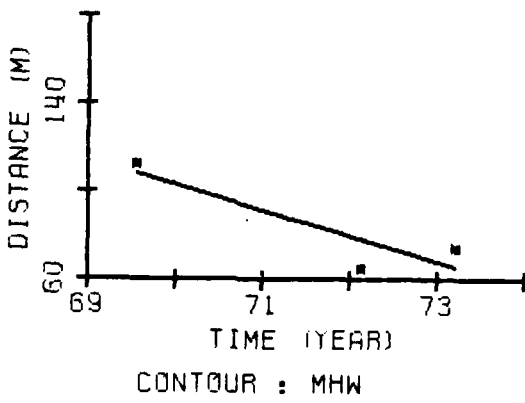
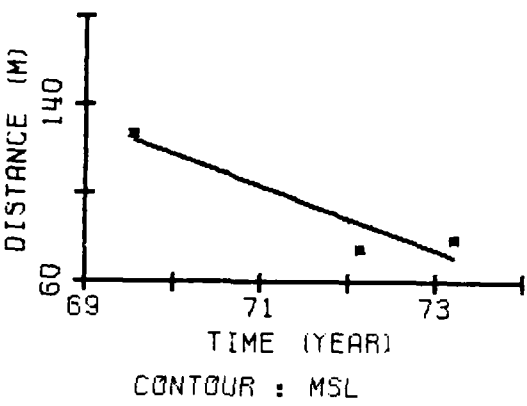
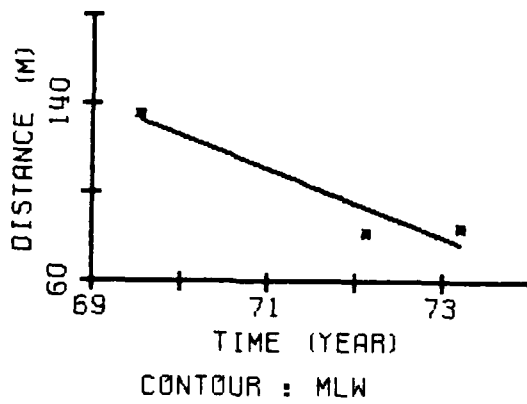


CONTOUR : MHW



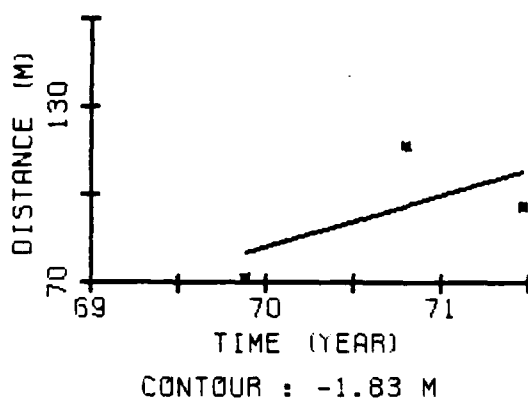
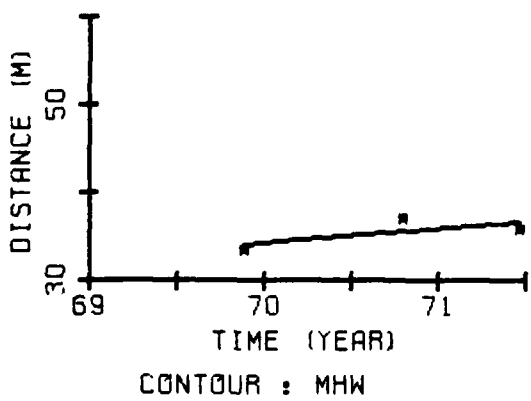
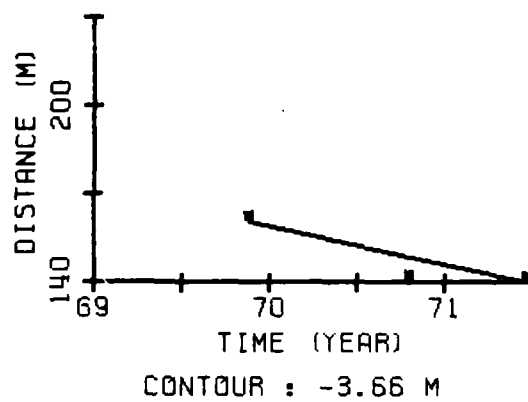
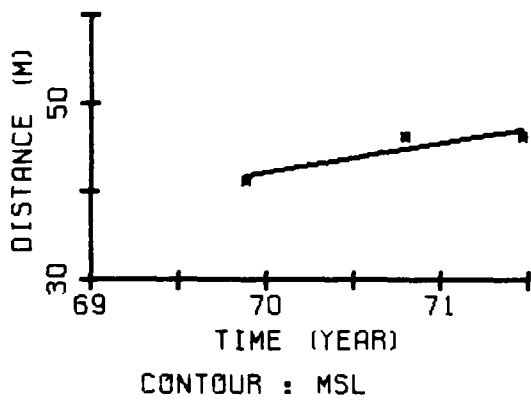
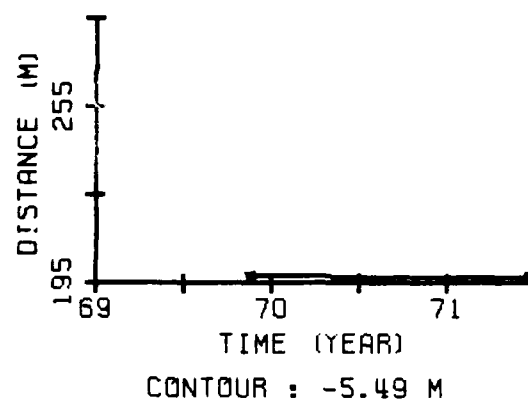
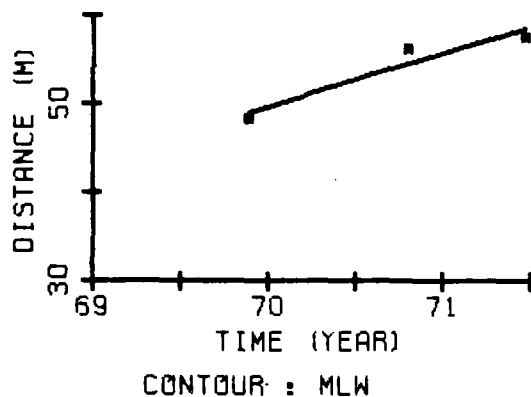
CONTOUR : -1.83 M

DISTANCE FROM THE BASE LINE TO STATED CONTOURS AT MB 29

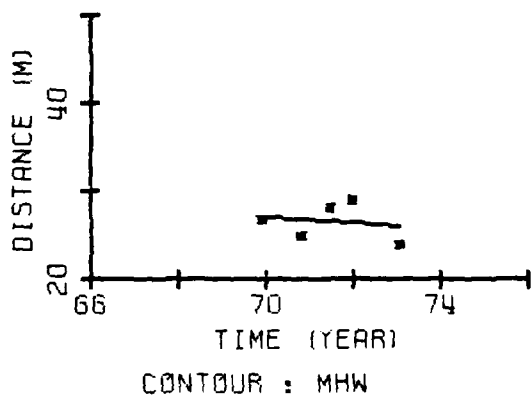
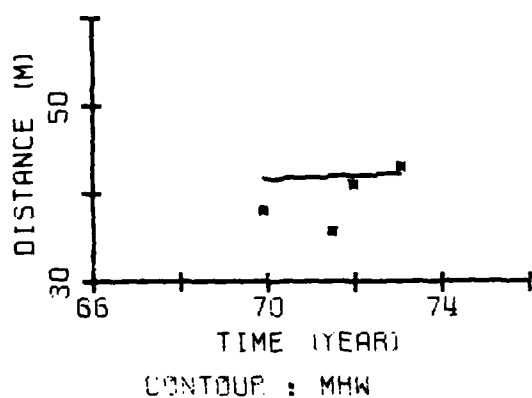
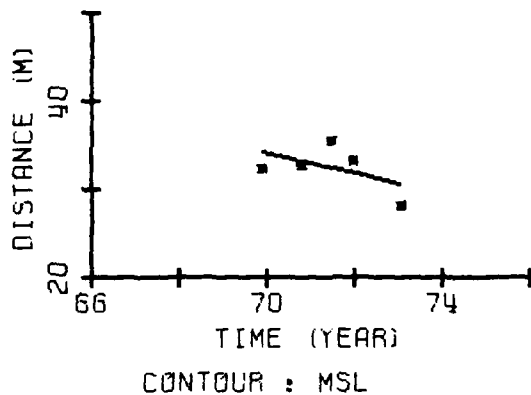
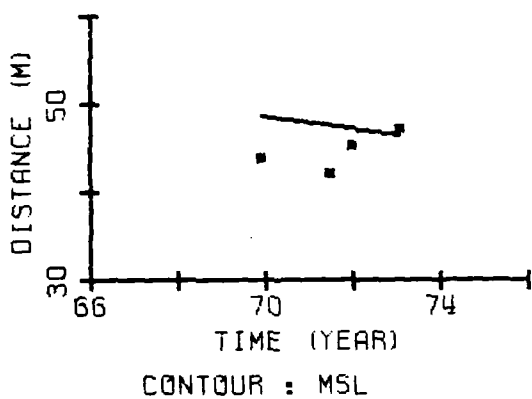
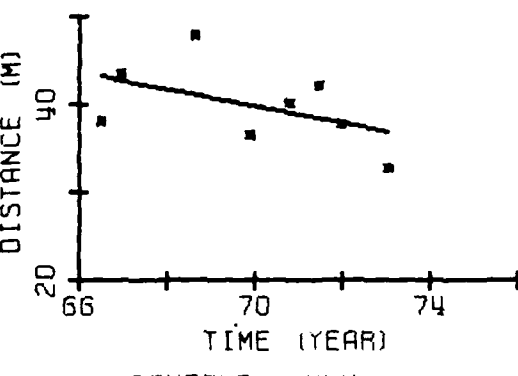
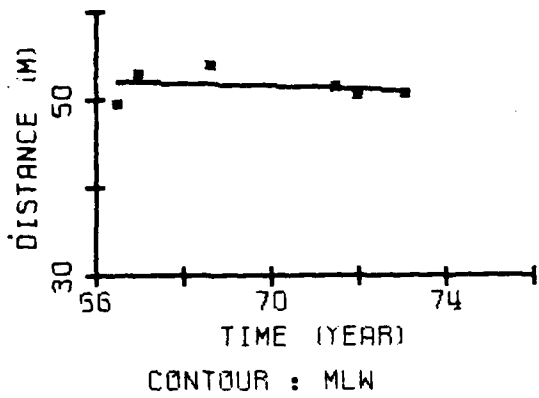


DISTANCE FROM THE BASE LINE TO STATED CONTOURS AT MB 31

APPENDIX D
KURE BEACH EXCURSION DISTANCE PLOTS



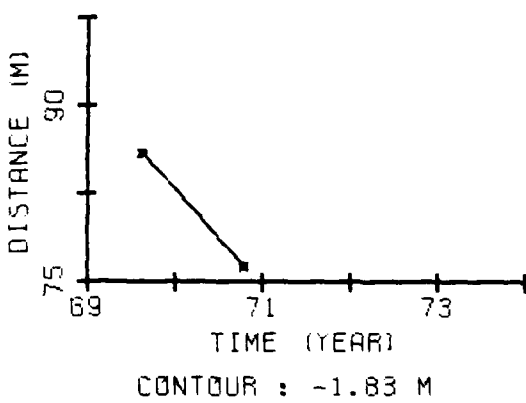
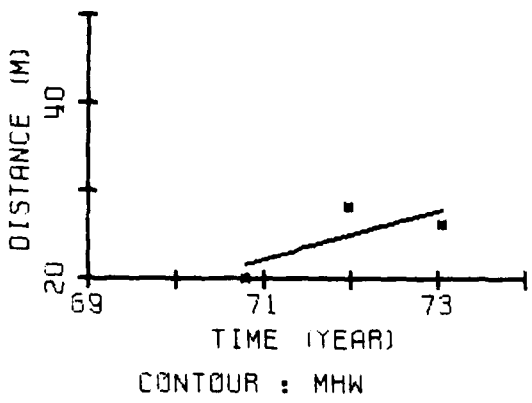
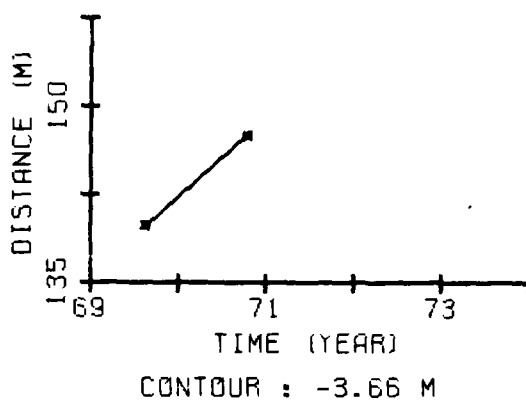
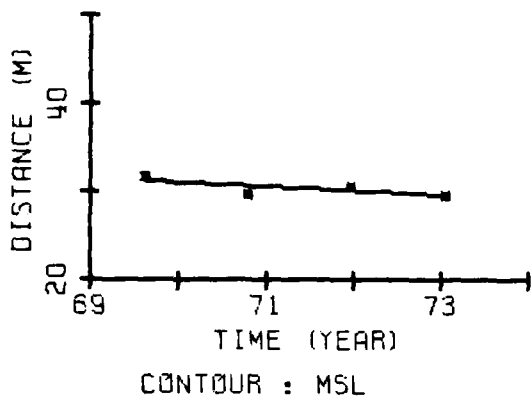
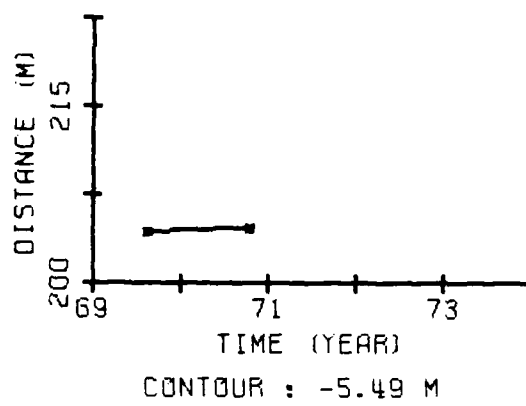
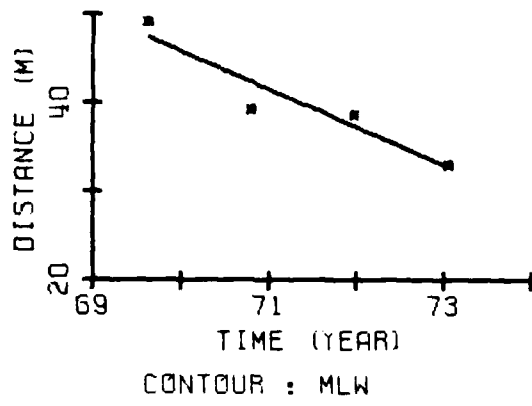
DISTANCE FROM THE BASE LINE TO STATED CONTOURS AT KB 3



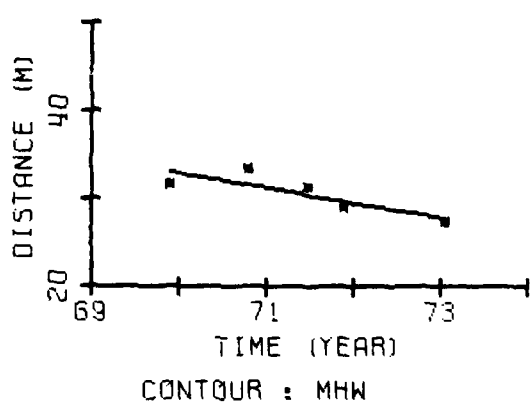
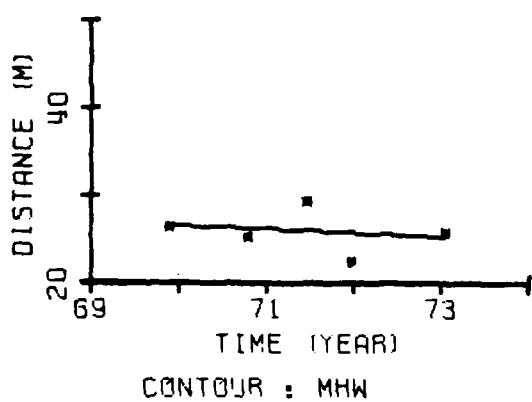
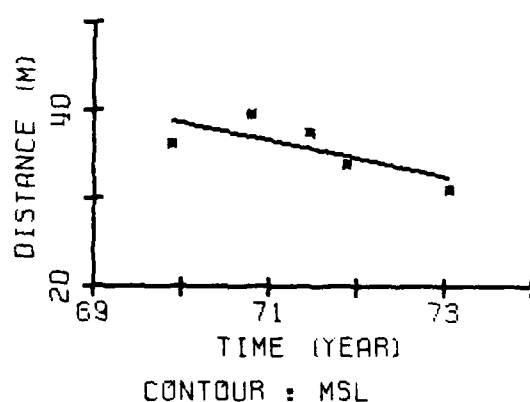
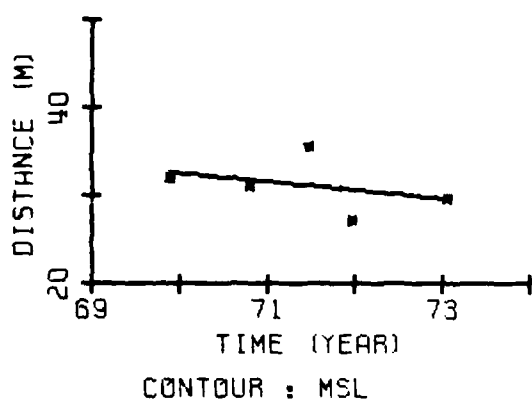
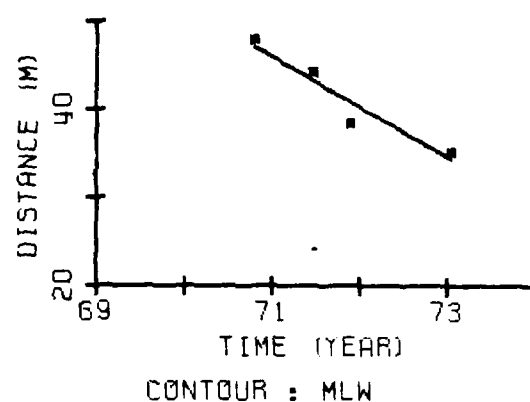
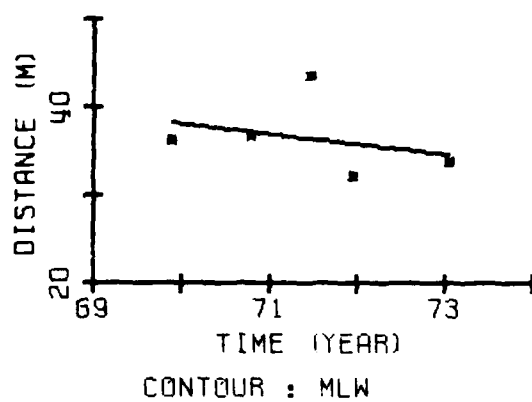
KB 4

KB 6

DISTANCE FROM THE BASE LINE TO STATED CONTOURS



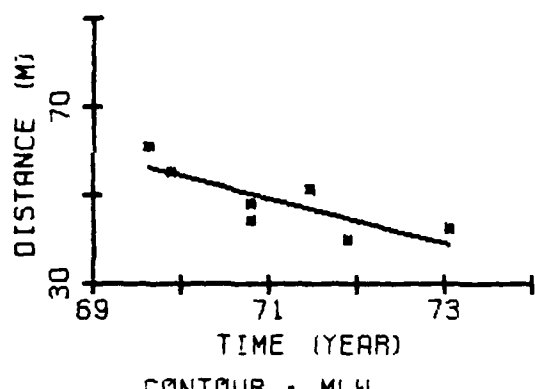
DISTANCE FROM THE BASE LINE TO STATED CONTOURS AT KB 7



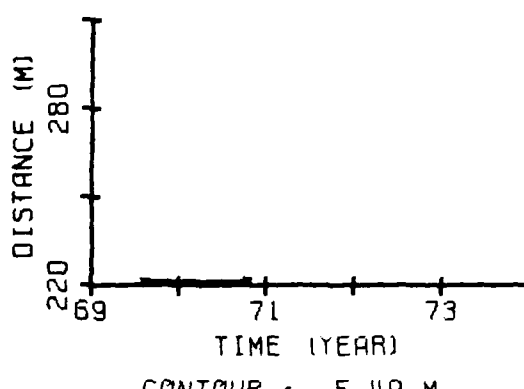
KB 8

KB 9

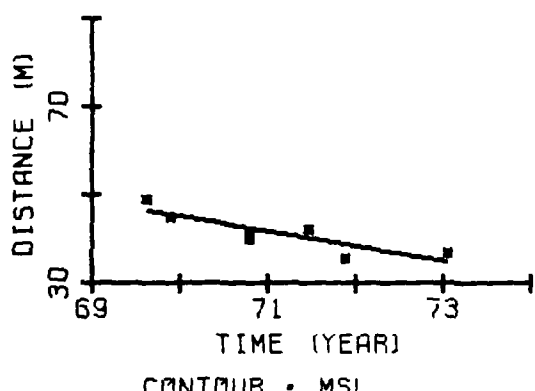
DISTANCE FROM THE BASE LINE TO STATED CONTOURS



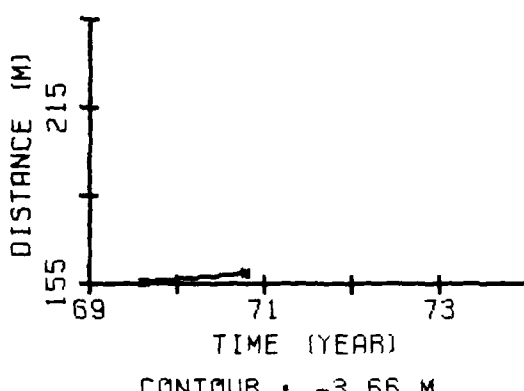
CONTOUR : MLW



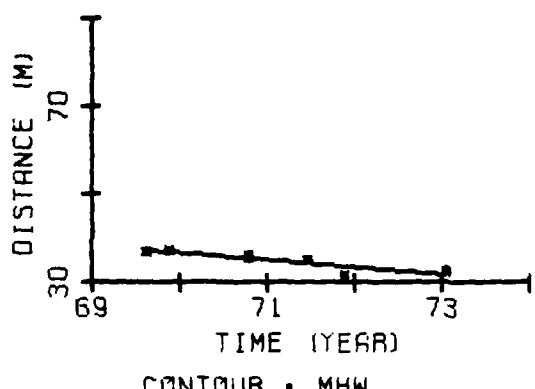
CONTOUR : -5.49 M



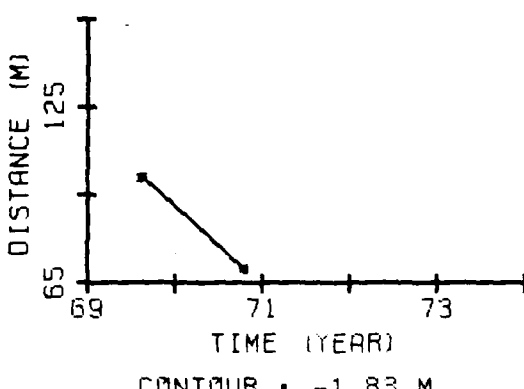
CONTOUR : MSL



CONTOUR : -3.66 M

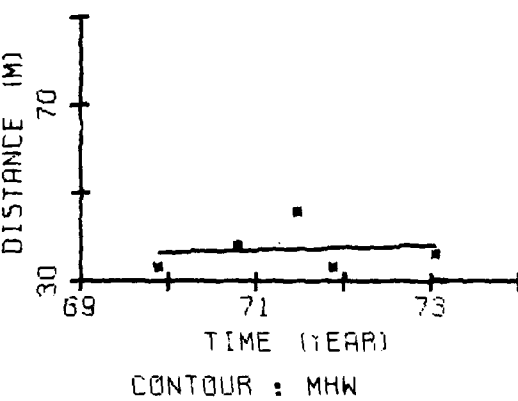
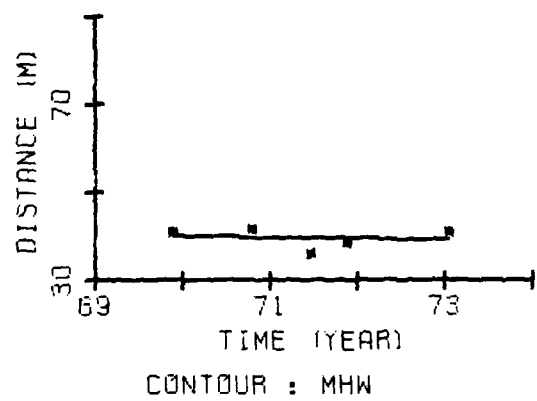
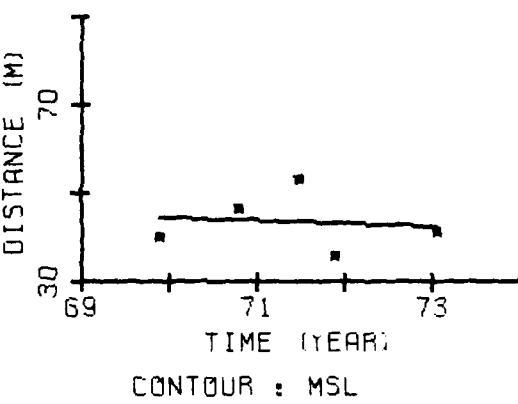
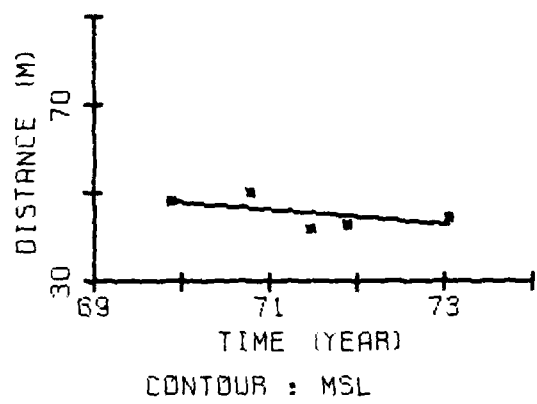
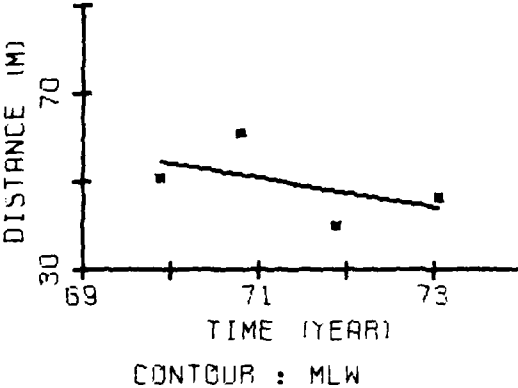
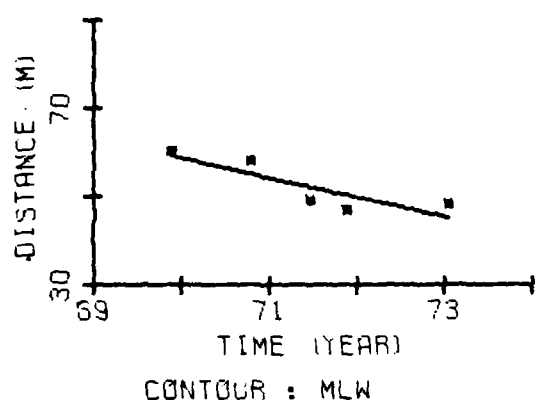


CONTOUR : MHW



CONTOUR : -1.83 M

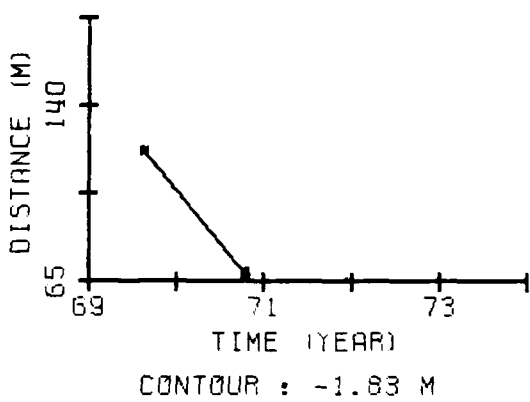
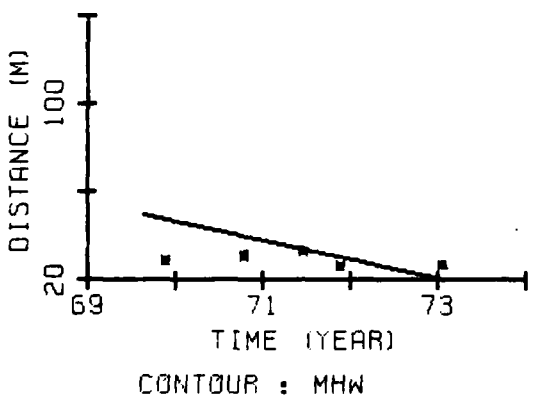
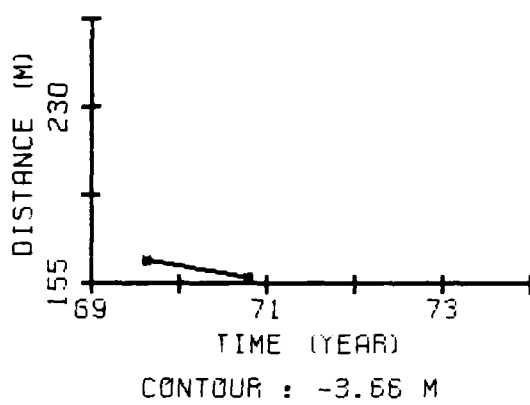
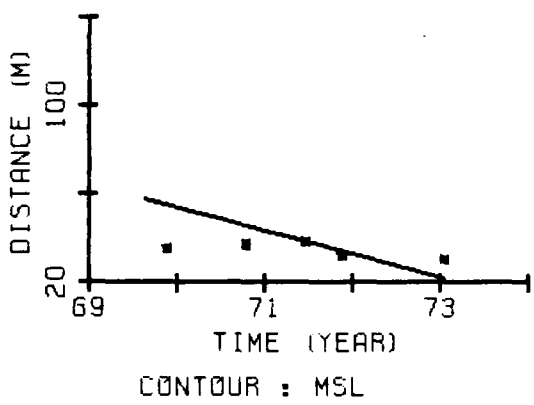
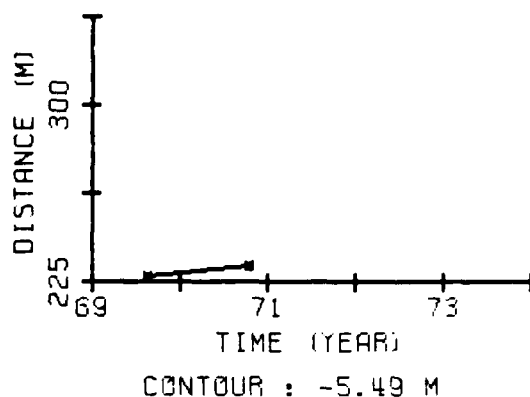
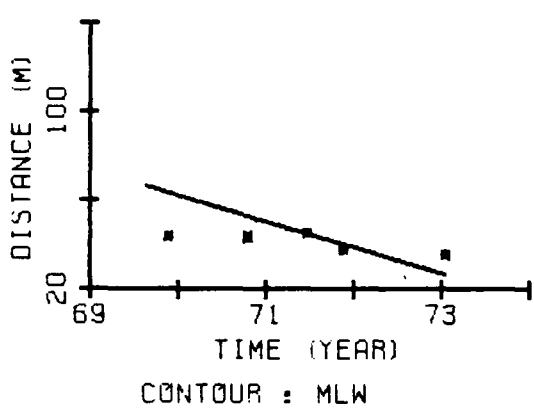
DISTANCE FROM THE BASE LINE TO STATED CONTOURS AT KB 10



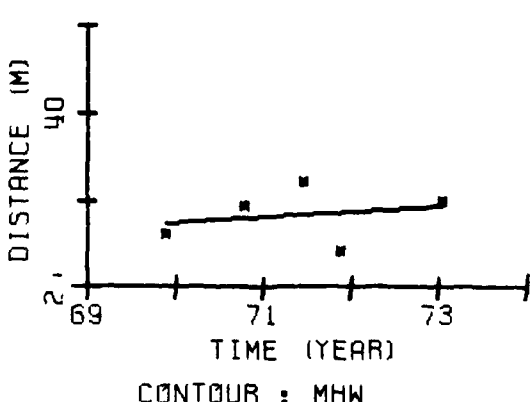
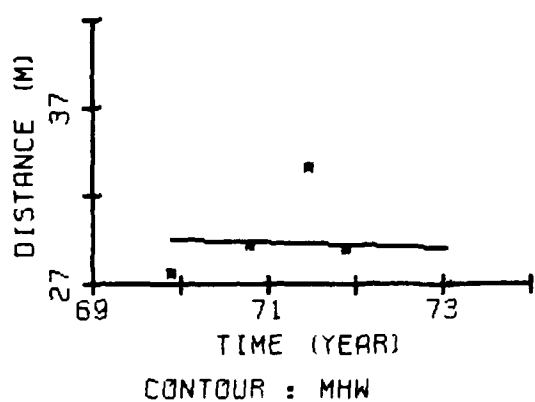
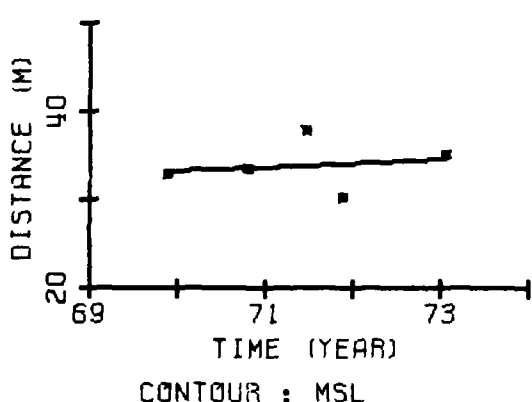
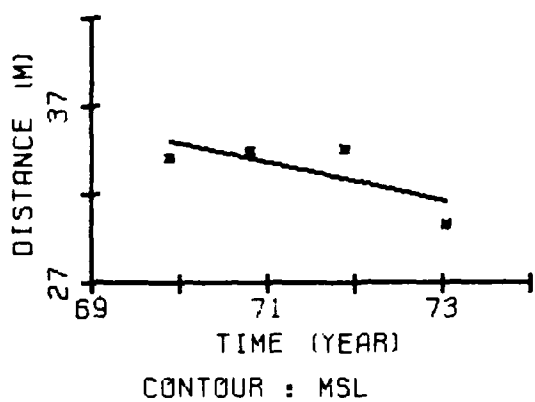
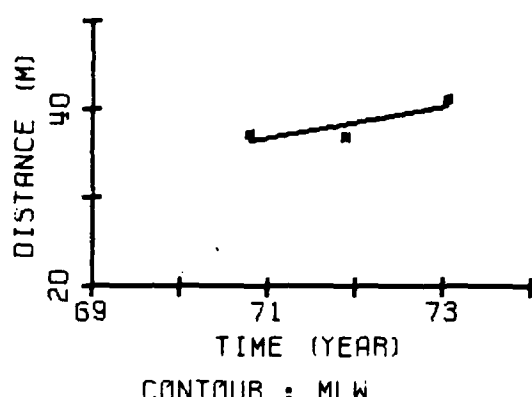
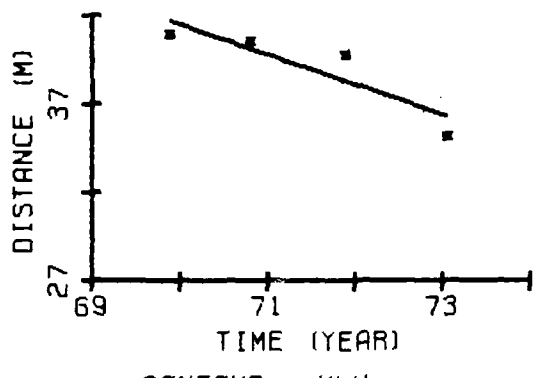
KB 11

KB 12

DISTANCE FROM THE BASE LINE TO STATED CONTOURS



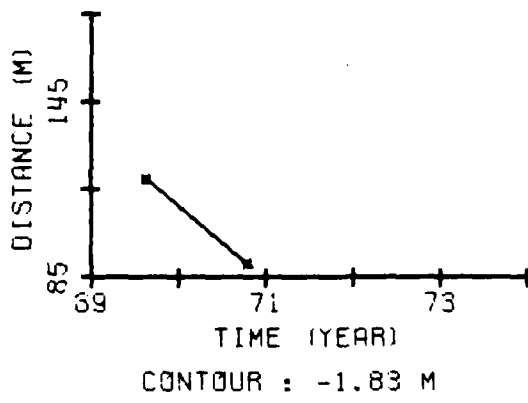
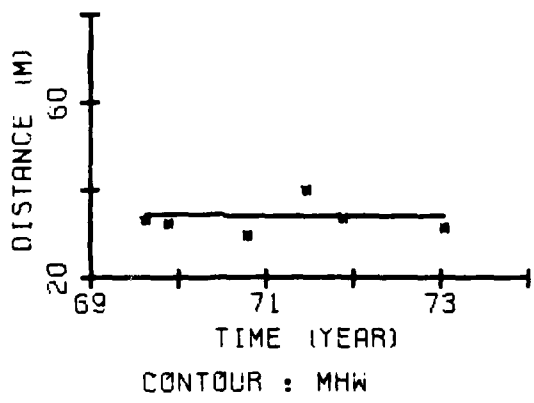
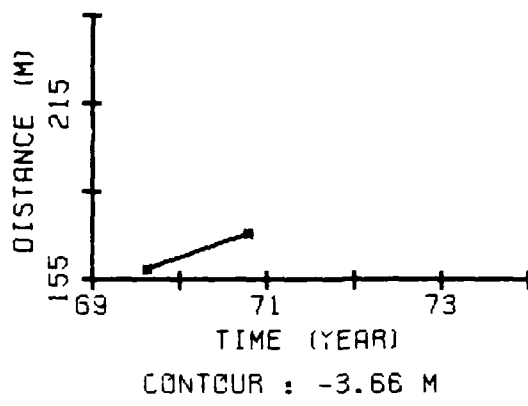
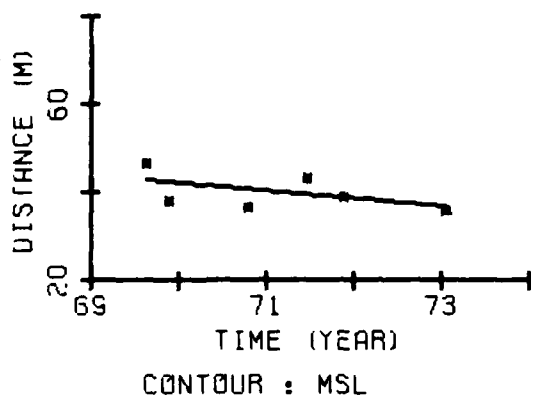
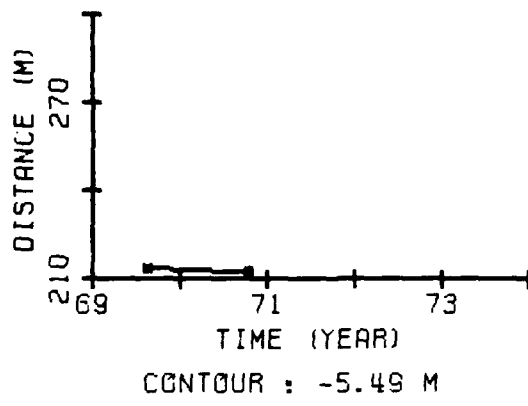
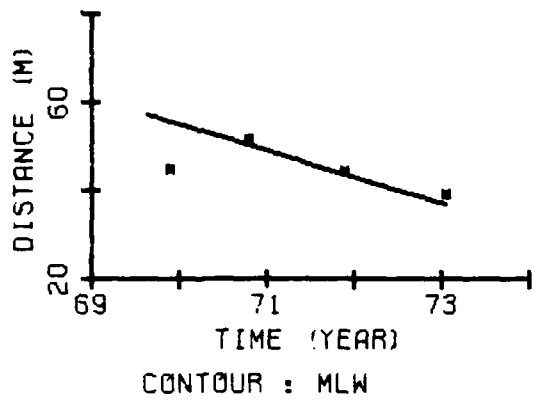
DISTANCE FROM THE BASE LINE TO STATED CONTOURS AT KB 13



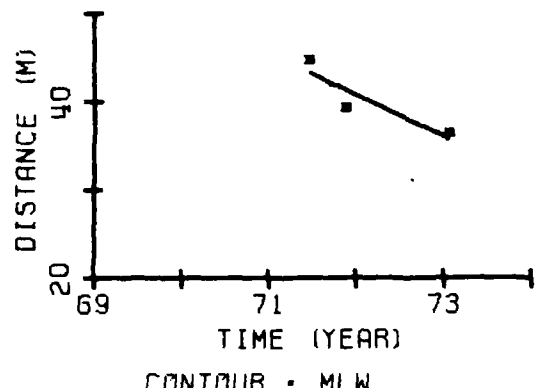
KB 14

KB 16

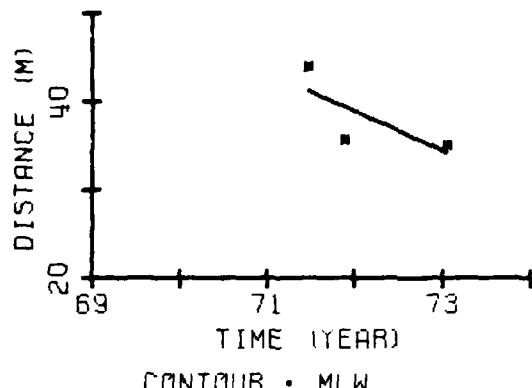
DISTANCE FROM THE BASE LINE TO STATED CONTOURS



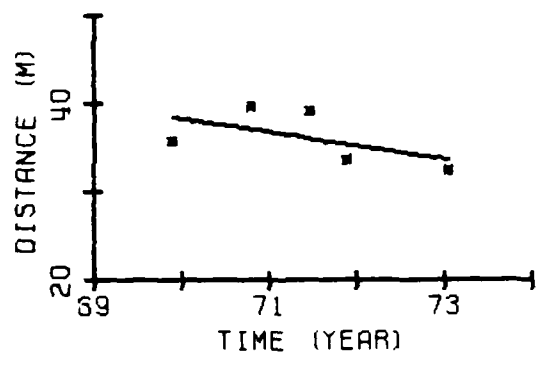
DISTANCE FROM THE BASE LINE TO STATED CONTOURS AT KB 17



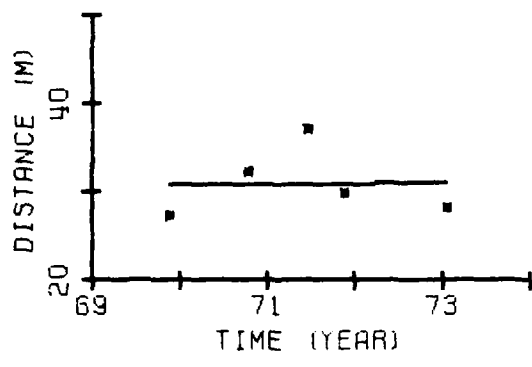
CONTOUR : MLW



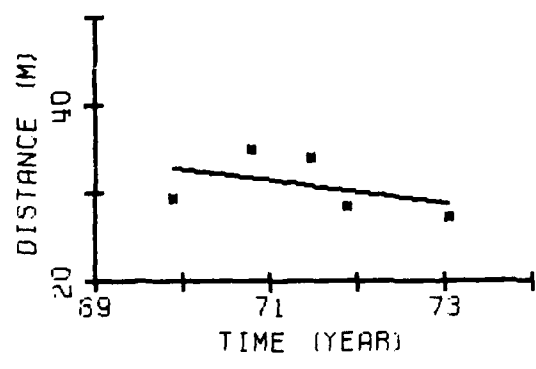
CONTOUR : MLW



CONTOUR : MSL

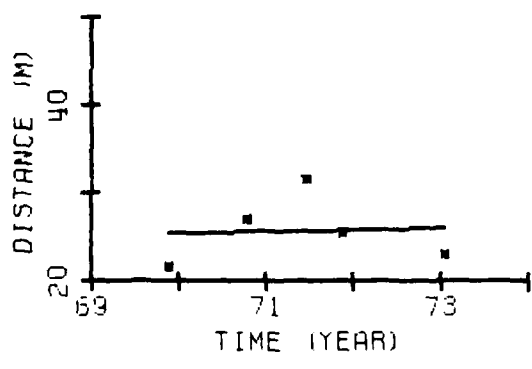


CONTOUR : MSL



CONTOUR : MHW

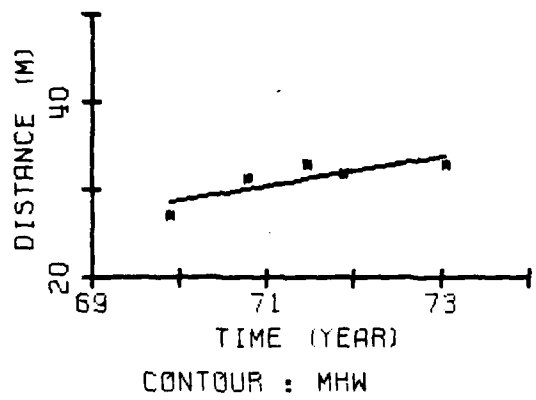
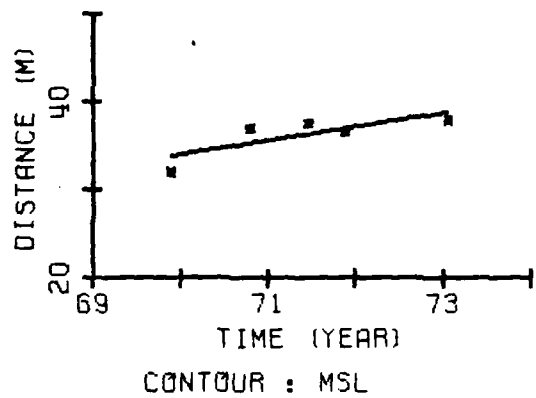
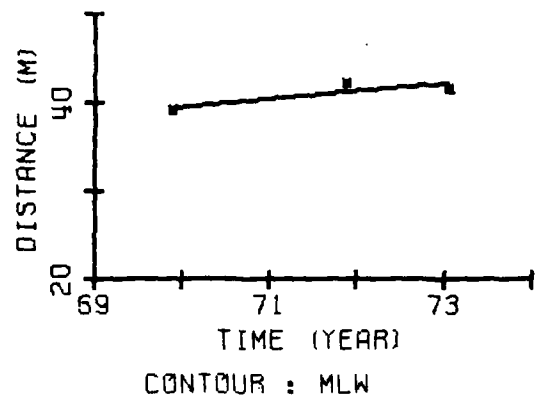
KB 18



CONTOUR : MHW

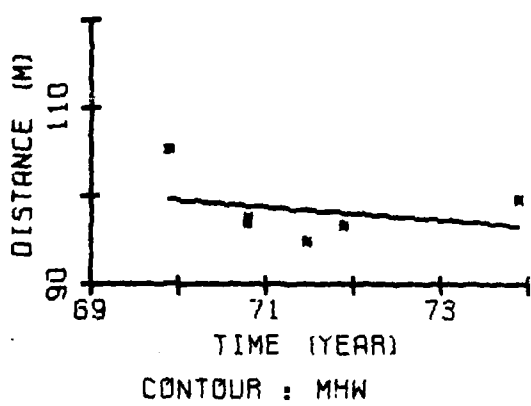
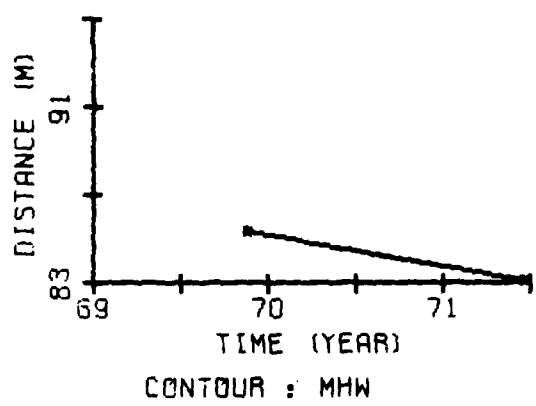
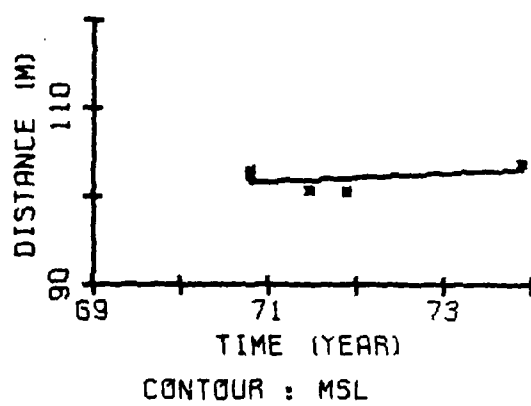
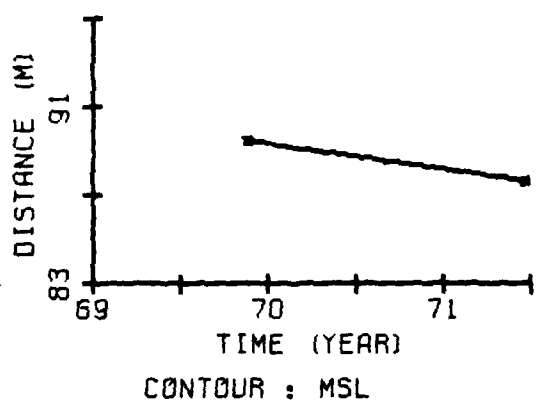
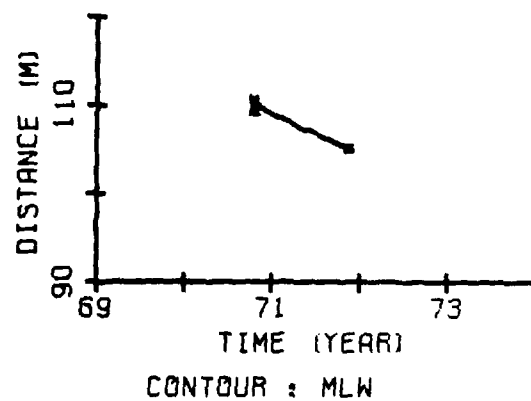
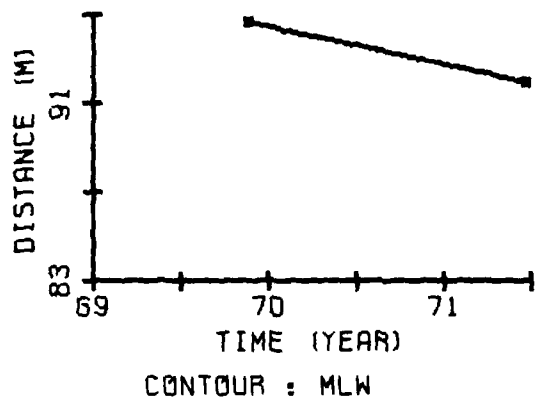
KB 19

DISTANCE FROM THE BASE LINE TO STATED CONTOURS



DISTANCE FROM THE BASE LINE TO STATED CONTOURS AT KB 20

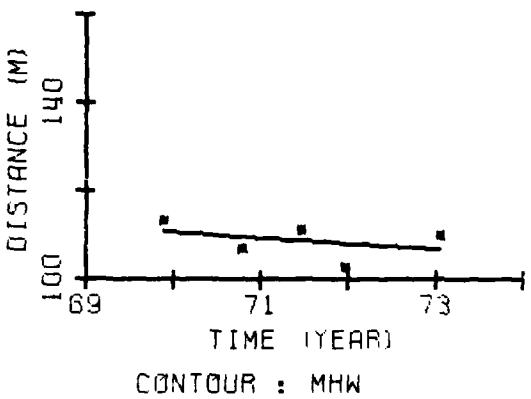
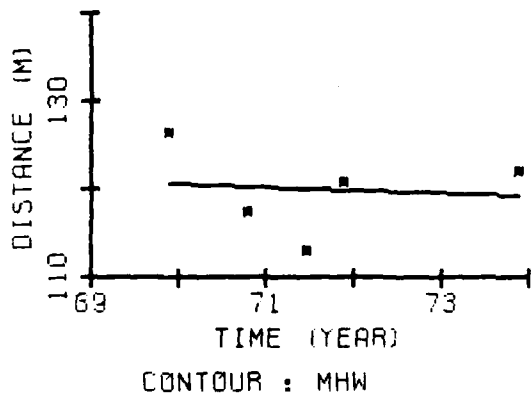
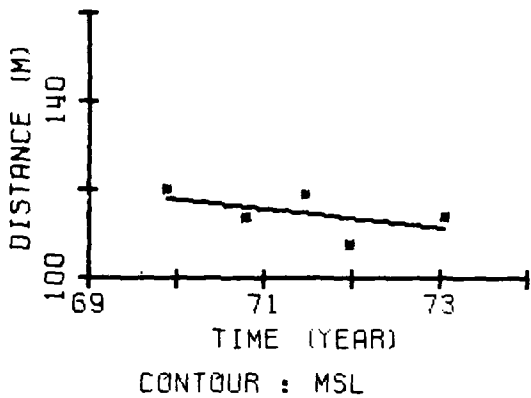
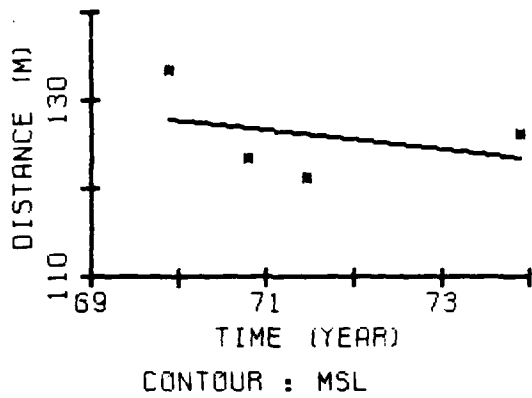
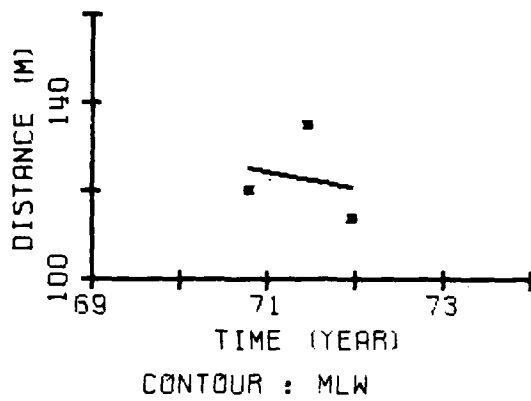
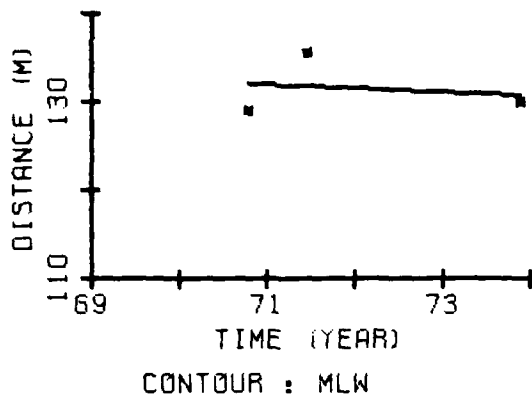
APPENDIX E
FISHER BEACH EXCURSION DISTANCE PLOTS



FB 1

FB 2

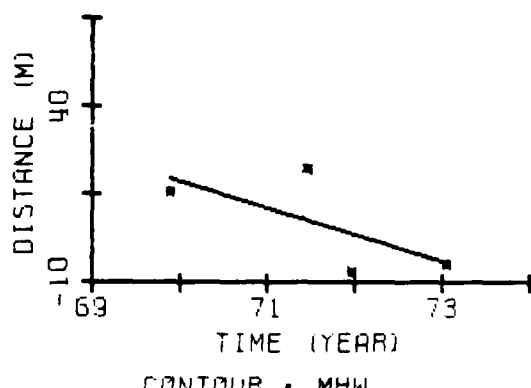
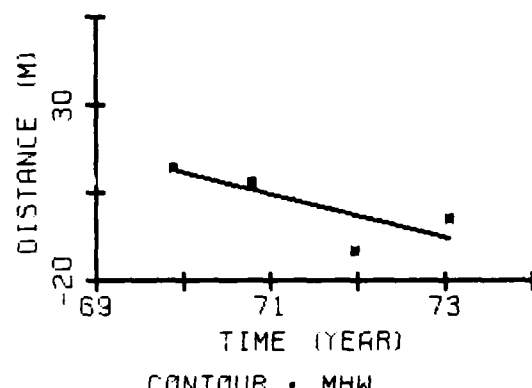
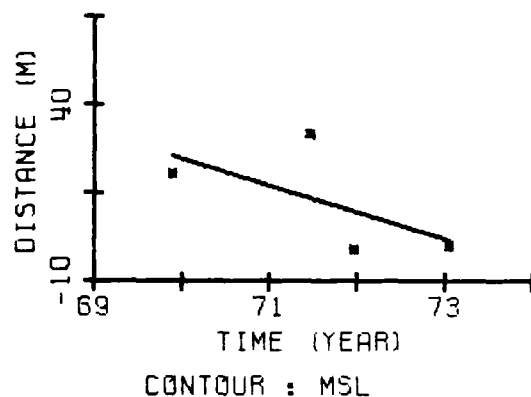
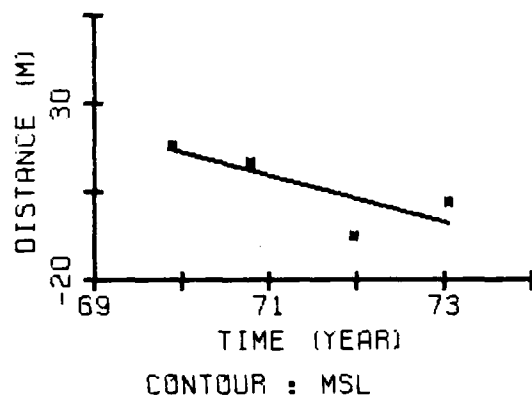
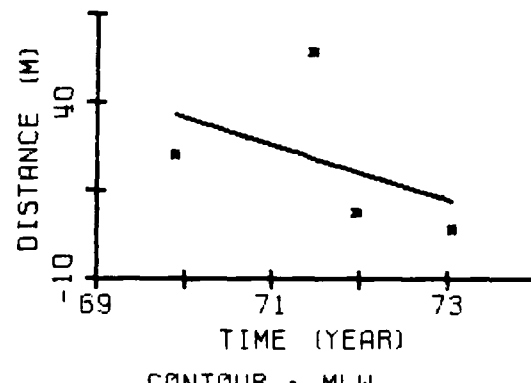
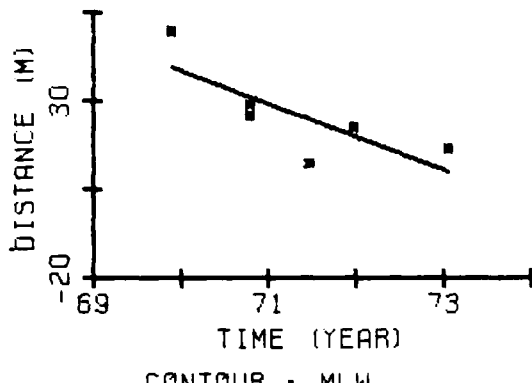
DISTANCE FROM THE BASE LINE TO STATED CONTOURS



FB 3

FB 4

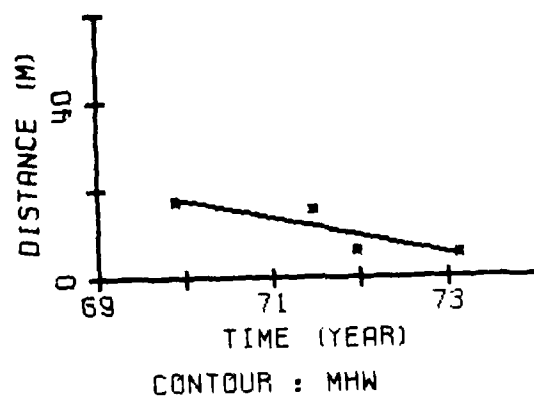
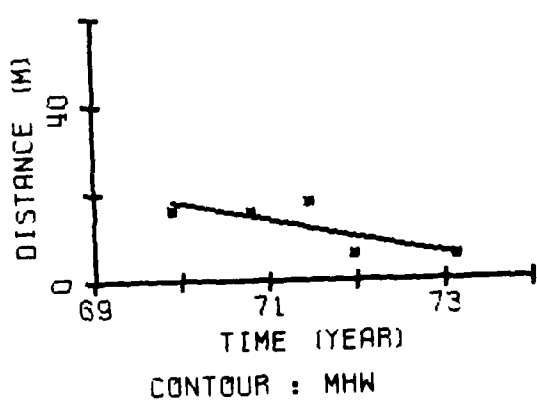
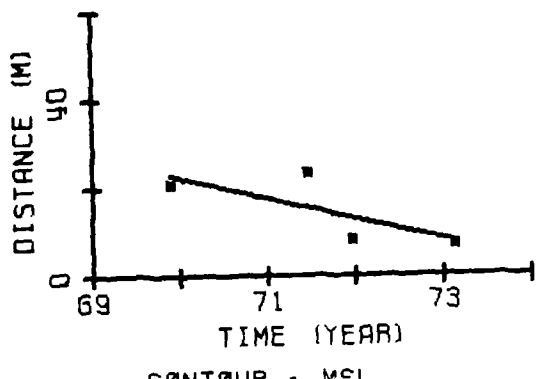
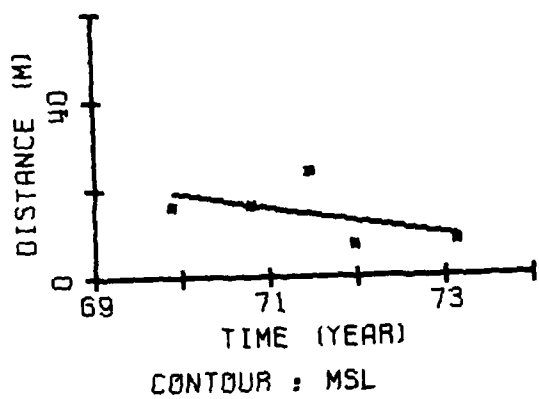
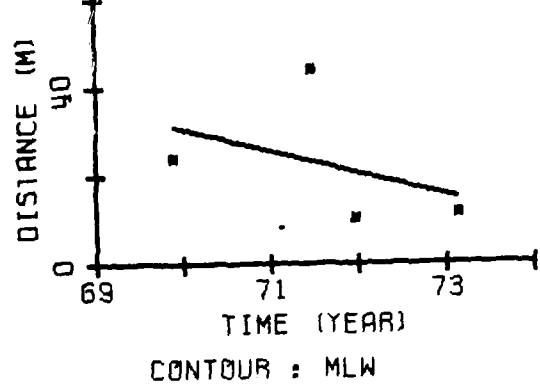
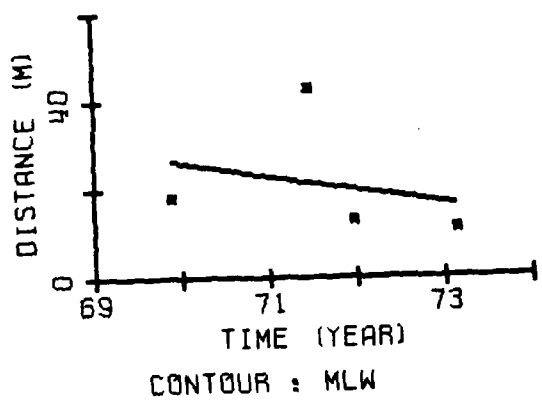
DISTANCE FROM THE BASE LINE TO STATED CONTOURS



FB 5

FB 6

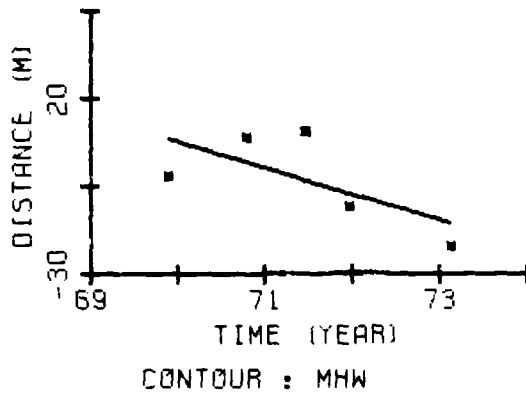
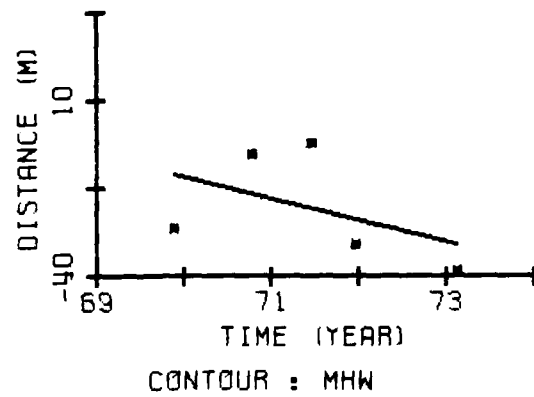
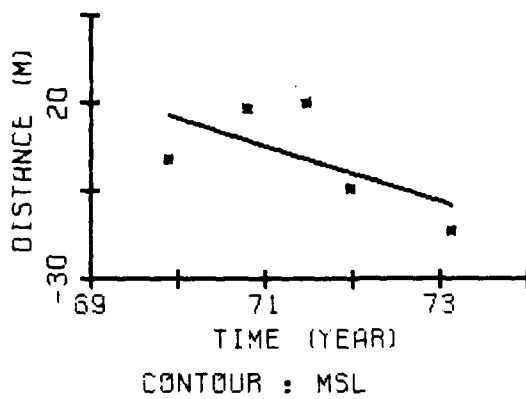
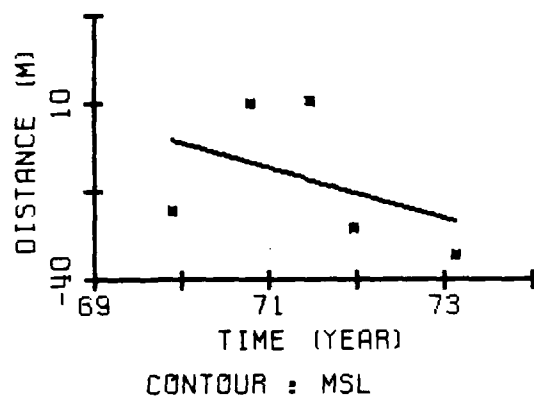
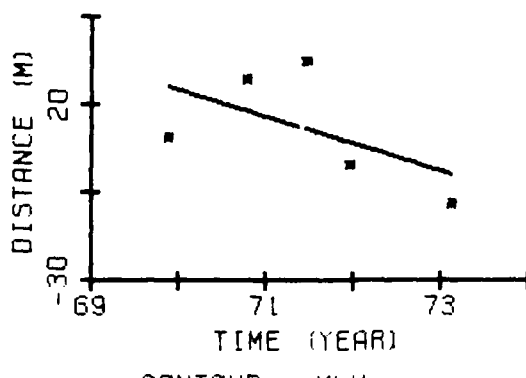
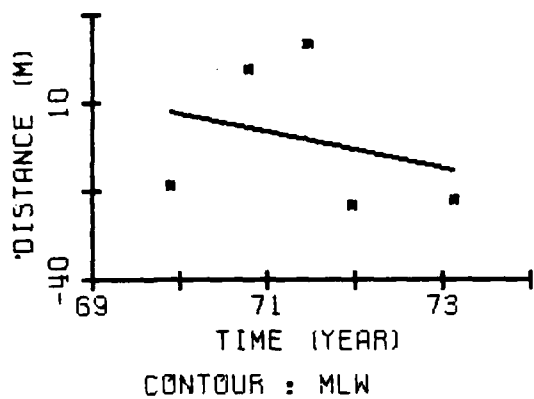
DISTANCE FROM THE BASE LINE TO STATED CONTOURS



FB 7

FB 8

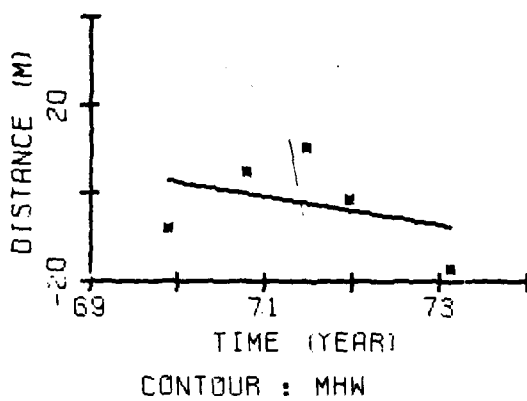
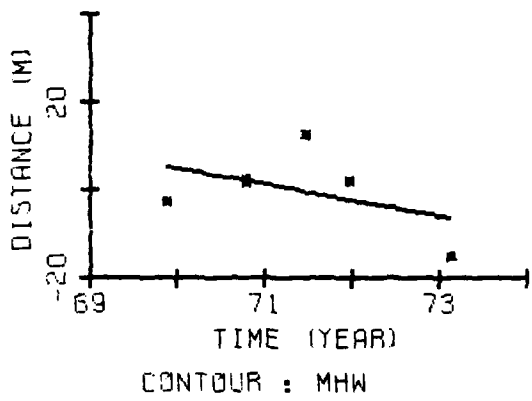
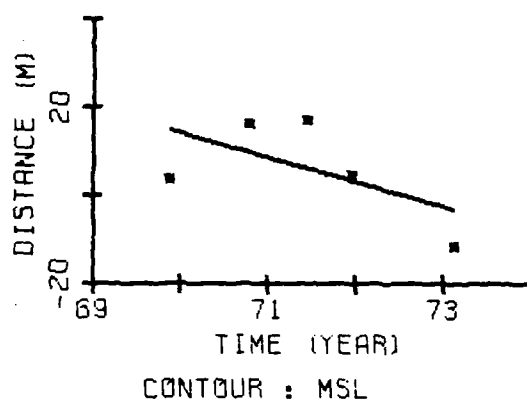
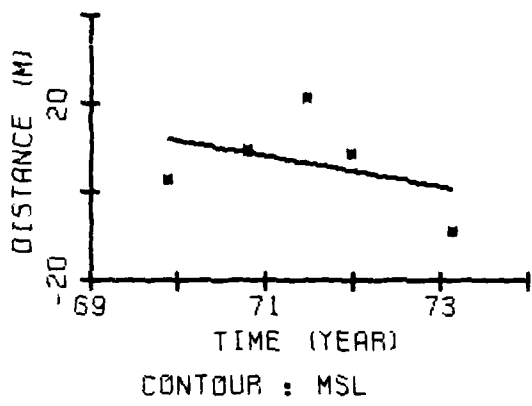
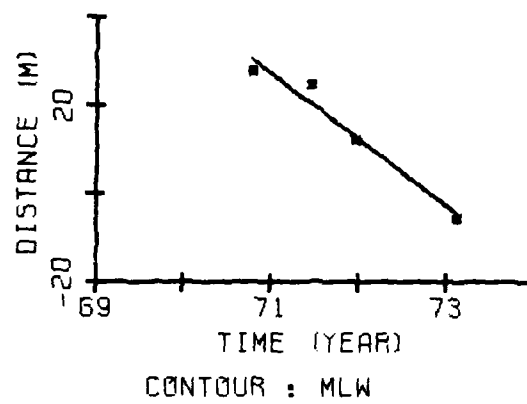
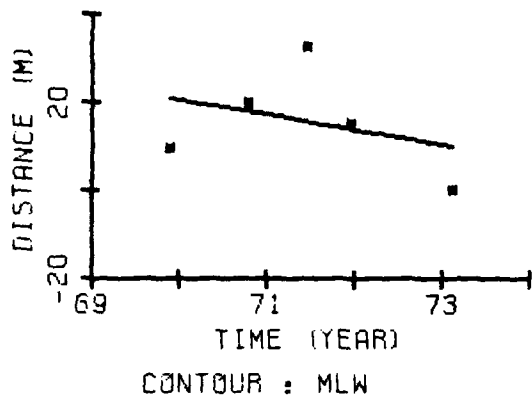
DISTANCE FROM THE BASE LINE TO STATED CONTOURS



FB 9

FB 10

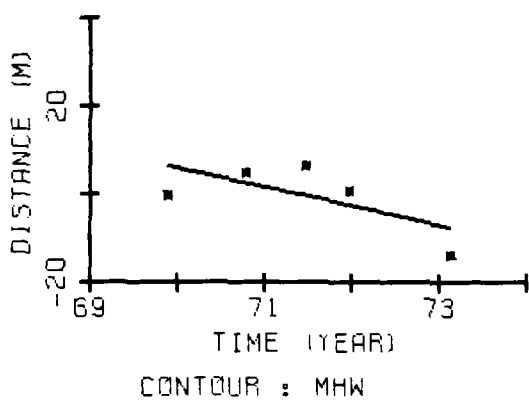
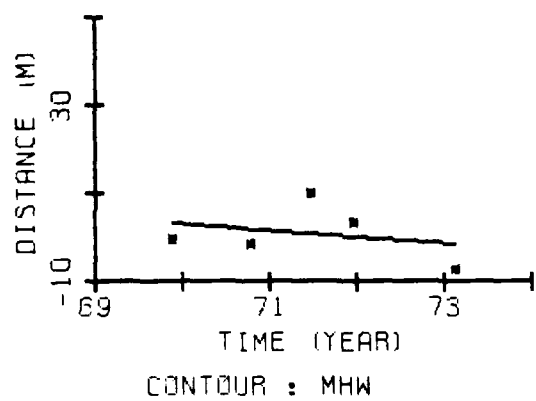
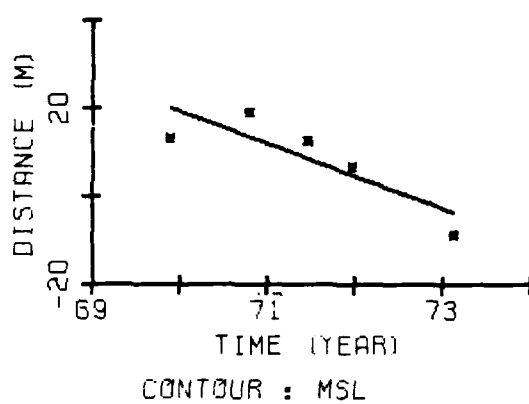
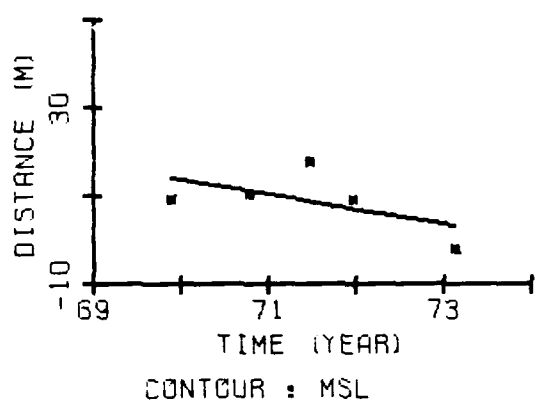
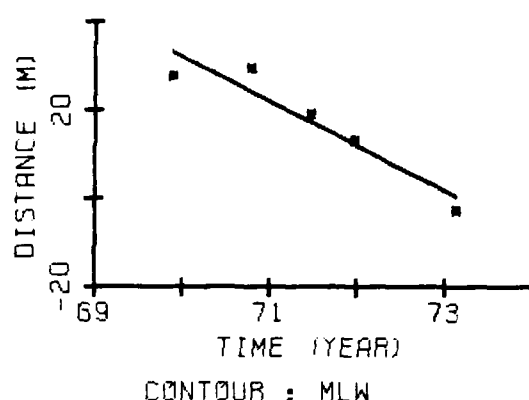
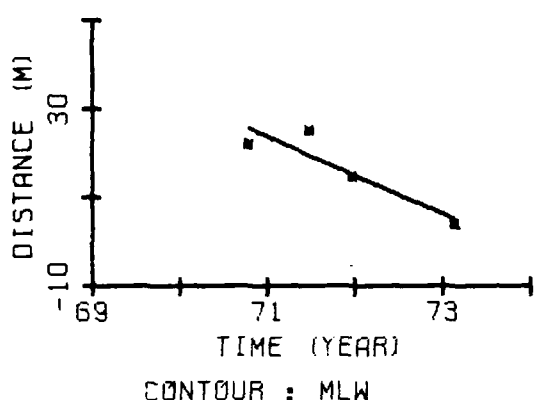
DISTANCE FROM THE BASE LINE TO STATED CONTOURS



FB 11

FB 12

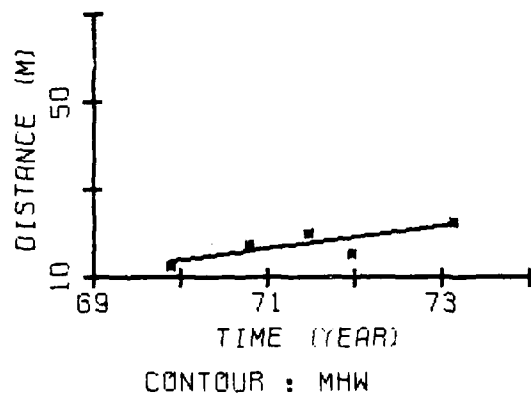
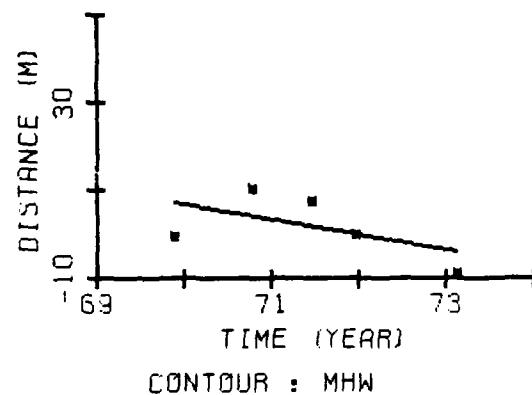
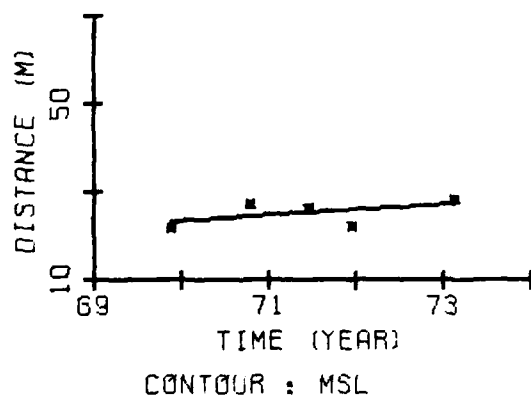
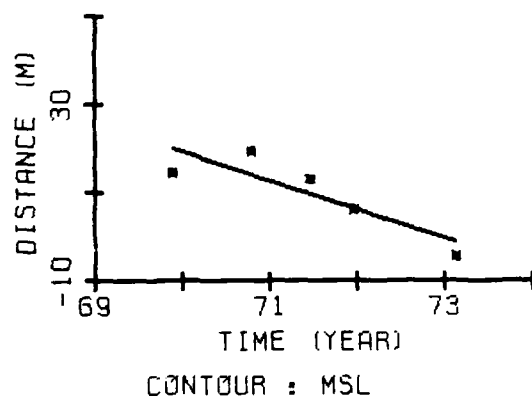
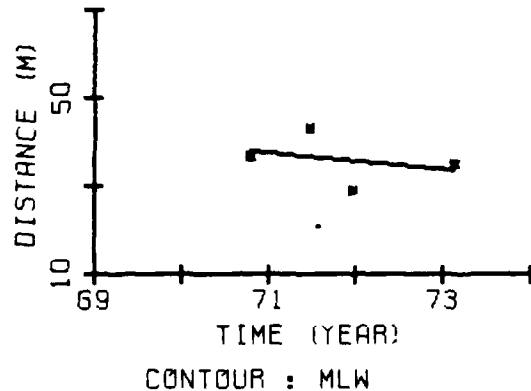
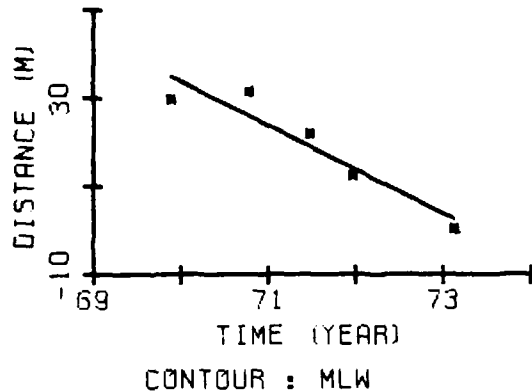
DISTANCE FROM THE BASE LINE TO STATED CONTOURS



FB 13

FB 14

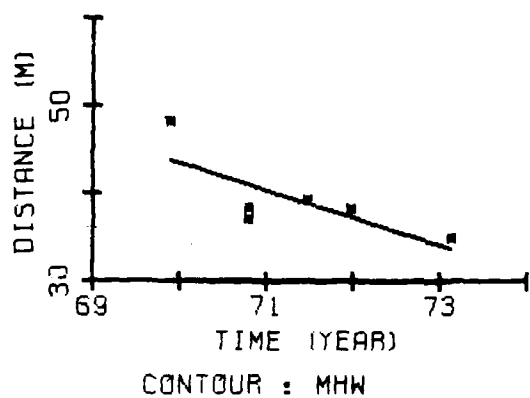
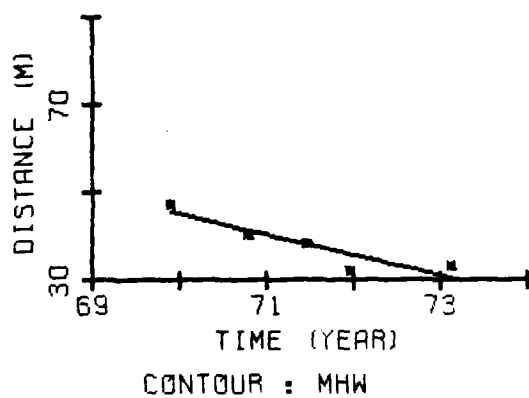
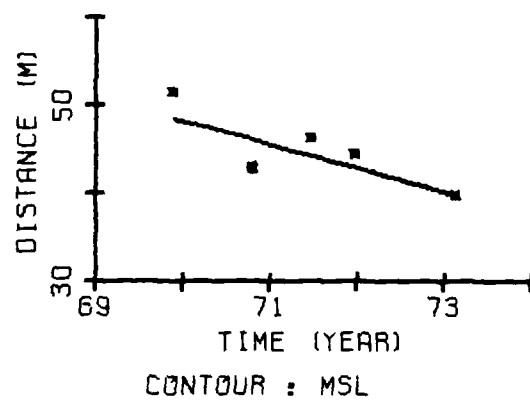
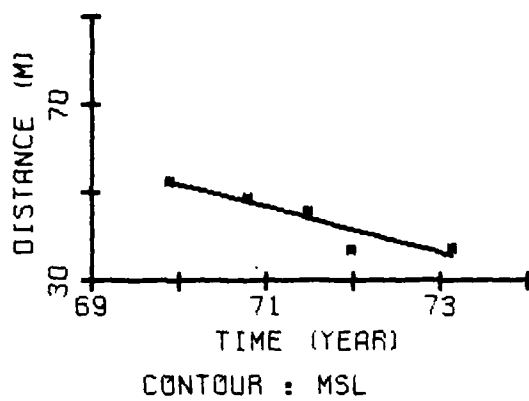
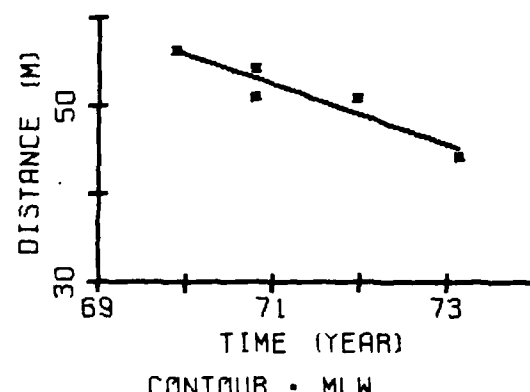
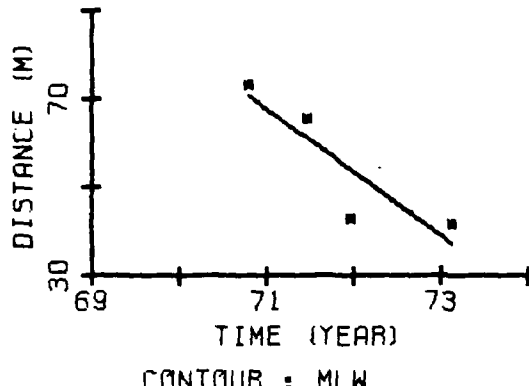
DISTANCE FROM THE BASE LINE TO STATED CONTOURS



FB 15

FB 16

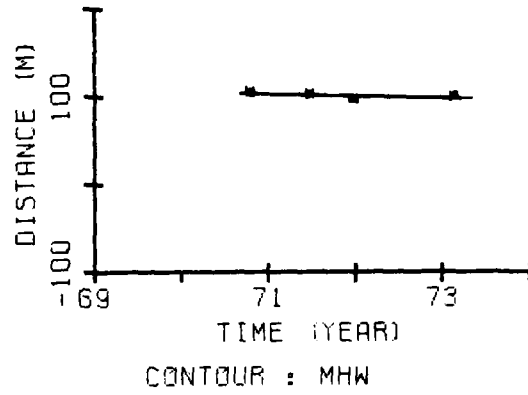
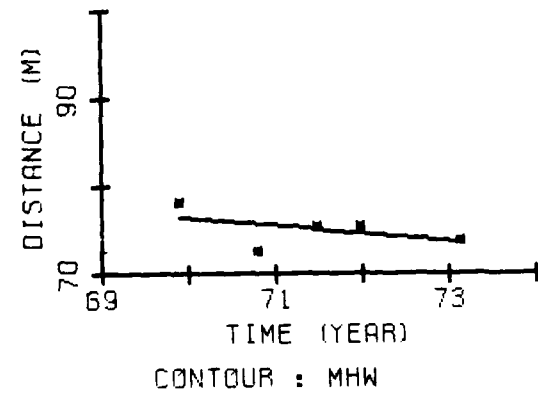
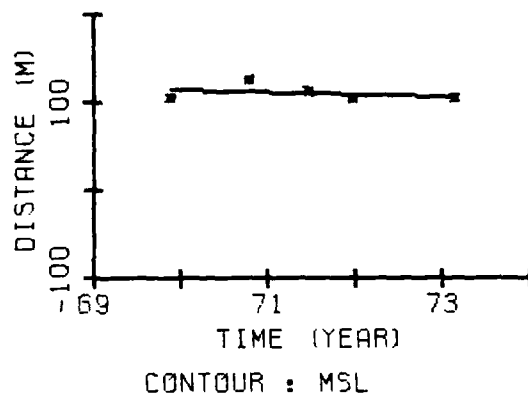
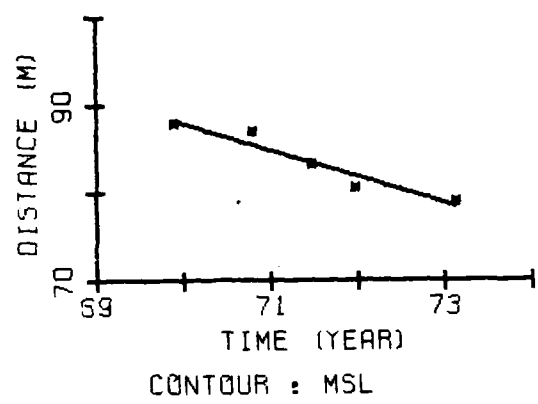
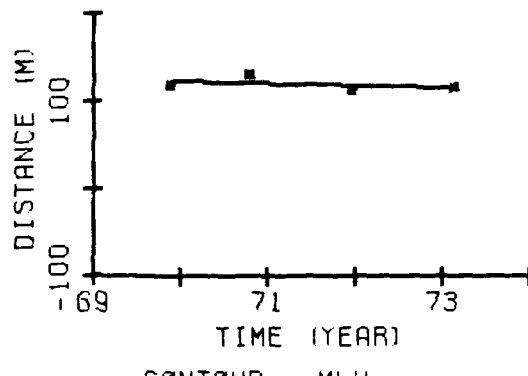
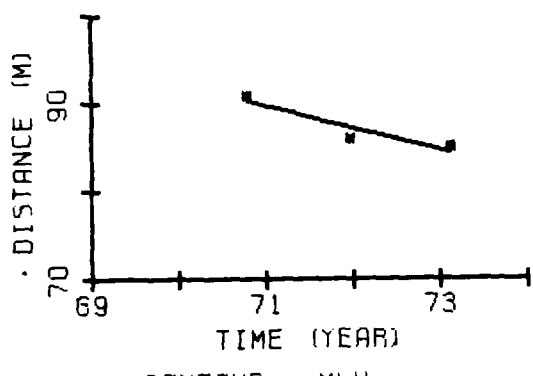
DISTANCE FROM THE BASE LINE TO STATED CONTOURS



FB 17

FB 18

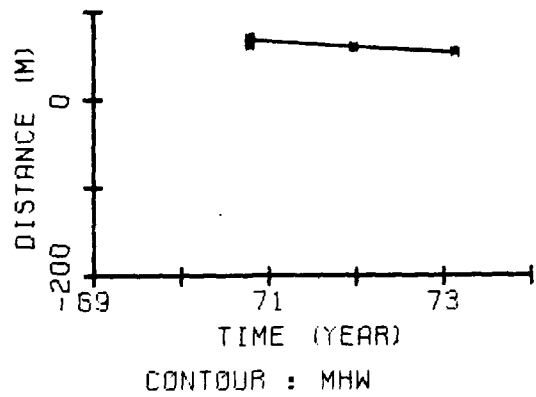
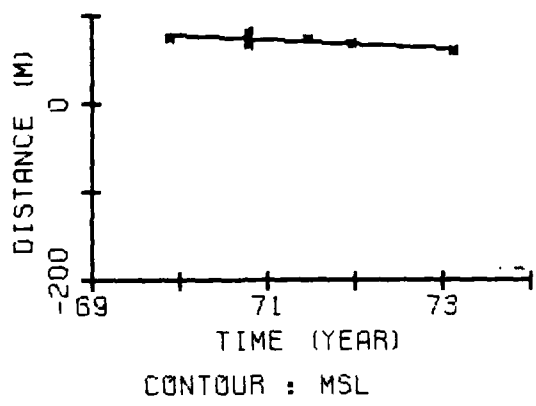
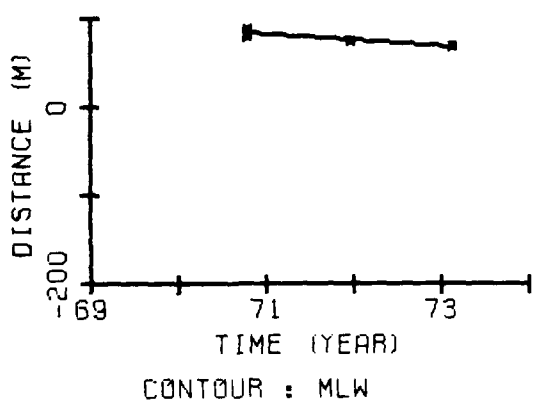
DISTANCE FROM THE BASE LINE TO STATED CONTOURS



FB 19

FB 20

DISTANCE FROM THE BASE LINE TO STATED CONTOURS



DISTANCE FROM THE BASE LINE TO STATED CONTOURS AT FB 21

APPENDIX F
COMPARATIVE SHORT BEACH PROFILES

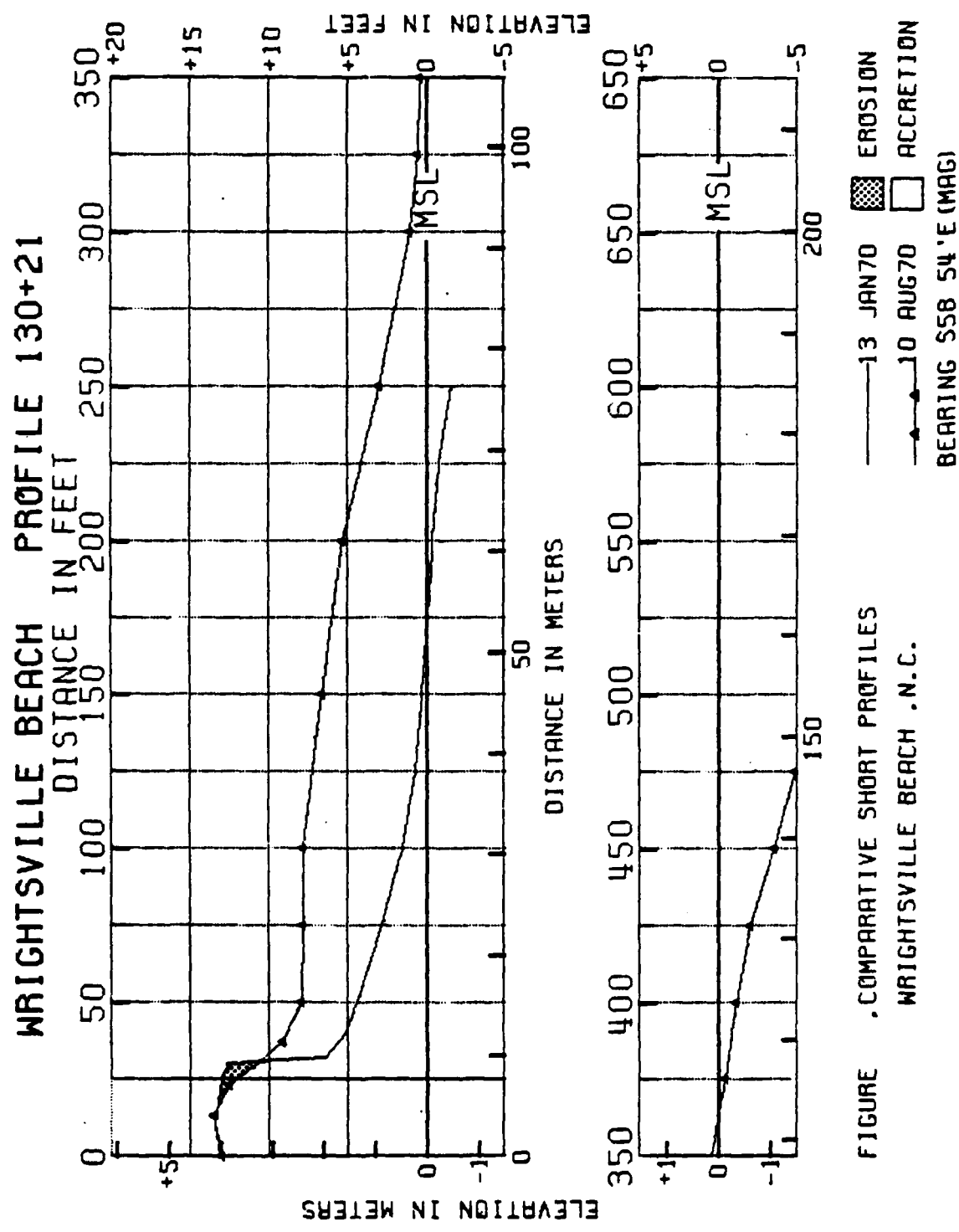


FIGURE . COMPARATIVE SHORT PROFILES
WRIGHTSVILLE BEACH . N.C.

WRIGHTSVILLE BEACH PROFILE 130+21

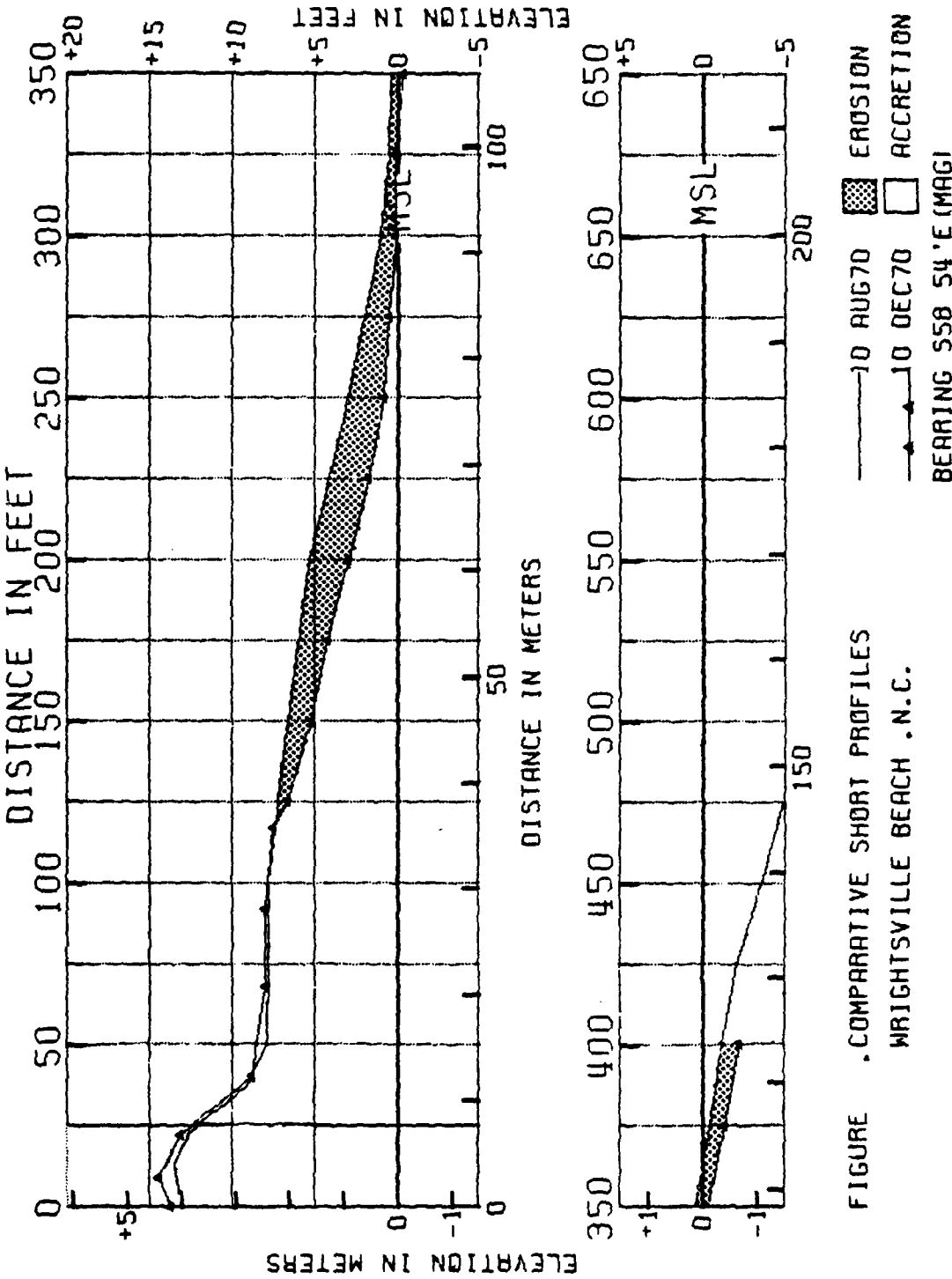


FIGURE .COMPARATIVE SHORT PROFILES
WRIGHTSVILLE BEACH .N.C.
BEARING 55° 54' E (MAG)

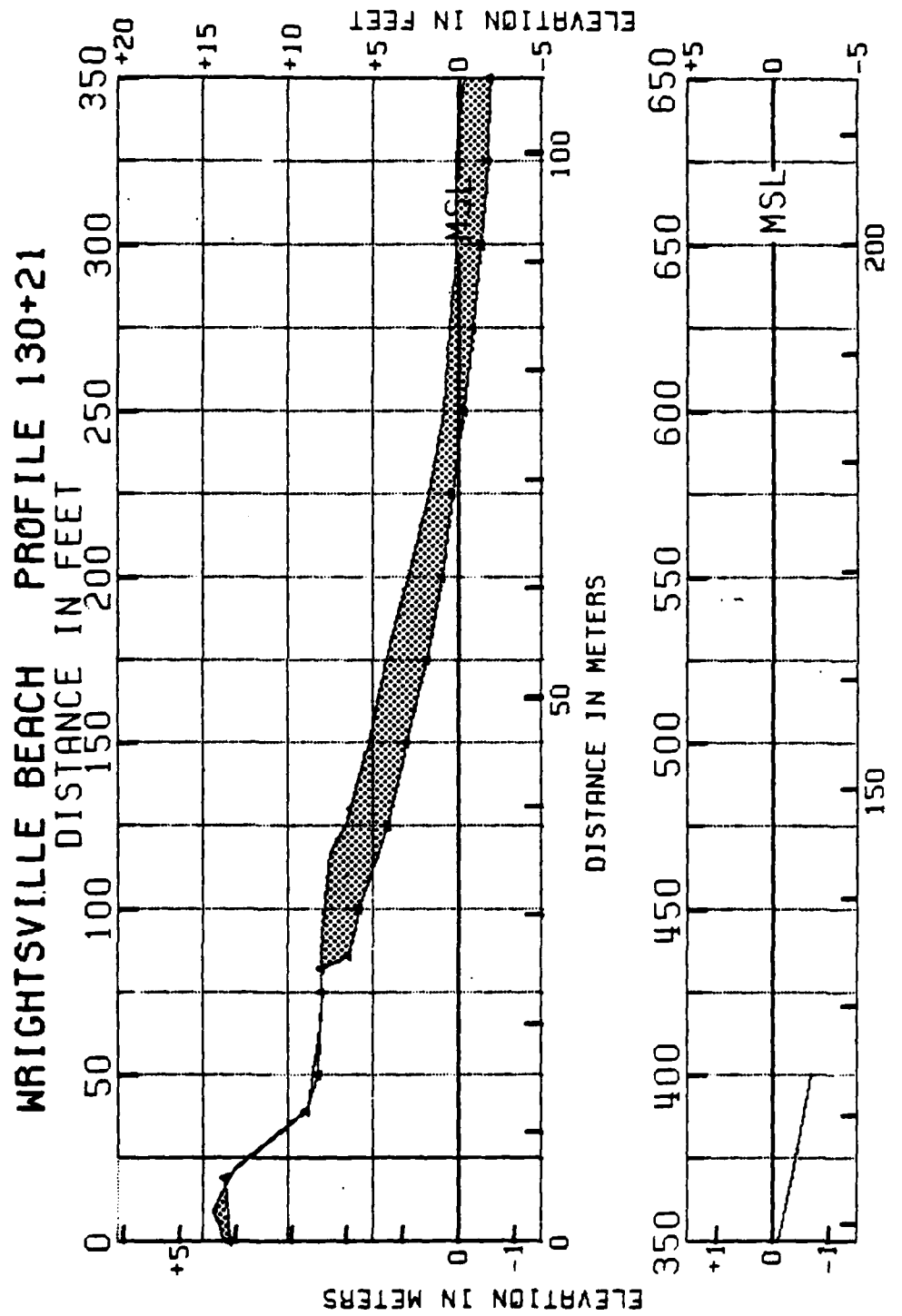


FIGURE . COMPARATIVE SHORT PROFILES
WRIGHTSVILLE BEACH , N.C.

— 10 DEC70 ■ EROSION
— 7 APR71 □ ACCRETION
BEARING 558 54'E (MAG)

WRIGHTSVILLE BEACH PROFILE 130+21

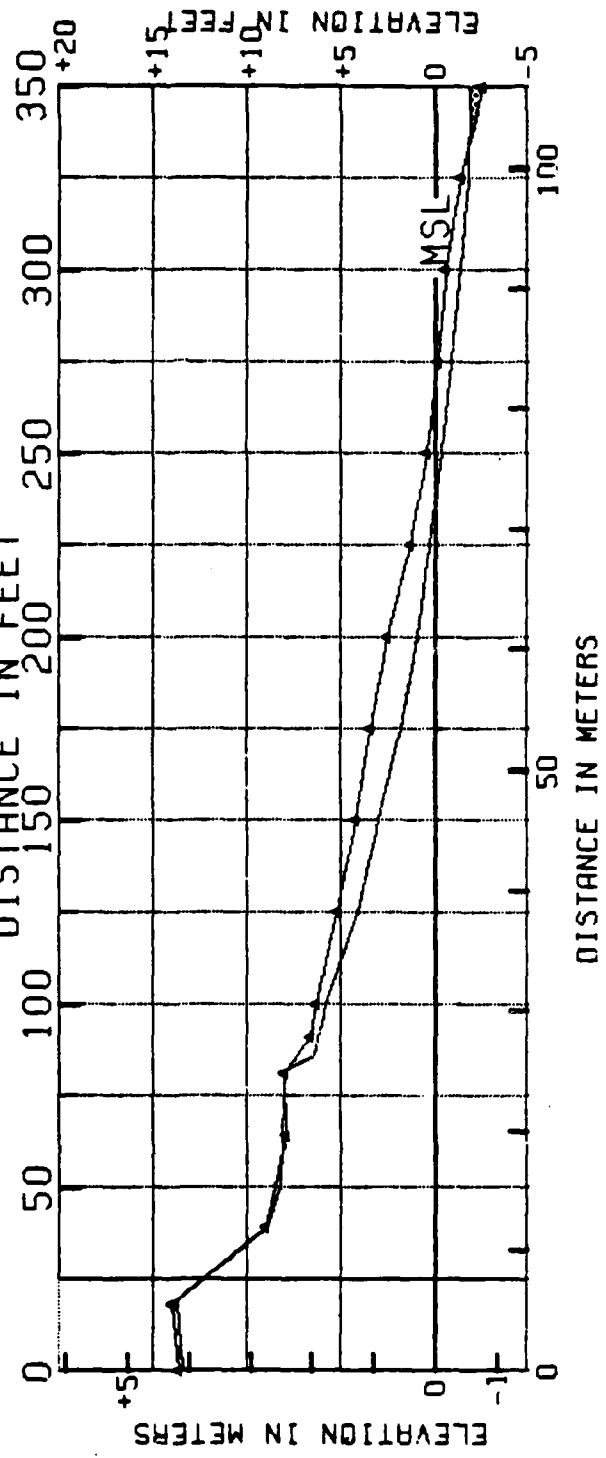


FIGURE . COMPARATIVE SHORT PROFILES
WRIGHTSVILLE BEACH , N.C.
BEARING 558 54'E (MAG)

— 7 APR71 ■ EROSION
— 29 AUG71 □ ACCRETION

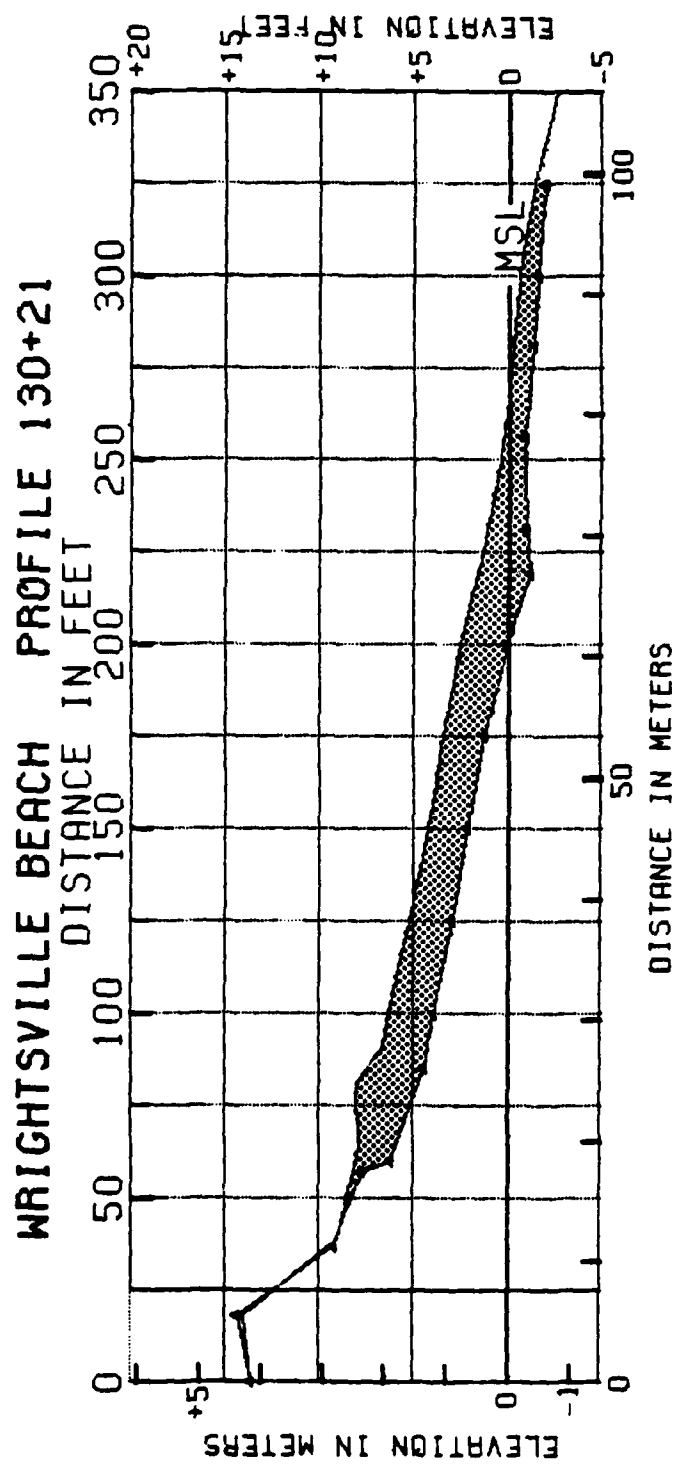


FIGURE . COMPARATIVE SHORT PROFILES
WRIGHTSVILLE BEACH . N.C.
29 AUG 71 EROSION
10 DEC 71 ACCRETION
BEARING S58 54'E (MAG)

WRIGHTSVILLE BEACH PROFILE 130+21

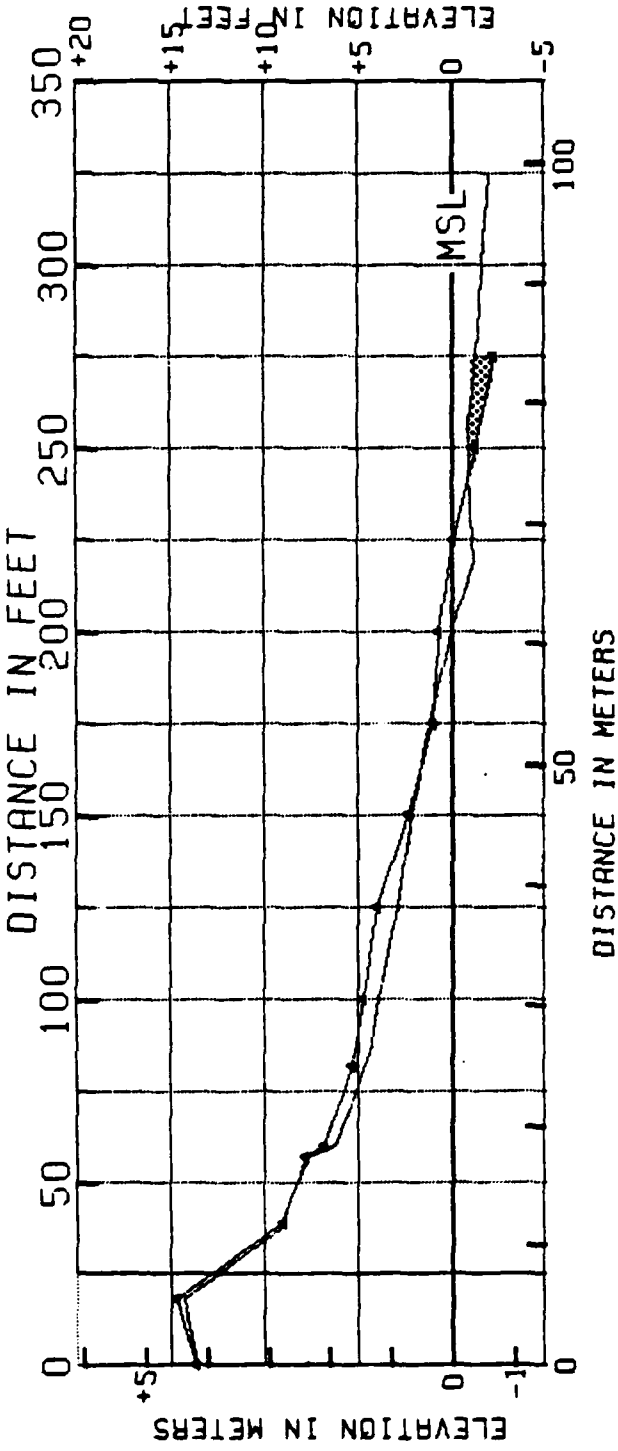


FIGURE . COMPARATIVE SHORT PROFILES
WRIGHTSVILLE BEACH , N.C.
BEARING 558 54'E (MAG)
— 10 DEC71 ■ EROSION
- - - 11 APR72 □ ACCRETION

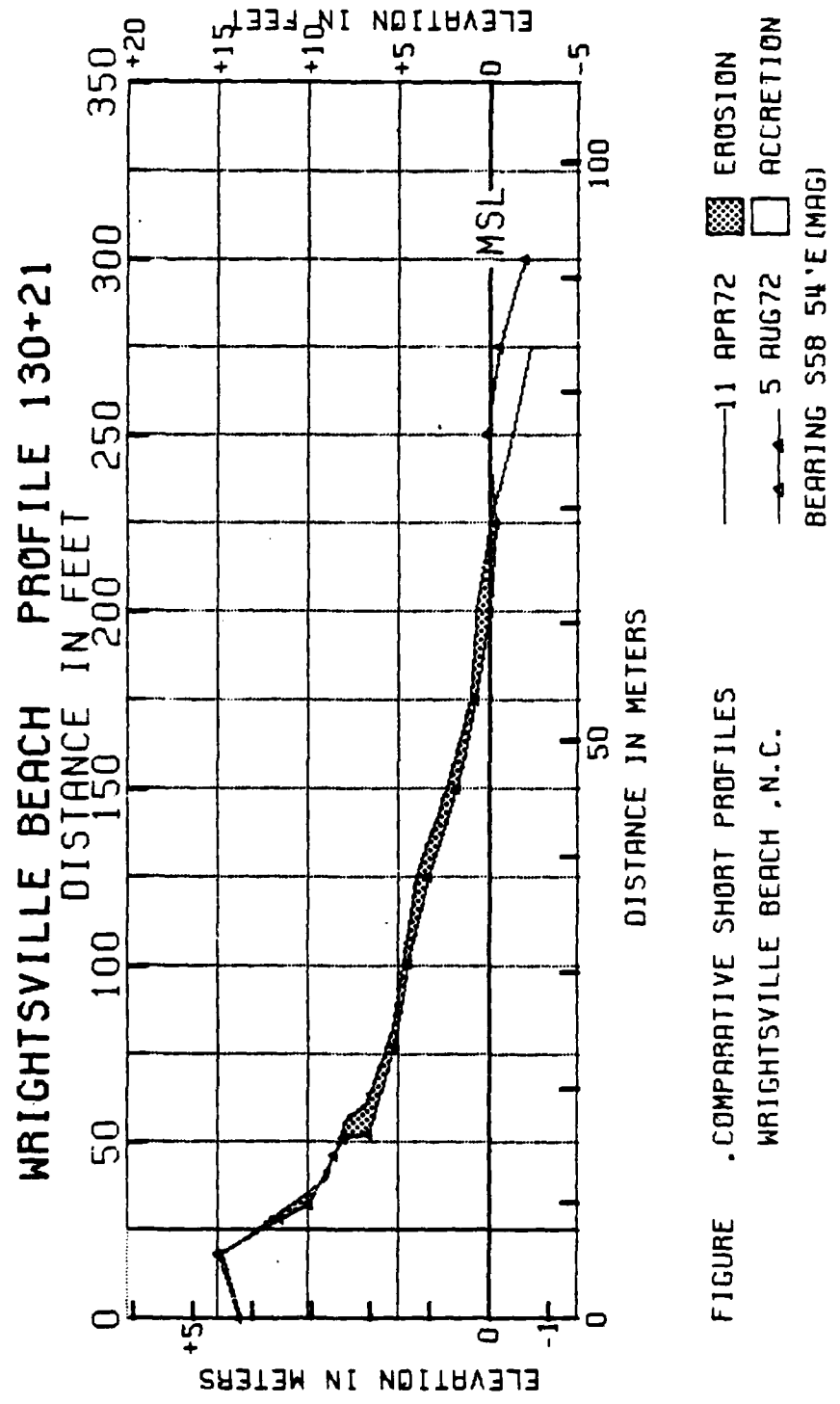


FIGURE . COMPARATIVE SHORT PROFILES
WRIGHTSVILLE BEACH , N.C.

WRIGHTSVILLE BEACH PROFILE 130+21

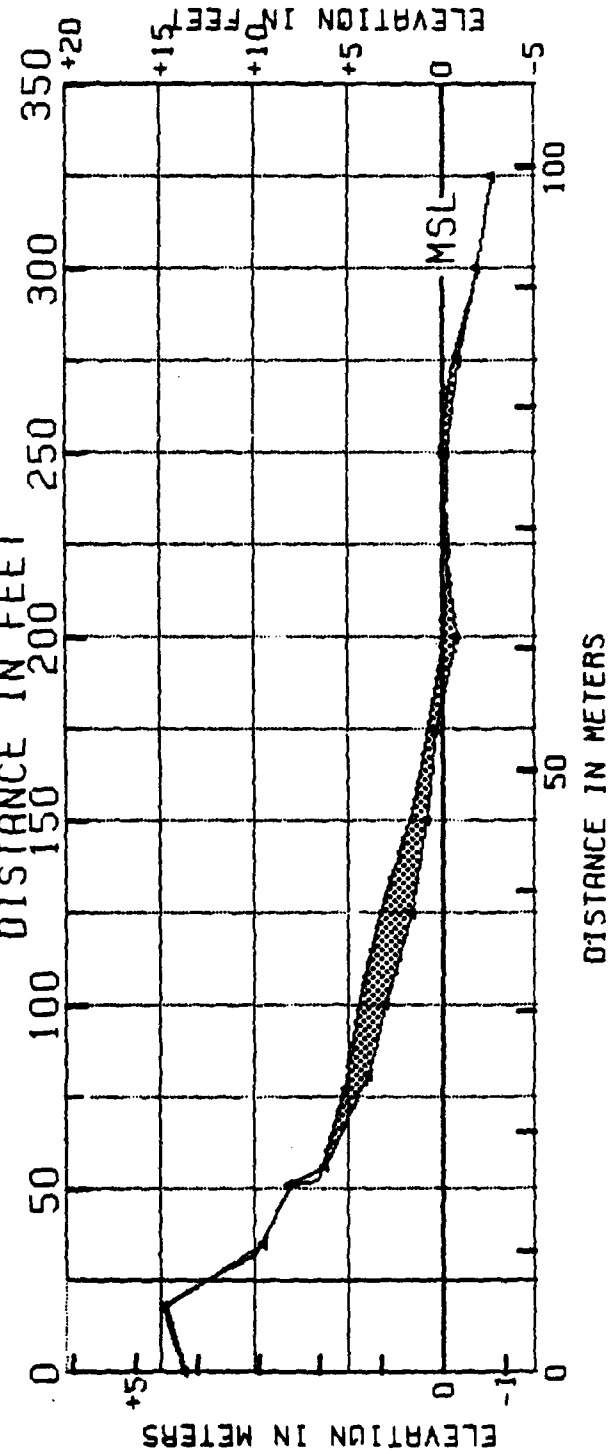
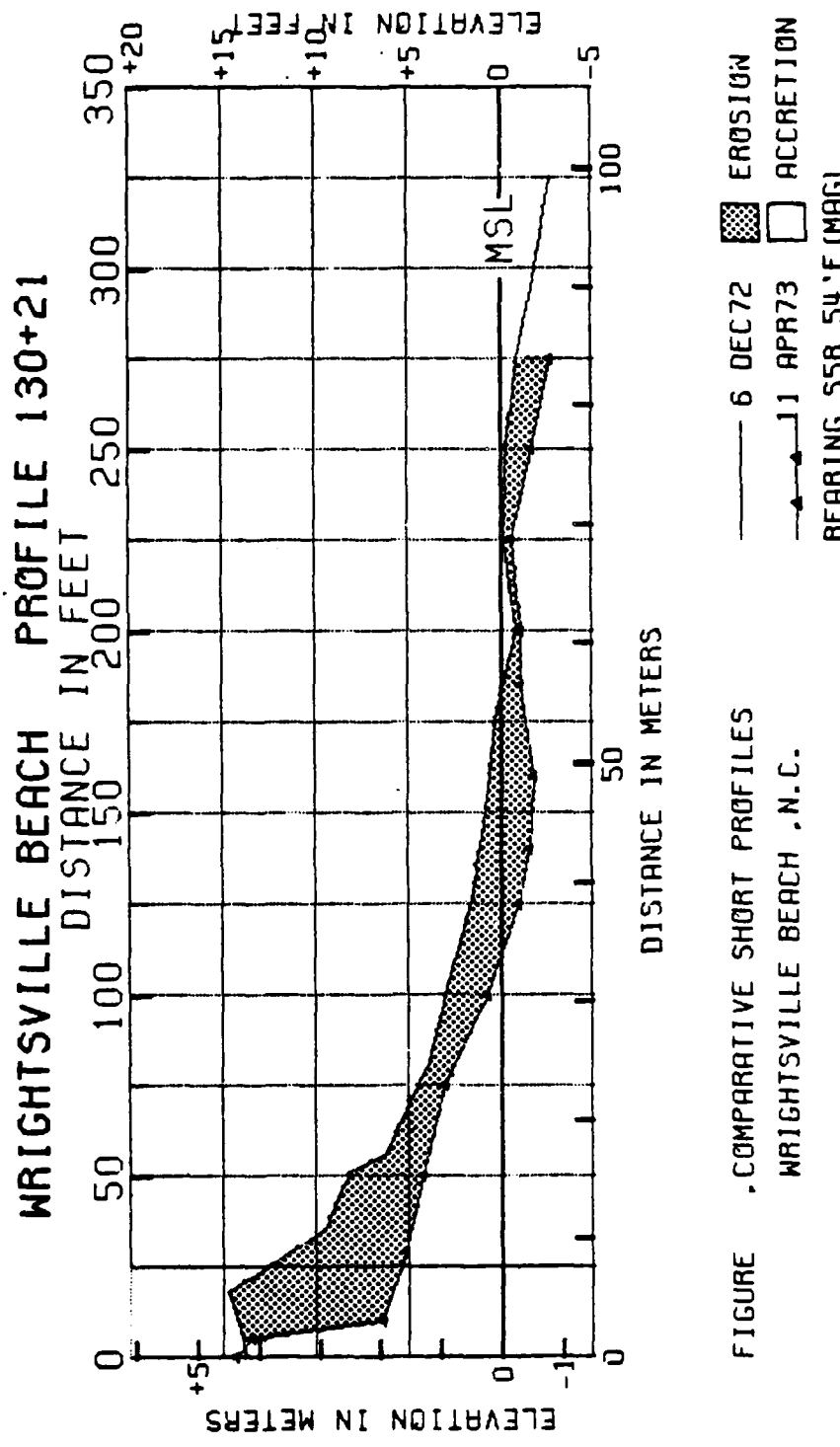


FIGURE 6 COMPARATIVE SHORT PROFILES
WRIGHTSVILLE BEACH - N.C.

BEARING 558 54'E (MAG)

■ EROSION
□ ACCRETION



AD-A103 168

ENVIRONMENTAL SCIENCE AND ENGINEERING INC GAINESVILLE FL F/6 8/10
ANALYSIS OF COASTAL SEDIMENT TRANSPORT PROCESSES FROM WRIGHTSVI--ETC(U)
JUN 81 T C WINTON, I B CHOU, G M POWELL
DACP72-79-C-0001

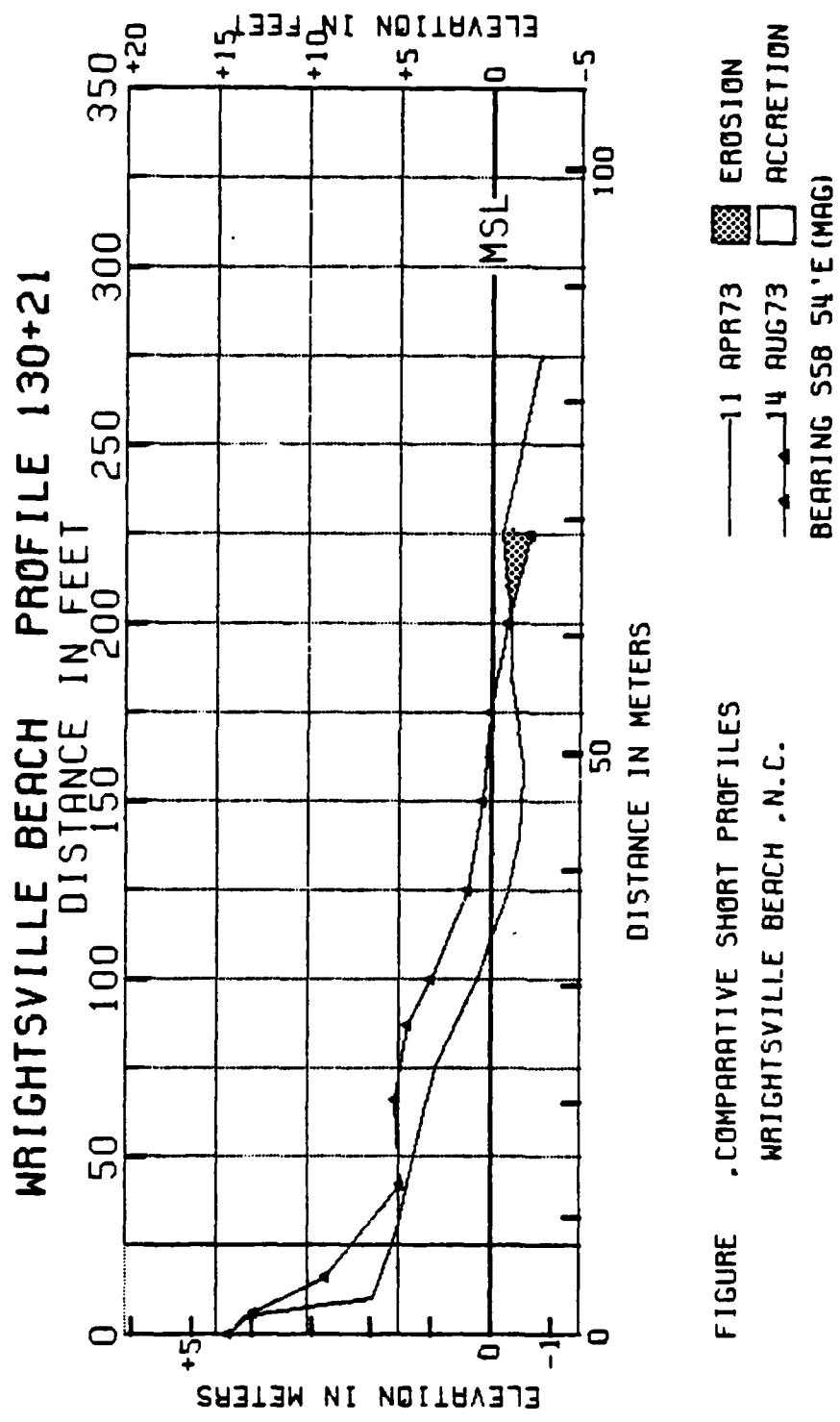
CERC-MR-81-6

NL

UNCLASSIFIED

3 of 3
AD &
10X16B

END
DATE
FILED
9-81
DTIC



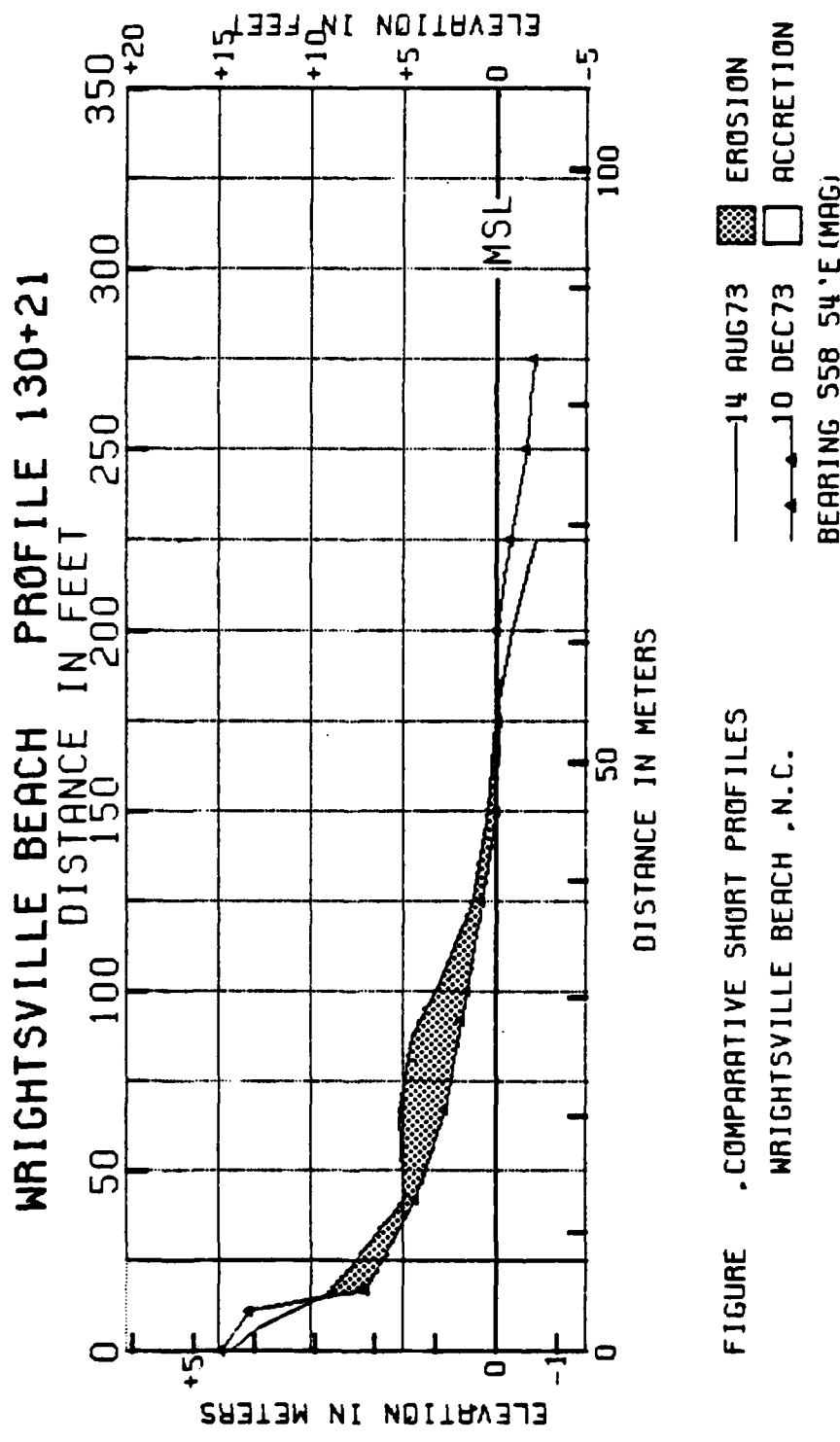


FIGURE . COMPARATIVE SHORT PROFILES

WRIGHTSVILLE BEACH , N.C.

WRIGHTSVILLE BEACH PROFILE 130+21

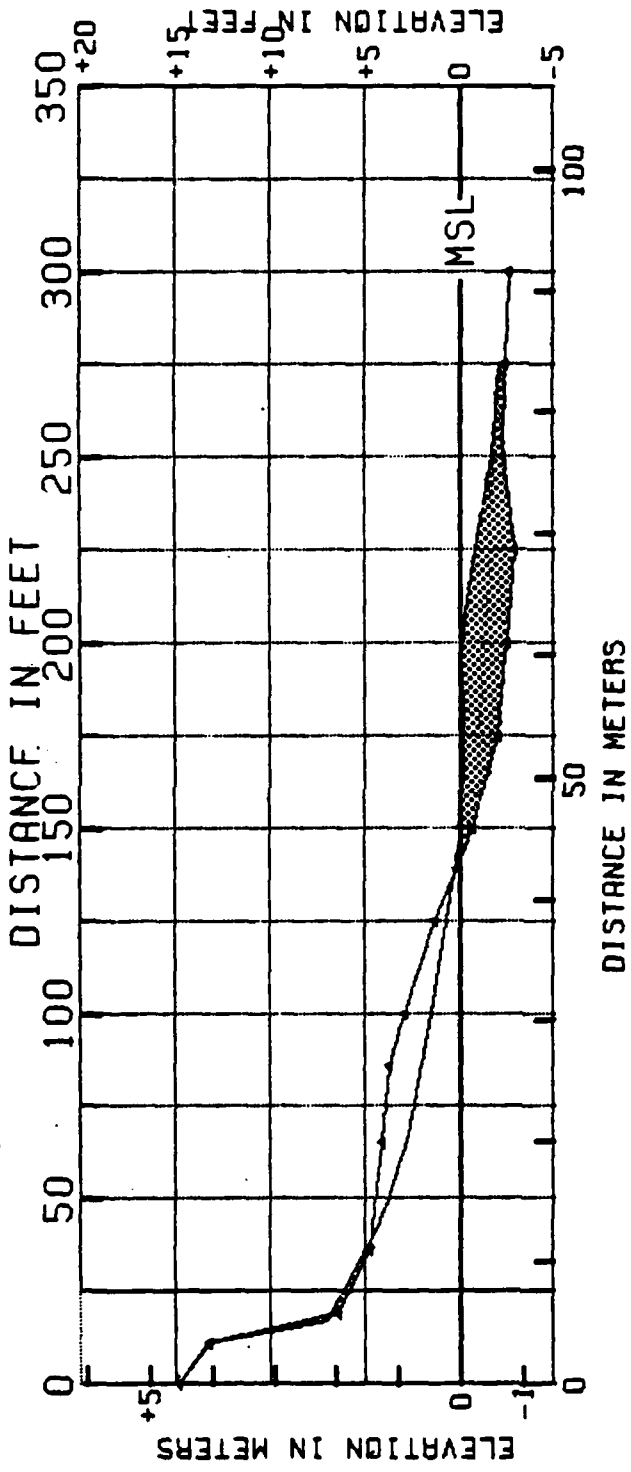


FIGURE . COMPARATIVE SHORT PROFILES
WRIGHTSVILLE BEACH . N.C.
— 10 DEC 73 ■ EROSION
— 4 APR 74 □ ACCRETION
BEARING 558° 54' E (MAG)

WRIGHTSVILLE BEACH PROFILE 130+21

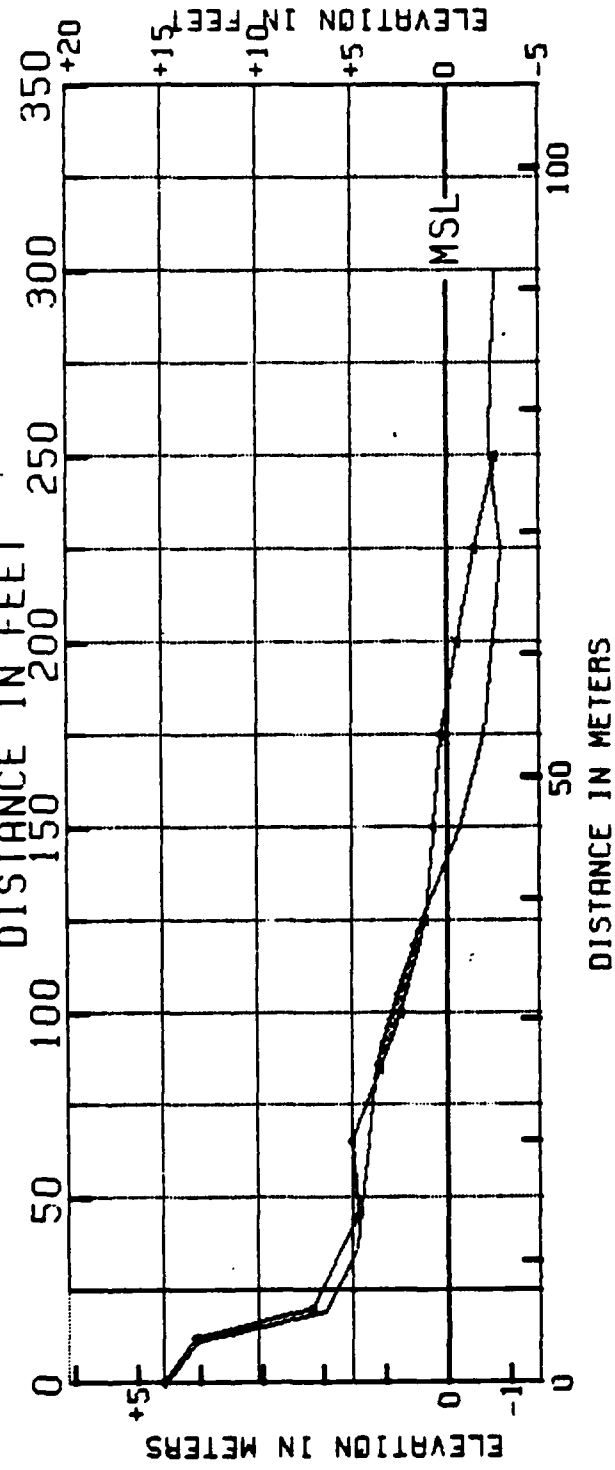
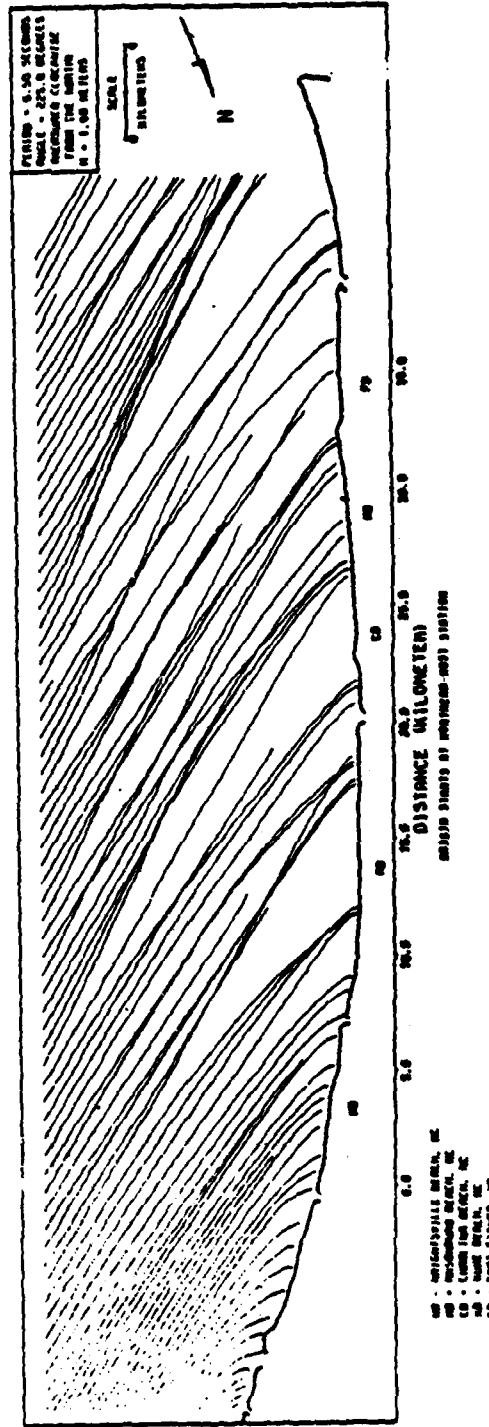
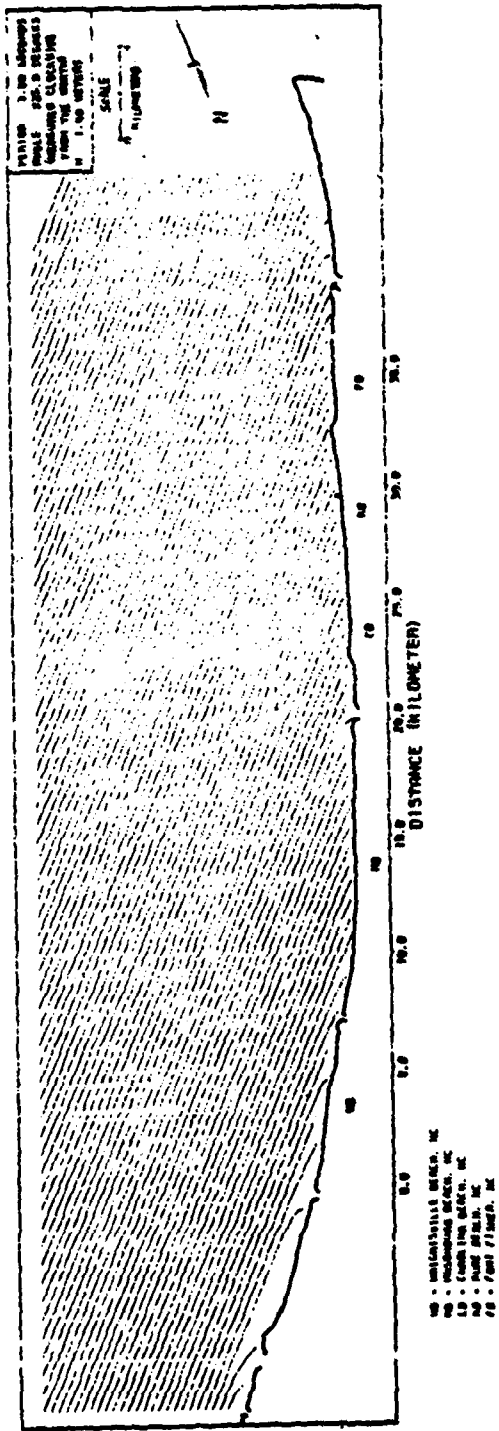
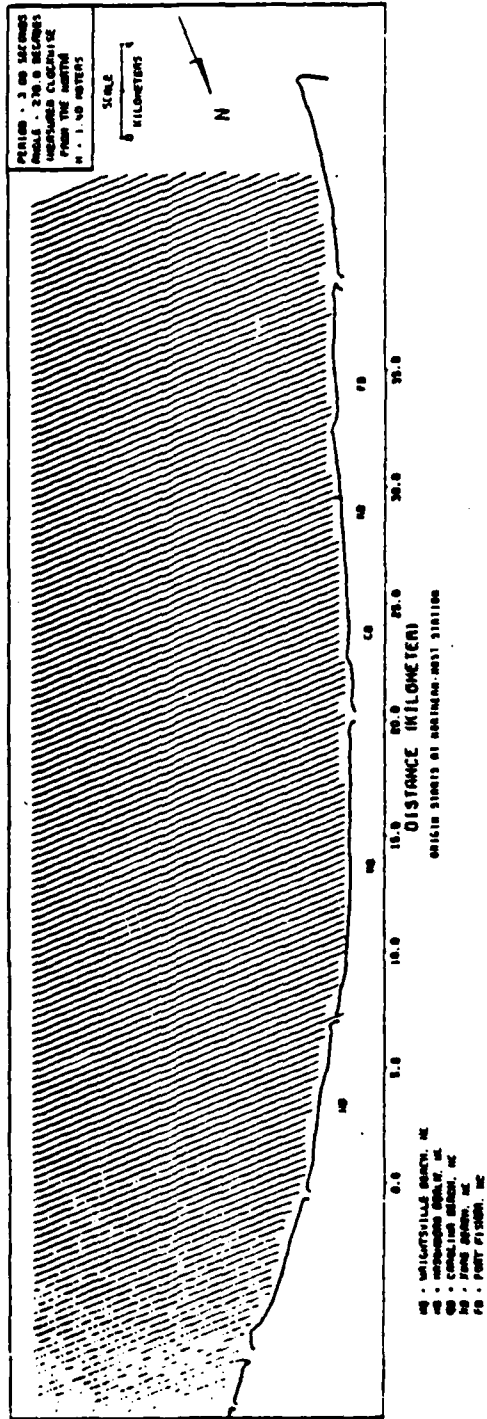
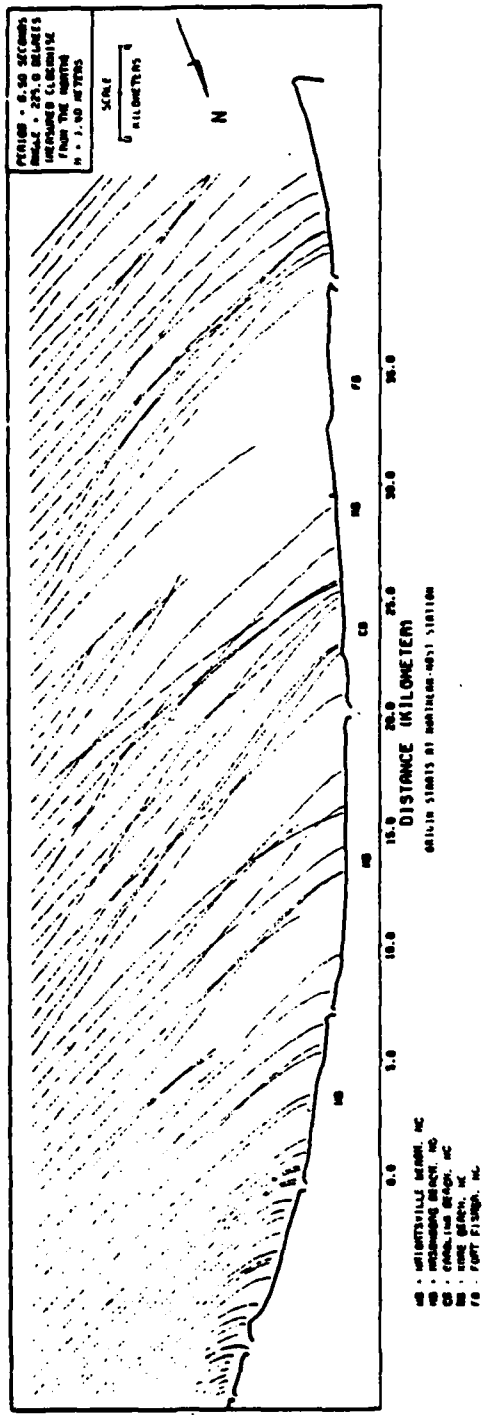


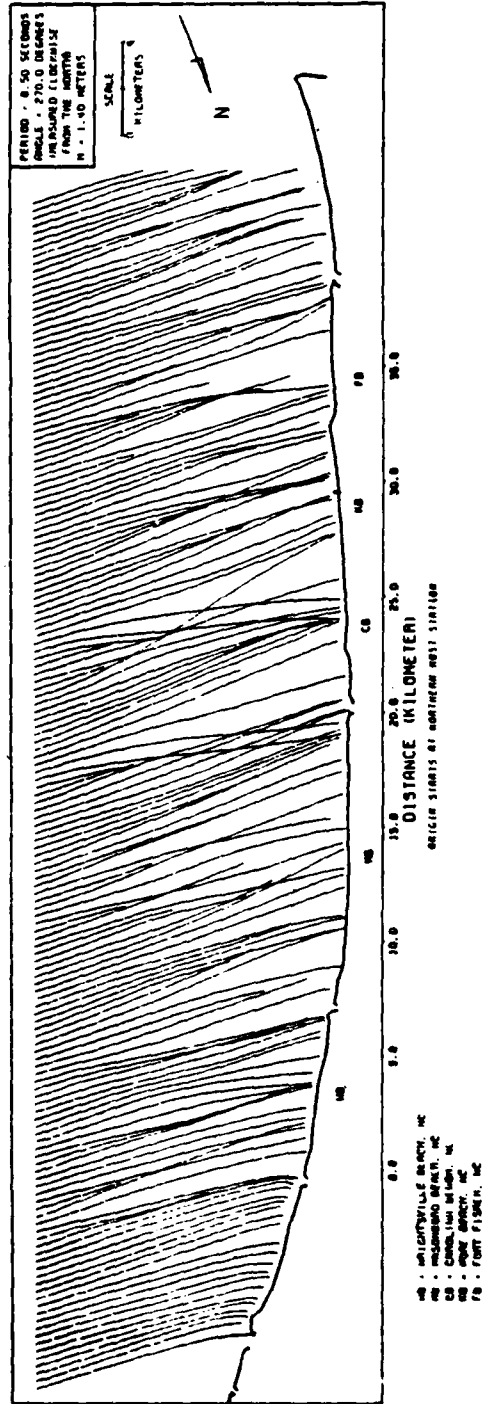
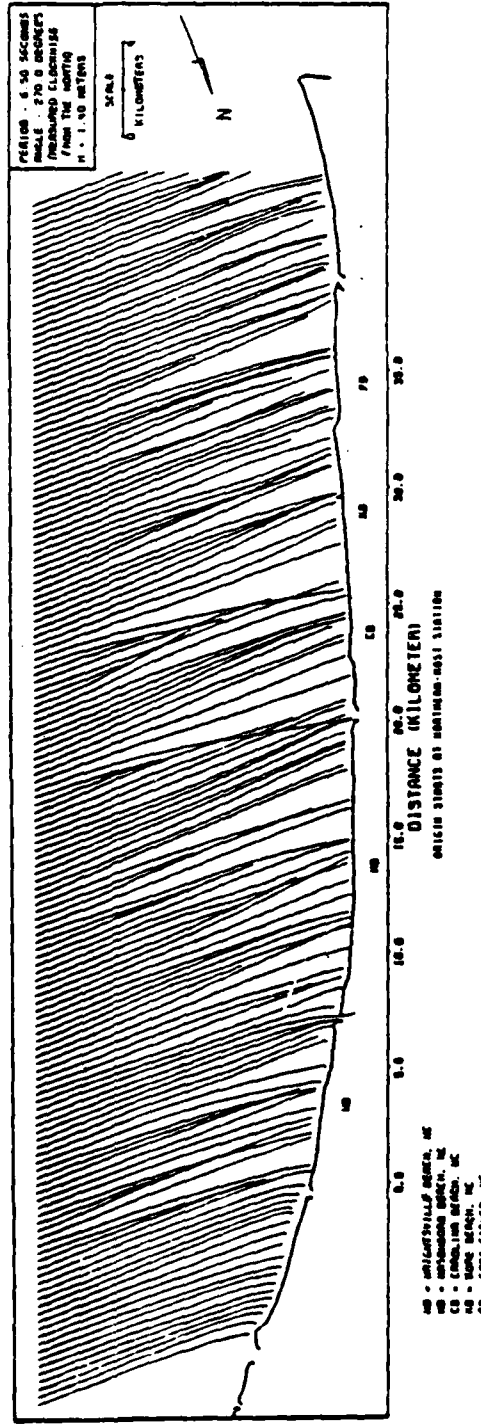
FIGURE . COMPARATIVE SHORT PROFILES
WRIGHTSVILLE BEACH , N.C.

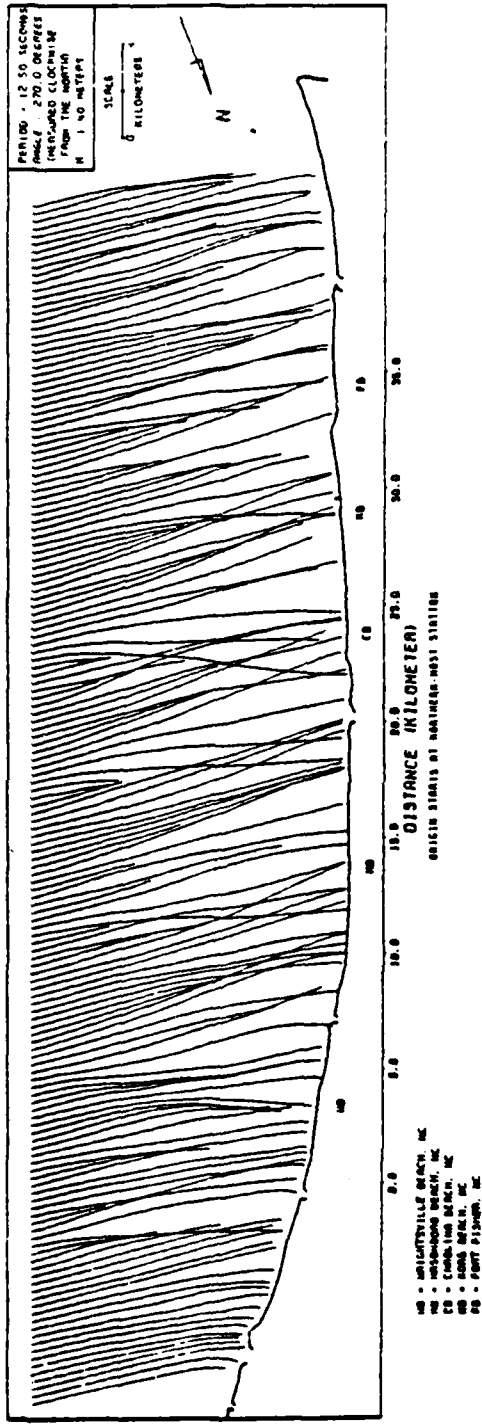
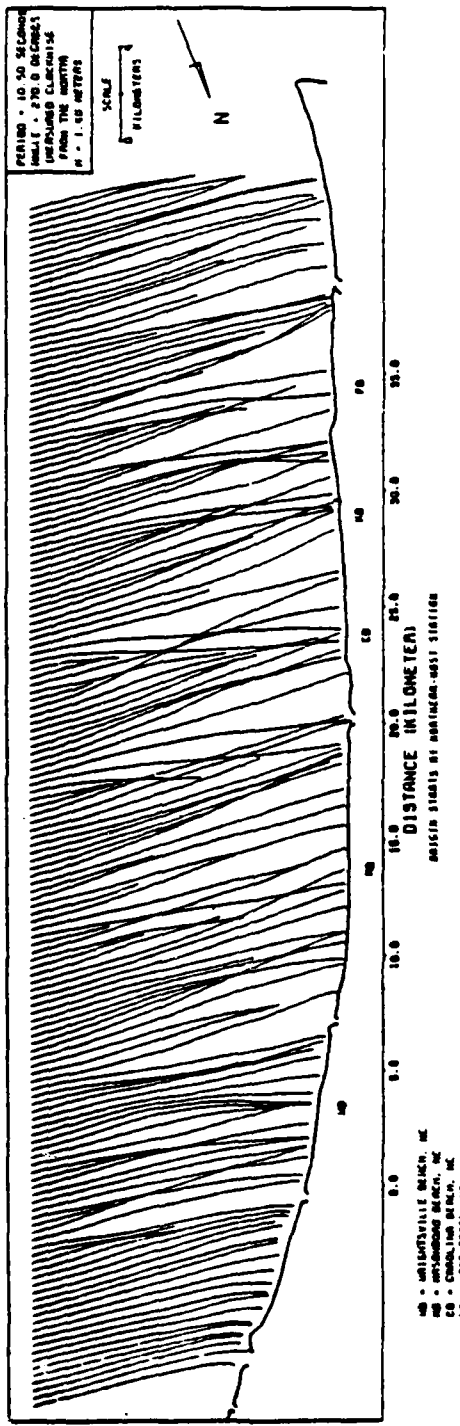
— 4 APR 74 ■ EROSION
— 13 AUG 74 □ ACCRETION
BEARING 558 54° E (MAG)

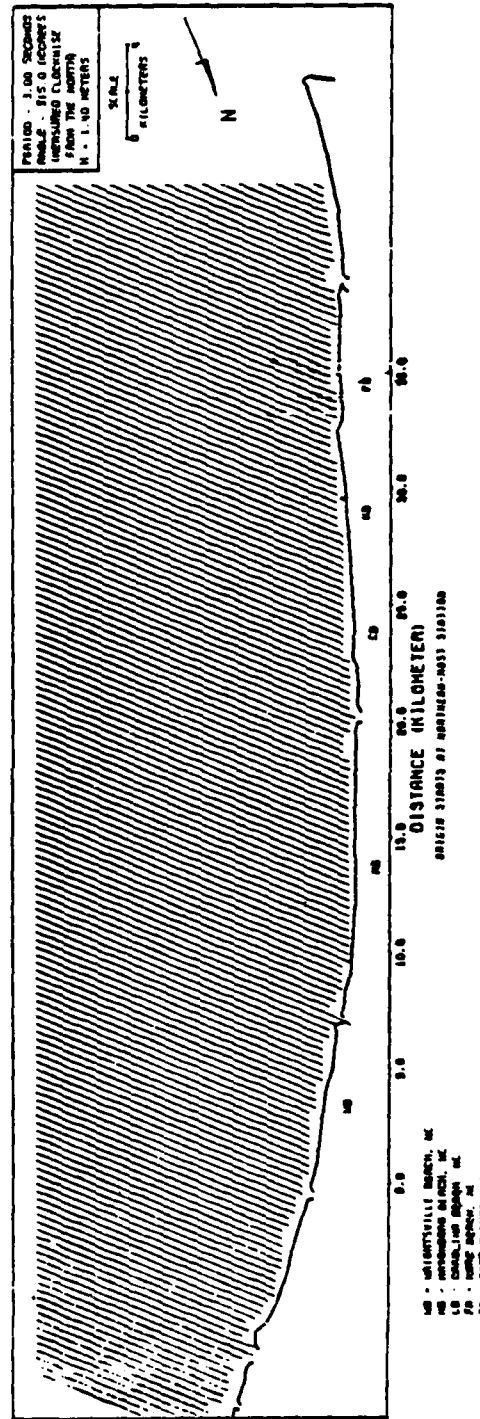
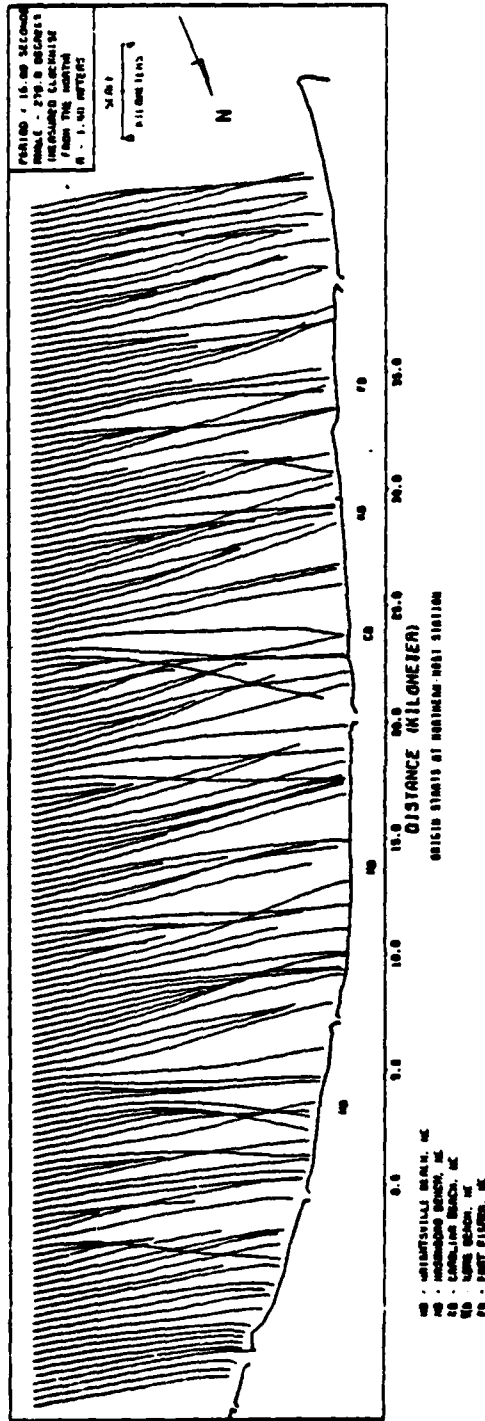
APPENDIX G
WAVE REFRACTION PLOTS

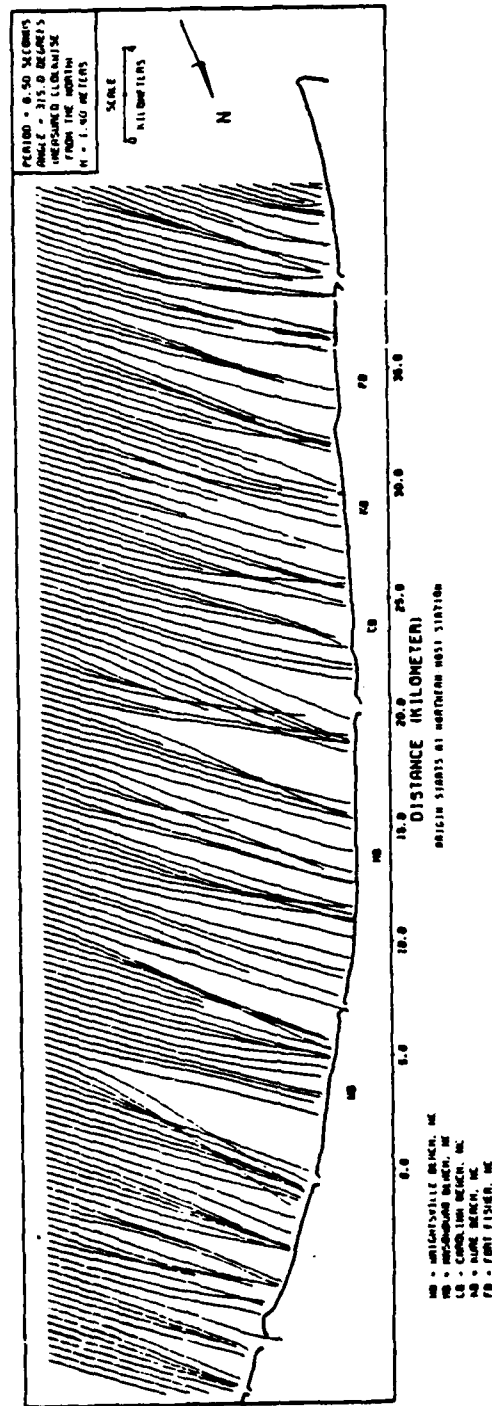
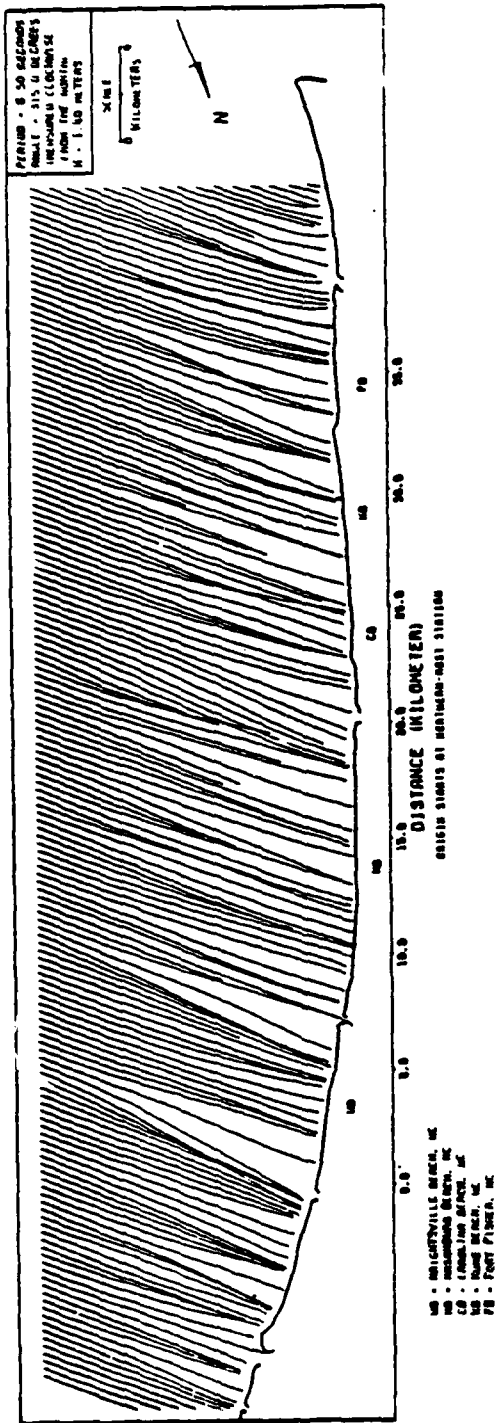


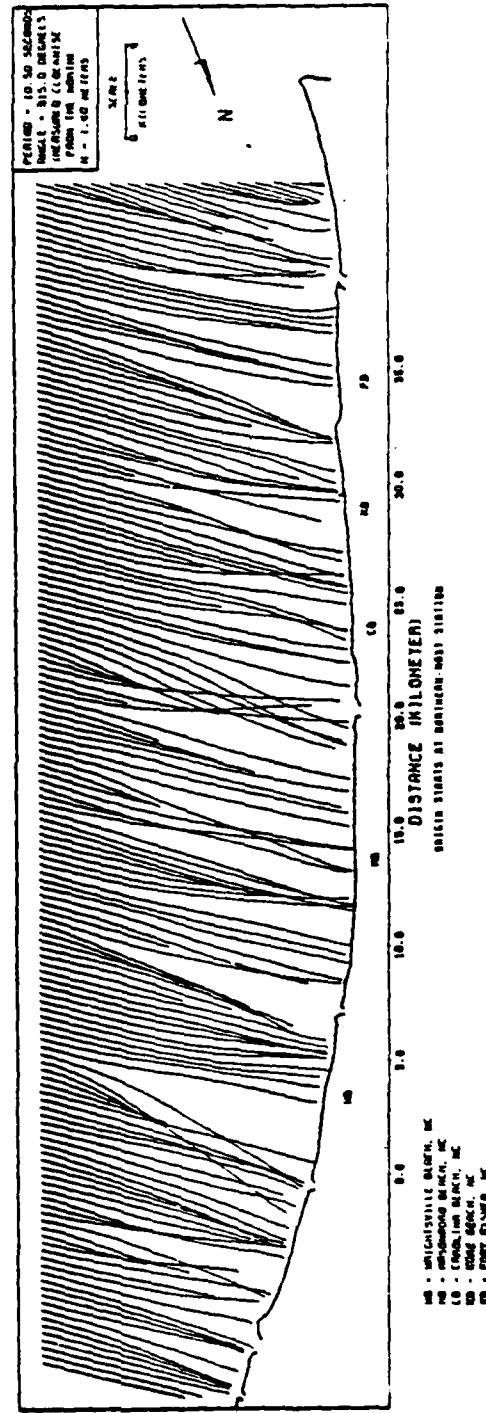
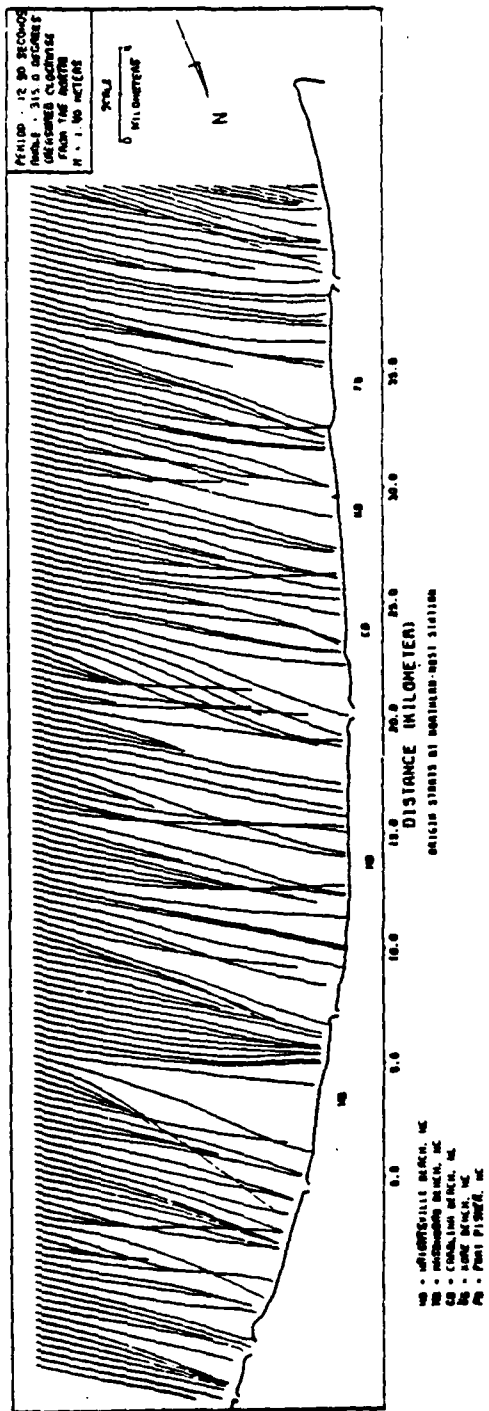


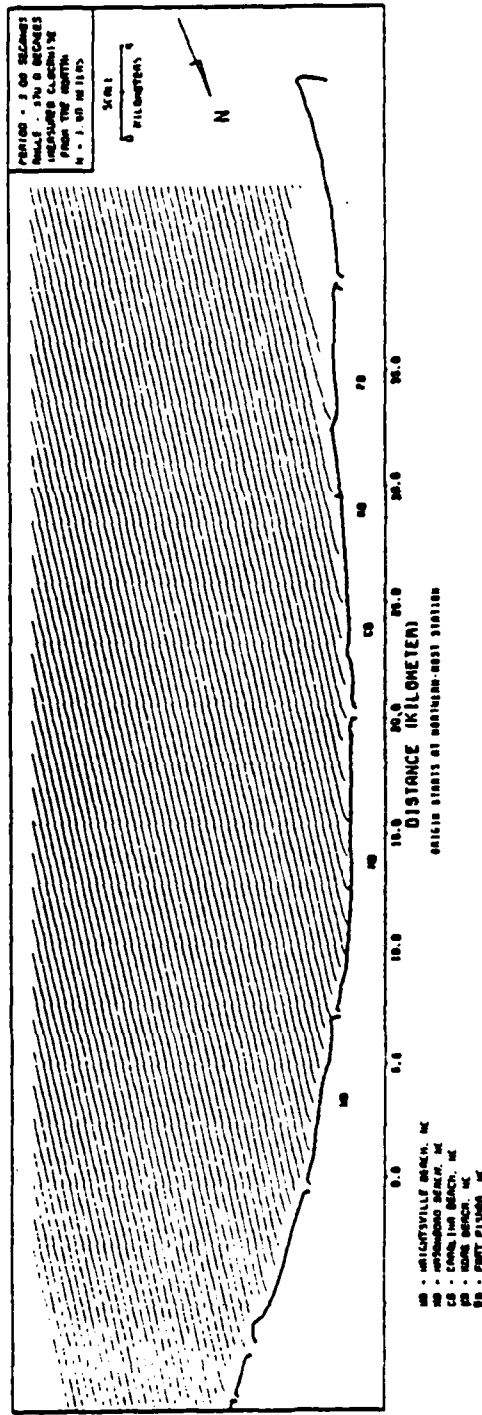
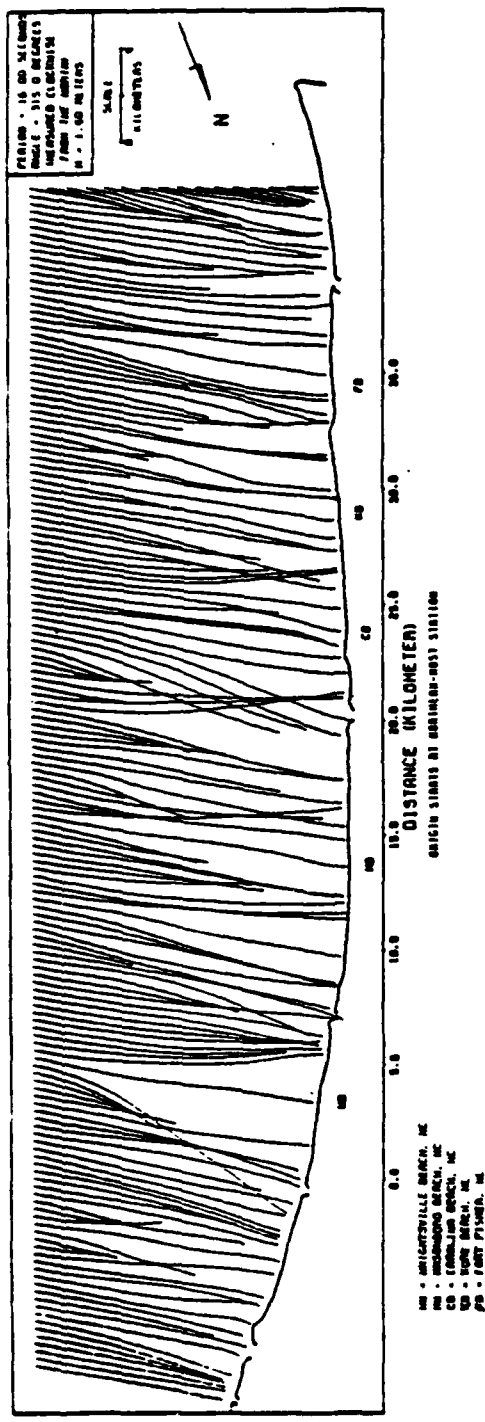


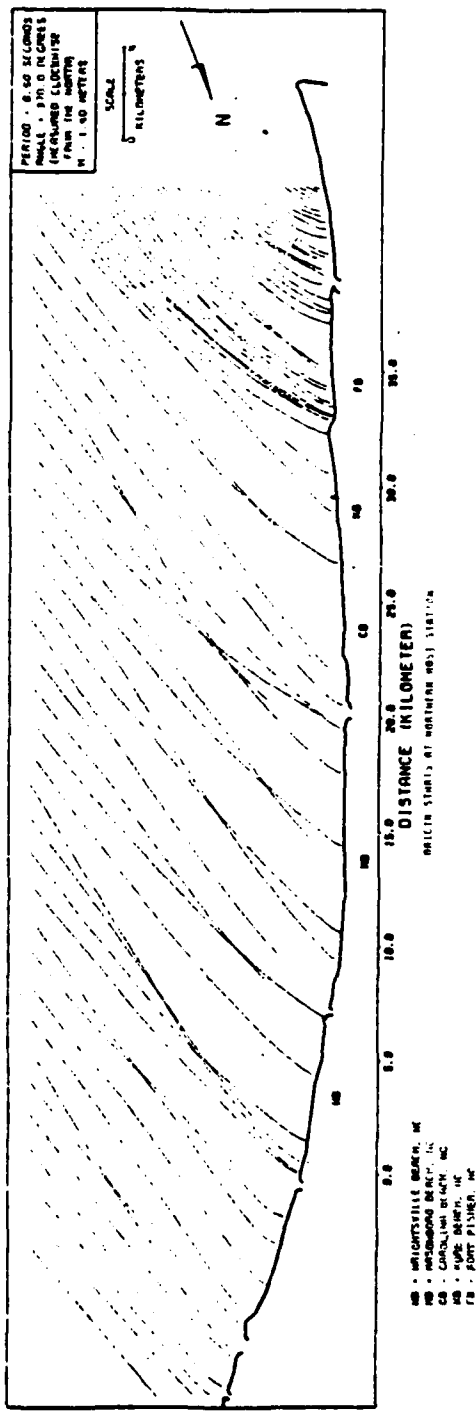
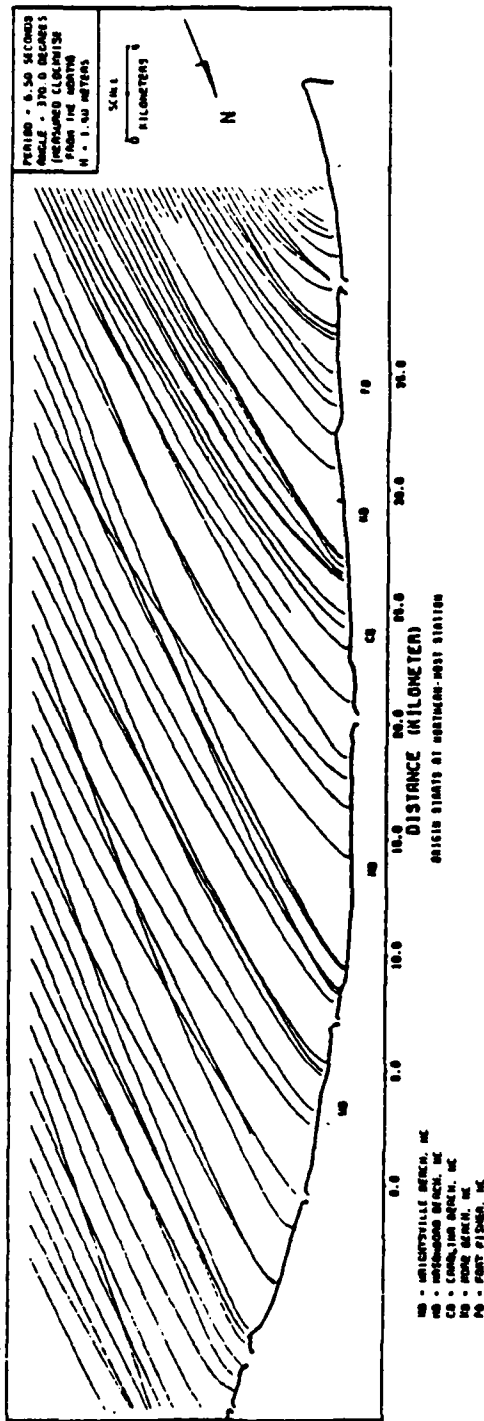












Analysis of coastal sediment transport processes from Wrightsville Beach to Fort Fisher, North Carolina / by T.C. Winton ... [et al.].—Fort Belvoir, Va. : U.S. Army Coastal Engineering Research Center ; Springfield, Va. : available from NTIS, 1981. [205] p. : ill., maps ; 27 cm.—(Miscellaneous report / U.S. Army Coastal Engineering Research Center ; no. 81-6) (Contract DACW ; 72-79-C-0001). Cover title.

"June 1981."

"Prepared for U.S. Army, Corps of Engineers, Coastal Engineering

Research Center."

Report presents a comprehensive engineering analysis of the coastal

sediment transport processes along a 42-kilometer segment of the North Carolina shoreline from Wrightsville Beach to Fort Fisher.

1. Sediment transport—North Carolina. 2. Littoral processes—

North Carolina. 3. Beach nourishment—North Carolina. I. Winton, T.C. II. Coastal Engineering Research Center (U.S.). III. Series: Miscellaneous report (Coastal Engineering Research Center (U.S.)) ; no. 81-6. IV. Series.

TC203 .US81mr no. 81-6 627

Analysis of coastal sediment transport processes from Wrightsville Beach to Fort Fisher, North Carolina / by T.C. Winton ... [et al.].—Fort Belvoir, Va. : U.S. Army Coastal Engineering Research Center ; Springfield, Va. : available from NTIS, 1981. [205] p. : ill., maps ; 27 cm.—(Miscellaneous report / U.S. Army Coastal Engineering Research Center ; no. 81-6) (Contract DACW ; 72-79-C-0001). Cover title.

"June 1981."

"Prepared for U.S. Army, Corps of Engineers, Coastal Engineering

Research Center."

Report presents a comprehensive engineering analysis of the coastal

sediment transport processes along a 42-kilometer segment of the North Carolina shoreline from Wrightsville Beach to Fort Fisher.

1. Sediment transport—North Carolina. 2. Littoral processes—

North Carolina. 3. Beach nourishment—North Carolina. I. Winton, T.C. II. Coastal Engineering Research Center (U.S.). III. Series: Miscellaneous report (Coastal Engineering Research Center (U.S.)) ; no. 81-6. IV. Series.

TC203 .US81mr no. 81-6 627

Analysis of coastal sediment transport processes from Wrightsville Beach to Fort Fisher, North Carolina / by T.C. Winton ... [et al.].—Fort Belvoir, Va. : U.S. Army Coastal Engineering Research Center ; Springfield, Va. : available from NTIS, 1981. [205] p. : ill., maps ; 27 cm.—(Miscellaneous report / U.S. Army Coastal Engineering Research Center ; no. 81-6) (Contract DACW ; 72-79-C-0001). Cover title.

"June 1981."

"Prepared for U.S. Army, Corps of Engineers, Coastal Engineering

Research Center."

Report presents a comprehensive engineering analysis of the coastal

sediment transport processes along a 42-kilometer segment of the North Carolina shoreline from Wrightsville Beach to Fort Fisher.

1. Sediment transport—North Carolina. 2. Littoral processes—

North Carolina. 3. Beach nourishment—North Carolina. I. Winton, T.C. II. Coastal Engineering Research Center (U.S.). III. Series: Miscellaneous report (Coastal Engineering Research Center (U.S.)) ; no. 81-6. IV. Series.

TC203 .US81mr no. 81-6 627

Analysis of coastal sediment transport processes from Wrightsville Beach to Fort Fisher, North Carolina / by T.C. Winton ... [et al.].—Fort Belvoir, Va. : U.S. Army Coastal Engineering Research Center ; Springfield, Va. : available from NTIS, 1981. [205] p. : ill., maps ; 27 cm.—(Miscellaneous report / U.S. Army Coastal Engineering Research Center ; no. 81-6) (Contract DACW ; 72-79-C-0001). Cover title.

"June 1981."

"Prepared for U.S. Army, Corps of Engineers, Coastal Engineering

Research Center."

Report presents a comprehensive engineering analysis of the coastal

sediment transport processes along a 42-kilometer segment of the North Carolina shoreline from Wrightsville Beach to Fort Fisher.

1. Sediment transport—North Carolina. 2. Littoral processes—

North Carolina. 3. Beach nourishment—North Carolina. I. Winton, T.C. II. Coastal Engineering Research Center (U.S.). III. Series: Miscellaneous report (Coastal Engineering Research Center (U.S.)) ; no. 81-6. IV. Series.

TC203 .US81mr no. 81-6 627

DATE
ILMED
- 8